Development and Mechanistic Investigation of Indium(III)-Catalysed Hydrosilane Reduction of Imines

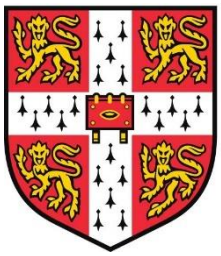

Nadia Nasser Petersen

This dissertation is submitted for the Degree of Doctor of Philosophy at the University of Cambridge.

January 2019

Abstract

Asymmetric catalysis continues to be of utmost importance *inter alia* for the development of enantiomerically pure drugs. The application of computational methods in understanding how enantioselectivity is induced in specific reactions is a powerful time-saving tool for organic chemists. By investigating the reaction pathway, specifically the enantiodetermining transition state, factors that result in an increased energy difference between the two enantiomeric transition states can be identified and thus employed for increasing the enantiomeric excess. Little is known regarding the achievement of enantioselectivity in indium(III)-catalysed reactions. Hence, the project described in this dissertation has started from scratch by generating the experimental data from which to build computational models. This dissertation starts with an introduction to the field of asymmetric catalysis, the advantages of indium as a catalyst and recent progress within indium-catalysed reactions. Following is a discussion of an extensive methodology project where complexes of In(III) and various functionalised BINOL ligands or BINOL derivatives have been investigated as catalysts for the hydrosilane reduction of imines. The functionalised BINOL ligands employed include a range of C_1-symmetric BINOL ligands, which were synthesised as part of a project on optimising BINOL phosphoric acid ligands described in Chapter 2. Significant progress has been made towards the development of a catalyst complex capable of achieving an enantioselective In(III)-catalysed reduction. The developed methodology presented in this thesis represents a novel method for achieving enantioselectivity in prochiral substrates by the use of chiral ligands co-ordinating to an indium metal-centre. Enantiomeric excess was obtained only in polar, protic solvent systems, where up to 73% e.e. was achieved. The experimental work has been combined with computational investigations of potential complexes and mechanistic pathway calculations. The most plausible pathway, established from the computational investigations presented in this thesis, proceeds via the formation of an In(III)-hydride species. This hydride is then transferred to the imine in the manner observed in ruthenium-catalysed reactions. Preliminary results for an alternative active In(III)-In(III) dimeric complex is discussed. Extensive experimental mechanistic investigations are presented along with a substrate scope of the reaction. Finally, future perspectives are given on how the knowledge obtained regarding the enantiodetermining mode in the investigated hydrosilane reduction might be employed to achieve enantioselectivity in other In(III)-catalysed reactions.

Contents

Declaration

This dissertation is submitted in partial fulfilment of the requirements for the Ph.D. in Chemistry. It describes the work carried out in the Department of Chemistry between January 2016 and January 2019. Hereby I declare, that this dissertation is a result of my own work and except if specified, nothing has been carried out by another individual. I further state that this dissertation is not substantially the same as any that I have submitted or will be submitting for a degree or diploma or other qualification at this or another University. In accordance with the Board of Graduate Studies guidelines, this document does not exceed 60,000 words.

Nadia Nasser Petersen

January 2019

Acknowledgements

I would like to express my gratitude to my supervisor Professor Jonathan M. Goodman for welcoming me in his research group and for giving me this opportunity to pursue a PhD at the University of Cambridge.

I wish to thank Professor Ian Paterson for encouraging me to apply to return to Cambridge for a PhD and for his input over the years. I am grateful to all those members of lab 122 who has contributed to providing a pleasant working environment.

Jolene Reid is acknowledged for her computational work behind and design of the C_1 catalyst along with initial synthesis, from which I took over the project described in Chapter 2. Kristaps Ermanis is acknowledged for his help with the project in synthesising the starting material for testing the catalyst along with doing the extra tests of this catalyst. Kristaps has also been a highly valued colleague for scientific discussions of my main project.

I am sincerely grateful to my two collaborators Prof. Scott E. Denmark and Assoc. Prof. Peter Brandt. Prof. Denmark provided a library of 32 BINOL ligands that I have employed for testing my developed system. Assoc. Prof. Peter Brandt has provided a constant stream of highly valuable ideas for the project and we have had many scientific discussions, that has made the project progress. Peter also hosted me visiting BMC in Uppsala for three weeks, and these were invaluable for the computational part of the project. Assoc. Prof. Peter Brandt and Dr. Fredrik Svensson has taught me all I know about computational chemistry and I am very thankful for this.

I am very grateful to Dr. Robert Phipps for his valuable input on my project both at my 1st year viva and over the last three months.

I am thankful to my wonderful student Miss Eilidh Bodfish, who carried out a 6-weeks summer project with me, synthesising imines and amines for me.

I am also grateful to: Mr. Nic Davies and Miss Naomi Hobbs for providing excellent technical support ensuring the lab is running smoothly; the Mass Spectrometry team; Dr. Andrew Bond for X-Ray crystallography and the NMR staff. The CMI support staff especially Mrs Susan Begg, who has kept the CMI running and helped with administrative work is very appreciated. I would like to thank Professor David Spring and the current and past Spring group HPLC team members for letting me use their RP-HPLC. Likewise, I wish to thank Prof. Leeper and the Leeper group for NP-HPLC, and Dr. Robert Phipps and the Phipps group for SFC.

Special thanks are expressed to Miss Eilidh Bodfish, Dr. Fredrik Svensson, Miss Madalina Mihai, Miss Lavinia Dunsmore and Dr. Kim Mortensen for proofreading this thesis.

I also wish to thank Avid, Eilidh, Fredrik, Madalina, Lavinia, Kim, Guillermo, members of GSNC and the three musketeers; Deborah, Alice and Rachel for all their support during my PhD. This has been invaluable especially towards the end.

Finally, I would like to thank Cambridge Trust and EPSRC for generous financial support along with Knud Højgaards foundation, Cambridge Leave to Work Away Research Fund, St Edmund's College and my grandfather for Travel funding.

Abbreviations

Ac	acyl
aq.	aqueous
AREA	A Remote Environment Angle
ASAP	atmospherical solid analysis probe
BINOL	1,1'-bi-2-napthol
BINAM	1,1'-Bi(2-naphthylamine)
BINAP	2,2′-bis(diphenylphosphino)-1,1′-binaphthyl)
Bn	benzyl
B3LYP	Becke, 3-parameter, Lee-Yang-Parr D3
Boc	*tert*-butyloxycarbonyl
CFT	crystal field theory
CFSE	crystal field splitting energy
CPA	chiral phosphoric acid
conc.	concentrated
COSY	correlation spectroscopy
DME	dimethoxyethane
DMF	dimethylformamide
DMSO	dimethylsulfoxide
DFT	density functional theory
DIPEA	*N*,*N*-diisopropylethylamine
e.e.	enantiomeric excess
EA	ethyl acetate
equiv	equivalent

ESI	electrospray ionization
EWG	electron withdrawing
FCC	flash column chromatography
FF	force field
FT	fourier transform
h	hour(s)
H_8	5,5',6,6',7,7',8,8'-octahydro
HMBC	heteronuclear multiple bond correlation
HMPA	hexamethylphosphoramide
HPLC	high performance liquid chromatography
HRMS	high resolution mass spectrometry
HSQC	heteronuclear single quantum coherence
IR	infrared
KHMDS	potassium hexamethyldisilazane
KS	Kohn-Sham
LA	Lewis acid
LACVP	Los Alamos national laboratory, outermost Core orbital, Valence only, People
LAE	ligand-acceleration effect
LANL2DZ	Los Alamos National Laboratory 2 Double Z
LAV3P	Los Alamos national laboratory, Valence only, Pople
m-CPBA	*meta*-chloroperbenzoic acid
min	minute(s)
M06	Minnesota 06
MM	molecular mechanics

MO	molecular orbital
MOM	methoxymethyl
MP	melting point
MPV	Meerwein-Ponndorf-Verley
MS	mass spectrometry
M.S.	molecular sieves, 4Å unless otherwise stated
MTBE	methyl tert-butyl ether
NFSI	*N*-fluorobenzenesulfonimide
NMP	*N*-methyl-2-pyrrolidone
NMR	nuclear magnetic resonance
NP	normal phase
O.N.	overnight
PE	40-60% petroleum ether
PES	potential energy surface
PBM	Poisson-Boltzmann model
PG	protection group
ppm	parts per million
QM	quantum mechanics
RE	rare-earth
rfx	reflux
RP	reverse phase
PYBOX	pyridine bis(oxazoline)
RT	room temperature
SALEN	*N*,*N*'-bis(salicylidene)ethylenediamine

sat.	saturated
SFC	supercritical fluid chromatography
SET	single electron transfer
SPE	single-point energy
TMEDA	*N,N,N′,N′*-Tetramethylethylenediamine
Tf	triflyl
THF	tetrahydrofuran
TLC	thin-layer chromatography
TMDS	1,1,3,3-tetramethyldisilazane
TMDSO	1,1,3,3-tetramethyldilisoxane
tfacac	triflouroacetylacetonate
TMS	trimethylsilyl
t_R	retention time
TRIP	3,3′-Bis(2,4,6-triisopropylphenyl)-1,1′-binaphthyl-2,2′-diyl hydrogenphosphate
TS	transition state
VAPOL	2,2′-Diphenyl-(4-biphenanthrol)
VANOL	3,3′-Diphenyl-2,2′-bi-1-naphthol
Å	ångstrøm

Chapter 1. Background

1.1. Asymmetric Catalysis

With the discovery of chirality through the isolation of the first optical isomers by Louis Pasteur in 1848,[1] the fundamental concept for what was to become the field of asymmetric catalysis was established. Following the thalidomide tragedy of 1961, the importance of stereochemistry in drug development was acknowledged through international regulations encouraging the synthesis of single-enantiomer drugs.[2,3] With the increasing demand for effective enantioselective synthesis, especially within the pharmaceutical industry, the field of asymmetric catalysis has rapidly evolved[4] since its inception in 1966.[5] When the Nobel prize in Chemistry was awarded to Knowles, Noyori and Sharpless in 2001, the importance of asymmetric catalysis was recognised worldwide.[6] One of the most general and flexible methods for asymmetric synthesis is enantioselective catalysis using chiral metal complexes.[7] Several metals are able to perform catalytic activities which allow apparently impossible reactions to occur. Metals have labile co-ordination sites; thus, by employing chiral ligands, substrates and reagents can come together in a chiral environment, leading to highly enantioselective reactions. Racemic background reactions caused by basic (non-ligated) catalysis continue to hinder the successful development of asymmetric versions of well working reactions. Therefore, there is still need for further developments in the field of asymmetric catalysis.[8]

1.1.1 Ligand-Acceleration Effects

The nature of the ligand bound to a metal centre affects not only the selectivity but also the rate of the organic transformations catalysed by the metal-ligand complex. Examples exist of chiral ligands not only providing a chiral environment but also accelerating the reaction. Ligand acceleration can be essential for achieving rapid transformations in a highly enantioselective fashion. The concept is particularly valuable in reactions with dynamic ligand exchange processes and in reactions which proceed independently of the ligand binding (basic catalysis). In either case high selectivity is achieved through channelling the reaction through one particular metal-ligand complex.[9] Two famous examples of ligand-accelerated catalysis are the titanium-catalysed asymmetric epoxidation[10] and the osmium tetraoxide catalysed dihydroxylation.[11]

However, in the majority of asymmetric processes, no significant ligand promoted rate enhancement is observed. Rather, high levels of enantioselectivity are achieved through the creation of an efficient chiral pocket, where formation of the unwanted enantiomer is decelerated due to steric crowding.[9]

1.2. Indium as a Catalyst for Organic Reactions

The main-group metal indium was identified from and named after its indigo blue spectral line in 1863 by Ferdinand Reich and Hieronymus Theodor Richter.[12] Until the 1990s, indium received little attention from synthetic chemists. However, as this metal possesses remarkable properties, including the ability to catalyse reactions in aqueous media, the interest in the utility of indium reagents has increased within recent years. Cintas described some of the applications and properties of indium reagents in 1995. As the metal is without any significant toxicity and often allows for low catalyst loading, it is very appealing as an environmentally benign catalyst.[13]

In(III) compounds are mild but effective Lewis acids (LAs) which often exhibit high regioselectivity while tolerating a large variety of functional groups.[14] Furthermore, indium compounds catalyse many different reactions. For instance, reports have been published on In(III)-catalysed Strecker-type reactions,[15] reductive aminations and cyclisations,[16] Ritter reactions,[17] Blaise reactions,[18] Barbier reactions,[19,20] Reformatsky reactions,[21] reductive alkynylations,[22] reductive sulfidations,[23] asymmetric allylations,[24] Friedel crafts reactions,[25,26], aldol reactions,[27,28] Diels-Alder reactions,[29] acylations,[30] Biginelli reactions[31] and Wagner-Meerwein rearrangements,[30] as well as other rearrangement reactions.[32]

1.2.1 Indium Salts; the Effect of the Counterion

1.2.1.1 Lewis Superacids; Indium(III) Triflate and Indium(III) Triflimidate

Metal salts of triflic acid or triflimidic acid are often referred to as Lewis superacids. The delocalisation in these counteranions results in exposed metal cations with high positive charge, thus enhancing the LA character of the metal centre. The nucleophilicity of bistriflimide is significantly lower than triflate due to the presence of two highly electron-withdrawing substituents on the nitrogen atom, which strongly increases the acidity of the *N*-bound hydrogen atom. Furthermore, triflimidic acid is a poorer Brønsted acid than triflic acid. Generation of the latter through partial hydrolysis of metal triflates can result in undesirable side reactions. Both metal triflates and metal triflimidates often outperform their metal halide analogues.[33] In aromatic sulfonylations, the triflate counterion in $In(OTf)_3$ was even found to participate in the reaction through ligand exchange with the chloride anion in the substrate to generate an activated intermediate, a role $InCl_3$ could not perform.[34]

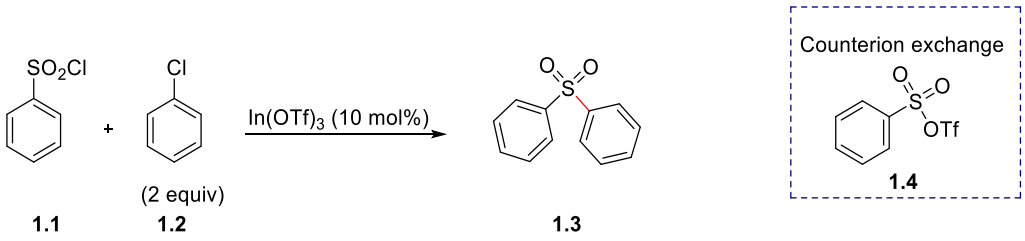

Scheme 1.2.1.1.1: In(OTf)$_3$-catalysed aromatic sulfonylation. Adapted from Frost et al.[34]

Both In(Tf$_2$N)$_3$ and In(OTf)$_3$ are recoverable, air-stable and moisture-tolerant catalysts (section 1.2.2.3); there are even examples of water accelerating reactions catalysed by In(Tf$_2$N)$_3$.[35]

1.2.1.2. Effects of Fine-Tuning LA Properties

Changing the counteranion in the In(III) salt can have profound effects. In 2016, Ogiwara et al.[16] reported a reductive amination of keto acids with hydrosilane. Depending on which In(III)-catalyst was used, this yielded selectively either lactams or cyclic amines (**Scheme 1.2.1.2.1**).

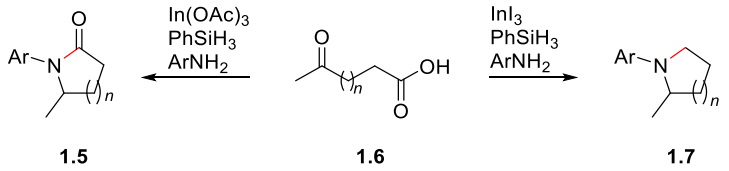

Scheme 1.2.1.2.1: In(III)-catalysed reductive amination of keto acids; with In(OAc)$_3$ lactams are obtained whereas the use of InI$_3$ yields cyclic amines. Adapted from Ogiwara et al.[16]

In this case the InI$_3$ is a much stronger LA and thus capable of over-reducing the lactam to yield cyclic amines.[16]

Shen et al.[36] found a [2+2] cycloaddition to be efficiently catalysed by In(III) trifluoroacetylacetonate (tfacac) in combination with trimethylsilyl bromide (TMSBr), whereas the reaction did not proceed at all when the similar In(III) acetylacetonate was employed in the same combination (**Scheme 1.2.1.2.2**). Furthermore, by adding water to the reaction they could switch from a [2+2] cycloaddition to a dearomatizing cascade reaction.

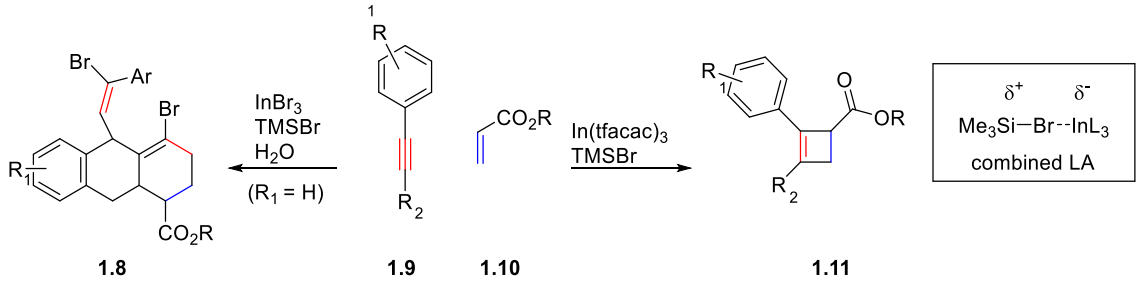

Scheme 1.2.1.2.2: In(III)-catalysed [2+2] reaction or dearomatizing cascade reaction. Adapted from Shen et al. [36]

This is one of the recent examples in literature of using combined LA systems. In(III) forms weaker LA salts than the other group III elements. Thus, the addition of TMS halides has been widely used as a means of increasing the Lewis acidity to improve or even allows for otherwise implausible transformations.[37–40]

1.2.2. Indium and the Environment - a Sustainable Green Metal?

In a society with increasing focus on sustainability and the human induced effects on the environment, it is necessary to address the environmental aspects of using a critical metal such as indium as a catalyst in chemical reactions.

1.2.2.1 Indium Availability

Alongside gallium, germanium and neodymium, indium has critical metal status due to its low concentration in metal ores. No dedicated indium ores exist: it is mined as a by-product of zinc deposits. Indium is crucial for modern technology, primarily in electronic displays and energy technologies e.g. light emitting diodes and solar panels,[41] and the demand for indium is not likely to decrease in the years to come. Therefore, within recent years there has been increased focus on the development of economically favourable recycling procedures (up to 78% in 2015)[41] to enable the continuing demand for indium to be met.[41–47] Already in 2017 more than half of the In used (650 of 1130 tonnes) was obtained from recycled sources.[47] In the grand scheme of the global substance flow of indium, the amount of indium used within research constitutes only a fraction.[46] From the perspective of indium's continuing importance in electronic products and the increased focus on development of sustainable recycling procedures, there is reason to believe that indium will continue to be available for chemical research in the years to come.

1.2.2.2 Green Indium-Mediated Reactions?

Within green chemistry, water is not necessarily considered a green solvent, due to the contamination of the water as a result of the chemical reaction taking place. However, water still possess favourable abilities as a solvent; water is non-toxic, non-flammable and allows for more biologically-related reactions to take place. Thus, reactions capable of being performed in an aqueous environment naturally attract attention.[48]

Examples of In(III)-catalysed Mukaiyama Aldol[49] and Mannich[50] reactions in water were reported in the late 1990s.

The first instance of an indium-mediated allylation in water (**Scheme 1.2.2.2.1**) was reported by Li and Chan in 1991. This reaction could be carried out at room temperature and without the need for

an inert atmosphere. Though the reaction required stochiometric In(0), it facilitated the reaction in high yield in contrast to both zinc and tin.[51]

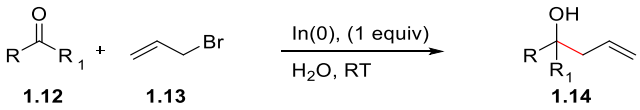

1.12 1.13 1.14

Scheme 1.2.2.2.1: Indium-mediated allylation in water. Adapted from Li and Chen.[51]

Several reports have followed since on In(0)-catalysed Barbier-type reactions in water, aqueous media or even under solvent free conditions.[52–54] In 2017, there followed an example of an enantioselective In(0)-mediated Barbier-reaction in water using a PYBOX-ligand (**Scheme 1.2.2.2.2**).[55]

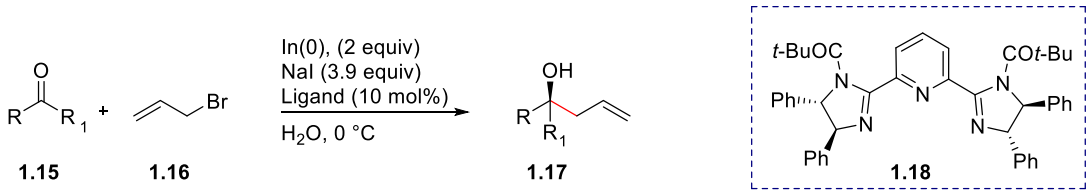

1.15 1.16 1.17 1.18

Scheme 1.2.2.2.2: Enantioselective In(0)-catalysed Barbier-type reaction in water. Adapted from Nakamura et al.[55]

In early 2018, a procedure was reported[56] for synthesising alkenyl iodides under aqueous conditions and with only 2.5 mol% In(III) iodide (**Scheme 1.2.2.2.3**). Compared with previous methods for this type of transformation, which employed stochiometric or sub-stoichiometric amounts of iron catalyst, this shows potential for applications within industry.

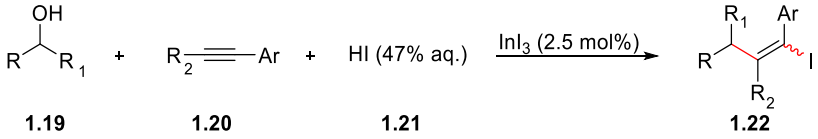

1.19 1.20 1.21 1.22

Scheme 1.2.2.2.3: InI_3 catalysed synthesis of alkenyl iodides. Adapted from Wu et al.[56]

An earlier example of In(III)-catalysed iodine incorporation under aqueous conditions was published in 2001, where Amantini et al. reported bromo- and iodolysis of epoxides in water (**Scheme 1.2.2.2.4**).[57]

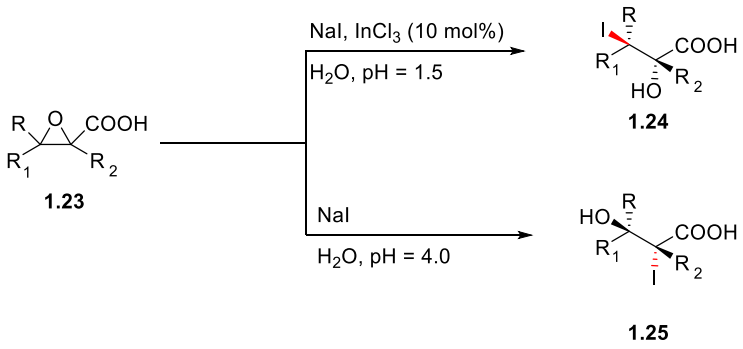

Scheme 1.2.2.2.4: $InCl_3$ catalysed bromo and iodolysis of epoxides in water. Adapted from Amantini et al.[57] The In(III) ion acts as a LA chelating the epoxy oxygen and the acid carbonyl.

Even In(III)-catalysed Diels-Alder reactions have been achieved with water as the solvent (**Scheme 1.2.2.2.5**).[29]

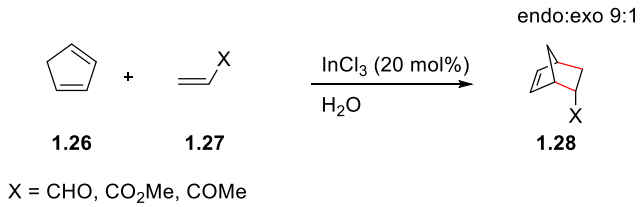

Scheme 1.2.2.2.5: In(III)-catalysed Diels-Alder reaction in water. Adapted from Loh et al. [29]

Another driving force within green chemistry is the development of solvent-free reactions. Within this field, too, indium catalysis has offered solutions. In 2007, In(III)-catalysed acylation and Wagner-Meerwein rearrangement was reported with high selectivity and low catalyst loading under solvent-free conditions (**Scheme 1.2.2.2.6** [a]),[30] and in 2014, an $In(OTf)_3$-catalysed solvent-free Biginelli reaction was also reported (**Scheme 1.2.2.2.6** [b]).[58]

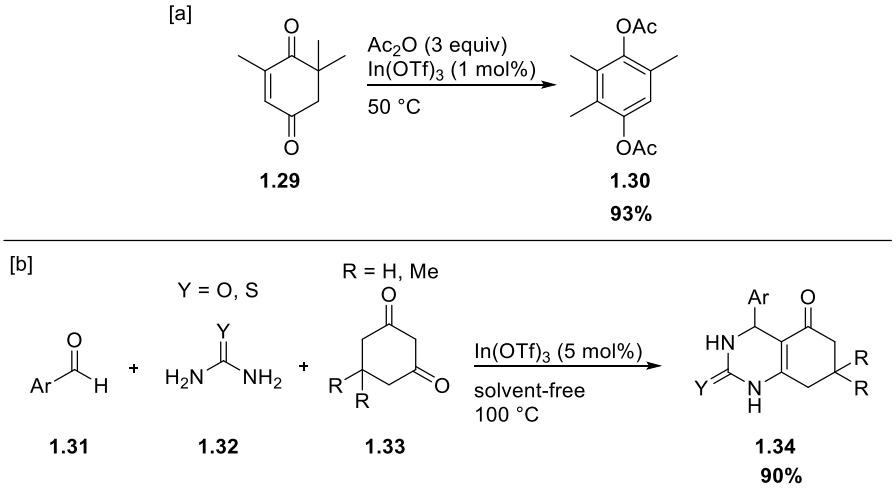

Scheme 1.2.2.2.6: [a] In(III)-catalysed acylation and Wagner-Meerwein rearrangement, adapted from Wildermann et al.[30] [b] $In(OTf)_3$ catalysed solvent-free Biginelli reaction, adapted from Karami et al.[58]

In 2018, a solvent-free $In(OTf)_3$-catalysed Friedel Crafts reaction (**Scheme 1.2.2.2.7**) with high atom economy, high reaction mass efficiency and high carbon efficiency was reported.[25] The protocol was operationally simple and since $In(OTf)_3$ is stable towards air and moisture, the reaction could be performed in a "open flask", leaving water as the only by-product. An additional advantage was that the In(III) catalyst could be recycled and reused for an additional five catalytic cycles without significantly compromising the yield.

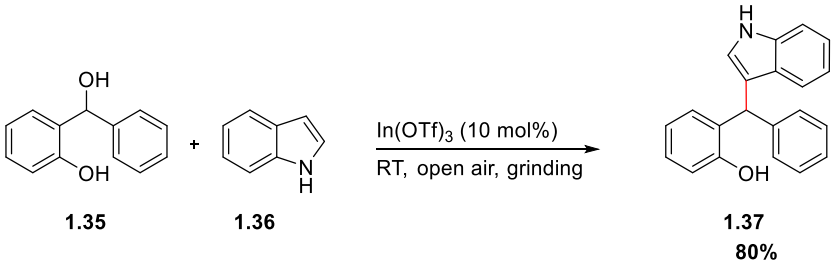

Scheme 1.2.2.2.7: Solvent-free $In(OTf)_3$ catalysed Friedel Crafts reaction. Adapted from Mondal et al.[25]

1.2.2.3 Indium-Catalyst Recovery

In(0) is recoverable through HCl leaching, which is also the method by which In(0) is recovered from Indium-Tin-Oxide.[45] This yields $InCl_3$ which can be used directly, employed for generating low valent indium salts, converted to In(III) hydroxide[59] or reduced to metallic indium, In(0)[60]. In(III) hydroxide can be dehydrated to form In(II) oxide[59] which is used for preparing In(III) triflimide[34] and In(III) triflate[61,62] through aqueous reflux with their corresponding acid counter-ions. In(III) halides are prepared with from In(0) with concentrated acid or with halide gas,[60,63] and these can be used for synthesising other In(III) compounds such as In(III) acetates.[64]

Water-stable indium salts include $InCl_3$, $In(OTf)_3$ and $In(Tf_2N)_3$, and are easily recovered by evaporation of the aqueous phase, allowing for their reuse in reactions without lowering the quality of the reaction.[25,34,50,58]

1.2.2.4 Indium and Transition Metal Catalysis

Over the past decade, indium has attracted attention even within typical transition metal-catalysed reactions.

Indium organometallics have been found to offer advantageous solutions to the cross-coupling reactions of alkyl, alkenyl, alkynyl and aryl substituents. Unlike other metals used in cross-coupling reactions (other group III elements, tin, or zinc), which can only transfer one group, the indium organometallics can transfer all three groups, allowing for the use of sub-stoichiometric amounts.[65] The use of organoindium compounds for cross-coupling reactions has been reported for nickel-,[66] rhodium-[67] and palladium-catalysed[68] reactions. Further progress in this field was reported in 2016 by Gil-Negrete et al., who published a transition-metal-free cross-coupling of indium organometallics with chromene and isochroman acetals mediated by $BF_3{\cdot}OEt_2$ (**Scheme 1.2.2.4.1**).[69]

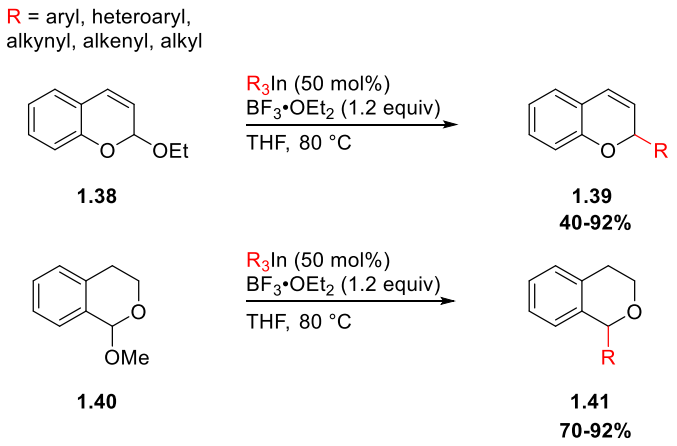

Scheme 1.2.2.4.1: LA catalysed coupling of In-Organometallics with chromene and isochroman acetals. Adapted from Gil-Negrete et al..[69]

In 2015, an In(III)-catalysed intramolecular hydroarylation of aryl propargyl ethers was reported (**Scheme 1.2.2.4.2**).[70] This reaction was regioselective and afforded only the 6-endo-dig cyclisation product. Additionally, a palladium-catalysed copper-free Sonogashira coupling could be performed in the same reaction vessel.

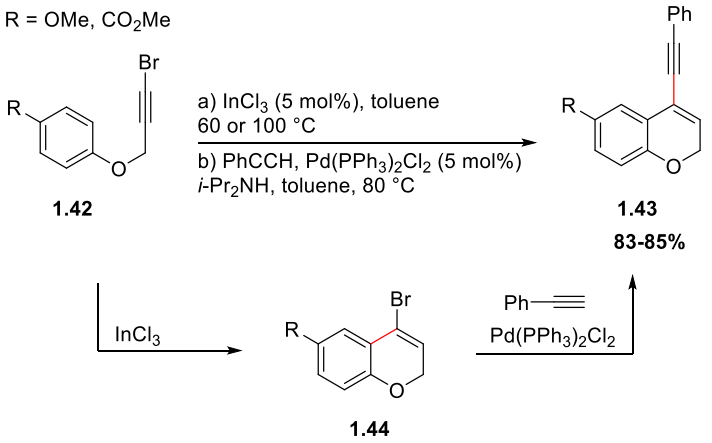

Scheme 1.2.2.4.2: A one-pot $InCl_3$ catalysed intramolecular hydroarylation of aryl propargyl ethers and subsequent Sonogashira coupling. Adapted from Alonso-Marañón et al.[70]

In 2016, a co-operative Indium(III)/Silver(I) system was reported for the oxidative coupling/annulation of 1,3-dicarbonyls and styrenes for the construction of five-membered heterocycles (**Scheme 1.2.2.4.3**).[71] This reaction was unable to proceed without the presence of silver oxide. When silver oxide was used as the sole metal catalyst the reaction proceeded in low yield. However, when these two catalysts were combined, the reaction proceeded in good yield and was three times faster.

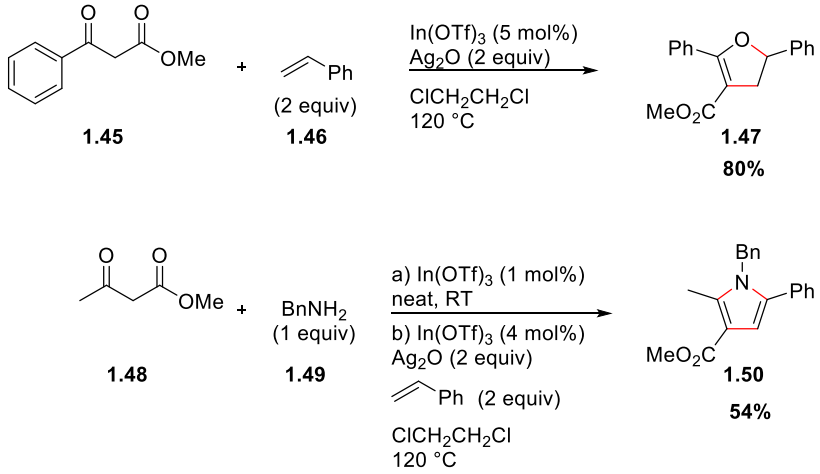

Scheme 1.2.2.4.3.: $In(OTf)_3/Ag_2O$ catalysed oxidative coupling/annulation of 1,3-dicarbonyles and styrenes yielding five-membered heterocycles. Adapted from Ko et al.[71]

Another example of co-operative indium-transition-metal-catalysis was published in 2018 (**Scheme 1.2.2.4.4**).[72] Here, indium was found to mediate a palladium-catalysed allylic alkylation by acting

both as a reductant and an LA, leading to good yield, broad substrate scope and high atom and step economy for the reaction.

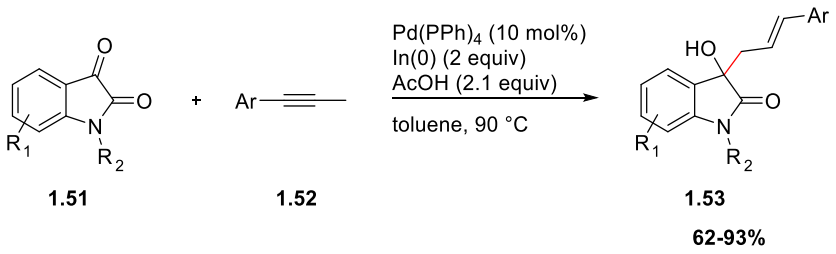

Scheme 1.2.2.4.4.: Co-operative In/Pd catalysed allylic alkylation. Adapted from Wu et al.[72]

In early 2018, Yonekura et al. reported a novel procedure for coupling amines with electron-rich five-membered heteroaryl electrophiles through the use of In(III)-salts (**Scheme 1.2.2.4.5**).[73]

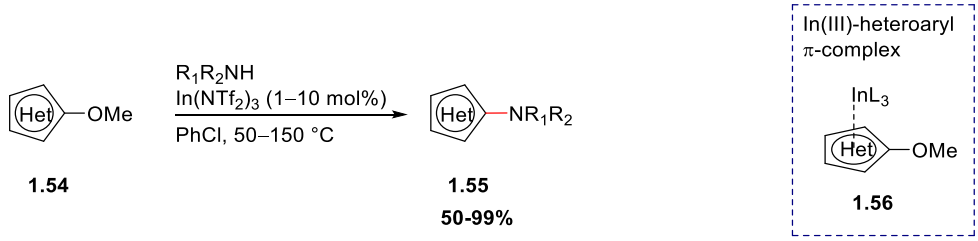

Scheme 1.2.2.4.5: $In(Tf_2N)_3$ catalysed coupling of amines with electron-rich five-membered heteroaryl electrophiles. Adapted from Yonekura et al.[73]

In contrast with the corresponding traditional aromatic substitution amination, this method allowed for the coupling of amines and heteroaryls, which intrinsically are both electron-rich, without the need for an electron withdrawing group (EWG) on the heteroaryl electrophiles or enhanced nucleophilicity of the metal amides. The key for this transformation was the temporary formation of an indium-heteroaryl π-complex, where the In(III) LA behaves as an EWG, thus facilitating the reaction.

1.2.3. Indium Catalysed Hydrosilane Reductions.

Hydrosilanes are organosilicon compounds with at least one Si-H bond. Hydrosilane reductions are carried out under mild conditions and found to demonstrate excellent chemoselectivity. In general, hydrosilanes do not react spontaneously with organic compounds as they have little to no nucleophilicity. The reduction process occurs when either the hydrosilane or the substrate is activated; therefore, the choice of activator allows for a high degree of control of the reaction. A wide variety of metals effectively catalyse hydrosilane reductions. In the simple cases, metals act directly as LAs and promote hydride transfer through addition to the electron-rich end of a bond. In more

complex cases, a reactive intermediate with a metal-hydrogen bond is thought to form via hydrogen transfer from the silane to the catalytic metal centre. The hydrogen is subsequently delivered from the metal to the substrate, freeing the metal for additional catalytic cycles.[74] This type of mechanism, with a reactive indium hydride species, has been suggested in the literature[75–77] for In(III)-catalysed hydrosilylations (**Scheme 1.2.3.1.**).

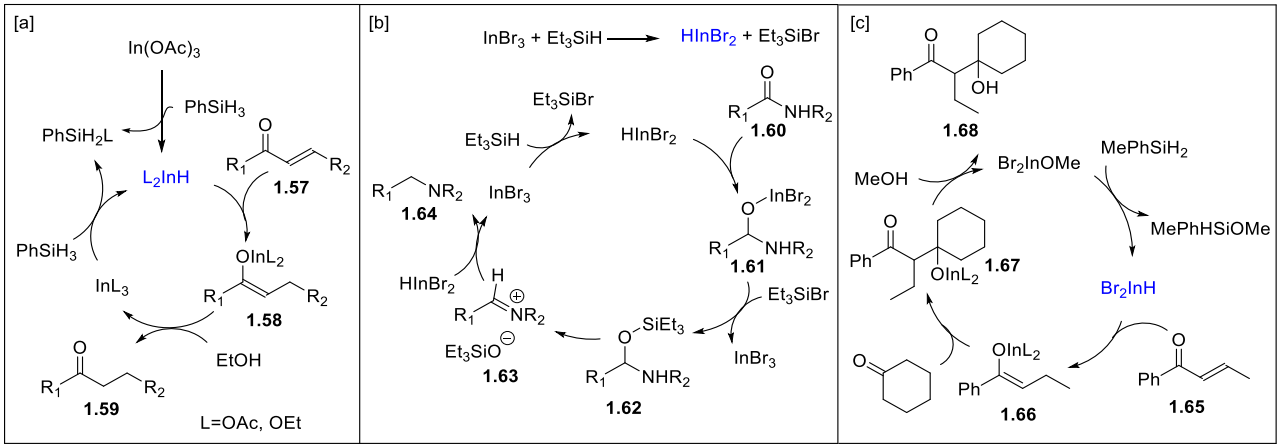

Scheme 1.2.3.1.: The proposed mechanism for the In(III)-catalysed hydrosilane reductions: [a] Suggested mechanism for the In(III)-H catalysed reduction of the alkene in conjugated carbonyls, adapted from Miura et al.[76] [b] Suggested mechanism for the In(III)-H catalysed reduction of the amides to amines, adapted from Sakai et al.[75] [c] Suggested mechanism for the In(III)-H catalysed aldol reaction, adapted from Ieki et al.[77]

If the ligands at the catalytic metal centre are chiral, the hydrogen transfer from the metal can lead to a high degree of enantioselectivity when reducing prochiral substrates.[74]

Several In(III)-catalysed reductive aminations with hydrosilane have been reported in the literature.[16,78,79] The mechanisms have not been fully examined, but In(III) is suggested to act as a LA in these three cases for activating the substrate as illustrated in **Scheme 1.2.3.2.**

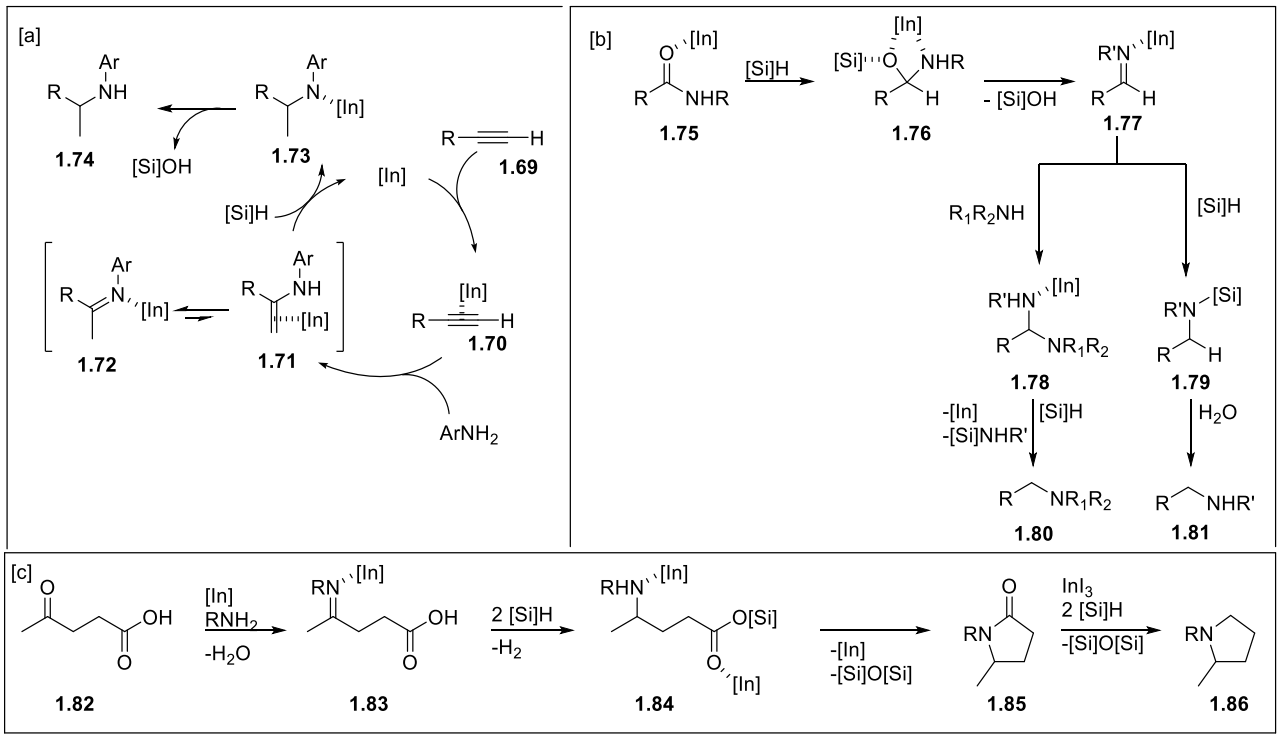

Scheme 1.2.3.2: Examples of proposed mechanisms for In(III)-catalysed reductive amination with hydrosilane. [a] In(III) first activated the alkyne to facilitate amination, then activates the imine tautomer for hydrosilane readuction. Adapted from Sakai et al.[78] [b] In(III) activates first the amide then the imine facilitating two sequential hydrosilane reductions. In the presence of an amine activation of the imine facilitates *N*-alkynylation resulting in an tertiary amine after addition of the second equiv hydrosilane. Adapted from Ogiwara et al.[79] [c] In(III) activates first the ketone facilitating imine formation, then the imine facilitating hydrosilane reduction and finally the silane ester resulting in cyclisation yielding a lactone. When InI_3 is used as the In(III) source, this LA further activates the lactam allowing for additional hydrosilane reduction to afford a cyclic amine. Adapted from Ogiwara et al.[16]

It is noteworthy in mechanism [c] that depending on the indium reagent employed the reduction goes selectively to the lactam or continues to the cyclic amine.

Hitherto, no examples of enantioselective In(III)-catalysed hydrosilane reductions have been reported.

1.2.4. Enantioselective Indium-Catalysed Reactions

In 2005, Teo et al. [80] reported an enantioselective allylation of ketones (**Scheme 1.2.4.1**) mediated by a chiral In(III)-(*R*)-BINOL complex prepared from (*R*)-BINOL and $InBr_3$. This complex was not characterised but they suggested that a tetrahedral In(III)-centre with a single (*R*)-BINOL ligand might be formed.

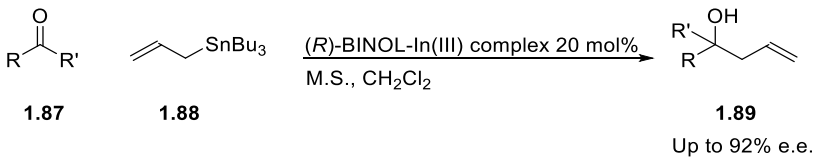

Scheme 1.2.4.1: Enantioselective allylation of ketones by Teo et al.[80]

They suggested that the stereochemical course of this allylation was a *re*-face attack on the ketone resulting from the *si*-face being blocked by co-ordination to the preformed chiral In(III)-complex as depicted in **Figure 1.2.4.1**.[80]

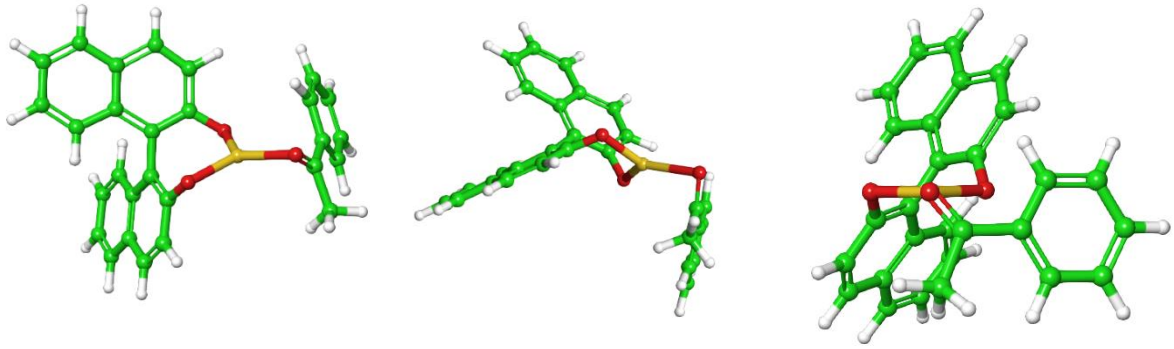

Figure 1.2.4.1: Teo *et al.*[80] suggested enantioselectivity to be induced through the *si*-face being blocked through co-ordination from to the BINOL ligand as depicted. NB this maestro model was constructed with (*S*)-BINOL. Complex shown from three different angles.

This followed a report on enantioselective allylation of aldehydes in up to 94% e.e using a chiral In(III)-PYBOX (**Scheme 1.2.4.2**).[81]

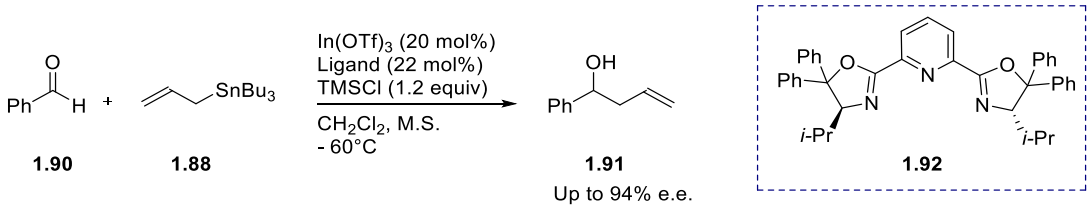

Scheme 1.2.4.2: Enantioselective In(III)-catalysed allylation of aldehydes using PYBOX ligands. Adapted from Lu et al.[81]

They further reported the development of this system to use ketones as substrates in the In(III)-PYBOX-catalysed enantioselective allylation.[82]

In 2005, Takita and co-workers employed In(III) bromide and (*R*)-BINOL for asymmetric alkynylation of aldehydes (**Scheme 1.2.4.3**).[83]

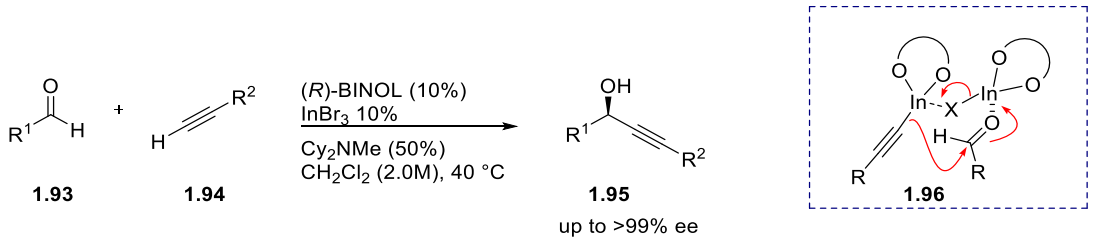

Scheme 1.2.4.3: Asymmetric alkynylation of aldehydes by Takita *et al.* [83]

This was based on their previous work with In(III) as a catalyst for ketone allylation through dual activation of the ketone both as a hard LA and as an activator of the alkyne. By combining the In(III) salt with enantiomerically pure (*R*)-BINOL they thus achieved an asymmetric version of the alkynylation. They suggested that this reaction might proceed via a bimetallic dual activation mechanism (one In(III)-BINOL complex activating the carbonyl, another complex activating the alkyne) as depicted in **Scheme 1.2.4.3**, albeit the catalytic complex of In(III) and BINOL was not characterised.[83] The bimetallic dual activation mechanism was based on the finding that 3,3'-phenyl substituted BINOL was unable to facilitate product formation. Phenyl substituents would result in significant steric hindrance, which could inhibit assembly of a bimetallic complex.

In 2007, *N*,*N*'-dioxides were also reported as chiral ligands for In(III)-catalysed enantioselective allylation of ketones in up to 83% e.e. These ligands were thought to bridge around the indium-metal-centre as depicted in **Scheme 1.2.4.4**.[84]

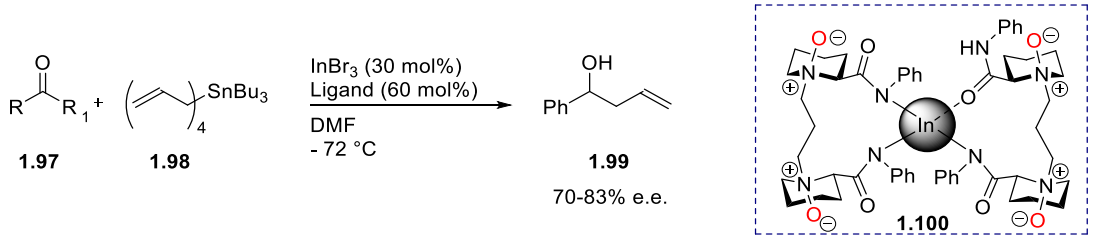

Scheme 1.2.4.4: Enantioselective In(III)-catalysed allylation of ketones with *N*,*N*'-dioxide ligand bridging around the In(III) metal-centre. Adapted from Zhang et al. [84]

Another example followed in 2008, this time with a Ramipril-derived *N*,*N*'-dioxide as the ligand for In(III) in enantioselective allylations of aromatic α-keto-phosphonates in up to 91% e.e.[85]

Enantioselective In(I) reactions have also been reported. In 2005, an enantioselective indium-mediated allylation of hydrazones was reported. The reaction employed stoichiometric In(0) to generate allylindium. By using 3,3'-$(CF_3)_2$-BINOL as the chiral ligand, up to 97% e.e. was achieved (**Scheme 1.2.4.5**).[86]

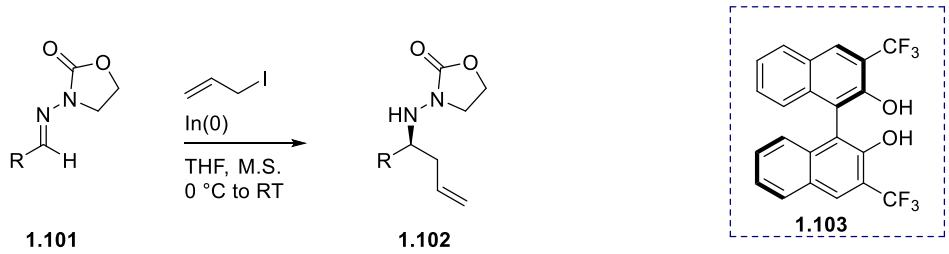

Scheme 1.2.4.5: Enantioselective allylation of hydrazones with In(0) and 3,3'-$(CF_3)_2$-BINOL-ligands. Adapted from Cook et al. [86]

In 2016, the e.e. of this reaction was found to increase when employing more Brønsted-acidic ligands, thus increasing the Lewis-acidity of the indium metal-centre. With a new class of 3,3'-$(SO_2R^F)_2$-ligands e.g. (*R*)-3,3'-$(SO_2CF_3)_2$-BINOL, the allylation could be achieved in up to 99% e.e.[87]

1.3. Towards Understanding Enantioselectivity in Indium(III)-Catalysed Reactions

Though examples of enantioselective In(III)-catalysis are present in the literature, as described in section 1.2.4, hitherto little is known of how the enantioselectivity in these In(III)-catalysed reactions is achieved. The project described in this thesis (from chapter 3 onwards) aspires to understand how enantioselectivity can be induced in ligated In(III)-catalysed reactions, through the combination of experimental investigations and computational mechanistic calculations. Establishing a plausible reaction mechanism and understanding the interactions in the enantiodetermining transition state will allow for future computational predictions to choose the best ligand for achieving enantioselectivity in other In(III)-catalysed reactions.

The developed methodology presented in this thesis represents a novel method for achieving enantioselectivity in prochiral substrates by the use of a chiral ligand co-ordinating to an indium metal-centre.

The ligand type initially examined in this project is BINOL-based, since the Goodman group has worked extensively with computational studies of this scaffold. As will be described in chapter 3, these BINOL-based ligands were found to outperform the other ligand types investigated. The mechanistic starting point for the project was based on the previously described work by Takita,[83] Teo,[88] Miura[76] and Sakai.[75] The reaction pathway was hypothesised to proceed via ligand exchange yielding an In(III)-BINOL complex, which upon addition of a silane would generate an active In(III) hydride species. By transferring the hydride to a prochiral substrate such as a carbonyl equivalent in the chiral environment induced by the co-ordinating ligand an enantioselective reduction is achieved. The hypothesised mechanism is depicted in **Scheme 1.3.1**.

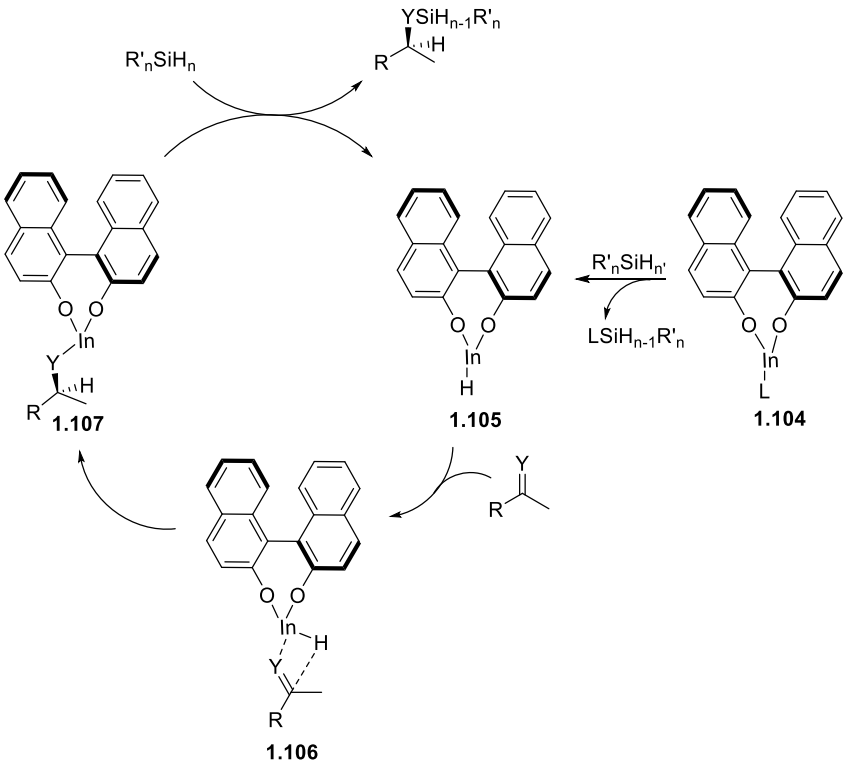

Scheme 1.3.1: The hypothesised mechanism of hydrosilane reduction of a carbonyl equivalent, catalysed by a chiral In(III)-BINOL complex.

Chapter 2: C_1-Symmetric Chiral Phosphoric Acid

The work presented in this chapter represents a side project and was carried out in order to experimentally assess calculations by Reid[i] on enantioselective hydrogenation of imines using chiral phosphoric acids (CPAs). Some of the compounds synthesised as part of this project have been used in the main project, which will be presented in Chapter 3 and onwards.

2.1 Towards Unified Steric Descriptors

Identifying the optimal ligand for achieving the highest possible stereoselectivity can be a troublesome and time-consuming process when led only by trial and error experimental work. Hence, the computational prediction of the enantioselective outcome of reactions is desirable. However, to achieve accuracy in such predictions, the mechanism of the reaction must be known and the steps along the enantiodetermining pathway, including all possible substrate-catalyst interactions, must be examined. Increased energy difference between the two enantiomeric transition states leads to increased e.e. Generally, these energy differences result from favourable interactions such as opposing dipoles, stabilising interactions such as hydrogen bonds or unfavourable steric clashes.

Several parameters (**Figure 2.1.1**) have been developed to describe steric effects. The early work in this area includes Taft's steric parameter, based on linear free energy in a range of esterification and ester hydrolysis reactions.[89,90] This parameter was later modified to include van der Waals radii for specific substituents by Charton.[91–95] In addition to these Taft-type parameters, other steric descriptors have been developed. Winstein-Holness parameters,[96] also known as A-values, are used for determining the most stable configuration of substituents (based on axial-equatorial flip on cyclohexanes); the interference value[97,98] also known as the rotation barrier, describes the rotational barrier in biphenyls; the Tolman Cone Angle[99,100] is widely used within organometallic chemistry to measure the size of the ligand; buried volume[101] gives the percentage of a sphere which is occupied by the ligand co-ordinating to the metal centre; the Sterimol parameters[102] (B_1, minimum width; B_5, maximum width; L, length) are used to describe the steric profile of a single substituent.

[i] Jolene Reid, previous PhD student in the Goodman Group, University of Cambridge.

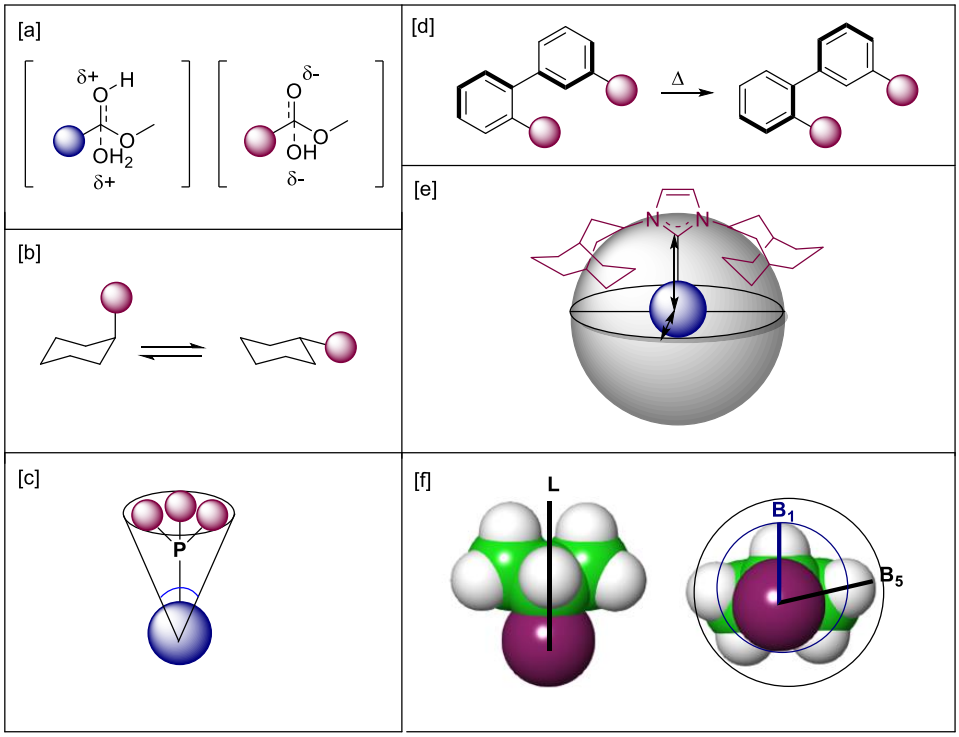

Figure 2.1.1: Different parameters used as steric descriptors. [a] Taft's parameter examining the effect from partial charges on the reaction rate. [b] A-values for axial-equatorial flip on cyclohexanes. [c] Tolman cone-angle. [d] Interference value based on rotation barriers of biaryls. [e] Buried volume of *N*-heterocyclic carbene ligand co-ordinating to a metal centre. [f] Sterimol parameter, adapted from Milo et al.[102]

Chiral phosphoric acids have become popular in organic synthesis as chirality-inducing ligands for many important transformations.[103–105] The 3,3'-substituents are central to the selectivity; generally, large steric bulk leads to high enantioselectivity. However, seemingly minor modifications can often result in profound non-intuitive changes in the enantioselectivity. Therefore, the stereoselective outcome cannot always be easily identified. Computational strategies have been employed, often with positive results, to predict enantioselectivity through the examination of the key interactions in competing diastereomer transition states.[106,107] With advances in computational methods, their ability to accurately model complex interactions continues to improve and the prediction of enantioselectivity *in silico* as the basis for catalyst design becomes a reality.[108] In 2016, a new measure, A Remote Environment Angle (AREA),[109] was introduced for measuring the space further from the phosphoric acid (**Figure 2.1.2**).

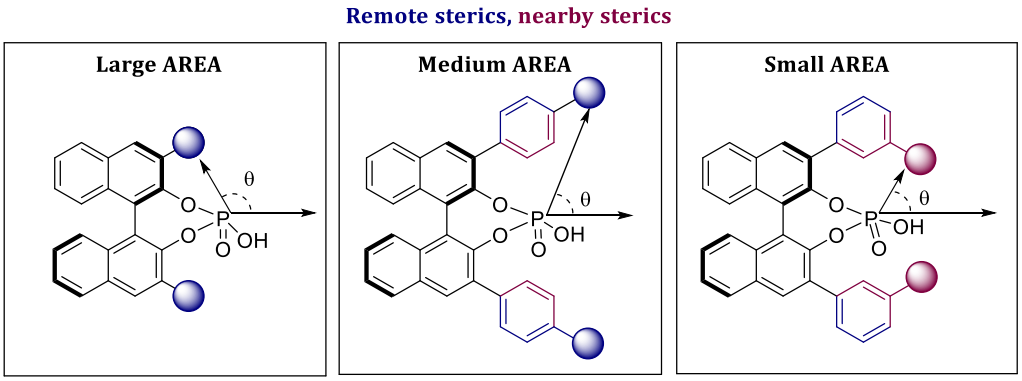

Figure 2.1.2: A Remote Environment Angle for CPAs; the size of the 3,3'-substituent and the proximity to the phosphor results in small to large AREA. Adapted from Reid et al. [109]

In combination with the rotation barrier, which quantifies the proximal sterics, AREA was employed for the successful identification of catalyst features necessary for efficient stereoinduction in imine hydrogenation reactions (**Figure 2.1.3**), suggesting that both proximal and remote sterics are important for the stereoinduction.[109] The calculations suggested that the imine orientation (*Type I* vs *Type II*) was controlled by the proximal bulk, while the stereoisomer (*E* vs *Z*) of the imine would be controlled by the remote sterics (AREA).

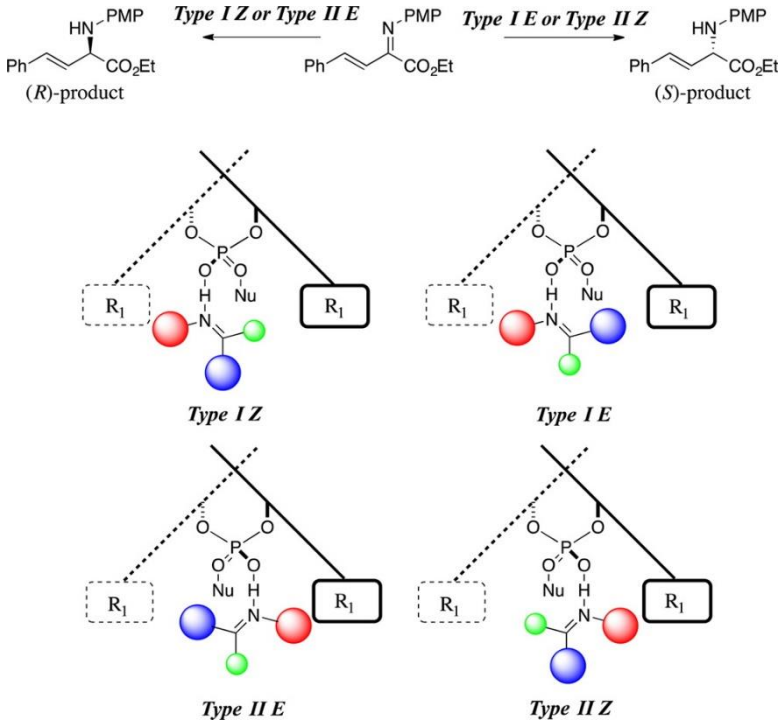

Figure 2.1.3:[109] Transition state models for the imine transfer hydrogenation used for the prediction of the enantioselective outcome. Reprinted from Reid[110] (CC-BY).

2.2. Second Generation BINOL-Derived C_1-Symmetric Catalysts

3,3′-Bis(2,4,6-triisopropylphenyl)-1,1′-binaphthyl-2,2′-diyl hydrogenphosphate (TRIP) belongs to the class of C_2-symmetric ligands. The C_2-symmetry offers several advantages: the symmetric axis limits the number of competing diastereomeric reaction pathways, allows for more straightforward analysis of interactions between the catalyst and the substrate, and thus overall simplifies the mechanistic and structural studies. Though TRIP continues to be a superior catalyst for many reactions, this is not always the case. As a continuation on the work on AREA as a means to computationally predict the best catalyst for high stereoinduction, Reid examined the addition of nucleophiles to conjugated imines. TRIP was found to be selective for seven out of eight possible permutations (**Figure 2.2.1**[110]). The pathway for which TRIP was not selective was *Type II E*, which involves large displaced nucleophiles. [110]

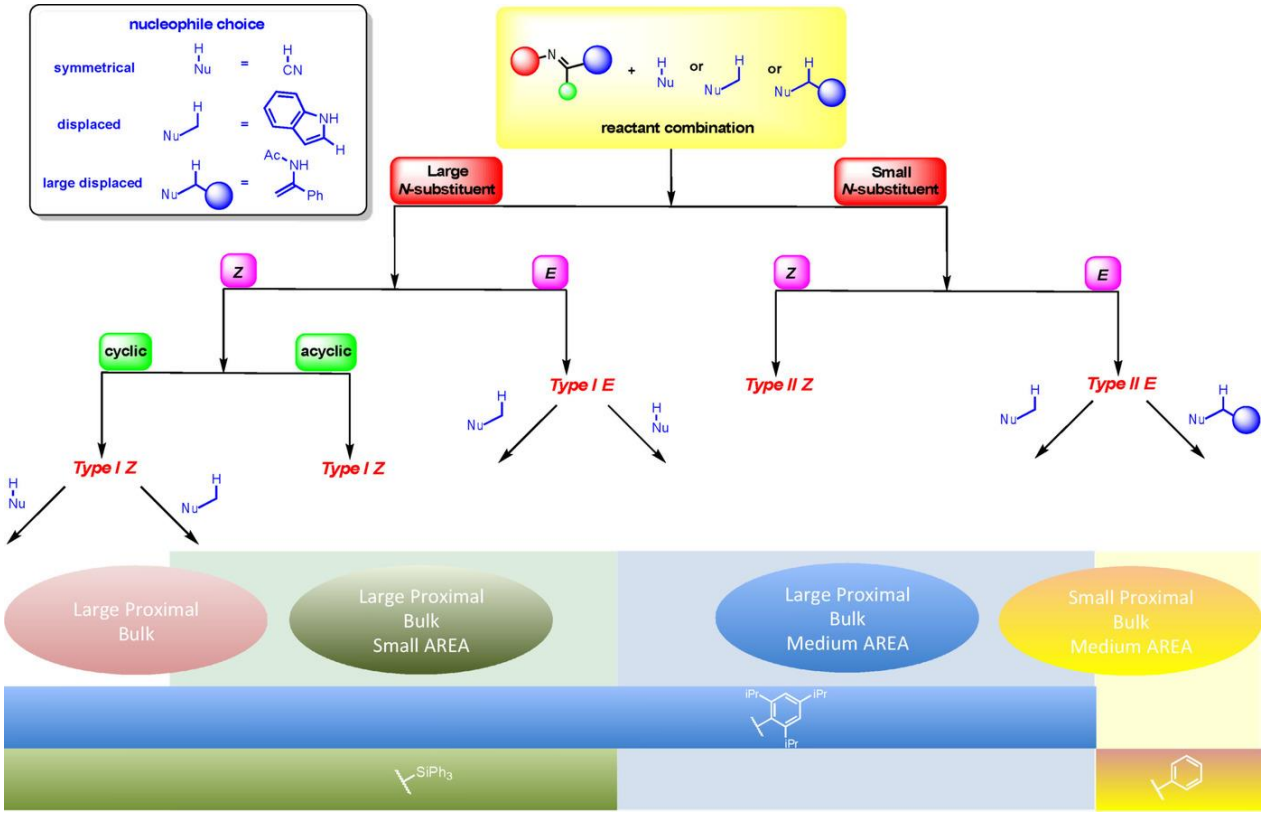

Figure 2.2.1[110]: Qualitative model for catalyst choice controlled by size of the *N*-substituent, imine configuration, acyclic or cyclic imine and size of the displaced nucleophile. Reprinted from Reid[110] (CC-BY).

Aiming for a catalyst selective in all eight possible permutations, Reid carried out computational predictions to find a single catalyst with both large and small proximal sterics.[111] Chiral phosphoric acids can be modelled in quadrant diagrams as depicted in **Figure 2.2.2**. By employing non-equivalent 3 and 3'-substituents, thus shifting from a C_2-symmetry to a C_1-architecture, more

versatile catalysts can be designed. In the C_1-catalyst, quadrant II continues to be fully blocked, while quadrant III is only partially blocked.

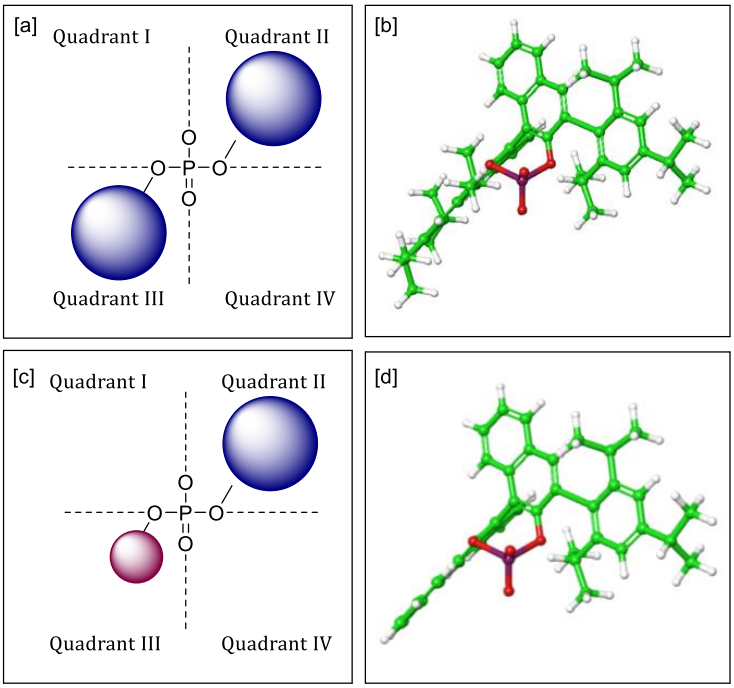

Figure 2.2.2: Quadrant diagram depicting the steric environment of a [a] C_2-symmetric catalyst and [c] C_1-symmetric catalyst. 3D representations of [b] TRIP and [d] the novel C_1-CPA. [a] and [c] adapted from Reid et al.[110]

The *Type II E* TS pathways with large nucleophiles were displaying poor enantioselectivity due to the clash between the 3'-substituent and the large nucleophile. Thus, it was hypothesised that a smaller 3'-substituent would allow for the accommodation of both the large displaced nucleophile and the imine, while retaining the stereoinduction caused by the 3-substituent in the remaining combinations.[111] Reid carried out computational investigations on five different pathways and found a strong preference for the *Type II* reaction pathway in four out of five of the examined reactions (**Figure 2.2.1**). For all five reactions examined, Reid predicted very high enantioselectivity (>99%) and suggested that this smaller phenyl substituent might be able to bias the mechanism towards a *Type II* TS pathway regardless of the reactants employed.[111] A further advantage of the C_1-catalyst is the possibility of late stage introduction of diversity at the 3'-position, thus allowing for the rapid synthesis of a library of catalysts from a common intermediate. This allows for faster evaluation of the effect of varying the size of these 3'-substituents, through experimental test.

2.3. Synthesis of a C_1-CPA

The synthesis suggested by Reid in her thesis[111] is outlined in **Scheme 2.3.1**. The route follows steps proven to be robust for a variety of C_2-CPAs and adds only two additional steps to allow for differentiation of the 3 and 3' substituents. Starting with a MOM-protection of (*S*)-BINOL, then selectively brominating the 3-position followed by a Kumada coupling gives (*S*)-3-(2,4,6-triisopropylphenyl)-MOM-BINOL. The 3'-substituent would then be installed by a second bromination and successive cross-coupling reaction. Removal of the MOM group in an acidic hydrolysis and subsequent phosphorylation would afford the final catalyst.

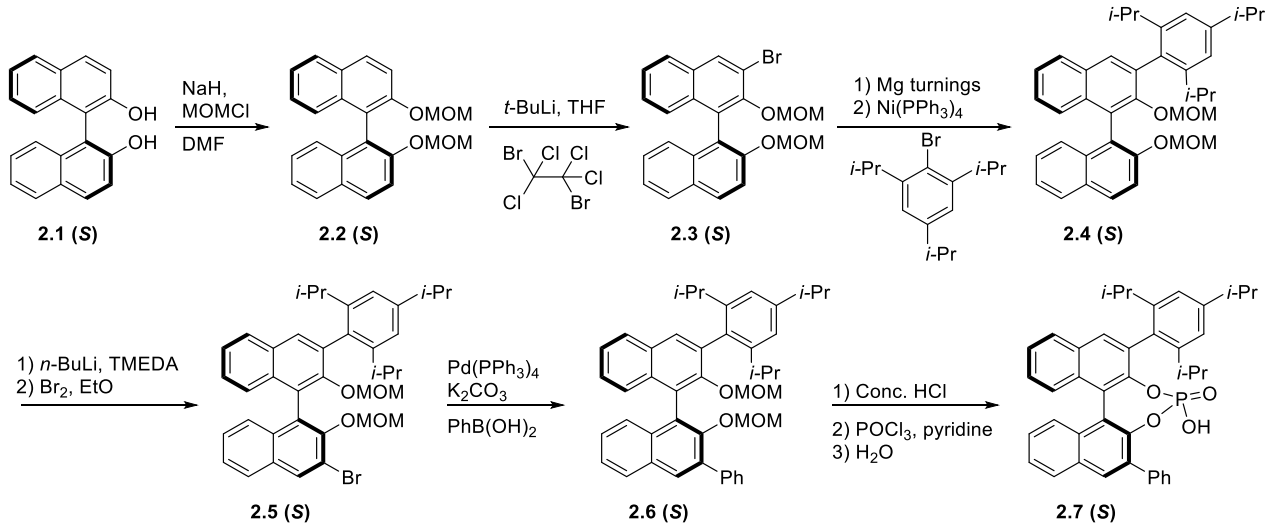

Scheme 2.3.1: First synthetic route to the C_1-symmetric catalysts proposed by Reid.

This synthesis was attempted by both Reid and Lam,[ii] however purification issues were encountered, particularly after the first bromination as well as after the Kumada coupling.

My contribution to the synthesis of the catalysts started by proposing a modified route to the (*R*)-enantiomer of the target CPA, **2.7 (*R*)** (**Scheme 2.3.4**). Commercially cheaper (*R*)-BINOL was employed. The bromination steps were switched to iodination steps, allowing for a cleaner halogenation; this had been found to be a robust and straightforward procedure for the ligands synthesised and described in Chapter 3. In the lithium-halogen exchange steps, *t*-BuLi was substituted with the considerably safer *n*-BuLi, which has been reported to provide equally good yields for mono-iodination.[112,113] At the stage of mono-iodination, the pathway was divided into two; one pathway installed the bulky substituent first through a Kumada coupling, while the second pathway employed a Suzuki coupling to install the less bulky phenyl group first. This allowed for the evaluation of the ease of purification of the product along with possible identification of side-

[ii] PhD Student in the Paterson Group, University of Cambridge.

products in each pathway. Each product was then to follow the reverse cross coupling after a second iodination. Subsequent MOM-deprotection and phosphorylation would yield the final catalyst.

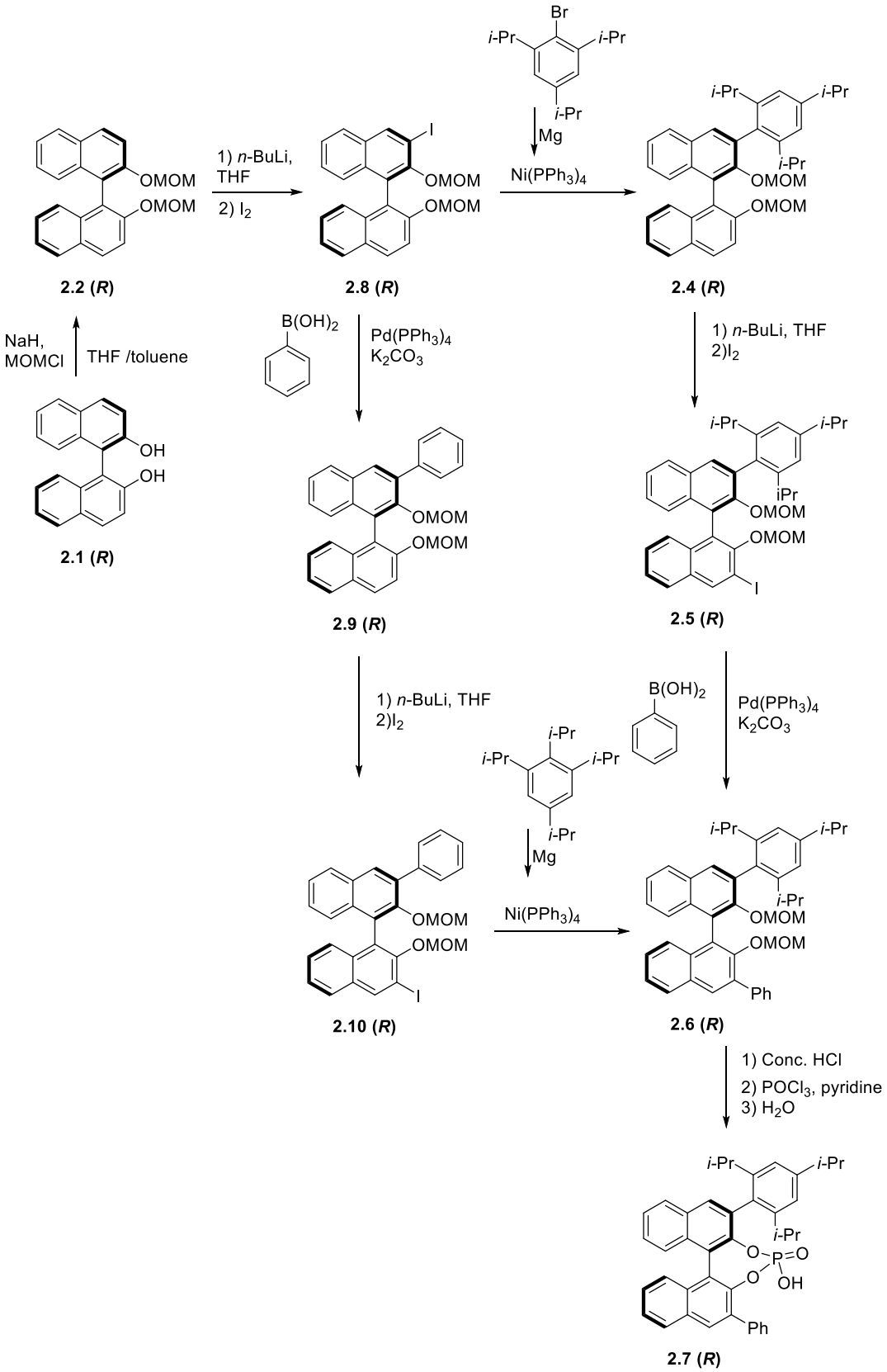

Scheme 2.3.4: Second synthetic route to the C_1-symmetric catalyst.

Commercially available (*R*)-BINOL was first MOM protected following a reported procedure[114] with minor modifications, using with freshly prepared MOMCl[115] in 92% yield (**Scheme 2.3.5**).

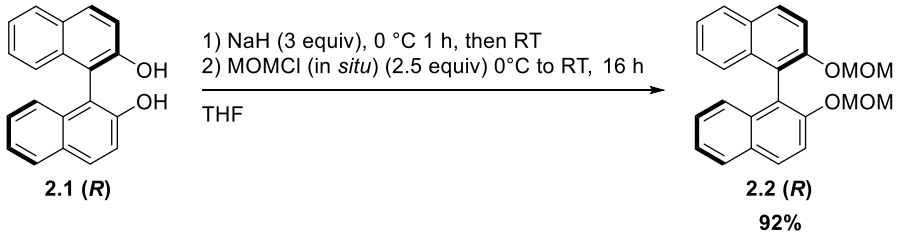

Scheme 2.3.5: MOM protection of (*R*)-BINOL yielding **2.2 (R).**

Selective iodination of the 3-position by cautious *n*-BuLi deprotonation and lithium-halogen exchange afforded the pure (*R*)-3-I-BINOL after recrystallisation (**Scheme 2.3.6**) as reported in the literature.[112]

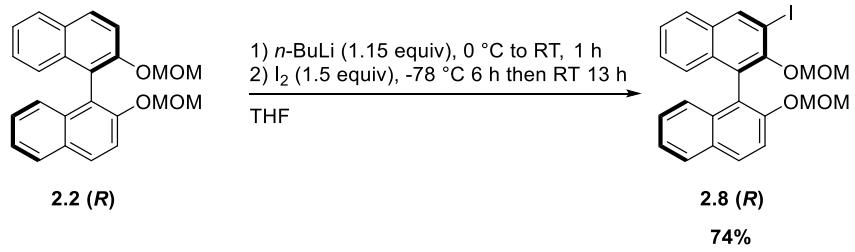

Scheme 2.3.6: Selective monoiodination of (*R*)-MOM-BINOL.

At this point the material was split into two batches. On a small-scale test reaction both cross couplings suffered from incomplete conversion (**Scheme 2.3.7**); however, in both cases pure products were obtained after column chromatography.

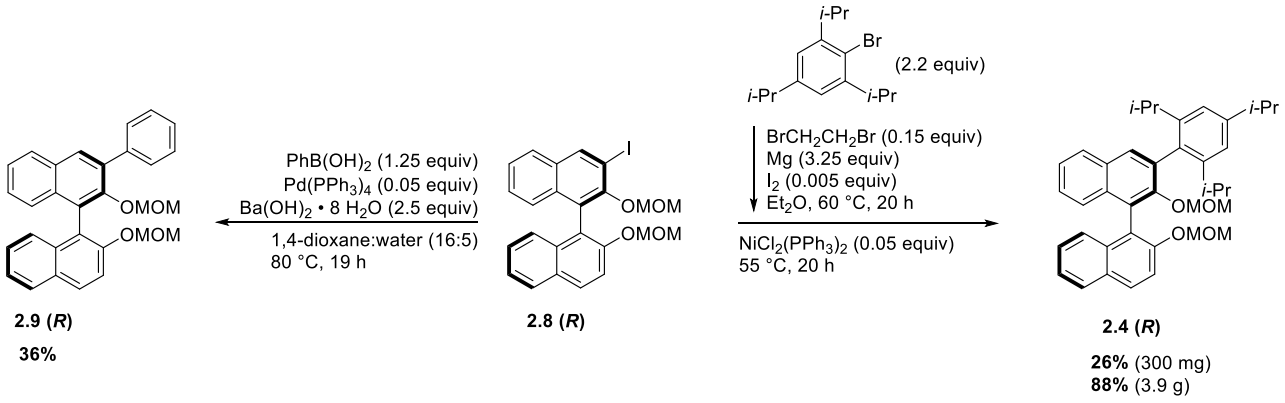

Scheme 2.3.7: Left Suzuki cross-coupling, right Kumada cross coupling of (*R*)-3-I-BINOL.

Potential lithiation of other benzylic positions would be eliminated in the route performing the Kumada coupling prior to the Suzuki coupling and, unlike previously, no issues with the purification

of the Kumada coupling product were encountered. Therefore, this route was repeated on a larger scale in good yield (**Scheme 2.3.7**). The second iodination proceeded in low yield on a test scale, due to incomplete conversion, but proceeded in high yield on large scale (**Scheme 2.3.8**).

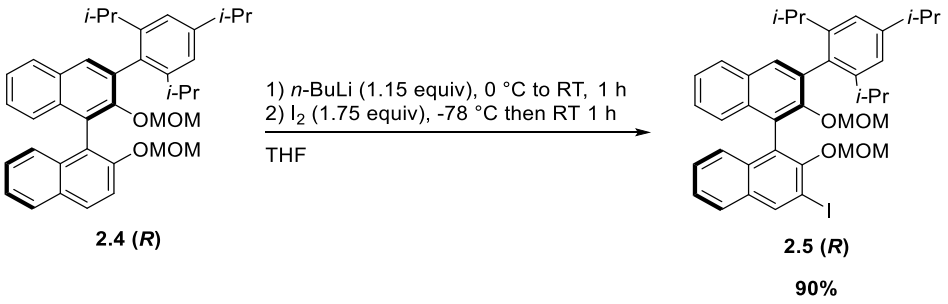

Scheme 2.3.8: Iodination of the 3'-position.

The Suzuki coupling was performed with an increased catalyst loading (10% palladium) since achieving full conversion with a lower catalyst loading had proven troublesome on smaller scale. The product **2.5 (*R*)** was obtained in 90% yield (**Scheme 2.3.9**).

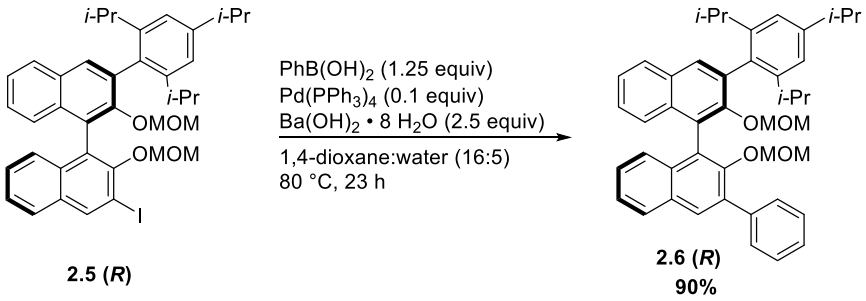

Scheme 2.3.9: Suzuki cross-coupling installing the 3'-phenyl group.

The MOM PG was hydrolysed with concentrated HCl to afford the diol **2.6 (*R*)** in quantitative yield (**Scheme 2.3.10**).

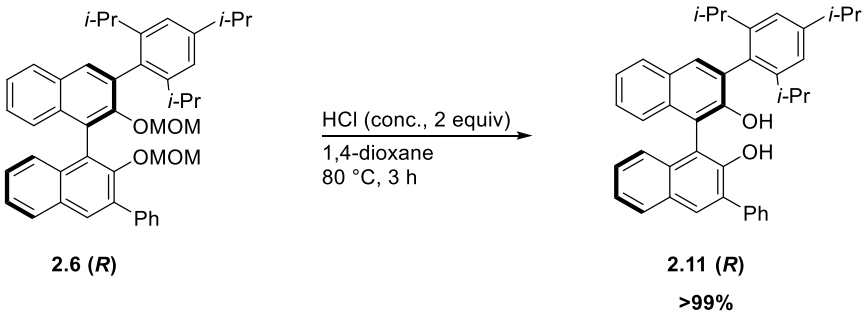

Scheme 2.3.10: Removal of the MOM PG to yield the diol **2.11 (*R*).**

Finally, phosphorylation of **2.11 (*R*)** provided the target C_1-CPA in 68% yield over two steps (**Scheme 2.3.11**).

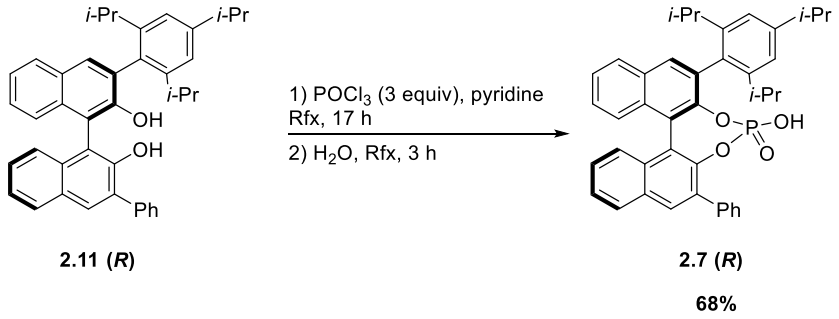

Scheme 2.3.11: Phosphorylation of the diol **2.11 (*R*)** yielding the target **CPA 2.7 (*R*).**

2.4: Testing the C_1-CPA

The first reaction for which the C_1-CPA was tested as a catalyst was an enamine self-coupling (**Scheme 2.4.1**). The enamine substrate **2.12** was synthesised by Ermanis,[iii] who also carried out one of the test reactions along with the reference reaction with TRIP. The outcome proved disappointing, despite the fact this novel C_1-CPA had been predicted to be a highly enantioselective catalyst, it afforded the product in only 8-9% e.e. while 22% e.e. could be achieved employing TRIP as catalyst.

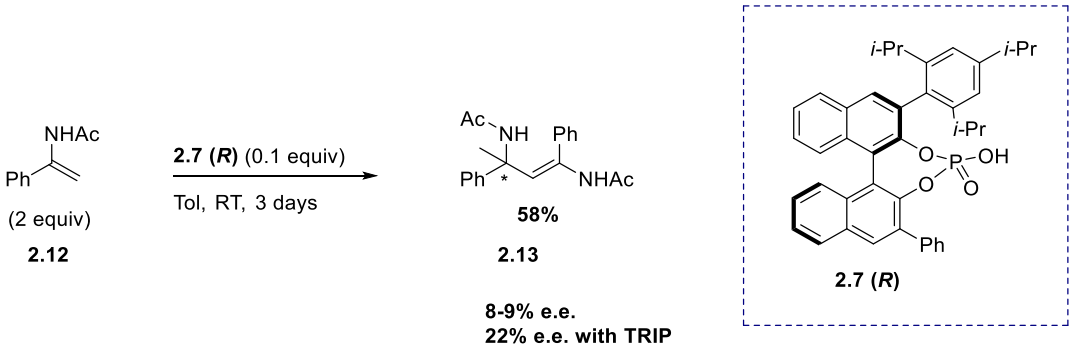

Scheme 2.4.1: Self-coupling of enamines to generate quaternary carbon stereocenter catalysed by the C_1-CPA predicted to yield high e.e.

At this point it was realised that the proton transfer of the phosphoric acid had not been considered when the computational analysis had been performed. In CPAs the proton can shift between the two oxygens, which is an insignificant equilibrium (**Scheme 2.4.2**) in the case of a C_2-scaffold, where the 3 and 3' substituents are the same. However, in the case of a C_1-CPA this proton transfer results in

[iii] PostDoc in the Goodman Group, University of Cambridge

the proton experiencing two different environments depending on whether its closest to the 3 or the 3' substituent.

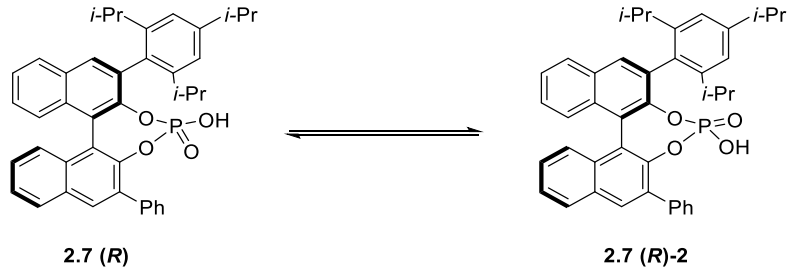

Scheme 2.4.2: Phosphoric acid proton equilibration yielding two diastereomeric C_1-CPAs.

It is known that the proton is favoured on the nitrogen in the case of *N*-triflyl phosphoramides[116,117] thus synthesising **2.14 (*R*)** from **2.11 (*R*)** could be one option for avoiding the equilibrating proton, as this *N*-triflyl phosphoramide would exist mainly as **2.14 (*R*)-1** (**Scheme 2.4.3**).

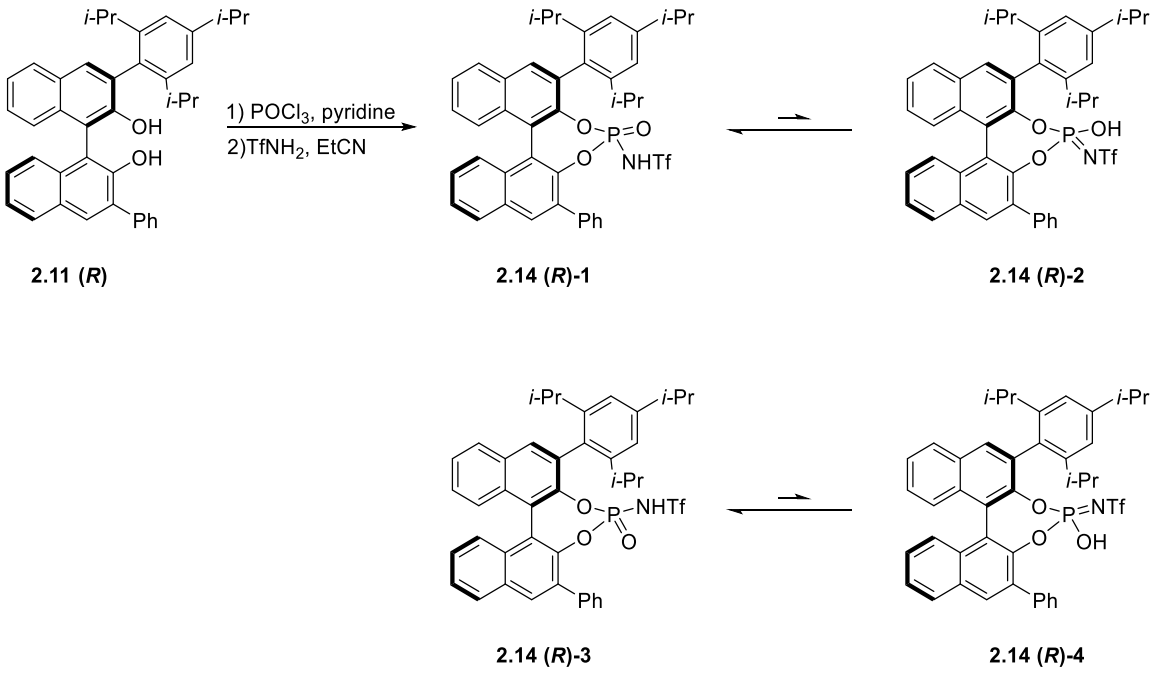

Scheme 2.4.3: Synthetic route to *N*-triflyl phosphoramide **2.14 (*R*)**, for which the major isomer would be **2.14 (*R*)-1**.

However, a new problem arises with CPA **2.14 (*R*)-1**, namely the chirality on phosphorous; the proton will yet again experience different environments, now based on whether it is closes to the 3 of the 3'- substituent **(2.14 (*R*)-1** and **2.14 (*R*)-3**. Likewise, attempting to solve this issue through an imido-linked[118] CPA, **2.15 (*R*)-1 / 2.15 (*R*)-2**, as shown in **Scheme 2.4.4**, will not solve the issue as

the proton continues to be closes to either the 3-substituent on one CPA or the 3'-substituent on the other CPA.

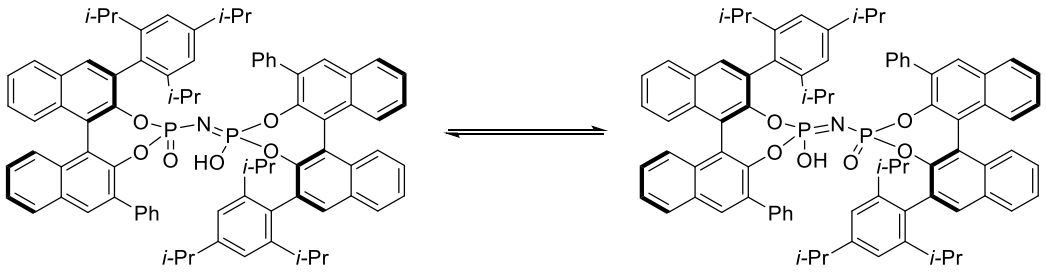

Scheme 2.4.4: Imido-linked CPA based on the target CPA **2.7 (*R*).**

Alternatively, two CPA's could be linked through the BINOL scaffold (**Figure 2.4.1**). However, **2.16 (*R*)** presents a different class of C_1-CPAs and computational investigations would be needed to evaluate the performance of this class of CPA catalysts and whether a preferred conformer is taken during catalysis favouring a certain conformation of the protons, whether the scaffold simply folds out when one of these protons involves in catalysis, in which case the equilibrating proton continue to result in the proton experience different environments.

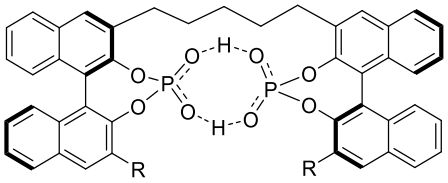

Figure 2.4.1: C_1-CPA linked through the BINOL scaffold.

2.5: C_1-Symmetric BINOL Ligands for In(III)-Catalysis

As the C_1-symmetric BINOL intermediates **2.8 (*R*)**, **2.4 (*R*)** and **2.5 (*R*)** from the synthesis of C_1-CPA **2.7 (*R*),** potentially could provide useful knowledge for the project described in Chapter 3, they were MOM-deprotected and purified (**Scheme 2.5.1**).

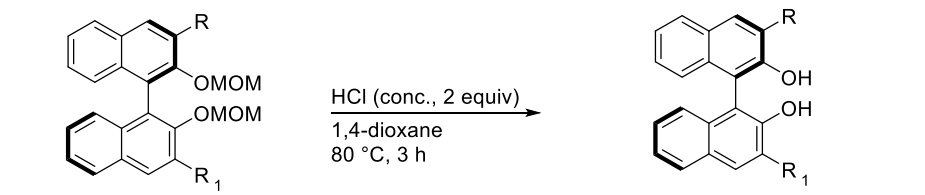

2.4 (*R*): R=(2,4,6-*i*-Pr)Ph R_1=H

2.5 (*R*): R= (2,4,6-*i*-Pr)Ph R_1=I

2.17 (*R*): R= (2,4,6-*i*-Pr)Ph R_1=H **>99%**

2.18 (*R*): R= (2,4,6-*i*-Pr)Ph R_1=I **94%**

Scheme 2.5.1: MOM-hydrolysis of the C_1-CPA intermediates yielding C_1-BINOL ligands for In(III)-Catalysis.

2.6. Conclusions

The target C_1-CPA **2.7 (*R*)** was successfully synthesised in 33% overall yield in eight steps from commercially available (*R*)-BINOL. This C_1-CPA, which had been predicted by Reid[i] to be a highly stereoselective CPA for all eight possible permutations of transfer hydrogenation of imines, did not outperform commercially available TRIP in the test reaction. This is hypothesised to be caused by the equilibrating phosphoric acid proton leading to this proton experiencing different environment.

The intermediates from the synthesis of this C_1-CPA were MOM-deprotected to yield 3,3'-substituted BINOL ligands which were used in the project described in Chapter 3.

Chapter 3: Methodology

As described in Chapter 1, the project presented in this thesis aspires to understand how enantioselectivity can be induced in In(III)-catalysed reactions through the application of chiral ligands. Though examples of enantioselective In(III)-catalysed reactions are present in the literature, little is hitherto known about the mode of enantioselectivity in these reactions. Hence, an extensive experimental methodology project has been carried out in order to develop and optimise an enantioselective In(III)-catalysed reaction, as described in this chapter.

3.1. Choosing a suitable In(III)-Catalysed Reaction

The examples of enantioselective In(III)-catalysed reactions presented in Chapter 1 share a common motif; they are all reactions on prochiral carbonyls or carbonyl-equivalents; ketones, aldehydes, hydrazones or alpha-ketone phosphonates. Of the In(III)-catalysed reactions reported within the last decade, several examples of hydrosilane reductions are found as presented in Chapter 1. Hydrosilane reductions of ketones have been widely known for decades.[119,120] This project aims to explore the induction of enantioselectivity in In(III)-catalysed hydrosilane reductions. Herein, is presented data which allow for the analysis and mechanistic understanding towards an enantioselective reduction mediated by In(III) salts.

3.1.1. Hydrosilane Reduction of a Ketone

Acetophenone was chosen as a commercially available starting material. BINOL was chosen as the initial chiral ligand, since the Goodman group has worked extensively with computational studies of this scaffold. In(III) bromide was chosen, as in the enantioselective allylations reported by Teo et al.[80] and Takita et al.[83] in 2005 both used In(III) bromide with BINOL for achieving enantioselectivity.

Prior to testing the reaction, NMR studies examining complex formation between indium and BINOL were performed. In(III) bromide and racemic BINOL were mixed together in dichloromethane. However, the ^{1}H NMR spectrum of the mixture was identical to the ^{1}H NMR of BINOL, thus not indicating complex formation. Complex formation was studied under alkaline conditions employing *N*,*N*-diisopropylethylamine (DIPEA) to increase the reactivity of the hydroxy groups towards complex formation. A slight change in the chemical shift was observed for the aromatic protons upon addition of In(III) bromide to the deprotonated BINOL solution, and this was interpreted as an indication of formation of an In(III)-BINOL complex.

The first hydrosilane reduction test reactions was performed (**Table 3.1.1**).

Table 3.1.1: Reaction performed to examine factors affecting the ketone reduction.

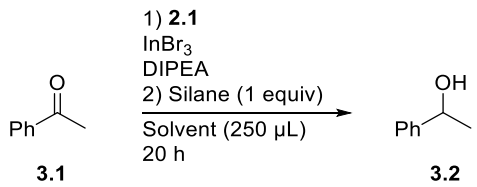

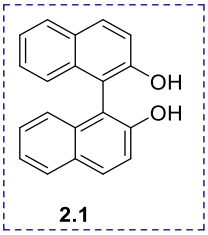

Entry	Solvent	Temperature	$InBr_3$:2.1:DIPEA [mol%]	Silane	Conversion[a] [%]
1	CH_2Cl_2	RT	10:10:50	$PhSiH_3$	0
2	CH_2Cl_2	40 °C	10:10:50	$PhSiH_3$	7
3	CH_2Cl_2	40 °C	50:50:50	$PhSiH_3$	20
4	EtOH	RT	10:10:50	$PhSiH_3$	14
5	EtOH	40 °C	10:10:50	$PhSiH_3$	17
6	CH_2Cl_2	40 °C	-	$PhSiH_3$	0
7	CH_2Cl_2	40 °C	10:10:50	Et_3SiH	0
8	EtOH	40 °C	10:10:50	Et_3SiH	0
9[b]	CH_2Cl_2	40 °C	10:10:50	$PhSiH_3$	6
10	CH_2Cl_2	40 °C	10:0:50	$PhSiH_3$	11
11	CH_2Cl_2	40 °C	10:10:10	$PhSiH_3$[c]	6
12	CH_2Cl_2	40 °C	10:10:12	$PhSiH_3$	2

Each entry represents a single experiment. All reactions were carried out with 143 µmol imine. [a] Conversion from ketone to alcohol determined from crude NMR. [b] Reaction time: 3 days. [c] 1.3 equiv.

There was no indication of product formation at room temperature in CH_2Cl_2 (**Table 3.1.1**, entry 1). Increasing the temperature to 40 °C facilitated the reaction in CH_2Cl_2, though the conversion was still low (entry 2). The reaction did not proceed without In(III)-catalyst (entry 6), whereas ligand **2.1** was not necessary for facilitating the reaction (entry 10). The reaction could proceed at room temperature in EtOH (entry 4). The use of EtOH as solvent, was based upon findings by Miura et al.,[76] who reported higher enantioselectivity for a hydrosilane reduction in polar protic solvents. To eliminate the low conversion resulting from the silane being an insufficient reducing agent a different silane, $EtSiH_3$, was tested. However, $EtSiH_3$ was not capable of reducing the ketone neither in CH_2Cl_2 nor in EtOH (entries 7, 8). The reaction time was prolonged but did not result in increased conversion (entry 9). Increasing the catalyst loading to 50 mol% did not lead to a proportional increase in conversion (entry 3), indicating a problem with catalyst turnover. The cause for this remains unknown. As the reaction proceeds well in EtOH it is not caused by In(III) being too oxophillic. The highest conversion achieved under these various conditions tested for reducing acetophenone did

not exceed 20% and therefore, it was decided to examine a different class of prochiral substrates as substrates for this In(III)-catalysed reaction.

3.2. Silane Reduction of Imines

The next class of prochiral substrates tested for the In(III)-catalysed hydrosilane reduction was chosen to be imines, which are easily accessible from the ketones in hand. A simple imine, *N*-methyl-(1-phenylethylidene)amine **3.3**, was prepared from methylamine and acetophenone in 91% yield (**Scheme 3.2.1**) in accordance with the literature.[121]

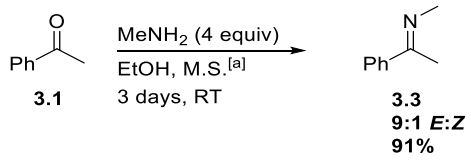

Scheme 3.2.1: Synthesis of *N*-methyl-(1-phenylethylidene)amine **3.3** from methylamine and acetophenone. [a] 3 Å.

The imine **3.3** was then reduced with phenylsilane and the In(III)-BINOL catalyst (**Table 3.2.1**). The product was evident by ^{1}H NMR; the conversion of the imine in the test reaction was 29% (entry 1).

Table 3.2.1: Hydrosilane reduction of **3.3** with varying conditions.

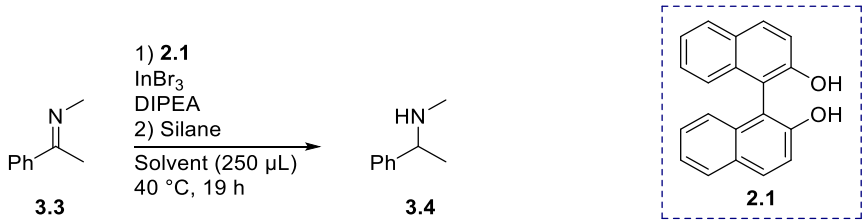

Entry	Solvent	$InBr_3$:2.1 [mol%]	DIPEA [mol%]	Silane	Conversion[a] [%]
1	CH_2Cl_2	10:10	50	$PhSiH_3$	29
2	CH_2Cl_2	10:10	50	Et_3SiH	0
3	CH_2Cl_2[b]	10:10	50	$PhSiH_3$	48
4	EtOH	10:10	50	$PhSiH_3$	14
5	CH_2Cl_2	10:10	20[c]	$PhSiH_3$	48
6	CH_2Cl_2	10:10	10[c]	$PhSiH_3$	48

Each entry represents a single experiment. All reactions were carried out with 143 µmol imine. [a] Based on the amount of amine present in the crude product. [b] M.S. added. [c] $InBr_3$, **2.1** and DIPEA premixed.

As had been observed when reducing acetophenone, Et_3SiH did not facilitate the reduction in CH_2Cl_2 (entry 2). Unlike the reduction of acetophenone, the conversion for the imine reduction was significantly lower in EtOH (entry 4) than in CH_2Cl_2. An increase in the conversion to 48% was

obtained both by adding molecular sieves (entry 3) and by premixing In(III), ligand and base using a decreased amount of base (entry 5 and 6).

To obtain a racemic reference compound for HPLC analysis of the e.e., imine **3.3** was reduced using sodium borohydride (**Scheme 3.2.3**).

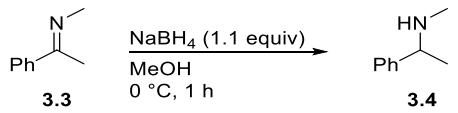

Scheme 3.2.3: Sodium borohydride reduction of **3.3**.

TLC analysis indicated the presence of multiple products and purification of the amine **3.4** product proved troublesome both by acidic work-up and column chromatography. To enable easy purification, it was decided to synthesise a stabilised imine.

N-Benzyl-1-phenylethan-1-imine **3.5**, was synthesised from benzylamine and acetophenone (**Scheme 3.2.4**) in accordance with the literature.[122,123] After recrystallisation the imine was obtained as light yellow crystals in 78% yield.

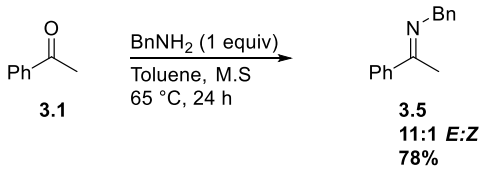

Scheme 3.2.4: Synthesis of *N*-benzyl-(1-phenylethylidene)amine **3.5** from acetophenone and benzylamine.

A racemic sodium borohydride reduction was carried out to afford a racemic reference (**Scheme 3.2.5**) for HPLC analysis of the e.e.

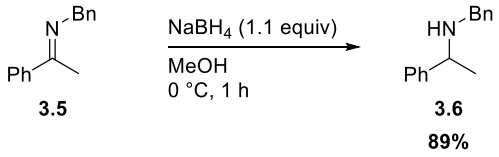

Scheme 3.2.5: Sodium borohydride reduction of **3.5** to yield racemic **3.6**.

The imine **3.5** was then reduced (**Scheme 3.2.6**) by the developed procedure using BINOL, In(III) bromide, phenylsilane and DIPEA in dichloromethane at 40 °C to afford 69% of the amine **3.6** isolated by column chromatography.

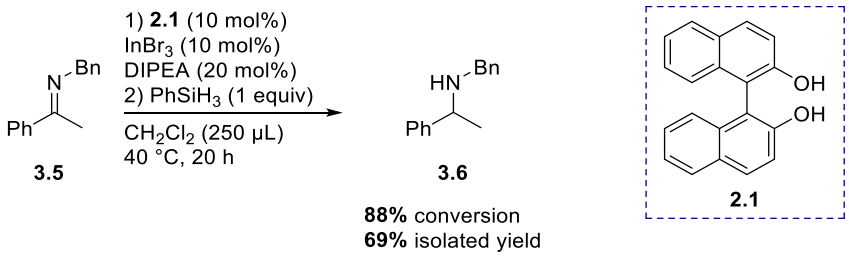

Scheme 3.2.6: Phenylsilane reduction of **3.5** with In(III) bromide and BINOL.

3.3. Optimisation Towards the Development of an Enantioselective Reaction

With the success of the In(III)-catalysed hydrosilane reduction further optimisation was performed. First it was found 0.5 equiv of phenylsilane was sufficient to afford 65% isolated amine. However, the reaction proceeded faster and to higher conversion with stochiometric amount of silane.

The reaction was tested with enantiomerically pure (*R*)-BINOL, **2.1 (*R*)**, obtaining the same yield as the initial test reaction. The enantiomeric excess of the amine was examined by NP-HPLC. However, the exchangeable amine proton resulted in very broad tailing peaks, inhibiting easy identification in the HPLC chromatogram. Therefore, the amines, were benzoylated to afford **3.7** (**Scheme 3.3.1**).

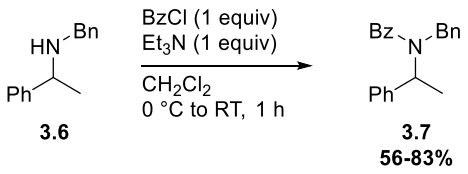

Scheme 3.3.1: Benzoylation of **3.6** yielding *N*-benzoyl-*N*-benzyl-(1-phenylethylidene)amide **3.7**.

Unfortunately, the amide from the In(III)-catalysed reduction was racemic. To examine which factors influenced the reduction several reactions were performed (**Table SI-3.3.1**). The conversion of imine to amine, determined by quantitative NMR, was found to be higher for reactions with base than without. The conversion did not depend on which base was used (DIPEA or *N,N*-dicyclohexylmethylamine), but too much base (more than 50 mol%) inhibited the reaction. The conversion was lower if BINOL was pre-dried and the reaction worked well with 10% of water present. Higher catalyst loading, higher temperature and longer reaction time all increased conversion. The reaction did not proceed without In(III) bromide, but proceeded regardless of the presence of BINOL. As there was no stereoselectivity this could also be caused by the In(III)-catalysed background reaction simply being faster than the reaction catalysed by a formed In(III)-BINOL complex. Therefore, the procedure was modified. In the asymmetric allylation employing an In(III)-BINOL species[88] (section 1.2.4) the In(III) salt had been co-evaporated with THF before mixed

with BINOL in THF. This is known to lead to co-ordination of two THF molecules to the In(III) metal-centre (**Scheme 3.3.2**).[124] Potentially, this species is more reactive towards the formation of a metallic complex.

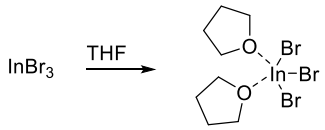

Scheme 3.3.2: In (III) bromide co-ordinates to two THF molecules when mixed.

Test reactions were performed (**Table 3.3.2**) and the reaction was faster when co-evaporating In(III) bromide with THF before adding BINOL, as the reaction proceeded in 67% conversion overnight at room temperature (entry 1).

Table 3.3.2: The screening reactions with THF co-evaporated In(III) bromide and (*R*)-BINOL.

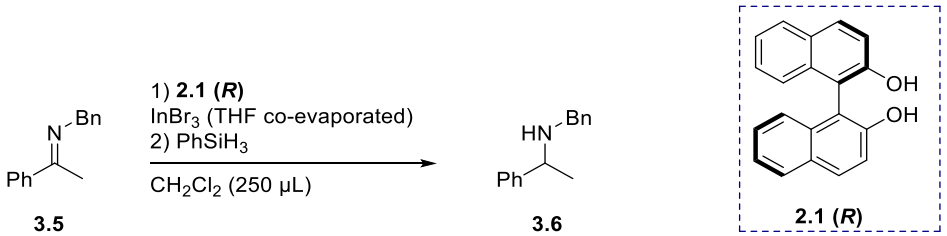

Entry	Temperature [°C]	$InBr_3$ [mol%]	2.1 (*R*) [mol%]	$PhSiH_3$ [equiv]	Conversion[a] [%] (time)
1	RT	-	-	1	0 (19 h), 0 (5 days)
2	30	-	-	1	0 (19 h), 0 (5 days)
3	30	-	10	1	0 (19 h), 0 (5 days)
4	RT	10	10	1	67 (19 h)
5	RT	10	-	1	63 (24 h), 78 (48 h), 95 (6 days)
6	30	10	10	1	79 (18 h)
7	30	10	-	1	49 (18 h)
8	RT	10	10	0.5	39 (17 h), 96 (5 days)
9	RT	10	10	1.5	39 (17 h)
10	RT	5	-	1	38 (16 h)
11	RT	5	5	1	29 (16 h), 90 (5 days)
12	RT	10	20	1	68 (16 h)

Each entry represents a single experiment. All reactions were carried out with 143 µmol imine. [a] Conversion of imine to amine determined by crude NMR with 1,3,5-trimethoxybenzene as internal standard.

As observed when reducing acetophenone (**Table 3.1.1**), the imine reduction does not proceed in the absence of the In(III)-catalyst (entries 1-3) and the ligand alone is not capable of facilitating the reaction (entry 3). However, the reaction proceeds independently of the presence of the ligand (entries 5, 7). A racemic background reaction could be outcompeted by a significant ligand-acceleration effect (LAE). A discussion of the kinetics will follow in Chapter 6. As the effect of adding ligand varies significantly with changes in the properties of the ligand, the option remains of finding a suitable 3,3'-substituted BINOL ligand, with the potential of outcompeting the background reaction through a LAE. Alternatively, the background reaction may be suppressed if complete binding of the In(III) ions.

The reaction continued towards full conversion after prolonged reaction time (entries 5, 8 and 11). The reaction proceeded significantly faster at 30 °C than at RT (entry 6). Interestingly, it was observed that the reaction appeared to proceed slower in the absence of **2.1 (*R*)** with 10 mol% In(III) (entry 5, 7), whereas increasing the amount of ligand did not appear to affect the rate (entry 12). However, the reaction proceeded to lower conversion in the presence of **2.1 (*R*)** within 16 hours when the catalyst loading was decreased (entry 11). The reaction proceeded slower with lower catalyst loading (entries 10, 11).

However, when the reaction time was prolonged the conversion reached 90% or more. It was discovered that the reaction proceeded to 96% conversion with only 0.5 equiv of $PhSiH_3$ when the reaction time was prolonged (entry 8). An increase in the reaction rate with increased silane stoichiometry was interestingly not observed (entry 9). The e.e. of each reaction presented in **Table 3.3.2** was examined by RP-HPLC and unfortunately found to be zero.[iv]

During each of the In(III)-catalysed reductions performed to this point, formation of a grey substance was observed. This grey substance originally formed as a grey powder resulting in the entire reaction mixture turning grey, and overnight the powder "assembled" into a grey metallic chunk. In the reactions with low conversion the solution remained grey. The formation of this metallic solid could indicate decomposition of initially formed indium hydride (InH_2) to give solid indium and hydrogen gas.[125] This correlates with the lack of enantioselectivity as this indium hydride is not coordinated to the BINOL ligand. Formation of this grey substance was limited to reactions affording racemic amines.

The lack of enantioselectivity in the reactions could have several explanations, of which one is that a In(III)-BINOL complex is not present. Chapter 4 will present the work performed on the attempt to

[iv] Analysis of the e.e. was from this point and onwards performed by chiral RP-HPLC, which became available in the laboratory and allowed for faster analysis.

form and characterise complexes of In(III) and BINOL. This work includes irreversible deprotonation of BINOL with NaH, resulting in the formation of a complex with 3 BINOLs co-ordinated to the In(III) metal-centre and THF molecules and sodium ions between the BINOL oxygens. To examine how such a complex performed in the hydrosilane reduction reactions were carried out (**Table 3.3.3**).

Table 3.3.3: Outcome of the test reactions performed in toluene.

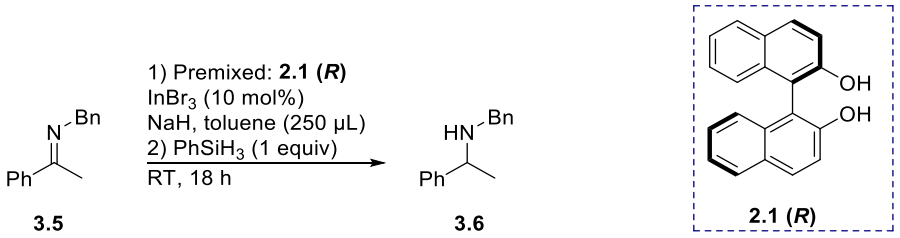

Entry	2.1 (*R*) [mol%]	NaH [mol%]	Conversion[a] [%]
1	30	95	0
2	30	140	0
3[b]	32	95	0
4	-	-	17
5	-	140	42

Each entry represents a single experiment. All reactions were carried out with 143 µmol imine. [a] Conversion of imine to amine determined by crude NMR with 1,3,5-trimethoxybenzene as internal standard. [b] Conditions used to form complex in Chapter 4.

It was attempted to form of a complex of In(III) and 3 BINOLs *in situ* in toluene avoiding further complications for co-ordination THF molecules (entries 1, 2). In contrast to when the complex was prepared in THF, formation of white precipitate from In(III) bromide was not observed in toluene. No amine product was found after 18 hours, which was also the case when the preformed crystallised complex was used (entry 3). Thus, this crystallised complex and whatever complex formed in toluene was unable to facilitate the reduction. Toluene had been chosen instead of CH_2Cl_2, in which insufficient deprotonation of BINOL had been observed. Control experiments (entries 4, 5) proved the reduction to proceed under the given reaction conditions when BINOL was absent. This non-ligated In(III)-catalysed reaction proceeded to higher conversion in the presence of NaH. The reactions in **Table 3.3.2** did not examine the effect of increasing the amount of NaH further, as the complex in Chapter 4 was formed with only 3 equiv NaH to 1 equiv BINOL. A detailed discussion of this complex is given in section 4.2.

3.3.1 Initial solvent screen and synthesis and screening of two 3,3'-substituted BINOLs

Reports were found in the literature regarding similar octahedral complexes of BINOL with either Fe(III) or Cr(III).[126] These were reported to be unstable in chlorinated solvents. This finding prompted a screen of 10 solvents (MeOH, EtOH, MeCN, THF, Et_2O, dichloroethane, DMSO, DMF, *n*-hexane and toluene, **Table SI-3.3.1.1**) with the hydrosilane using BINOL as ligand for the $InBr_3$ catalysed hydrosilane reduction of *N*-benzyl-(1-phenylethylidene)amine. The screen was performed both with and without base (DIPEA), but in all cases the resulting amine was found to be racemic. The reaction proceeded to full conversion in EtOH and MeOH, whereas 50-70% conversion was achieved in the remaining solvents. Addition of DIPEA further decreased the conversion except in MeOH and EtOH.

It was decided to synthesise 3,3'-modified BINOLs as it was expected steric bulk in the 3 and 3'-position could be important for achieving high e.e. With the synthesis of the TRIP-diol in mind, (*R*)-MOM-BINOL **2.2 (R)** was iodinated at the 3,3'-position through ortho-lithiation with and lithium-halogen exchange (**Scheme 3.3.1.1**) following a reported procedure,[114] to provide iodo-handles for a subsequent Kumada coupling.

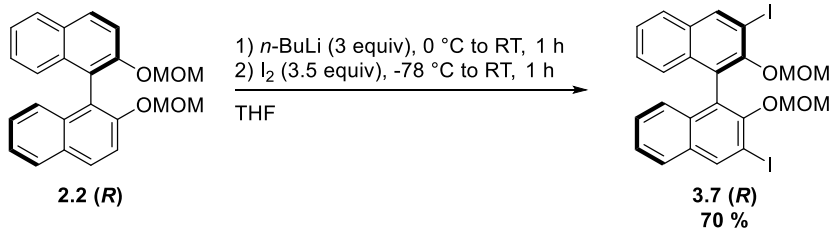

2.2 (*R*) **3.7 (*R*) 70 %**

Scheme 3.3.1.1: Synthesis of (*R*)-3,3'-I_2-MOM-BINOL **3.7 (*R*)**.

An aliquot of **3.7 (*R*)** was MOM-deprotected to yield the (*R*)-3,3'-I_2-BINOL **3.8 (*R*)** (**Scheme 3.3.1.2**), which was included in the ligand screen.

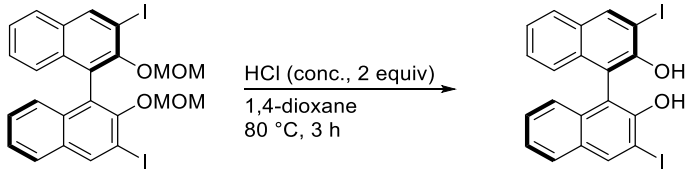

3.7 (*R*) **3.8 (*R*) 98%**

Scheme 3.3.1.2: MOM deprotection to yield (*R*)-3,3'-I_2 -BINOL **3.8 (*R*)**.

From **3.7 (*R*)** the bulky diol **3.10 (*R*)** was synthesised through a nickel(II)-catalysed Kumada coupling (**Scheme 3.3.1.3**) with *in situ* prepared (2,4,6-triisopropylphenyl)magnesium bromide. Full

conversion was observed for the Kumada coupling and the crude product was deprotected without further purification to yield **3.10 (*R*)** in 89% yield over two steps.

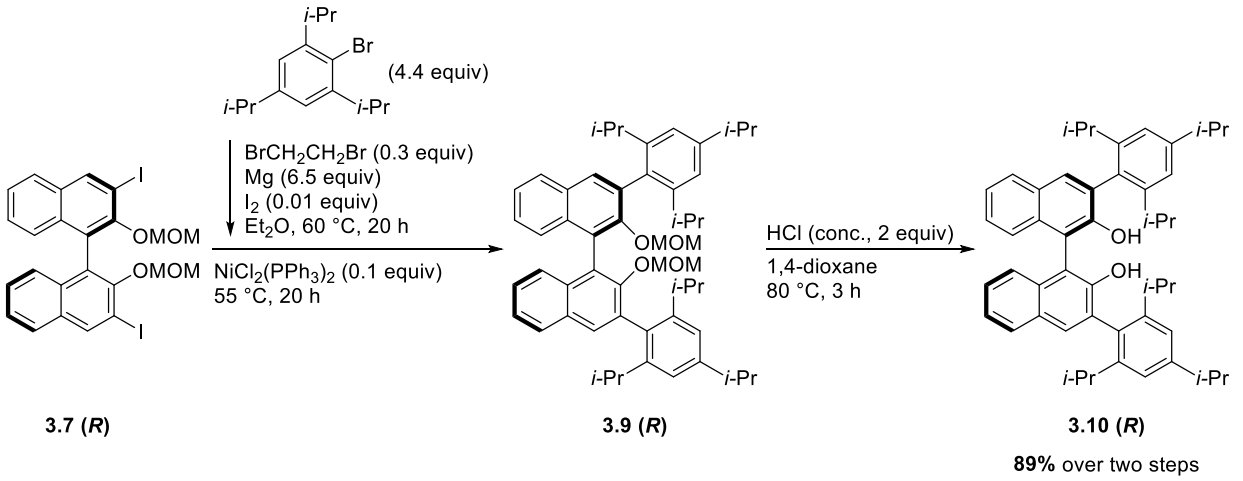

Scheme 3.3.1.3: Kumada coupling and subsequent MOM deprotection to yield **3.10 (*R*)**.

While synthesising TRIP diol **3.10 (*R*)**, screening of (*R*)-3,3'-I_2-BINOL **3.8 (*R*)** was performed (**Table 3.3.1.2**) in 11 different solvents with and without 20 mol% base, corresponding to 2 equiv per ligand and thus 1 equiv per alcohol proton.

Table 3.3.1.2: Solvent screen with and without base using (*R*)-3,3'-I_2-BINOL as ligand for In(III).

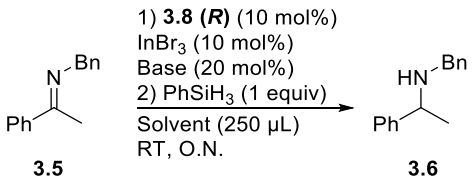

3.5 3.6

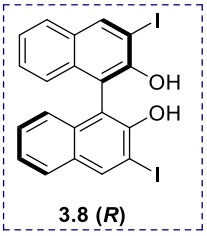

3.8 (*R*)

Entry	Solvent	Base	Conversion[a] [%]	e.e.[b] [%]
1	MeOH	-	>99	9
2	MeOH	DIPEA	78	5
3	EtOH	-	>99	6
4	EtOH	DIPEA	>99	6
5	MeCN	-	92	0
6	MeCN	DIPEA	26	0
7	THF	-	75	0
8	THF	DIPEA	17	0
9	Et_2O	-	83	0
10	Et_2O	DIPEA	20	0
11	CH_2Cl_2	-	75	0
12	CH_2Cl_2	DIPEA	17	0
13	$C_2H_4Cl_2$	-	75	0
14	$C_2H_4Cl_2$	DIPEA	6	0
15	DMSO	-	87	4
16	DMSO	DIPEA	61	5
17	DMF	-	85	0
18	DMF	DIPEA	50	0
19	*n*-hexane	-	17	0
20	*n*-hexane	DIPEA	15	0
21	toluene	-	75	0
22	toluene	DIPEA	9	0

Each entry represents a single experiment. All reactions were carried out with 143 µmol imine. [a] Conversion of imine to amine determined by crude NMR with 1,3,5-trimethoxybenzene as internal standard. [b] e.e. of amine determined by chiral stationary phase RP-HPLC.

The first non-racemic results were obtained: both in MeOH and EtOH indications of enantioselectivity was observed (Entry 1-4). The positive result in DMSO (Entry 15-16) was later found to be caused

by an impurity co-eluting with the (*R*)-enantiomer of **3.6** for the specific RP-HPLC method used to analyse the e.e. The reaction was found to be racemic in non-polar and polar aprotic solvents independent of the presence of base. The reaction in the absence of the ligand was not included in the solvent screen. Further investigations of the unligated reaction was carried out later in MeOH, revealing a faster racemic reaction compared to the ligand decelerated reaction in the presence of **3.8 (*R*)**. Further details hereon can be found in Chapter 6, were the kinetics of this reaction was investigated.

With this first positive indication of enantioselectivity in hand further screening in MeOH and EtOH was performed (**Table 3.3.1.3**) varying the stoichiometry of ligand and base. Both $InBr_3$ and $InCl_3$ were testes as In(III)-catalysts. Additionally, two other polar protic solvents, *i*-PrOH and *n*-butanol, were included as solvents to examine how elongating the carbon chain of the alcohol solvent affected the result. No conversion was obtained in *n*-butanol (not included in **Table 3.3.1.3**).

Table 3.3.1.3: Further screening of $InBr_3$ and $InCl_3$ in MeOH, EtOH and *i*-PrOH using (*R*)-3,3'-I_2-BINOL.

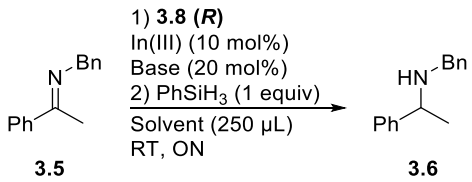

3.5 3.6

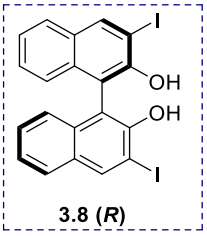

3.8 (*R*)

Entry	Solvent	In(III) source	3.8 (*R*) [mol%]	Base	[mol%]	Conversion[a] [%]	e.e.[b] [%]
1	MeOH	$InBr_3$	20	-	-	>99	20
2	MeOH	$InBr_3$	20	DIPEA	40	72	35
3	MeOH	$InBr_3$	30	-	-	91	18
4	MeOH	$InBr_3$	30	DIPEA	60	50	35
5	MeOH	$InCl_3$	10	-	-	90	18
6	MeOH	$InCl_3$	20	-	-	95	24
7	MeOH	$InCl_3$	20	DIPEA	40	50	32
8	MeOH	$InCl_3$	10	NaH	100	>99	20
9	EtOH	$InBr_3$	20	-	-	>99	12
10	EtOH	$InBr_3$	20	DIPEA	40	>99	25
11	EtOH	$InBr_3$	30	-	-	>99	12
12	EtOH	$InBr_3$	30	DIPEA	60	78	32
13	EtOH	$InCl_3$	10	-	-	90	16
14	EtOH	$InCl_3$	20	-	-	?[c]	18
15	EtOH	$InCl_3$	20	DIPEA	40	?[c]	32
16[d]	EtOH	$InCl_3$	20	-	-	>99	18
17	*i*-PrOH	$InCl_3$	10	-	-	?[c]	7

Each entry represents a single experiment. All reactions were carried out with 143 µmol imine. [a] Conversion of imine to amine determined by crude NMR with 1,3,5-trimethoxybenzene as internal standard. [b] e.e. of amine determined by chiral stationary phase RP-HPLC. [c] Unable to shim NMR and thus unable to measure the conversion. [d] Non-dry EtOH.

In both EtOH and MeOH e.e. above 30% was achieved in several reactions, the highest being 35% e.e. in MeOH using $InBr_3$ in the presence of DIPEA (entry 2,4). In MeOH the conversion was decreased in the presence of DIPEA (entries 2,4,6), whereas this effect was not observed in EtOH (entries 10,12) or when NaH was used as the base in MeOH (entry 8). Comparing the results in **Table 3.3.1.3** (entries 1-2 and 9-10) with **Table 3.3.1.2** (entries 1-2 and 3-4) an important observation is made: the e.e. is

increased with 50% or more, when changing from a 1:1 relationship between In(III) and ligand to a 1:2 ratio. This suggest either two molecules of ligand are bound to each In(III) ion or the excess ligand ensures no non-ligated In(III), preventing the racemic background reaction to proceed (**Table 3.3.2**, entries 2,4,7 – the reaction proceeds independent of the presence of the ligand).

Upon completing the synthesis of the TRIP-diol **3.10 (*R*)**, screening was performed with this ligand for the In(III)-catalysed hydrosilane reduction of imine **3.5** (**Table 3.3.1.4**). Screening was performed primarily in the two polar protic solvents MeOH and EtOH, which had resulted in up to 35% e.e. for the bisiodide diol **3.8 (*R*).** A few representative non-polar and aprotic polar solvents were included, to examine the solvent effect was different with this much more hydrophobic ligand.

Table 3.3.1.4: Solvent screen with and without base using (*R*)-3,3'-bis(2,4,6-triisopropylphenyl)-BINOL **3.10 (*R*)** as ligand for In(III).

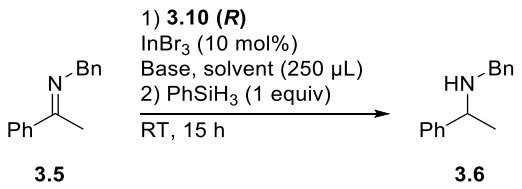

3.5 **3.6**

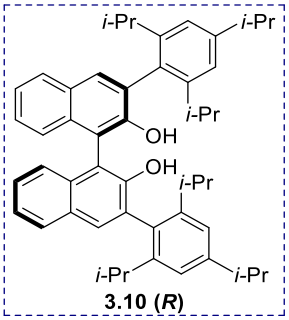

3.10 (*R*)

Entry	Solvent	3.10 (*R*) [mol%]	Base	[mol%]	Conversion[a] [%]	e.e.[b] [%]
1	MeOH	10	-	-	>99	6
2	MeOH	10	DIPEA	20	>99	6
3	MeOH	20	-	-	>99	4
4	MeOH	20	DIPEA	40	>99	6
5[c]	MeOH	10	NaH	100	14	0
6	EtOH	10	-	-	>99	7
7	EtOH	10	DIPEA	20	>99	5
8	EtOH	20	-	-	>99	6
9	EtOH	20	DIPEA	40	>99	6
10	CH_2Cl_2	10	-	-	50	0
11	CH_2Cl_2	10	DIPEA	20	23	0
12	toluene	10	-	-	50	0
13	toluene	10	DIPEA	20	13	0
14	MeCN	10	-	-	85	4
15	MeCN	10	DIPEA	20	50	4
16	Et_2O	10	-	-	85	4
17	Et_2O	10	DIPEA	20	43	0

Each entry represents a single experiment. All reactions were carried out with 143 µmol imine. [a] Conversion of imine to amine determined by crude NMR with 1,3,5-trimethoxybenzene as internal standard. [b] e.e. of amine determined by chiral stationary phase RP-HPLC. [c] with $InCl_3$ as In(III) source only 8% conversion to a racemic product was observed.

The results in **Table 3.3.1.4** shows that the TRIP-diol **3.10 (*R*)** induced low to no selectivity. The highest obtained e.e. was 7% (entry 6) in EtOH. The e.e. was generally unaffected by the presence of base, whereas the conversion was decreased. The reaction proceeded to afford racemic amines in non-polar solvents (entries 10-13), whereas weak indications of enantioselectivity was observed in

the aprotic polar solvents MeCN and Et_2O (entries 14-17). Results of further optimisation with **3.10 (*R*)** are included in a number of tables in the following sections.

3.3.2 Expanding the screening of BINOL ligands, metal sources, bases and reducing agents

Based hereon it was hypothesised if this ligand was too bulky to fit around the indium metal centre. It was decided to synthesise (*R*)-3,3'-Ph_2-BINOL as a less bulky non-polar 3,3'-substituted BINOL.

(*R*)-3,3'-Ph_2-BINOL **3.12 (*R*)** was synthesised from bisiodide **3.7 (*R*)**. The phenyl groups were installed by a Suzuki coupling followed by deprotection of the MOM groups afforded the diol in high yield over two steps (**Scheme 3.3.2.1**).

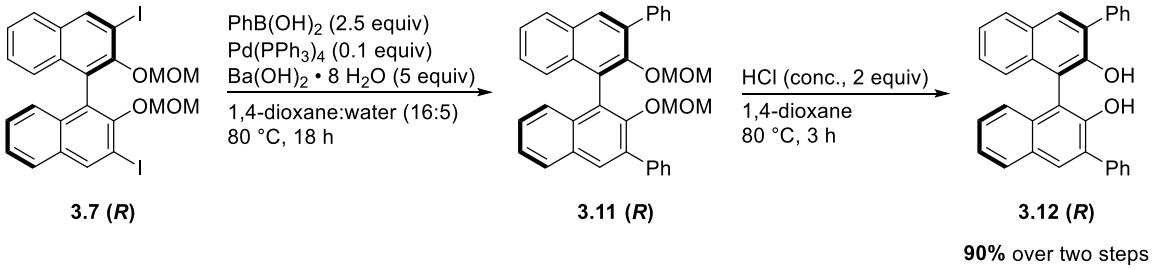

Scheme 3.3.2.1: Synthesis of (*R*)-3,3'-bisphenyl-BINOL **3.12 (*R*)**.

It was decided to examine both $In(OTf)_3$ and $GaBr_3$ as catalysts for the reduction. Gallium has been reported to be afford superior e.e. compared to In(III) in when ketones are reduced with the aid of catecholboranes.[127] However, as most gallium compounds dictate strict use of inert atmosphere (glovebox), In(III)-catalysts poses the opportunity for a more straightforward procedure.

(*R*)-3,3'-Ph_2-BINOL was then screened as ligand for the hydrosilane reduction of **3.5** (**Table 3.3.2.1**). All reactions were performed in MeOH as this had shown the most promising enantioselectivity on 35% and furthermore results based on conversion and enantioselectivity.

Table 3.3.2.1: Screening of **3.12** along with screening new In(III) catalyst and gallium(III).

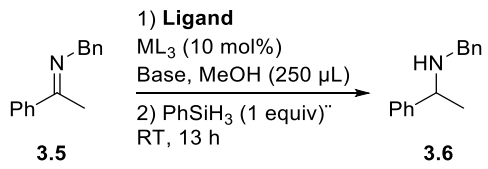

3.5 **3.6**

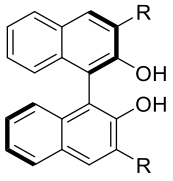

3.8 (*R*), R=I
3.10 (R), R=(2,4,6-*i*-Pr)-Ph
3.12 (R), R=Ph

Entry	Catalyst	Ligand	[mol%]	Base	[mol%]	Conversion[a] [%]	e.e.[b] [%]
1	$InBr_3$	**3.12 (*R*)**	10	-	-	>99	7
2	$InBr_3$	**3.12 (*R*)**	10	DIPEA	20	>99	7
3	$InBr_3$	**3.12 (*R*)**	20	-	-	>99	7
4	$InBr_3$	**3.12 (*R*)**	20	DIPEA	40	>99	7
5	$In(OTf)_3$	**3.12 (*R*)**	20	-	-	98	19
6	$In(OTf)_3$	**3.12 (*R*)**	20	DIPEA	40	45	22
7	$GaBr_3$	**3.12 (*R*)**	20	-	-	>99	9
8	$GaBr_3$	**3.12 (*R*)**	20	DIPEA	40	78	12
9	$InCl_3$	**3.12 (*R*)**	20	-	-	>99	12
10	$InCl_3$	**3.8 (*R*)**	20	-	-	95	29
11	$InCl_3$ [c]	**3.8 (*R*)**	20	-	-	90	19
12	$In(OTf)_3$	**3.8 (*R*)**	10	-	-	>99	29
13	$In(OTf)_3$	**3.8 (*R*)**	20	-	-	>99	29
14	$GaBr_3$	**3.8 (*R*)**	20	-	-	>99	29
15	$InBr_3$	**3.8 (*R*)**	20	DIPEA	40	42	33
16	$InBr_3$[c]	**3.8 (*R*)**	20	DIPEA	40	50	34
17	$In(OTf)_3$	**3.8 (*R*)**	10	DIPEA	20	72	33
18	$In(OTf)_3$	**3.8 (*R*)**	20	DIPEA	40	36	27
19	$InBr_3$	**3.8 (*R*)**	20	Et_3N	40	93	41
20	$GaBr_3$	**3.8 (*R*)**	20	DIPEA	40	88	28
21	$In(OTf)_3$	**3.10 (*R*)**	20	DIPEA	40	>99	6
22	$In(OTf)_3$	**3.10 (*R*)**	20	-	-	>99	7

Each entry represents a single experiment. All reactions were carried out with 143 μmol imine. [a] Conversion of imine to amine determined by crude NMR with 1,3,5-trimethoxybenzene as internal standard. [b] e.e. of amine determined by chiral stationary phase RP-HPLC. [c] 4 μL water added.

The highest e.e. obtained using **3.12 (*R*)** as ligand was 22% (entry 6). The conversion was affected when DIPEA was used as base in $In(OTf)_3$ catalysed reactions (entries 6, 17, 18) for ligands **3.8 (*R*)** and **3.12 (*R*),** but not for ligand **3.10 (*R*)** or when **3.12 (*R*)** was combined with $InBr_3$. The e.e. was increase to entire 41% when Et_3N was used as base in combination with $InBr_3$ and **3.8 (*R*)** (entry 19). $GaBr_3$ was examined as catalyst for the reaction (entries 7, 8, 14, 20) and found to afford e.e. similar to InX_3 (entries 10, 15) but lower than $In(OTf)_3$ (entries 5, 6) under the same conditions. The $In(OTf)_3$ catalysed reaction also proceeded to full conversion in the absence of ligand. The unligated reaction catalysed by $GaBr_3$ was not investigated.

From the screening reactions performed to this stage it seemed that the electronic effects rather than the steric effects of the 3,3'-positions posed the greater influence on the e.e. Based hereon, various ligands were synthesised. As the (*R*)-3,3'-I_2-BINOL ligand had proven superior up to this point, three other halogenated ligands were synthesised for comparison. The bromine was installed in the 3,3'-positions in accordance with the literature procedure[114,128] through ortho-lithiation and lithium halogen exchange on **2.2 (*R*)** (**Scheme 3.3.2.3**).

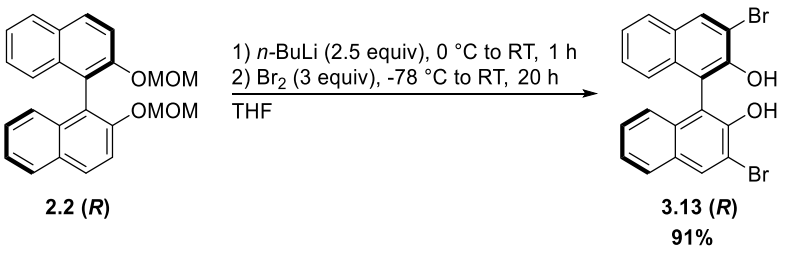

Scheme 3.3.2.2: Synthesis of (*R*)-3,3'-Br_2-BINOL **3.13 (*R*)**.

It was discovered that the product of the bromination was the diol **3.13 (*R*)**. TLC analysis after 4 hours had shown two compounds; the minor product was the sole product after 20 hours, suggesting the major product after 4 hours was the MOM protected ligand, whereas the deprotection proceeded when left stirring for further 16 hours. This indicate that the batch of bromine used contained HBr, which would catalyse MOM deprotection. However, as the diol was the target molecule, this was rather convenient.

(*R*)-3,3'-Cl_2-BINOL **3.15 (*R*)** was synthesised in accordance with the literature[129] using C_2Cl_6 as chlorination agent. MOM deprotection of crude **3.14 (*R*)** afforded the diol **3.15 (*R*)** in high yield over two steps (**Scheme 3.3.2.3**).

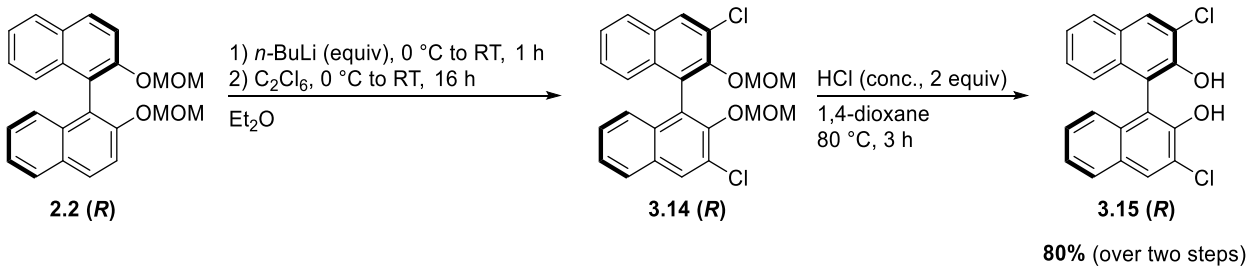

Scheme 3.3.2.3: Synthesis of (*R*)-3,3'-Cl_2-BINOL **3.15 (*R*).**

For synthesising (R)-3,3'-F_2-BINOL, *N*-fluorobenzenesulfonimide (NFSI) was used as fluorination agent, as reported by Zhang et al.[130] followed by crude deprotection of the MOM groups to afford the target ligand **3.17 (*R*)** in 75% yield over two steps (**Scheme 3.3.2.4**).

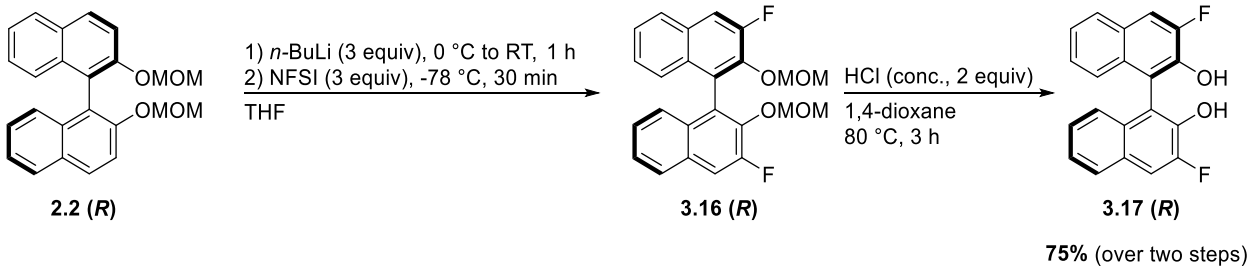

Scheme 3.3.2.4: Synthesis of (*R*)-3,3'-F_2-BINOL **3.17 (*R*).**

To examine the effect of an electron donating group in the 3,3'-position a sulfur substituent was installed. In this case the 3,3'-substituent was chosen to be thiobenzyl. Deprotonation with *n*-BuLi followed by addition of the disulphide yielded the thioether **3.18 (*R*)** in 74% yield in accordance with the literature.[131] MOM deprotection gave the target diol **3.19 (*R*)** in 88% yield (**Scheme 3.3.2.5**).

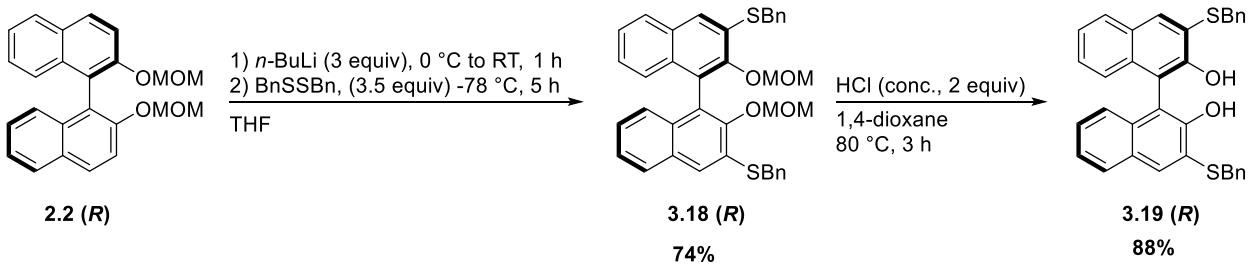

Scheme 3.3.2.5: Synthesis of (*R*)-3,3'-$(SBn)_2$-BINOL **3.19 (*R*)**.

With the thiobenzyl substituted ligand in hand, oxidation of the sulphur with meta-chloroperoxybenzoic acid (*m*-CPBA) yielded the sulfoxide **3.20 (*R*)** (**Scheme 3.3.2.6**) following a general procedure.[132]

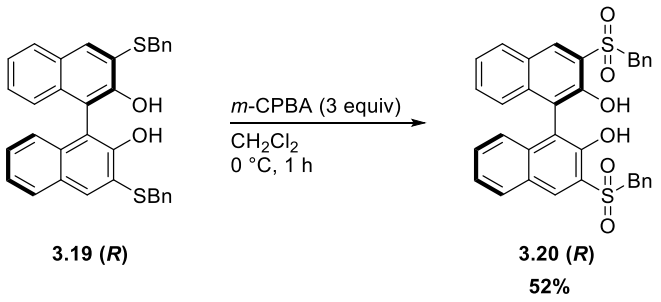

3.19 (*R*) **3.20 (*R*)**

52%

Scheme 3.3.2.6: Oxidation of the thiobenzylether to yield sulfoxide **3.20 (*R*) .**

(*R*)-3,3'-SO_2CF_3-BINOL **3.22 (*R*)** had been reported as a highly enantioselective ligand for the In(0)-catalysed allylation of hydrazones.[133] Attempts were made to make this following a reported procedure,[134] (*R*)-BINOL was first reacted with triflic anhydride to yield **3.21 (*R*)** in 80% yield (**Scheme 3.3.2.7**).

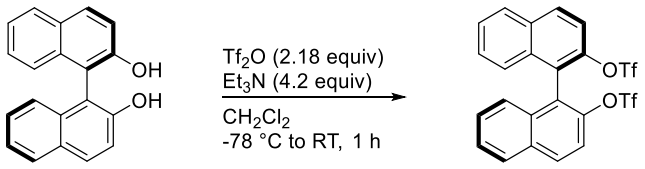

2.1 (*R*) **3.21 (R)**

80%

Scheme 3.3.2.7: Synthesis of (*R*)-BINOL-triflate **3.21 (*R*)**.

Exposing **3.21 (*R*)** to lithium diisopropylamide should result in a thia-Fries rearrangement[134,135] (**Scheme 3.3.2.8**) to give **3.22 (*R*)**.

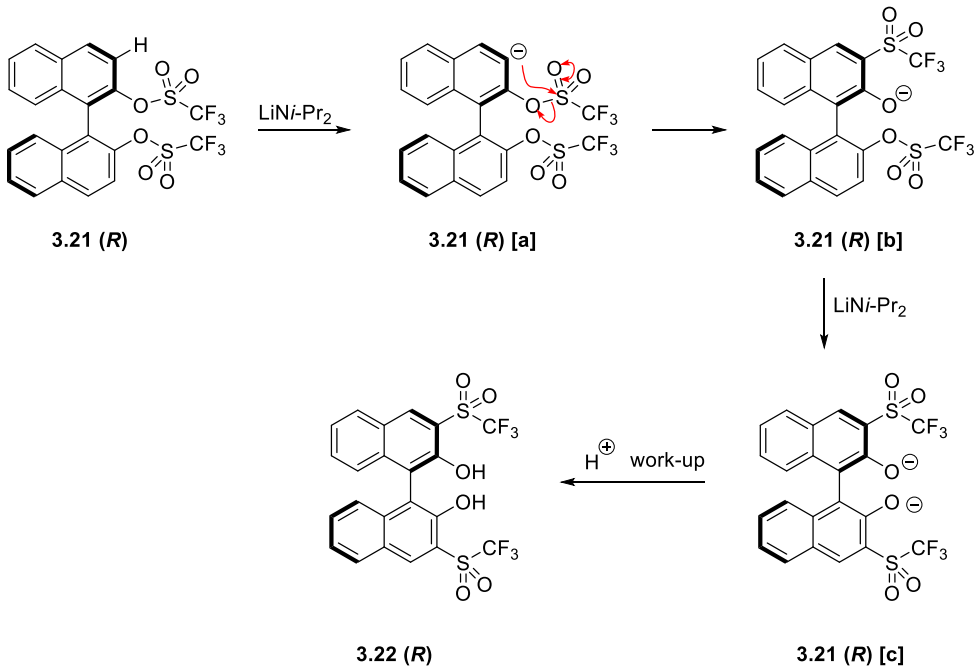

Scheme 3.3.2.8: Mechanism of the anionic thia-Fries rearrangement. Adapted from Dyke et al.[135]

The reaction was attempted twice without success following a reported procedure[134] using *in situ* prepared lithium diisopropylamide (**Scheme 3.3.2.9)**.

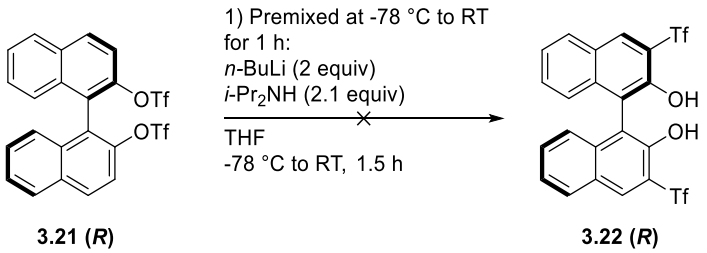

Scheme 3.3.2.9: Synthetic route attempted to **3.22 (*R*).**

At the point it was decided to focus on screening the ligands in hand.

The substituted BINOL ligands successfully synthesised were screened in the hydrosilane reduction (**Table 3.3.2.2**). The ligand was premixed with the In(III)-catalyst to examine if the complex formation could be optimised by allowing prolonged time for assembly of the complex. The amount of base was varied to examine the effect on e.e. and conversion with decreased amount of base.

Table 3.3.2.2: Screening new ligands, solvents and additives along with investigating premixing In(III) and ligand at RT.

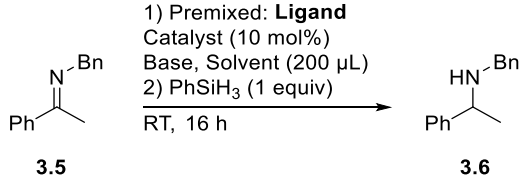

3.5 **3.6**

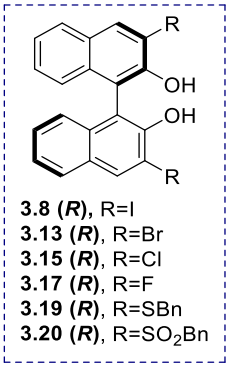

Entry	Solvent	Catalyst	Ligand	[mol %]	Base	[mol %]	Premix [h]	Conversion[a] [%]	e.e.[b] [%]
1	MeOH	$InCl_3$	**3.8 (*R*)**	10	Et_2NH	20	16	5	32[c]
2	MeOH	$InCl_3$	**3.8 (*R*)**	10	Et_3N	10	16	91	27
3	MeOH	$InCl_3$	**3.8 (*R*)**	10	Et_3N	20	16	31	25[c]
4	MeOH	$InBr_3$	**3.8 (*R*)**	20	-	-	16	>99	42
5	MeOH	$InBr_3$	**3.8 (*R*)**	10	Et_3N	10	16	96	17
6	MeOH	$InBr_3$	**3.8 (*R*)**	20	Et_3N	20	16	55	22[c]
7	MeOH	$InBr_3$	**3.8 (*R*)**	10	Et_2NH	10	16	81	20
8	MeOH	$InBr_3$	**3.8 (*R*)**	20	Et_2NH	20	16	42	27[c]
9	MeOH[d]	$InCl_3$	**3.8 (*R*)**	10	-	-	16	>99	42
10	DME	$InCl_3$	**3.8 (*R*)**	20	-	-	1	80	18
11	DME	$InCl_3$	**3.8 (*R*)**	20	Et_3N	40	1	22	15
12	CH_2Cl_2[e]	$InCl_3$	**3.8 (*R*)**	20	-	-	1	>99	6
13	MeOH	$In(OTf)_3$	**3.8 (*R*)**	20	DIPEA	20	1	97	30
14	MeOH	$In(OTf)_3$	**3.8 (*R*)**	20	Et_3N	20	1	72	24
15	MeOH	$In(OTf)_3$	**3.8 (*R*)**	20	Et_2NH	20	1	38	27
16	MeOH	$In(OTf)_3$	**3.8 (*R*)**	20	NaH[f]	20	1	92	18
17	MeOH	$InCl_3$	**3.13 (*R*)**	10	-	-	1	>99	25
18	MeOH	$InCl_3$	**3.13 (*R*)**	20	-	-	1	>99	28
19	MeOH	$InCl_3$	**3.13 (*R*)**	20	Et_3N	40	1	33	45
20	MeOH	$InBr_3$	**3.13 (*R*)**	20	-		1	>99	36

Table 3.3.2.2 continued: Screening new ligands, solvents and additives along with investigating premixing In(III) and ligand at RT.

Entry	Solvent	Catalyst	Ligand	[mol %]	Base	[mol %]	Premix [h]	Conversion[a] [%]	e.e.[b] [%]
21	MeOH	$InBr_3$	**3.13 (*R*)**	20	Et_3N	40	1	21	39
22	EtOH	$InCl_3$	**3.13 (*R*)**	20	-		1	>99	19
23	EtOH	$In(OTf)_3$	**3.13 (*R*)**	20	Et_3N	40	1	>99	42
24	MeOH	$In(OTf)_3$	**3.8 (*R*)**	20	Et_3N	20	1	59	28
25	MeOH	$InCl_3$	**3.15 (*R*)**	10	-	-	1	>99	32
26	MeOH	$InCl_3$	**3.17 (*R*)**	10	-	-	1	97	18
27	MeOH	$InCl_3$	**3.17 (*R*)**	20	-	-	1	83	13
28	MeOH	$InCl_3$	**3.20 (*R*)**	10	NaH[f]	30	1	>99	8
29	MeOH	$InCl_3$	**3.19 (*R*)**	20	-	-	1	>99	22
30	MeOH	$InCl_3$	**3.19 (*R*)**	10	-	-	1	>99	10
31	MeOH	$InBr_3$	**3.19 (*R*)**	10	-	-	1	>99	16
32	MeOH	$InBr_3$	**3.19 (*R*)**	20	Et_3N	20	1	69	16
33	MeOH	$In(OTf)_3$	**3.19 (*R*)**	20	-	-	1	>99	24
34	EtOH	$InCl_3$	**3.19 (*R*)**	10	-	-	1	>99	7
35	MeOH	$GaBr_3$	**3.19 (*R*)**	10	-	-	1	>99	16

Unless otherwise noted each entry represents a single experiment. All reactions were carried out with 143 μmol imine. [a] Conversion of imine to amine determined by crude NMR with 1,3,5-trimethoxybenzene as internal standard. [b] e.e. of amine determined by chiral stationary phase RP-HPLC [c] Average of two reactions. [d] 5 mol% In(III)-catalyst. [e] with 20 μL MeOH added. [f] Deprotonation in THF, which was afterwards evaporated.

Table 3.3.2.2 shows a subset of the results obtained from the screenings with the new ligands and with the 3,3'-I_2 -ligand **3.8 (*R*)**. With few exceptions (entries 5, 13, 23) the conversion decreased to below 90% when amine bases were used (entries 1-3, 6-8, 11, 14-15, 19, 21, 24, 32), whereas the same trend was not observed in the presence of NaH (entries 16, 28). Up to 45% e.e. was achieved with the dibromide **3.13 (*R*)** (entry 19) in MeOH and 42% (entry 23) in EtOH, both when combined with $In(OTf)_3$ and in the presence of Et_3N. The e.e. was increased to 42% with the bisiodide **3.8 (*R*)** by prolonging the premixing time to 16 hours (entries 4, 9). No clear trend between the e.e. and the halide on the BINOL ligand was observed. Weak e.e. was observed in CH_2Cl_2 when MeOH additive was used (entry 12). Many more were carried out, however, several of these were in EtOAc, and it was later found these reactions contained impurities co-running with the enantiomers in the HPLC analysis. When properly separated the result indicated very low e.e. to racemic results for all

reactions performed in EtOAc. Therefore, these results have been excluded from this thesis. The reaction was found to be racemic in acetone and no conversion was observed when ethylene glycol was used as the solvent (entries excluded from **Table 3.3.2.2**).

Commercially available enantiomeric pure (*R*)-BINAM **3.23**, (*R*)-BINAP **3.24** and (*R*)-TRIP **3.25** (**Figure 3.3.2.1**) were included in the screen. BINAM and BINAP were included to examine if these ligands would bind stronger to In(III) metal-centre, resulting in e.e. without 3,3'-substituents. TRIP was included to compare the result with that of the TRIP diol. It was expected BINAM would not afford higher e.e. than BINOL, based on the observed problem with catalyst turnover for the ketone reduction. These three ligands all afforded racemic amines in the In(III)-catalysed reaction independent on the presence of base.

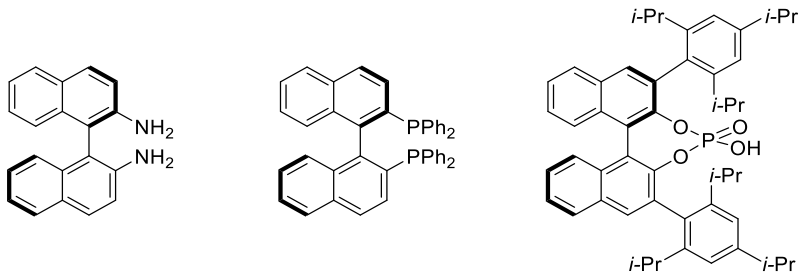

3.23 (*R*) **3.24 (*R*)** **3.25 (*R*)**

Figure 3.3.2.1: (*R*)-BINAM **3.23 (*R*),** (*R*)-BINAP **3.24 (*R*)** and (*R*)-TRIP **3.25 (*R*).**

3.3.3 HPLC analysis of the e.e.

Examination of the e.e. of the screening reactions was carried out using RP-HPLC with 0.05 M ammonium bicarbonate in MeCN. Commercially available enantiomeric pure **3.6 (*R*)** was used as reference to determine the stereoisomer of the enantiomer in excess, which also was **3.6 (*R*)**. Over time the separation of the two enantiomeric peaks decreased as a result of alkaline contamination of the chiral column. This is a known issue for alkaline RP-HPLC,[136,137] and as it proved difficult to restore the chiral phase and thus the separation of the enantiomeric peaks, it was decided to derivatise the obtained amines to amides and examine the e.e. of the amides instead. Different procedures for synthesising and separating the synthesised amides were examined (**Table SI-3.4.1**) and a straightforward acylation with Et_3N and Ac_2O was found to be the most efficient and straightforward procedure. This provided acylated amines with well-defined narrow enantiomeric peaks with excellent separation. The majority of the amides were subjected to HPLC analysis directly from the crude mixture after sufficient filtration. Further details are given in the SI.

For HPLC reference acyl amine **3.26** was synthesised from the racemic amine from $NaBH_4$ reduction (**Scheme 3.4.1**).

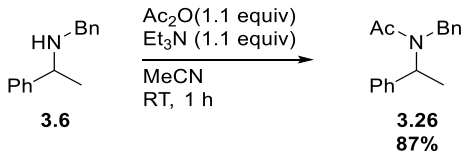

Scheme 3.4.1: Synthesis of HPLC reference amides **3.26**.

It was decided to use MeCN as solvent for the acylations, as this allowed for direct examination of the e.e. from the crude reaction mixtures as the solvent is tolerated by the HPLC chiral column. The enantiomerically pure **3.6 (*R*)** was used to synthesise **3.26 (*R*)**, which as a crude mixture was used to distinguish the enantiomer peaks in the HPLC chromatogram.

3.3.4 Lowering the catalyst loading

The results to this stage was presented at ISySyCat conference in 2017, where Prof. Scott Denmark, University of Illinois, offered to collaborate, sending a library of substituted BINOLs to test as ligands for the reaction. To minimise the consumption of these precious ligands, optimisation was performed to decrease either the scale or the catalyst loading (**Table 3.3.4.1**).

Table 3.3.4.1: Screening-results for lowering the scale or catalyst loading.

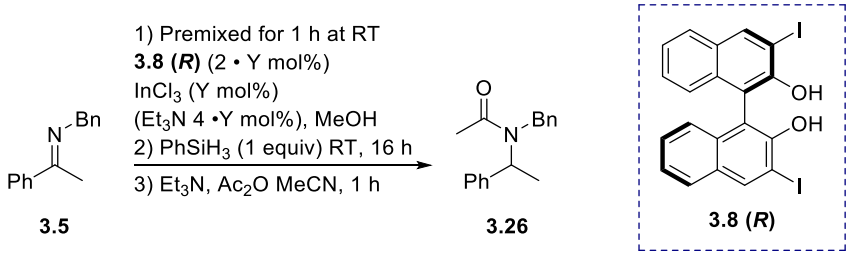

Entry	MeOH [µL]	3.5 [µmol]	Y	Base	Conversion[a] [%]	e.e.[b,c] [%]
1	200	143	5	Et_3N	49	29
2	100	72	10	Et_3N	40	26
3	200	143	5	-	>99	22
4	100	72	10	-	>99	19
5	200	143	10	-	>99	26
6	200	143	10	Et_3N	30	26

All reactions were carried out with 143 µmol imine. [a] Conversion of imine to amine determined by crude NMR with 1,3,5-trimethoxybenzene as internal standard. [b] e.e. of amine determined by chiral stationary phase RP-HPLC. [c] Each entry represents an average over two reactions.

The conversion was in all cases affected by the addition of Et_3N (entries 1, 2, 6). The e.e. of the control reactions (entries 5-6) was 26% independent on the presence of base. The e.e. was found to be 22-29% when the catalyst loading was decreased to 5% and 19-26% when the scale was halved. Based on this it was decided to carry on examining the reaction with a decreased catalyst loading. Further screenings were carried out (**Table SI-3.3.4.1**) to see how much the catalyst loading could be decreased and still yield reproducible results. Decreasing the amount of indium to 2.5 mol% seemed optimal. Decreasing the loading further resulted in a decrease in the conversion (2.5 mol% full conversion, 2 mol% - 94% conversion, 1.5 mol% - 94% conversion, 1 mol% - 90% conversion, 0.5 mol% - 88% conversion). New 300 µL vessels were found (**Figure SI-3.3.4.1**) allowing for carrying out the screening reaction of 72 µmol scale in only 100 µL solvent without risking loss of material from spreading it over the insides of the vessel. Hereby the scale was halved and the catalyst loading quartered, thereby, decreasing the amount of ligand needed per reaction by a factor 8.

Several reduction agents, mainly hydrosilanes, were screened including Et_3SiH, 1,1,3,3-tetramethyldisilazane (TMDS), 1,1,3,3-tetramethyldilisoxane (TMDSO), $SiCl_3H$, $PhSiHMe_2$ and Hantzsch ester. Most of these reduction agents led to low conversion, others were incapable of reducing the imine. Only $PhSiH_3$ was efficient as reduction source in this In(III)-catalysed reaction, capable of fully reducing the imine. Some reduction agents were screened in different solvent

systems, ensuring the lack of conversion was not caused by the choice of solvent. A full overview is given in **Table SI-3.3.4.2**.

Several screenings were carried out varying the stoichiometry of the silane. The reaction was found to proceed to full conversion with only 0.5 equiv of silane. When less silane was used the conversion started to decrease. However, full conversion with sub-stoichiometric equiv of silane could be achieved by performing the reaction to 60 °C. Unfortunately, this resulted in a decrease in the e.e. Furthermore, the effect on the e.e. varied from reaction to reaction. The stoichiometry of the silane was generally kept to one equiv, to ensure full conversion and eliminate variations in the results caused by varying conversion. As will be described in the following section the increase in the e.e. caused by lowering the silane concentration was a result of a general dilution, and a more robust method for achieving the same increase in e.e. will be presented.

3.4 Mixed solvent systems and premixing at elevated temperatures

Before screening the Denmark BINOL library, several screenings were carried out trying to optimise the conditions further. Two aspects that were attempted to further optimise were solubility and base addition. From the results obtained it is not clear what effect addition of base has. In some cases, an increase in e.e. as a result of adding base was observed, in other cases the e.e. appear similar with and without base being present in the reaction mixture. In several reactions, addition of base influenced the conversion, resulting in the reduction not proceeding to full conversion. The halogenated ligands were generally not particular soluble in polar protic solvents; however, the degree of solubility was difficult to judge by visual inspection, and to be sure the more hydrophobic ligands were not underperforming due to insufficient ligand solubility, screenings were carried out with mixed solvents systems to ensure full solubility of both the ligand and the indium salt. To avoid wasting any of the precious compounds in the library from Prof. Denmark, these screenings were carried out with commercially available ligands (**Figure 3.4.1 3.27 (*R*), 3.28 (*S*)** & **3.29 (*R*)**) and synthesised ligands. The (*R*)-3,3'-bis(2,4,6-tricyclohexylphenyl)-BINOL **3.30 (*R*)** (**Figure 3.4.1**) was kindly donated by Dr. Robert Phipps' group at University of Cambridge.

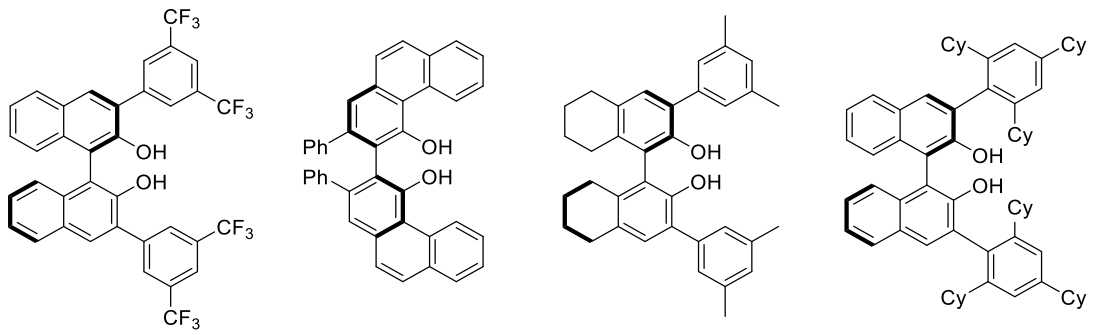

3.27 (*R*) **3.28 (*S*)** **3.29 (*R*)** **3.30 (*R*)**

Figure 3.4.1: New ligands included in the screenings to test the effect of solubility

All ligands but (*S*)-VAPOL afforded racemic amines. This surprising result prompted a hypothesis of whether these ligands were soluble enough in MeOH to facilitate the assembly of a In(III)-ligand complex. Screening of these new ligands were repeated with addition of 10 µL of various solvent additive (**Table 3.4.1**). All solvent additives were tested with **3.8 (*R*)** as control experiments, examining a general effect of the solvent on the e.e. Due to the previously discussed varying effect on the conversion caused by based addition, this was avoided.

Table 3.4.1: Examing effect of solvent additive.

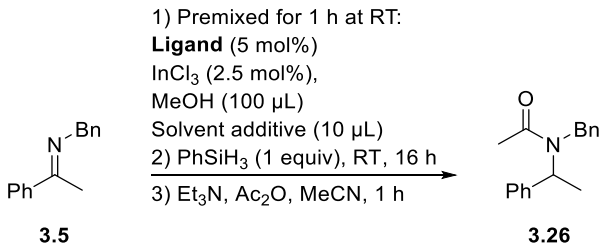

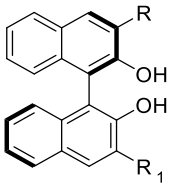

2.17 (*R*) R= (2,4,6-*i*-Pr)-Ph, R_1=H
2.18 (*R*) R = (2,4,6-*i*-Pr)-Ph, R_1=I
3.8 (*R*), R,R_1=I
3.13 (*R*) R,R_1=Br
3.19 (*R*), R,R_1=SBn
3.27 (*R*), R,R_1=(3,5-CF_3)-Ph
3.28 (*S*), (*S*)-VAPOL
3.29 (*R*), R,R_1=(3,5-Me)-Ph **H_8-BINOL**
3.30 (*R*), R,R_1=(2,4,6-Cy)-Ph

Entry	Ligand	Additive	Conversion[a] [%]	e.e.[b] [%]
1	**3.8 (*R*)**	THF	>99	14
2	**3.8 (*R*)**	MeCN	>99	18
3	**3.8 (*R*)**	CH_2Cl_2	>99	16
4	**3.8 (*R*)**	toluene	50	19
5	**3.8 (*R*)**	Et_2O	>99	20
6	**3.8 (*R*)**	hexane	>99	18
7	**3.8 (*R*)**	NMP	?[c]	16
8	**3.8 (*R*)**	DMSO	88	23
9	**3.8 (*R*)**	1,4-dioxane	92	27
10	**3.8 (*R*)**	MTBE	93	30
11	**3.8 (*R*)**	*i*-PrOH	96	20
12	**3.8 (*R*)**	ethylene glycol	68	21
13	**3.8 (*R*)**	PhCN	94	27
14	**3.8 (*R*)**	THF-co-evaporated	>99	18
15	**3.8 (*R*)**	*i*-PrOH/toluene	95	36
16	**3.8 (*R*)**	benzene	?[c]	28
17	**3.8 (*R*)**	DMF	?[c]	16
18	**3.27 (*R*)**	THF	>99	4
19	**3.27 (*R*)**	toluene	55	0
20	**3.27 (*R*)**	Et_2O	95	0
21	**3.30 (*R*)**	THF	>99	3
22	**3.30 (*R*)**	MeCN	>99	6

Table 3.4.1 continued: Examing effect of solvent additive.

Entry	Ligand	Additive	Conversion[a] [%]	e.e.[b] [%]
23	**3.29 (*R*)**	THF	60	0
24	**3.29 (*R*)**	MeCN	63	2
25	**3.29 (*R*)**	toluene	49	0
26	**3.29 (*R*)**	Et_2O	72	0
27	**3.28 (*S*)**	THF	>99	11[d]
28	**3.28 (*S*)**	MeCN	>99	8[d]
29	**3.28 (*S*)**	toluene	20	19[d]
30	**3.28 (*S*)**	Et_2O	75	16[d]
31	**3.19 (*R*)**	THF	>99	18
32	**3.19 (*R*)**	MeCN	75	20
33	**3.13 (*R*)**	toluene	41	33[e]
34	**3.13 (*R*)**	Et_2O	79	34
35	**2.17 (*R*)**	toluene	38	0
36	**2.17 (*R*)**	Et_2O	>99	0
37	**2.18 (*R*)**	toluene	53	0
38	**2.18 (*R*)**	Et_2O	>99	4

Unless otherwise noted each entry represents a single experiment. All reactions carried out with 72 μmol imine. [a] Conversion of imine to amine determined by crude NMR with 1,3,5-trimethoxybenzene as internal standard. [b] e.e. of the acylated amine determined by chiral stationary phase RP-HPLC. [c] Conversion unknown as unable to shim NMR spectrum. [d] (*S*)-enantiomer in excess. [e] Average over three reactions.

The result in **Table 3.4.1** are from reactions not all performed on the same day. However, these results are all shown here to allow for comparison. As presented earlier the majority of the solvents included in this table as additive afforded racemic amines when MeOH was not present. From the first round of screenings (entries 1-8) it was decided for further investigate Et_2O and toluene as additives. Being respectively polar aprotic and non-polar it was hoped either one of these would ensure full solubility of whatever ligand used. Both Et_2O and toluene appeared to not affect the e.e. (entries 4, 5). It was noticed that toluene resulted in a decreased conversion (entry 4). However, the focus was on increasing the e.e., and it was furthermore found interesting to examine whether a potential decrease in the rate of the reaction was the cause of the lower conversion. This will be described in Chapter 6. The increase in e.e. when MTBE, PhCN or 1,4-dioxane was added was found later, along with the result in entry 15. It is noted here how the combination of toluene and *i*-PrOH result in an increase in e.e. (36%) neither are capable of facilitation alone (19 and 20% respectively). Mixed solvent systems containing *i*-PrOH will be further discussed from **Table 3.4.4** and onwards.

As will be discussed in the coming sections the effect of the additive solvent depends on both the ligand and the source of In(III) used. The course for this variation remains unknown.

In section 3.3 it was described how (*R*)-3,3'-Ph_2-BINOL **3.12 (*R*)** afforded the highest e.e. (19-22%) in combination with $In(OTf)_3$ (**Table 3.3.2.1**, entry 5,6). In the interest of examining whether this was a general trend for non-polar 3,3'-substituents, screening with mixed solvents systems with Et_2O and toluene were carried out with $In(OTf)_3$ (**Table 3.4.2**). **Table 3.4.2** also includes results from reactions performed with In(III) iodide. In(III) iodide is known to exist as dimer crystals,[138] why it was of interest to examine whether significantly different results were obtained compared to monomeric sources of In(III).

Table 3.4.2: Screening $In(OTf)_3$ and InI_3 as sources of In(III) in mixed solvent systems with MeOH and Et_2O or toluene.

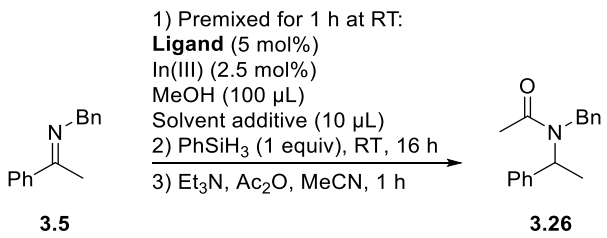

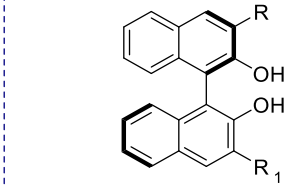

2.18 (*R*) R = (2,4,6-*i*-Pr)-Ph, R_1=I
3.8 (*R*), R,R_1=I
3.13 (*R*) R,R_1=Br
3.15 (*R*) R,R_1=Cl
3.17 (*R*) R,R_1=F
3.19 (*R*), R,R_1=SBn
3.27 (*R*), R,R_1=(3,5-CF_3)-Ph
3.28 (*S*), (*S*)-VAPOL
3.29 (*R*), R,R_1=(3,5-Me)-Ph **H_8-BINOL**

Table 3.4.2 continued: Screening $In(OTf)_3$ and InI_3 as sources of In(III) in mixed solvent systems with MeOH and Et_2O or toluene.

Entry	Ligand	In(III) source	Additive	Conversion[a] [%]	e.e. [b] [%]
1	**3.8 (*R*)**	$In(OTf)_3$	toluene	41	35
2	**3.8 (*R*)**	$In(OTf)_3$	Et_2O	95	22
3	**3.8 (*R*)**	InI_3	-	98	29
4	**3.8 (*R*)** [c]	InI_3	-	96	33
5	**3.8 (*R*)** [d]	InI_3	-	90	33
6	**3.8 (*R*)**	InI_3	toluene	37	54
7	**3.8 (*R*)** [c]	InI_3	toluene	37	42
8	**3.29 (*R*)**	$In(OTf)_3$	toluene	51	0
9	**3.29 (*R*)**	$In(OTf)_3$	Et_2O	79	0
10	**3.28 (*S*)**	$In(OTf)_3$	toluene	50	9 [e]
11	**3.28 (*S*)**	$In(OTf)_3$	Et_2O	73	10 [e]
12	**3.28 (*S*)**	InI_3	toluene	45	9 [e]
13	**3.13 (*R*)**	$In(OTf)_3$	toluene	45	34
14	**3.13 (*R*)**	$In(OTf)_3$	Et_2O	95	32
15	**3.13 (*R*)**	InI_3	toluene	74	23
16	**3.15 (*R*)**	$In(OTf)_3$	Et_2O	>99	30
17	**3.17 (*R*)**	$In(OTf)_3$	Et_2O	>99	26
18	**3.19 (*R*)**	$In(OTf)_3$	toluene	44	24
19	**3.19 (*R*)**	$In(OTf)_3$	Et_2O	91	10
20	**3.19 (*R*)**	InI_3	toluene	51	23
19	**2.18 (*R*)**	$In(OTf)_3$	toluene	53	0
20	**2.18 (*R*)**	$In(OTf)_3$	Et_2O	>99	4
21	**2.18 (*R*)**	InI_3	-	>99	3
22	**2.18 (*R*)** [c]	InI_3	-	>99	3
23	**2.18 (*R*)** [c]	InI_3	toluene	49	0
24	**3.27 (*R*)**	$In(OTf)_3$	toluene	51	0
25	**3.27 (*R*)**	$In(OTf)_3$	Et_2O	79	0
26	**3.8 (*R*)**	$In(OTf)_3$	toluene	43	33
27	**3.8 (*R*)** [c]	$In(OTf)_3$	toluene	40	35

Each entry represents a single experiment. All reactions carried out with 72 μmol imine. [a] Conversion of imine to amine determined by crude NMR with 1,3,5-trimethoxybenzene as internal standard.. [b] e.e. of the acylated amine determined by chiral stationary phase RP-HPLC. [c] 10 mol% ligand [d] 15 mol% ligand. [e] (*S*)-enantiomer in excess.

It is striking how entire 54% e.e. was obtained when InI_3 was used in a MeOH-toluene system (entry 6). In contrast hereto, the e.e. is only increased to 35% for $In(OTf)_3$ with toluene additive in MeOH (entry 1), which is not nearly as impressive in comparison with the 42-45% e.e. achieved with $In(OTf)_3$ through base addition (**Table 3.3.2.2**). The majority of the results in **Table 3.4.2** exhibit weak to no influence from the solvent additive. The e.e. obtained with the screened system using the ligands with non-polar substituents (**3.29 (R)**, **3.28 (*S*)**, **3.27 (*R*)**) does not show the increase that it was hoped they would, thus indicating lacking solubility is not the cause of the low performance of the ligands with non-polar 3,3'-substituents investigated to this state.

No obvious difference between using one, two or three equiv of ligand to In(III) was observed for InI_3 (entries 3-5 and 6-7). Even though InI_3 is known to exist as a dimer this could very well change the moment ligands co-ordinate to the In(III) metal-centre. Likewise, it is not known if the active catalyst for other In(III)-sources forms dimers. Thus the results presented here indicate, that either InI_3 is no longer a dimer as the active catalyst or In(III) obtained from another In(III)-source dimerises to form the active In(III)-catalyst.

Selected ligands from the Denmark Library was screened with toluene additive under the conditions above. Unfortunately, all resulting in less than 5% e.e. (**Table SI-3.4.3**).

The highest achieved e.e.'s to this stage was found either by premixing for prolonged time (42% e.e. with $InCl_3$ in MeOH, **3.8 (*R*)** premixed for 16 hours), addition of base (45% e.e. with **3.13 (*R*)** with Et_3N in MeOH) or through addition of solvent additive (InI_3 with toluene afforded 54% e.e.). These three factors could all be increasing the e.e. as a result of improving assembly of a catalyst complex. Solvent addition seems in general to increase the e.e. if the solvent addition effect causes lowered conversion. This indicates the increase in e.e. could be a result of the reaction rate decreasing, allowing for more time for the ligands and indium to interact.

Based on these observations screenings were carried out with dilution of the concentration to decrease the rate. The first rounds of experiments were carried out using MeOH, EtOH and *i*-PrOH (**Table 3.4.4**). As most previous experiments were carried out with $InCl_3$, it was decided to do the first rounds of dilution experiments continuing with this source of In(III) for comparison. To maximise In(III)-ligand interaction, it was decide also to increase the premixing temperature and time.

Table 3.4.4: Examining the effect of premixing In(III) and the ligand at elevated temperature for prolonged time.

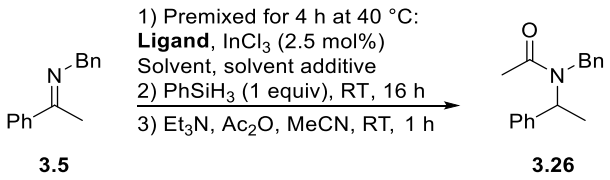

3.5 **3.26**

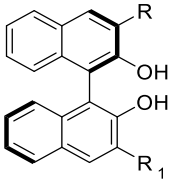

2.18 (*R*) R = (2,4,6-*i*-Pr)-Ph, R_1=I
3.8 (*R*), R,R_1=I
3.19 (*R*), R,R_1=SBn
3.28 (*S*), (*S*)-VAPOL

Entry	Solvent	[µL]	Additive	[µL]	Ligand	[mol%]	e.e. [a] [%]
1	*i*-PrOH	300	-	-	**3.8 (*R*)**	5	20
2	EtOH	300	-	-	**3.8 (*R*)**	5	38
3	*i*-PrOH	300	-	-	**3.28 (*S*)**	5	19 [b]
4	*i*-PrOH	300	toluene	10	**3.8 (*R*)**	5	20
5	MeOH	300	toluene	10	**3.8 (*R*)**	5	38
6	*i*-PrOH	300	-	-	**2.18 (*R*)**	5	0
7	*i*-PrOH	550	-	-	**3.8 (*R*)**	5	23
8	*i*-PrOH	300	-	-	**3.8 (*R*)**	5	24
9	*i*-PrOH	250	MeOH	50	**3.8 (*R*)**	5	42
10	*i*-PrOH	250	MeOH	50	**3.8 (*R*)**	10	44
11	*i*-PrOH	250	MeOH	50	**3.19 (*R*)**	5	36
12	EtOH	300	toluene	10	**3.8 (*R*)**	5	41
13	EtOH	300	MeOH	10	**3.8 (*R*)**	5	39
14	EtOH	250	MeOH	50	**3.8 (*R*)**	5	48
15	EtOH	250	MeOH	50	**3.8 (*R*)**	10	40
16	MeOH	300	-	-	**3.8 (*R*)**	5	32
17	MeOH	300	-	-	**3.8 (*R*)**	10	30
18	MeOH	300	-	-	**3.19 (*R*)**	5	25
19	EtOH	250	MeOH	20	**3.8 (*R*)**	5	43
20	EtOH	250	MeOH	30	**3.8 (*R*)**	5	41
21	EtOH	250	MeOH	40	**3.8 (*R*)**	5	35
22	EtOH	250	MeOH	50	**3.8 (*R*)**	5	41
23	EtOH	250	MeOH	75	**3.8 (*R*)**	5	35
24	EtOH	250	MeOH	100	**3.8 (*R*)**	5	33

Table 3.4.4 continued: Examining the effect of premixing In(III) and the ligand at elevated temperature for prolonged time.

Entry	Solvent	Vol (µL)	Additive	Vol (µL)	Ligand	mol%	e.e. [a] [%]
25	EtOH	250	MeOH/toluene	50/10	**3.8 (*R*)**	5	34
26	EtOH	250	MeOH/ *i*-PrOH	50/10	**3.8 (*R*)**	5	36
27	EtOH	250	MeOH/benzene	50/10	**3.8 (*R*)**	5	35
28	EtOH	250	MeOH/toluene	50/50	**3.8 (*R*)**	5	33
29	EtOH	250	MeOH	50	**3.28 (*S*)**	5	26 [b]

All reactions proceeded to full conversion. Conversion of imine to amine was determined by crude NMR with 1,3,5-trimethoxybenzene as internal standard. Each entry represents a single experiment. All reactions carried out with 72 µmol imine. [a] e.e. of the acylated amine determined by chiral stationary phase RP-HPLC. [b] (*S*)-enantiomer in excess.

A significant increase in the obtained e.e. is observed when the solvent system is switched around and *i*-PrOH becomes the major component reaching 44% (entry 10). It was previously noted (**Table 3.4.1)** how adding *i*-PrOH to MeOH had little influence on the e.e. The increase in e.e. was generally observed in mixed solvent systems of EtOH, *i*-PrOH to MeOH, where MeOH was the minor component (entry 9-11, 13-15, 19-28), consistently affording 30-44 % e.e. for 3,3'-halogen substituted BINOLs. An increase was also observed when toluene additive was added to EtOH (entry 12). However, the effect was less when MeOH was also present (entries 25, 28).

Prior to further investigate these mixed solvent systems with multiple polar protic solvents, it was decided to investigate the influence of the addition order and temperature of imine and silane. The following trends were observed: 1) The e.e. decreased when the silane was added prior to the imine; 2) adding the silane 10 or 60 minutes after the imine had no effect on neither e.e. nor conversion; 3) adding the silane at a lower temperature (0 or 4 °C) resulted in a slight increase in the e.e. and a significant decrease in the conversion; 4) addition of sub-stoichiometric equiv of silane resulted in a slight increase in e.e. and a significant decrease in conversion; 5) addition of sub-stoichiometric equiv of silane 60 °C did not affect neither the conversion nor the e.e. As none of these factors had a positive influence on the e.e. without affecting the conversion, the addition order and temperatures were kept for onwards experiments.

Furthermore, based on the previously made observation that InI_3 outperformed $InCl_3$ with 35% when both were used in combination with toluene additive and **3.8 (*R*)** as the ligand (**Table 3.4.2** entry 6 and **Table 3.4.1** entry 4), it was decided to carry out control experiments (**Table SI-3.4.5**) adding various sources of silver trying to remove the chlorine counterions from $InCl_3$ catalysed reductions, examining if the more exposed metal-cation was the reason for InI_3 and $In(OTf)_3$ outperforming $InCl_3$

and $InBr_3$. The larger iodine counterions results in a more Lewis acidic In(III) metal-centre, which potentially could be the cause of this significant difference, as a more Lewis acidic In(III) ion is expected to result in stronger and faster ligand exchange and thus formation of an active In(III)-ligand complex. However, it turned out silver catalyses an even faster racemic reaction. Therefore, this approached were abandoned. An additional control experiment was performed by adding tetrabutylammonium chloride to the reaction and as this caused a lower e.e. it was concluded there were issues with the chloride counterion equilibrium. Upon this realisation all In(III) halide salts were abandoned as sources of indium.

Returning to focus on the positive effect of dilution and preheating the complex further screenings were carried out. As the best results were obtained in *i*-PrOH or EtOH with added MeOH and variations of these solvent systems included mix all three solvents were used. It was decided to further decrease the catalyst loading to 2 mol% which was found to yield results similar to 2.5 mol%. Screening was carried out with either 40 or 60 °C and it was found that increasing the temperature increased the e.e. whereas, increasing the temperature to 70 °C did not improve the e.e. Premixing was carried out for 4 or 5 hours and on occasion overnight. However, it was found that the premixing time did not have much effect – 3.5 or 6 hours would yield the same e.e., whereas overnight premixing on occasion lowered the e.e., which could be a result of moisture entering the system. Based on the premixing time was set to 4 hours all reaction presented onwards.

It was decided to examine $In(OAc)_3$ as In(III)-catalyst (**Table 3.4.6**). Mixed solvent systems with the three polar protic solvents MeOH, EtOH and *i*-PrOH in various combinations was used.

Table 3.4.6: Testing various ligands under mixed solvent systems using $In(OAc)_3$.

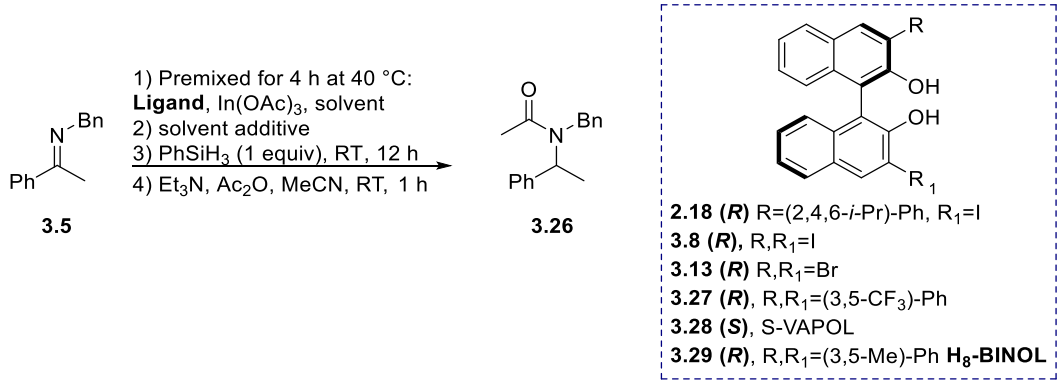

Table 3.4.6 continued: Testing various ligands under mixed solvent systems using $In(OAc)_3$.

Entry	Solvent	Vol [µL]	Additive[a]	Vol [µL]	In(III) [mol%]	Ligand	[mol %]	Premix temp [°C]	e.e.[b] [%]
1	*i*-PrOH	250	MeOH	50	2	**3.8 (*R*)**	2	60	24
2	*i*-PrOH	250	MeOH	50	2	**3.8 (*R*)**	4	60	24
3	*i*-PrOH	250	MeOH	50	2	**3.37 (*R*)**[c]	2	60	20
4	*i*-PrOH	250	MeOH	50	2	**3.13 (*R*)**	2	60	19
5	*i*-PrOH	250	MeOH	50	2	**3.29 (*R*)**	2	60	0
6	*i*-PrOH	250	MeOH	50	2	**3.27 (*R*)**	2	60	0
7	*i*-PrOH	250	MeOH	50	2	**2.18 (*R*)**	2	60	0
8	*i*-PrOH	250	toluene	50	2	**3.8 (*R*)**	2	60	3
9	*i*-PrOH	250	MeOH	50	0.5	**3.8 (*R*)**	1	60	17
10	*i*-PrOH	250	MeOH	50	2	**3.8 (*R*)**	2	60	17
11	EtOH	100	*i*-PrOH /MeOH	200/50	2	**3.8 (*R*)**	2	40	13
12	EtOH	100	*i*-PrOH /MeOH	200/50	2	**3.8 (*R*)**	4	40	17
13	EtOH	100	*i*-PrOH /MeOH	200/50	2	**3.13 (*R*)**	2	40	24
14	EtOH	300	MeOH	50	2	**3.8 (*R*)**	2	40	22
15	EtOH	100	*i*-PrOH /toluene	200/50	2	**3.8 (*R*)**	2	40	8
16	EtOH	100	*i*-PrOH /MeOH	200/50	0.5	**3.8 (*R*)**	1	40	45
17	EtOH	100	*i*-PrOH /MeOH	200/50	0.5	**3.8 (*R*)**	1	40	40
18	EtOH	100	*i*-PrOH /MeOH	200/50	0.5	**3.8 (*R*)**	0.5	40	41
19	EtOH	350	*i*-PrOH /MeOH	200/50	0.25	**3.8 (*R*)**	1	40	38
20	EtOH	100	*i*-PrOH /MeOH	200/50	0.25	**3.8 (*R*)**	0.5	40	45
21	EtOH	100	*i*-PrOH /MeOH	200/50	0.5	**3.13 (*R*)**	1	40	31

Unless otherwise noted each entry represents a single experiment. All reactions carried out with 72 µmol imine. All reactions proceeded to full conversion. Conversion of imine to amine was determined by crude NMR with 1,3,5-trimethoxybenzene as internal standard. [a] Added with the imine. [b] e.e. of the acylated amine determined by chiral stationary phase RP-HPLC. [c] Structure Figure 3.7.1

As the 3,3'-halide substituted BINOL had shown superior e.e. on up to 54%, ligand **3.37 (*R*)** from the Denmark library was included. This 3,3'-bisbromo-H_8-BINOL afforded 20% e.e. with $In(OAc)_3$ (entry 3) thus comparing well fully aromatic version, **3.13 (*R*)**, affording 19% e.e. under the same conditions (entry 4). Several of the ligands previously screened and found to afford racemic amines, continued to afford racemic amine (entry 5-7). Noteworthy, the e.e. decreased to 3% when MeOH is removed from the *i*-PrOH/toluene mixture (entry 8). Positively, it was observed how the e.e. was

increase significantly (38-45%) when the catalyst loading was decreased to 0.25-0.5% $In(OAc)_3$ (entries 16-20).

Returning to $In(OTf)_3$ further combinations of the three polar protic solvents were screened (**Table 3.4.7**).

Table 3.4.7: Testing various ligands under mixed solvent systems using $In(OTf)_3$.

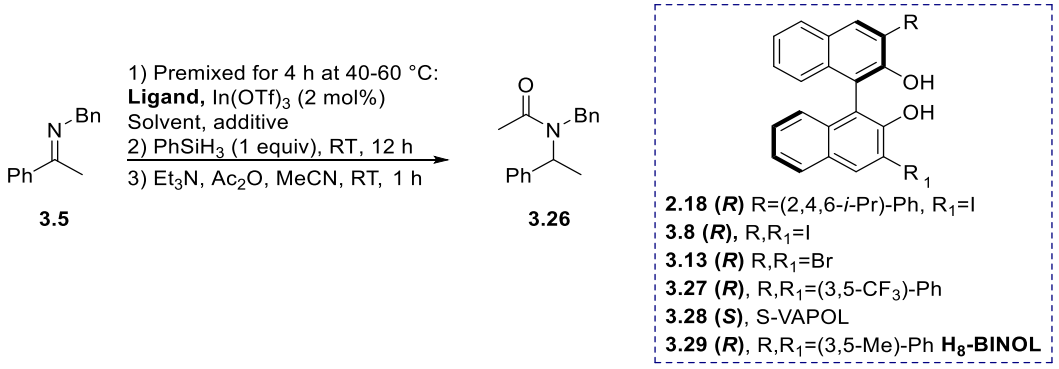

Table 3.4.7 continued: Testing various ligands under mixed solvent systems using $In(OTf)_3$.

Entry	Solvent	[µL]	Additive	[µL]	Ligand	[mol%]	Premix temp [°C]	e.e. [a] [%]
1	*i*-PrOH	250	EtOH	50	**3.8 (*R*)**	2	40	32
2	*i*-PrOH	250	EtOH	50	**3.8 (*R*)**	4	40	33
3	*i*-PrOH	250	MeOH	50	**3.8 (*R*)**	2	40	33
4	*i*-PrOH	250	MeOH	50	**3.8 (*R*)**	4	40	28
5	*i*-PrOH	250	toluene	50	**3.8 (*R*)**	4	40	30
6	*i*-PrOH	250	MeOH	50	**3.13 (*R*)**	4	40	30
7	*i*-PrOH	250	MeOH	50	**2.18 (*R*)**	4	40	-[b]
8	*i*-PrOH	250	EtOH	50	**3.8 (*R*)**	4	60	33
9	*i*-PrOH	250	MeOH	50	**3.28 (*S*)**	4	40	10[c]
10	*i*-PrOH	250	MeOH	50	**3.37 (*R*)**[c]	4	40	43
11	*i*-PrOH	250	MeOH	50	**3.8 (*R*)**	4	60	39
12	EtOH	200	MeOH	50	**3.8 (*R*)**	2	40	25
13	EtOH	200	MeOH	50	**3.8 (*R*)**	4	40	24
14	EtOH/ *i*-PrOH	100/200	MeOH	50	**3.8 (*R*)**	4	40	32
15	EtOH/ *i*-PrOH	100/200	toluene[d]	50	**3.8 (*R*)**	4	40	35
16	EtOH	200	MeOH	50	**3.8 (*R*)**	4	60	23
17	*i*-PrOH	400	MeOH	50	**3.36 (*R*)**[e]	4	60	12
18	*i*-PrOH	400	MeOH	50	**3.55 (*R*)**[e]	4	60	9
19	*i*-PrOH	400	MeOH	50	**3.27 (*R*)**	2	60	0
20	*i*-PrOH	400	MeOH	50	**3.29 (*R*)**	2	60	0
21	*i*-PrOH	250	MeOH	50	**3.8 (*R*)**	4	60	24

Unless otherwise stated all reactions proceeded to full conversion of imine to amine. Conversion was determined by crude NMR with 1,3,5-trimethoxybenzene as internal standard. Unless otherwise noted each entry represents a single experiment. All reactions carried out with 72 µmol imine. [a] e.e. of the acylated amine determined by chiral stationary phase RP-HPLC. [b] (*S*)-enantiomer in excess. [c] 0% conversion from imine to amine. [d] 50% conversion. [e] Structure Figure 3.7.1.

Selected ligands from the Denmark Library (entries 10, 17, 18) were included for initial screening under these new solvent systems. The 3,3'-bisbromide **3.37 (*R*)** (H_8-BINOL) yielded 43% (entry 10) thus comparing with the 3,3'-bisiodide **3.8 (*R*)** (up to 44% e.e. in **Table 3.4.4**). In the table above a decrease in the e.e. to 28% was observed for this ligand (**3.8 (*R*)**) (entry 4) compared to **Table 3.4.4**, for which the cause is unknown. However, based on the positive results for lowering the catalyst loading for $In(OAc)_3$ it was decided to examine this effect for $In(OTf)_3$ along with further dilution through an increase in the amount of *i*-PrOH (**Table 3.4.8**).

Table 3.4.8: Decreasing catalyst loading of $In(OTf)_3$ and concentration of imine.

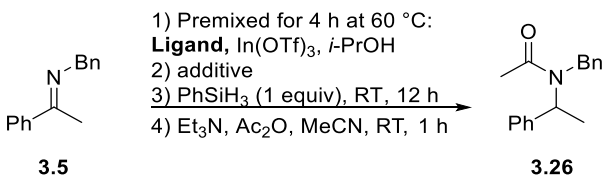

3.5 **3.26**

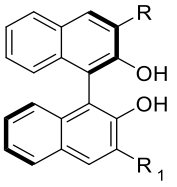

2.18 (*R*) R=(2,4,6-*i*-Pr)-Ph, R_1=I
3.8 (*R*), R,R_1=I
3.13 (*R*) R,R_1=Br

Table 3.4.8 continued: Decreasing catalyst loading of $In(OTf)_3$ and concentration of imine.

Entry	[µL]	Additive[a]	Vol [µL]	In(III) [mol%]	Ligand	[mol%]	e.e. [b] [%]
1	300	MeOH	50	0.5	**3.8 (*R*)**	0.5	55
2	300	MeOH	50	0.5	**3.8 (*R*)**	1	60
3	300	MeOH	50	1	**3.8 (*R*)**	1	50
4	300	MeOH	50	0.25	**3.8 (*R*)**	0.5	58
5	300	MeOH	50	0.25	**3.8 (*R*)**	1	63
6	300	MeOH	50	0.1	**3.8 (*R*)**	0.5	62
7	300	MeOH	50	0.5	**3.8 (*R*)**	1	66
8	300	MeOH	50	0.5	**3.13 (*R*)**	1	55
9	300	MeOH	50	0.5	**3.51 (*R*)**[c]	1	10
10	300	MeOH	50	0.5	**3.34 (*R*)**[c]	1	1
11	300	MeOH	50	0.5	**3.42 (*R*)**[c]	1	8
12	300	MeOH	50	0.5	**3.59 (*R*)**[c]	1	10
13[e]	300	MeOH	50	0.5	**3.48 (*R*)**[c]	1	0
14	300	toluene[d]	50	0.5	**3.8 (*R*)**	1	45
15	500	MeOH	50	0.5	**3.8 (*R*)**	1	69
16	300	MeOH	50	0.5	**3.8 (*R*)**	1	69
17	300	MeOH	50	0.25	**3.8 (*R*)**	1	61
18[e]	500	MeOH	50	0.5	**3.8 (*R*)**	1	**72**
19[f]	750	MeOH	50	0.5	**3.8 (*R*)**	1	**71**
20	1000	MeOH	50	0.5	**3.8 (*R*)**	1	**73**
21	1500	MeOH	50	0.5	**3.8 (*R*)**	1	**73**
22	500	MeOH	50	0.5	**3.8 (*R*)**	1	**72**
23[g]	500	MeOH	50	0.5	**3.8 (*R*)**	1	**71**
24	500	MeOH	50	0.5	**2.18 (*R*)**	1	1
25	500	MeOH	50	1	**3.8 (*R*)**	1	66
26	500	MeOH	50	0.5	**3.8 (*R*)**	1	68
27	1000	MeOH	50	1	**3.8 (*R*)**	1	68

Each entry represents a single experiment. All reactions carried out with 72 µmol imine. Unless otherwise stated all reactions proceeded to full conversion of imine to amine. Conversion was determined by crude NMR with 1,3,5-trimethoxybenzene as internal standard.. [a] Added with the imine. [b] e.e. of the acylated amine determined by chiral stationary phase RP-HPLC. [c] Structure in Figure 3.7.1. [d] 50% NMR conversion from imine to amine. [e] 0.5 equiv silane, 78% conversion. [f] 0.33 equiv silane, 52% conversion. [g] overnight premix.

The e.e. gradually increase with decreasing catalyst loading and decreased imine concentration reaching the above 70% for several reactions (entries 18-23). Entire 73% e.e. was reached with bisiodide ligand **3.8 (*R*)** (entry 20) by decreasing the imine concentration to 72 mM and using 0.5 mol% $In(OTf)_3$. Further dilution did not improve the e.e. which remained 73% (entry 21). It was observed that the 3,3'-I_2 ligand became fully soluble at 60 °C in the diluted (more than 500 µL) *i*-PrOH system. This is believed to be the reason for the increase in e.e. A similar increase in e.e. was found by decreasing the silane stoichiometry (entries 18, 19). However, this also decreased the conversion. The 73% e.e. in entry 20 will represent the optimised conditions for the remaining of this thesis.

3.5 Further examination of base addition and addition of an alcohol

Prior to screening the Denmark library, it was decided to complete examination of additives.

Extensive screenings had shown indications of increased e.e. upon base addition when $InCl_3$ or $InBr_3$ was used as source of In(III) (section 3.3). Screenings were carried out to test if the same effect was observed with InI_3 or $In(OTf)_3$ was used as In(III) source (**Table 3.5.1**).

Table 3.5.1 Testing the optimised reaction conditions with InI_3 and $In(OTf)_3$.

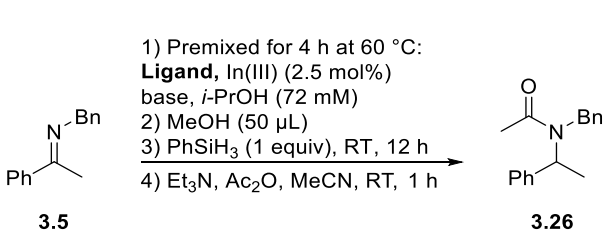

Entry	Ligand	[mol%]	In(III)	Base	[mol%]	Conversion[a] [%]	e.e.[b] [%]
1 [c, d]	**3.8 (*R*)**	5	InI_3	-	-	98	29
2 [c, d]	**3.8 (*R*)**	10	InI_3	-	-	96	33
3 [c, d]	**3.8 (*R*)**	15	InI_3	-	-	90	33
4	**3.8 (*R*)**	5	InI_3	Et_3N	10	84	28
5	**3.8 (*R*)**	10	InI_3	Et_3N	20	66	33
6	**3.8 (*R*)**	15	InI_3	Et_3N	30	51	35
7 [c, e]	**3.8 (*R*)**	10	$In(OTf)_3$	-	-	>99	29
8 [c, e]	**3.8 (*R*)**	10	$In(OTf)_3$	DIPEA	20	71	33
9 [c, e]	**3.8 (*R*)**	10	$In(OTf)_3$	DIPEA	40	36	27
10	**3.8 (*R*)**	10	$In(OTf)_3$	Et_3N	10	95	30
11	**3.8 (*R*)**	5	$In(OTf)_3$	Et_3N	20	88	32
12[f]	**3.8 (*R*)**	5	$In(OTf)_3$	Et_3N	10	41	30
13	**2.18 (*R*)**	5	InI_3	Et_3N	10	>99	3
14 [c, e]	**2.18 (*R*)**	10	InI_3	-	-	>99	3
15	**2.18 (*R*)**	5	$In(OTf)_3$	Et_3N	10	96	5
16 [c, e]	**3.8 (*R*)**	10	$InCl_3$	Et_3N	10	91	26
17[c,]	**3.8 (*R*)**	5	$InCl_3$	-	-	>99	42

Each entry represents a single experiment. All reactions carried out with 72 µmol imine. [a] Conversion of imine to amine determined by crude NMR with 1,3,5-trimethoxybenzene as internal standard. [b] e.e. of the acylated amine determined by chiral stationary phase RP-HPLC. [c] Entry is from previous table, reprinted here for comparison. [d] 5 mol% In(III), 100 µL MeOH no *i*-PrOH. [e] Only 250 µL *i*-PrOH. [f] 10 µL Toluene added

There is no obvious trend between e.e. and base addition. However, addition of base often, though not consistently, decreased the conversion. $In(OTf)_3$ afforded similar e.e. whether no base is present (entry 7) or base is present (entry 9-12). Different conditions are employed in these entries. However, as a decrease in catalyst loading based on previous findings should increase the e.e, addition of either base or toluene has limited to no effect in the results presented above. The same effect was found when InI_3 was employed as source of In(III) (entries 4-6 compared to 1-3).

Various other bases were screened early on, including K_2CO_3, $MeNH_2$ and NH_3 (**Table SI-3.5.2**). However, none of these improved the e.e. significantly. After the extensive screen of mixed solvent systems, it was decided to further examine base addition. As the biproduct from employing NaOMe would be MeOH, which is already present in the reaction mixture, this was though an important base to investigate (**Table 3.5.3**).

Table 3.5.3 Screenings with NaOMe.

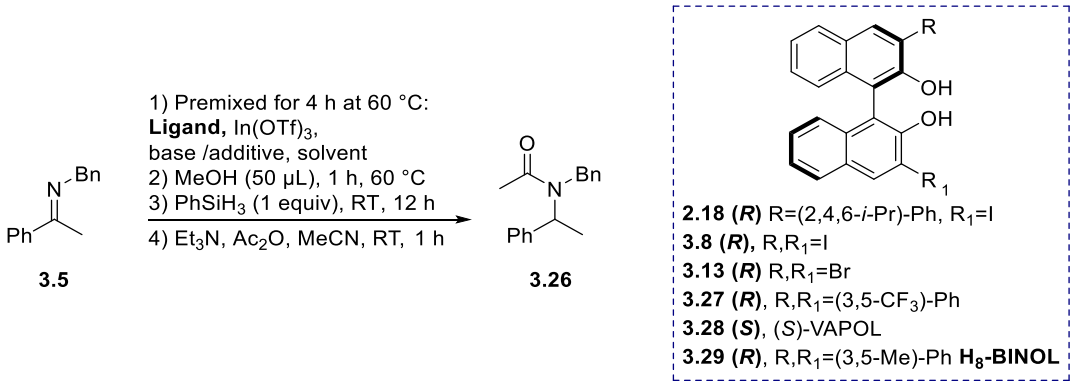

Entry	*i*-PrOH [µL]	In(III) [mol%]	Ligand	[mol %]	Base	[mol%]	Conversion[a] [%]	e.e.[b] [%]
1	400	0.5	**3.8 (*R*)**	1	NaOMe	2	>99	58
2	300	0.5	**3.8 (*R*)**	1	NaOMe	3.5	>99	58
3[c]	300	0.5	**3.8 (*R*)**	1	NaOMe	4	45	39
4	500	0.5	**2.18 (*R*)**	1	NaOMe	2	>99	6
5	500	0.5	**2.18 (*R*)**	1	NaOMe	4	>99	11
6	500	0.5	**3.8 (*R*)**	1	NaOMe	2	>99	61
7	1000	0.5	**3.8 (*R*)**	1	NaOMe	2	>99	58
8	1000	0.5	**2.18 (*R*)**	1	NaOMe	6	>99	9
9	1000	0.5	**2.18 (*R*)**	1	NaOMe	12	>99	9
10	1000	0.5	**3.28 (*S*)**	1	NaOMe	2	87	15[d]
11	1000	0.5	**2.18 (*R*)**	1	NaOMe	2	>99	9
12	1000	0.5	**3.29 (*R*)**	1	NaOMe	2	95	2
13	1000	0.5	**3.27 (*R*)**	1	NaOMe	2	>99	0

Each entry represents a single experiment. All reactions carried out with 72 µmol imine. [a] Conversion of imine to amine determined by crude NMR with 1,3,5-trimethoxybenzene as internal standard. [b] e.e. of the acylated amine determined by chiral stationary phase RP-HPLC. [c] Toluene instead of MeOH. [d] (*S*)-enantiomer in excess.

Addition of NaOMe to the optimised conditions with ligand **3.8 (*R*)** (entry 7) afforded only 58% e.e. compared with 73% e.e. without NaOMe. No obvious trend resulting from base addition appears to

exist at the different concentrations with this ligand (entries 1-3, 6, 7). A slight increase in e.e. is observed with increased NaOMe addition for ligand **2.18 (*R*)** (entries 4, 5). However, this ligand does not afford more than 11% e.e.

None of the results presented in **Table 3.5.1-3** succeeds the e.e. obtained in the same system without base addition (**Table 3.4.8**). Therefore, further screenings were carried out without addition of base.

Returning to focus on the alcohol additive. The amount of MeOH was found to have a high impact on the both the conversion and the e.e.: when less than 30 µL of MeOH was added the conversion decreased; when more than 50 µL was added the e.e. decreased (**Table 3.5.4**).

Table 3.4.5: Examining the affect of varying the amount of MeOH.

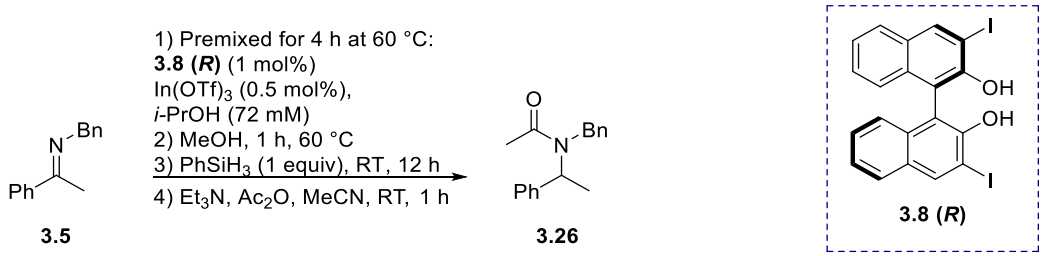

Entry	MeOH [µL]	Equiv	Conversion[a] [%]	e.e.[b] [%]
1	3	1	25	54
2	9	3	29	51
3	30	10	>99	62
4	50	17	>99	73
5	60	20	>99	57
6	180	60	>99	56
7	1000[c]	333	>99	23

Each entry represents a single experiment. All reactions carried out with 72 µmol imine. [a] Conversion of imine to amine determined by crude NMR with 1,3,5-trimethoxybenzene as internal standard. [b] e.e. of the acylated amine determined by chiral stationary phase RP-HPLC. [c] No *i*-PrOH added.

It is noted how the conversion is below 30% when 3 or less equiv of MeOH is added (entry 1, 2). The e.e. varies to some degree. This highest e.e. was obtained with 17 equiv of MeOH (entry 4), hereafter a drop in the e.e. is observed, and when MeOH is the sole solvent (entry 7) only 23% e.e. is obtained.

Various alcohols were screened to examine if MeOH was the optimal alcohol additive. These alcohols were initial screened in the presence of MeOH, as the imine was added from a MeOH stock solution. Those that did not cause a decrease in the e.e. were then re-examined in the absence of MeOH to

allow for comparison of how these alcohols affected the e.e. compared to the effect of MeOH on the e.e. The results are shown in **Table 3.5.5**.

Table 3.5.5 Screenings various alcohol additives.

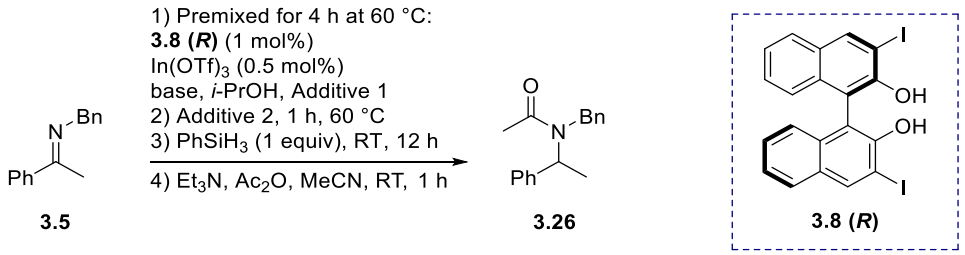

Entry	*i*-PrOH [µL]	Additive 1	[µL]	Additive 2	[µL]	Ligand	e.e. [a] [%]
1	1000	-	-	MeOH	50	**3.8 (*R*)**	73
2	1000	-	-	4-MeO-PhOH[b]		**3.8 (*R*)**	18
3	950	phenylethanol	50	MeOH	50	**3.8 (*R*)**	64
4	100	phenylethanol	900	MeOH	50	**3.8 (*R*)**	45
5	950	1,5-pentandiol	50	MeOH	50	**3.8 (*R*)**	63
6	100	1,5-pentandiol	900	MeOH	50	**3.8 (*R*)**	41
7	950	2,4-pentanediol	50	MeOH	50	**3.8 (*R*)**	64
8	100	2,4-pentanediol	900	MeOH	50	**3.8 (*R*)**	52
9	950	2-pyridinemethanol	50	MeOH	50	**3.8 (*R*)**	0
10	100	2-pyridinemethanol	900	MeOH	50	**3.8 (*R*)**	12
11	950	3-butyl-2-ol	50	MeOH	50	**3.8 (*R*)**	-[c]
12	100	3-butyl-2-ol	900	MeOH	50	**3.8 (*R*)**	0
13	1000	-	-	Phenylethanol	50	**3.8 (*R*)**	33
14	1000	-	-	1,5-pentanediol	50	**3.8 (*R*)**	56
15	1000	-	-	2,4-pentanediol	50	**3.8 (*R*)**	-[c]
16	500	hexane	500	MeOH	50	**3.8 (*R*)**	-[c]
17	500	cyclohexane	500	MeOH	50	**3.8 (*R*)**	61

Conversion minimum 99% for all entries. Conversion of imine to amine was determined by crude NMR with 1,3,5-trimethoxybenzene as internal standard. Each entry represents a single experiment. All reactions carried out with 72 µmol imine. [a] e.e. of the acylated amine determined by chiral stationary phase RP-HPLC. [b] 0.45 mg added. [c] e.e. could not be determined due to impurities.

When the hydrosilane reduction was performed on ketones the alcohol products were found to inhibit the catalyst turnover. As Verdaguer et al. reported an increase in e.e. with amine additives for a titanium catalysed hydrosilylation when aliphatic amines were added,[139] the effect of adding

n-decylamine or *n*-butyl amine was examined. In both reactions a slight decrease in conversion to 85% was observed. With *n*-decylamine the e.e. was determined to be 51%. With *n*-butyl amine impurities were co-running with the enantiomeric peaks, however, the e.e. was around 50% in this case too. Furthermore, addition of enantiomeric pure amine product **3.6 (*R*)** was added to the reaction mixture and found to not affect the conversion.

3.6 Choosing the best source of indium(III)

As described in section 3.4, In(III) halides were abandoned as source of In(III) due to the experiments conducted with $InCl_3$ showing addition of tetrabutylammonium chloride lowered the e.e. thus suggesting an insufficient ligand exchange process with between the chlorine counterions and the BINOL ligand **3.8 (*R*)**. Increased temperature and premix time increased the e.e. indicating this could affect the ligand exchange equilibrium. Several attempts were made towards obtaining a more exposed In(III)-metal centre. Commercially available In(III) compounds with alkoxy counterions, $In(OEt)_3$ and $In(i\text{-}PrO)_3$, were examined as In(III)-catalyst (**Table SI-3.6.1**). Protonation of these alkoxy anion would result in EtOH and *i*-PrOH, which first of all are better leaving group, and second, they are two of the polar protic solvents, which have been found to contribute positively to an increase in e.e. of the In(III)-catalysed hydrosilane reduction through dilution. Attempts to remove these counterions from the In(III) metal-centre were made using tetrafluoro boric acid (HBF_4), which can be used as a source of protons due to the non-co-ordinating nature of the BF_4^- anion. Upon mixing of $In(i\text{-}PrO)_3$ with HBF_4 the following reaction is expected to proceed:

$$In(i\text{-}PrO)_3 + 3\ HBF_4 \rightarrow In^{+3} + 3\ i\text{-}PrOH + 3\ BF_4^-$$

The non-co-ordinating anion BF_4^- should not co-ordinate to the In(III) metal-centre. Hence, this cation is exposed and hypothesised to be more prone to co-ordinate to the BINOL ligands.

However, none of these attempts outperformed the use of $In(OTf)_3$ in the *i*-PrOH/MeOH system that afforded up to 73% e.e. $In(OTf)_3$ were found to perform better than $In(OAc)_3$. As $In(OTf)_3$ is an In(III) LA superacid, the attention was led the other In(III) LA superacid; $In(NTf_2)_3$, which should be even more LA acidic on the In(III) metal-centre and therefore, thought to bind even stronger to the ligand oxygens.

$In(NTf_2)_3$ was synthesised as described in the literature.[34] This proved rather troublesome. The first batch contained In_2O_3 impurities. Commercially available In_2O_3 was found to catalyse the reaction, which suggested there could be other impurities present. Thorough cleaning of the synthesised $In(NTf_2)_3$ led to a white solid. However, a decrease in the e.e. from 65% to 59% was found for the

hydrosilane reduction when employing this batch of $In(NTf_2)_3$ which was expected to be caused by the difference in the water content compared to the first batch, as a result of thorough drying the second batch (72 hours *in vacuo* at 150 °C compared to 36 hours *in vacuo* at 130°C) . Different drying processes of new batches were attempted along with examination of the effect caused by water addition to the carefully dried $In(NTf_2)_3$. However, the e.e. was neither improved nor consistent with the different reaction conditions, which is why it was decided to solely use $In(OTf)_3$, which had afforded reproducible result. All results for screening $In(NTf_2)_3$ are found in **Table SI-3.6.2**.

3.7 Screening of a library of 3,3'-substituted BINOLs

Having pushed the optimisation of the system to achieve 73% e.e. with (*R*)-3,3'-I_2-BINOL **3.8 (*R*)**, it was decided to screen the library of 3,3'-substituted BINOL ligands from Prof. Scott Denmark (**Figure 3.7.1**). The results of the screening are found in **Table 3.7.1**.

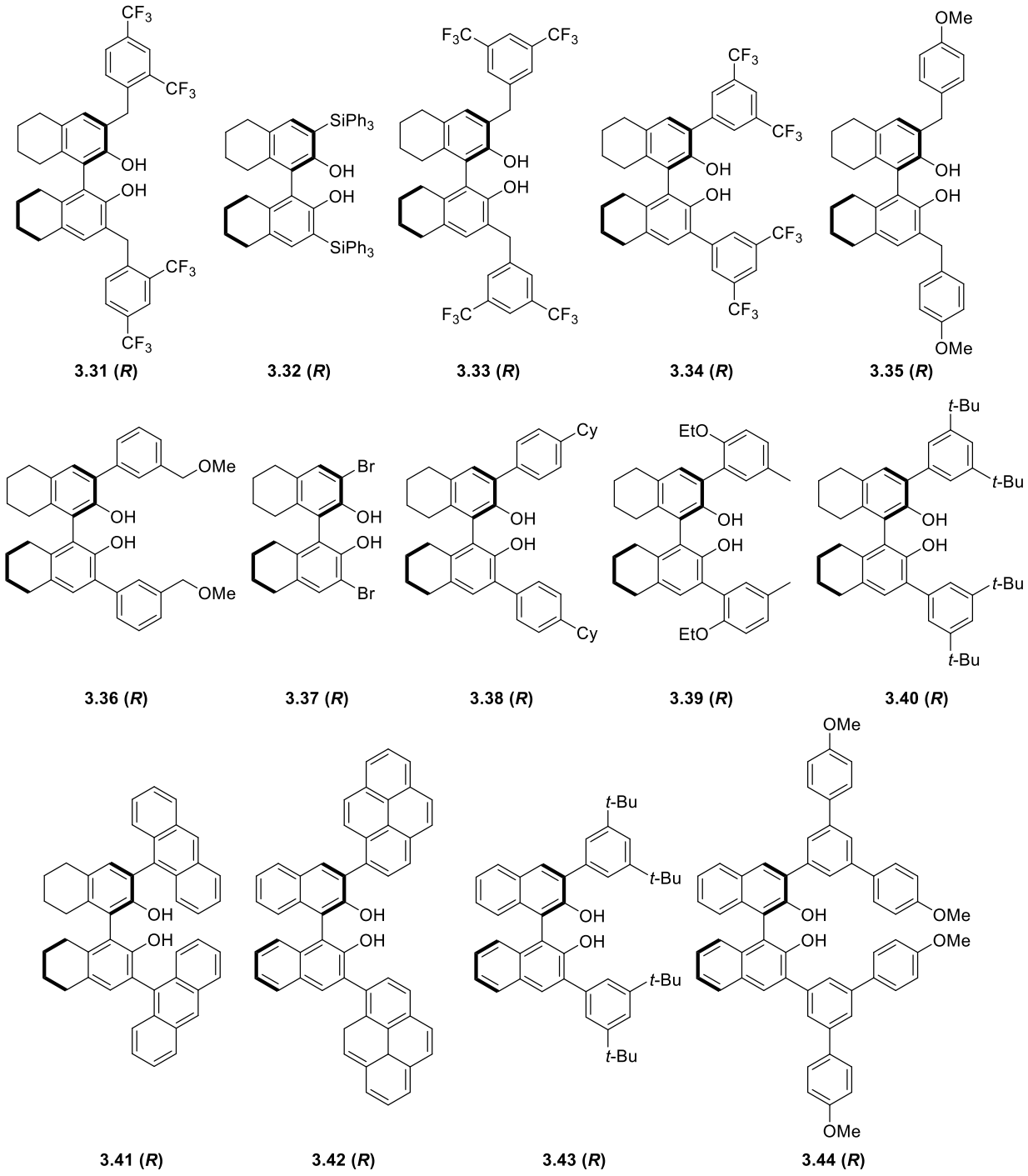

Figure 3.7.1: Library of 3,3'-substituted BINOLs from Prof. Denmark.

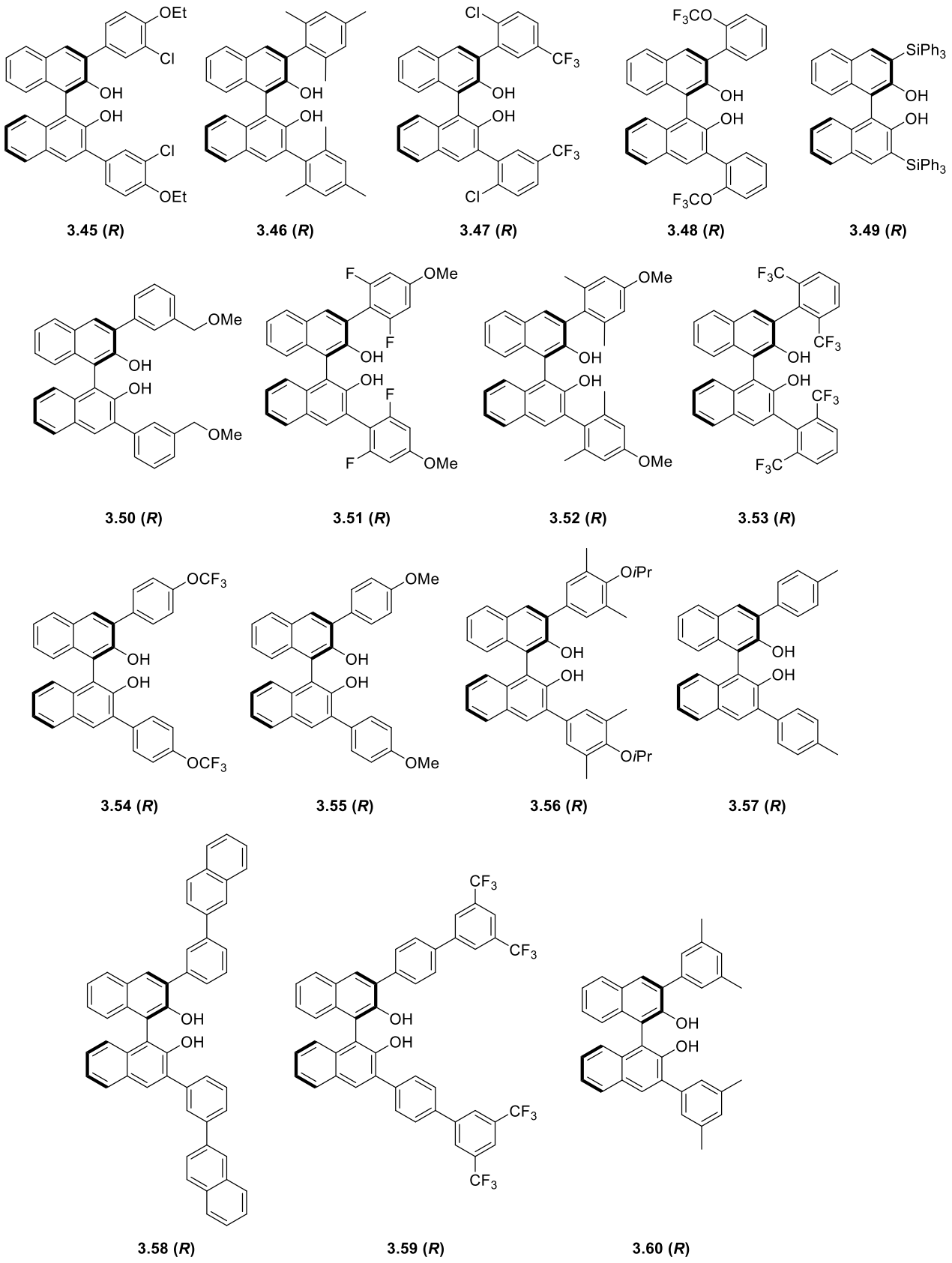

Figure 3.7.1 continued: Library of 3,3'-substituted BINOLs from Prof. Denmark continued.

Table 3.7.1: Screening of the Denmark Library.

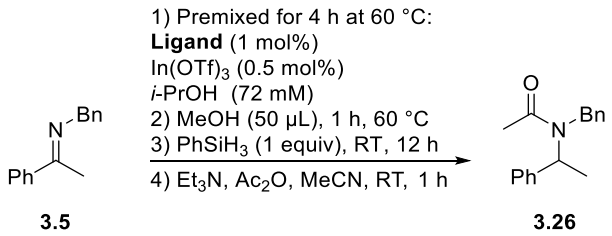

3.5 **3.26**

Entry	Ligand	e.e.[a] [%]	Entry	Ligand	e.e.[a] [%]
1	**3.31 (*R*)**	0	**16**	**3.46 (*R*)**	0
2	**3.32 (*R*)**	0	**17**	**3.47 (*R*)**	8
3	**3.33 (*R*)**	0	**18**	**3.48 (*R*)**	0[b]
4	**3.34 (*R*)**	1[b]	**19**	**3.49 (*R*)**	0
5	**3.35 (*R*)**	0	**20**	**3.50 (*R*)**	2
6	**3.36 (*R*)**	12[c]	**21**	**3.51 (*R*)**	10[b]
7	**3.37 (*R*)**	65	**22**	**3.52 (*R*)**	0
8	**3.38 (*R*)**	3	**23**	**3.53 (*R*)**	0
9	**3.39 (*R*)**	0	**24**	**3.54 (*R*)**	18
10	**3.40 (*R*)**	0	**25**	**3.55 (*R*)**	14
11	**3.41 (*R*)**	0	**26**	**3.56 (*R*)**	5
12	**3.42 (*R*)**	8 [b]	**27**	**3.57 (*R*)**	15
13	**3.43 (*R*)**	4	**28**	**3.58 (*R*)**	0
14	**3.44 (*R*)**	0	**29**	**3.59 (*R*)**	10 [b]
15	**3.45 (*R*)**	10	**30**	**3.60 (*R*)**	4

Each entry represents a single experiment. All reactions carried out with 72 µmol imine. Conversion minimum 99% for all entries. Conversion of imine to amine was determined by crude NMR with 1,3,5-trimethoxybenzene as internal standard. [a] e.e. of the acylated amine determined by chiral stationary phase RP-HPLC. [b] 500 µL *i*-PrOH. [c] 400 µL *i*-PrOH

The results of the screen strongly indicated that the e.e. of the reaction is not dictated by the steric effects of the 3,3'-substituents. The best performing ligand and the only to reach more than 20% e.e. is **3.37 (*R*)** (entry 7), which has bromine in the 3,3'-positions.

A few of the previous screened ligands were screened under these optimised condition (**Table 3.7.2**) to allow for comparison of the results under the optimised conditions. (*R*)-3,3'-(Et_3Si)-BINOL **3.61 (*R*)** [v] was included.

[v] Synthesised by Guillermo Caballero-Garcia, PhD Student, Goodman Group, University of Cambridge.

Table 3.7.2: Screening previously examined ligands under the optimised condtions..

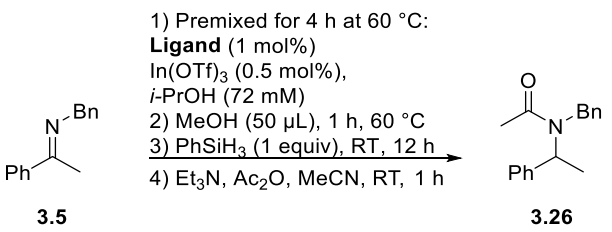

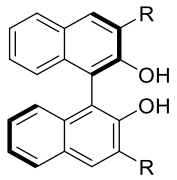

2.1 (*R*), R=H
3.8 (*R*), R=I,
3.10 (*R*), R=(2,4,6-*i*-Pr)-Ph
3.12 (*R*), R= Ph
3.13 (*R*), R=Br,
3.15 (*R*), R=Cl
3.17 (*R*), R=F
3.19 (*R*), R=SBn
3.20 (*R*), R=SO_2Bn
3.27 (*R*), R=(3,5-CF_3)-Ph
3.28 (*S*), S-VAPOL
3.29 (*R*), R=(3,5-Me)-Ph **H_8-BINOL**
3.30 (*R*), R= (2,4,6-Cy)-Ph
3.61 (*R*), R= $SiEt_3$

Entry	Ligand	e.e.[a] [%]
1	**2.1 (*R*)**	7
2	**3.10 (*R*)**	0
3	**3.12 (*R*)**	21
4	**3.13 (*R*)**	59
5	**3.15 (*R*)**	52
6	**3.17 (*R*)**	35
7	**3.19 (*R*)**	19
8	**3.20 (*R*)**	13[b]
9	**3.27 (*R*)**	2
10	**3.28 (*S*)**	15[c]
11	**3.29 (*R*)**	0
12	**3.30 (*R*)**	0
13	**3.61 (*R*)**	0

Unless otherwise noted each entry represents a single experiment. All reactions carried out with 72 µmol imine. NMR conversion of imine to amine: minimum 99% for all entries. Conversion was determined by crude NMR with 1,3,5-trimethoxybenzene as internal standard. [a] e.e. of the acylated amine determined by chiral stationary phase RP-HPLC. [b] average over two reactions. [c] (*S*)-enantiomer in excess.

It is noted how only ligands containing 3,3'-halides afford high e.e. above 30% (entries 4-6). The 3,3'-bisflouride only reach 35% (entry 6), however the bischloro ligand **3.17 (*R*)** afford 52% (entry 5), the bisbromide entire 59% (entry 4), thus the e.e. is found to increase with increasing size of the halide under the optimised conditions, with the bisiodide **3.8 (*R*)** affording 73% e.e. From entry 1 it

is noticed how BINOL afforded 7% e.e., whereas this was found to yield racemic amines with $InCl_3$ in MeOH. In contract, the TRIP-diol gave up to 7% e.e. and under the optimised conditions it affords racemic amines (entry 2). Thus, some variations are found with the source of In(III) employed.

The ligands **3.29 (*R*), 3.30 (*R*)** and **3.61 (*R*)** all afforded racemic products, which based on the results from screened the Denmark library, is not surprising.

3.8 Screening of NON-BINOL Based Ligands

Alongside the work with screening BINOL-based ligands, other types of chiral ligand classes were also screened (**Figure 3.8.1**). (*S*)-VAPOL **3.28 (*S*)** was included in several previous tables including **Table 3.7.2** where it was found to afford 15% e.e. under the optimised conditions. (*R*)-VANOL **3.62 (*R*)** was included to test if the phenyl rings flanking the hydroxy groups in (*S*)-VAPOL was too bulky to allow the ligand to bind to In(III). However, only 6% e.e. was obtained using (*R*)-VANOL, thus suggesting the pocket in VAPOL fits better around the indium metal centre. PYBOX ligands have previously been used for enantioselective indium catalysis, both of these ligand-types were screened. SALEN ligands has been reported through base catalysis to bind In(III) resulting in dinuclear In(III)-complexes.[140–142]

A SALEN ligand, (*R,R*)-(−)-*N,N*′-bis(3,5-di-*tert*-butylsalicylidene)-1,2-cyclohexanediamine **3.63 (*R*)**, was screened both with an without addition of base under the optimised conditions, however the e.e. did not exceed 14%. Two PYBOX ligands, 2,6-bis[(4*R*)-(+)-isopropyl-2-oxazolin-2-yl]pyridine **3.64 (*R*)** and 2,6-bis[(3a*R*,8a*S*)-(+)-*H*-indeno[1,2-*d*]oxazolin-2-yl)pyridine **3.65 (*R*)**, were screened under the optimised conditions, but were both found to afford racemic amines.

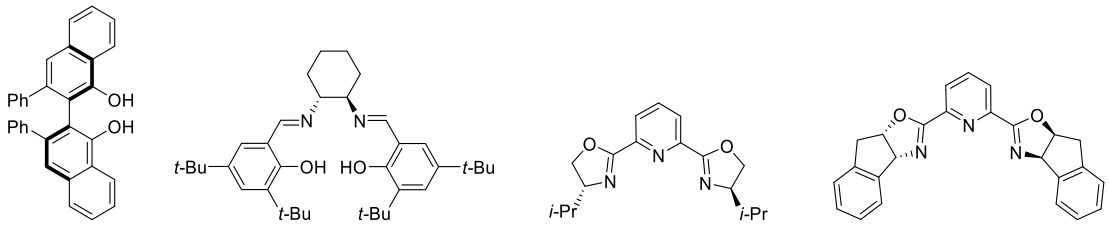

3.62 (*R*) **3.63 (*R*)** **3.64 (*R*)** **3.65 (*R*)**

Figure 3.8.1: Non-BINOL ligands screened as ligands for the In(III)-catalysed reaction.

3.9 Synthesis of New Ligands

As the best results from the previous screenings have been obtained with halogens in the 3- and 3'-position it was decided to synthesise two new ligands; 3,3'-CF_3 and 3,3'-C_6F_5.

(*R*)-3,3'-CF_3-MOM-BINOL **3.66 (*R*)** was synthesised according to the literature[114] (**Scheme 3.9.1**) from (*R*)-3,3-I_2-MOM-BINOL **3.7 (*R*)**. The first time the reaction was carried out it did not go to completion and it was discovered that the major product was (*R*)-3-CF_3-3'-I-BINOL **3.67 (*R*)**. Prolonging the reaction time resulted in the desired product **3.66 (*R*)** as the major product.

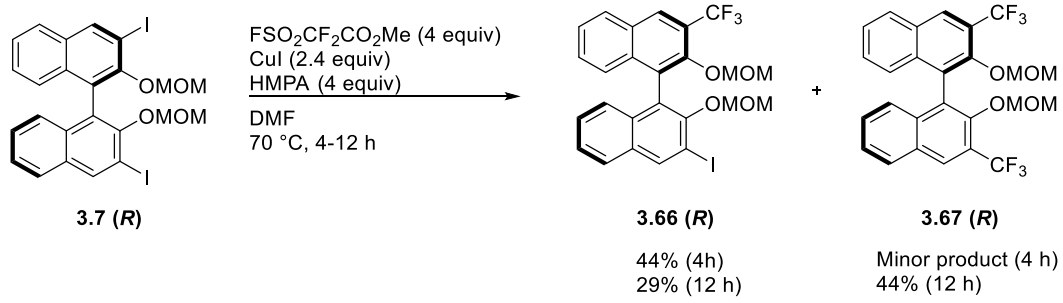

3.7 (*R*) | **3.66 (*R*)** 44% (4h) 29% (12 h) | **3.67 (*R*)** Minor product (4 h) 44% (12 h)

Scheme 3.9.1: Synthesis of **3.66** and **3.67**.

Both **3.66 (*R*)** and **3.67 (*R*)** were deprotected (**Scheme 3.9.10**) to yield the diols **3.68 (*R*)** and **3.69 (*R*)**, which were screened as ligands for the imine reduction (**Table 3.9.1**).

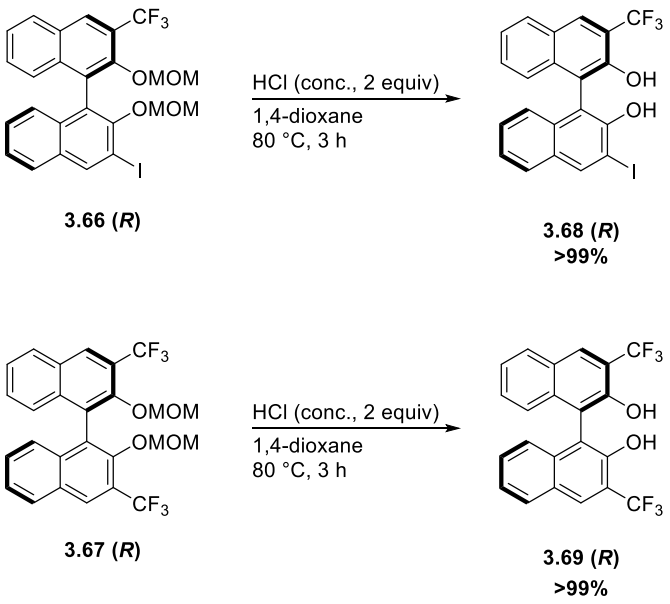

3.66 (*R*) | **3.68 (*R*)** **>99%**

3.67 (*R*) | **3.69 (*R*)** **>99%**

Scheme 3.9.2: Synthesis of **3.68 (*R*)** and **3.69 (*R*)**.

The 3,3'-$(C_6F_5)_2$-BINOL ligand **3.70 (*R*)** was synthesised from (*R*)-MOM-BINOL **3.8 (*R*)** in 72% yield in accordance with the literature[143] (**Scheme 3.9.3**). Subsequent deprotection yielded the desired diol ligand **3.71 (*R*)**.

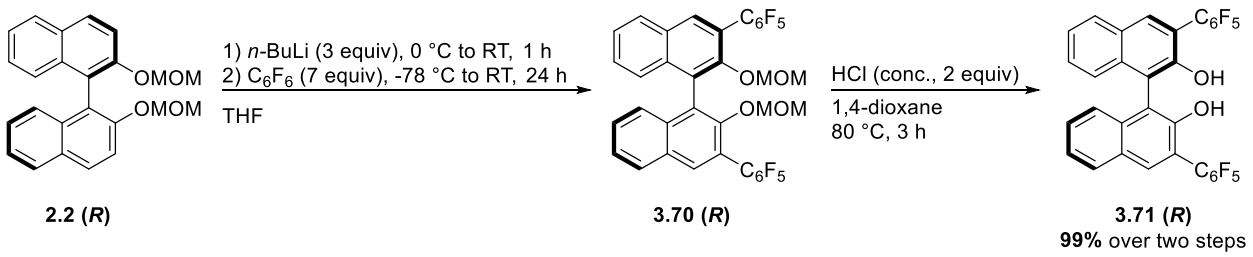

Scheme 3.9.3: Synthesis of **3.71 (*R*)**

Using (*R*)-3,3'-Br_2-H_8-BINOL (**3.37 (*R*)**, **Figure 3.7.1**) resulted in a higher e.e. (65%) than when (*R*)-3,3'-Br_2-BINOL **3.13 (*R*)**, was employed as ligand (59%). It was hypothesised the same trend could be observed for the (*R*)-3,3'-I_2-H_8-BINOL **3.73 (*R*)**. Therefore, also this ligand was synthesised (**Scheme 3.9.4**) as reported in the literature.[144]

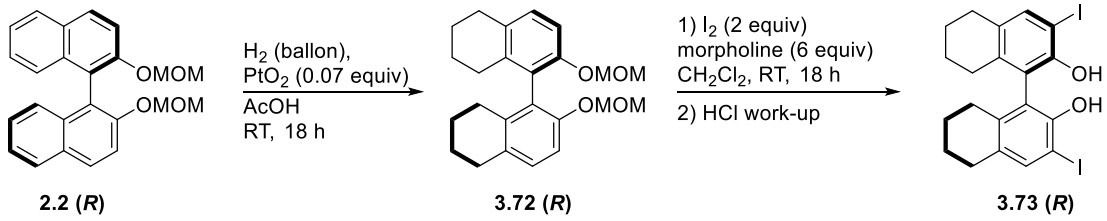

Scheme 3.9.4: Synthesis of **3.73 (*R*)**

Commercially available (*R*)-6,6'-Br_2-BINOL **3.74 (*R*)** (**Figure 3.9.1**) was also included in the screenings, to compare the effect of the halogens position on the naphthol ring.

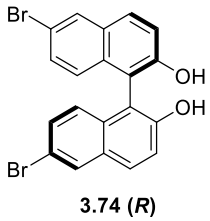

Figure 3.9.1: (*R*)-6,6'-Br_2-BINOL **3.74 (*R*)**

These ligands were screened under the optimised conditions (**Table 3.9.1**).

Table 3.9.1 Screening the new ligands under the optimised conditions.

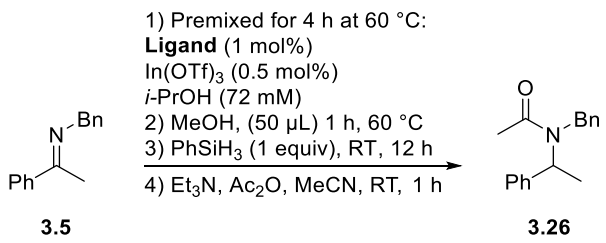

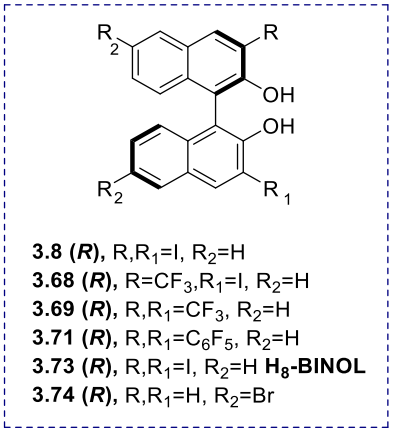

Entry	Ligand	e.e.[a] [%]
1	**3.8 (*R*)**	73[b]
2	**3.68 (*R*)**	64[b]
3	**3.69 (*R*)**	58[b]
4	**3.71 (*R*)**	15[b]
5	**3.73 (*R*)**	72[b]
6	**3.74 (*R*)**	6

Unless otherwise noted each entry represents a single experiment. All reactions carried out with 72 µmol imine. NMR conversion of imine to amine: minimum 99% for all entries. Conversion was determined by crude NMR with 1,3,5-trimethoxybenzene as internal standard. [a] e.e. of the acylated amine determined by chiral stationary phase RP-HPLC. [b] Average over two reactions.

The results in **Table 3.9.1** confirms the need of electronic effects directly in the 3,3'-position. The difference between the 3,3'-I_2-BINOL (entry 4) and the H_8 version of this ligand **3.73 (*R*)** (entry 5) is insignificant. The increase in e.e. from **3.69 (*R*)** affording 58% (entry 3) to 64% with **3.68 (*R*)** (entry 2) where one CF_3 substituent is replaced by iodine and finally **3.8 (*R*)** with 73% (entry 1) when both the 3 and 3'-substituent is iodine is remarkable.

Attempting to develope a better understanding of the correlation of the ligand properties and the e.e., computational investigations of different ligand properties such as the dihedral angle, the O-In bond length and the partial charge of the oxygen etc. were carried out. Unfortunately, no clear trends were observed. The majority of the ligands screened resulted in racemic amines which ultimately limited the meaningful entries in a multivariate analysis such as quantitative structure-activity relationship. At the point of submission of this thesis, no meaningful outcomes had been made and therefore these computational investigations are not included in this thesis.

3.10 The effect of the *N*-substituent

Two different imines were synthesised to examine the effect of the amine substituent.

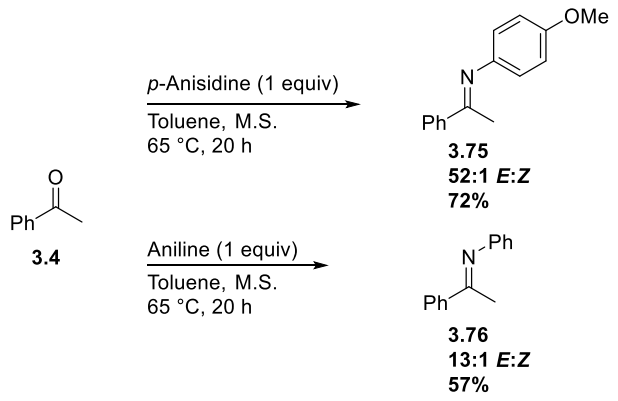

Scheme 3.10.1: Synthesis of two imines **3.75** and **3.76** with *N*-phenyl groups.

This imine was reduced with $NaBH_4$ to afford amine **3.84**, which was acetylated to be used as racemic reference for HPLC analysis of the e.e.

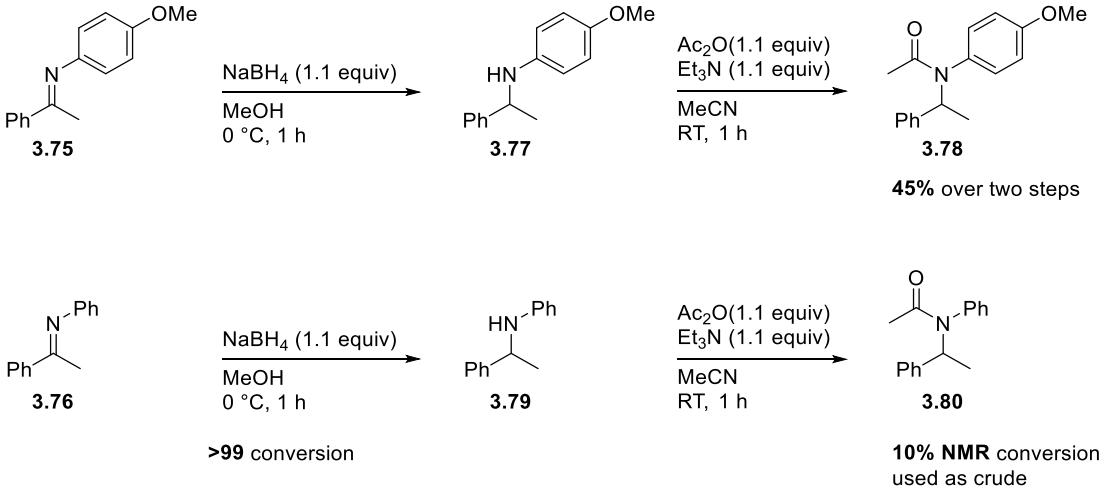

Scheme 3.10.2: Racemic reduction followed by acylation for afford **3.78** and **3.80** for HPLC references.

Both of these two imines resulted in racemic amines when reduced under the developed In(III)-catalysed system with **3.8 (*R*)** as ligand. This strongly suggest the CH_2 group plays and important role in the mechanism. Potentially steric bulk on this position could preventing LA interactions with an In(III) could. The CH_2 group in **3.5** enables the phenyl ring (red, **Figure 3.10.1**) to rotate, thus avoiding steric interactions with a co-ordinating In(III)-complex (**Figure 3.10.1 a** and **b**). In contrast hereto, the *N*-phenyl substituent is locked in its position resulting in what appear as a somewhat similar sized cavity on either side (**Figure 3.10.1 c**). Furthermore, this imine is flat,

whereas the *N*-benzyl imine the sp_3 hybridised CH_2 group allows the phenyl ring to bend out of the plane (**Figure 3.10 a** and **b**). The influence of the CH_2 group will be further discussed in Chapter 5.

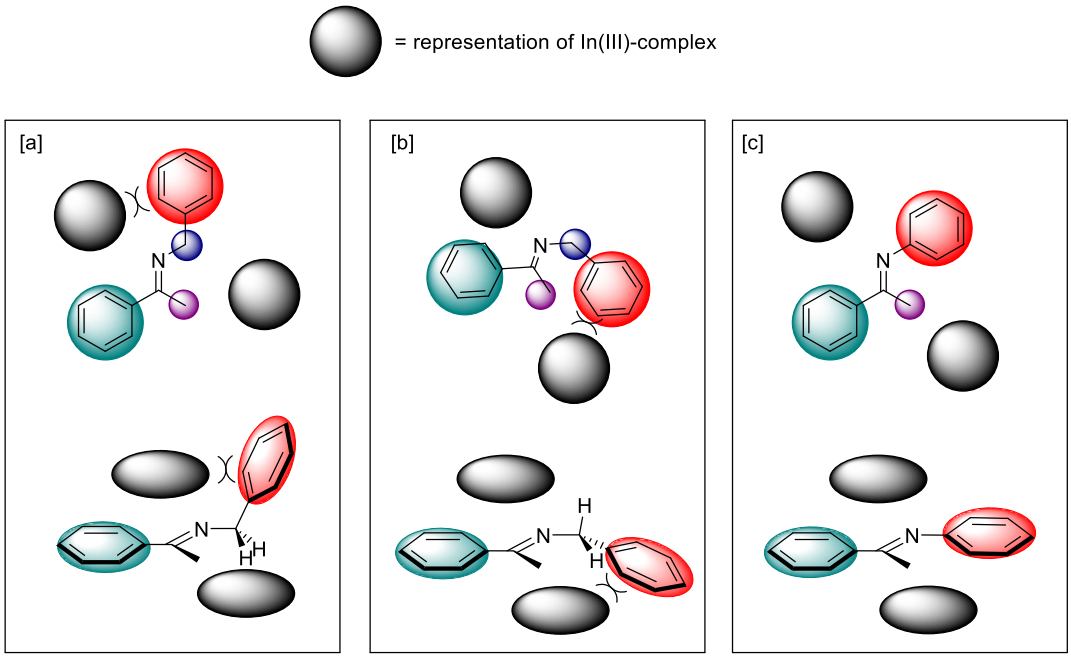

Figure 3.10.1: [a] and [b]: The flexible CH_2 position in imine 3.5 allows for rotation. [c] In imine **3.76** the *N*-phenyl substituent is locked in the plane.

Based on the influence of this CH_2 group it would have been very interesting to examine the effect of only partially blocking the *N*-α position as in imines **3.81**-**3.82** (**Figure 3.10.2**). As the new substituent introduce a second chiral centre, it would be interesting to examine how the results for a racemic mixture in **3.81** compare with the enantiomeric pure **3.81 (*R*)**. Furthermore, the electron influence from this position could be investigated using imine **3.82** with the electron withdrawing CF_3 substituent.

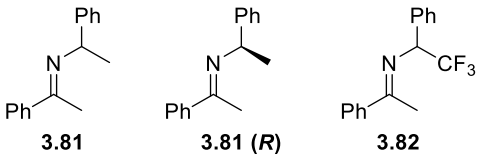

Figure 3.10.2: Imines with increased steric bulk α to the imine nitrogen.

Unfortunately, due to time constrains this imine was not synthesised.

An imine **3.83** with an extended chain between the nitrogen and the phenyl ring was synthesised (**Scheme 3.10.3**) to examine the effect of extending the alkyl chain increasing the space between the imine nitrogen and the phenyl ring.

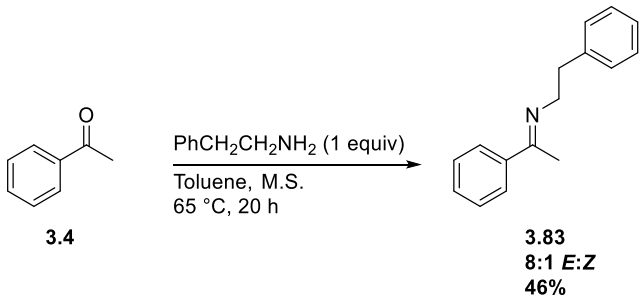

Scheme 3.10.3: Imine **3.83** with extended alkyl chain on the imine nitrogen.

This imine was reduced with $NaBH_4$ to afford amine **3.84**, which was acetylated to be used as racemic reference for HPLC analysis of the e.e.

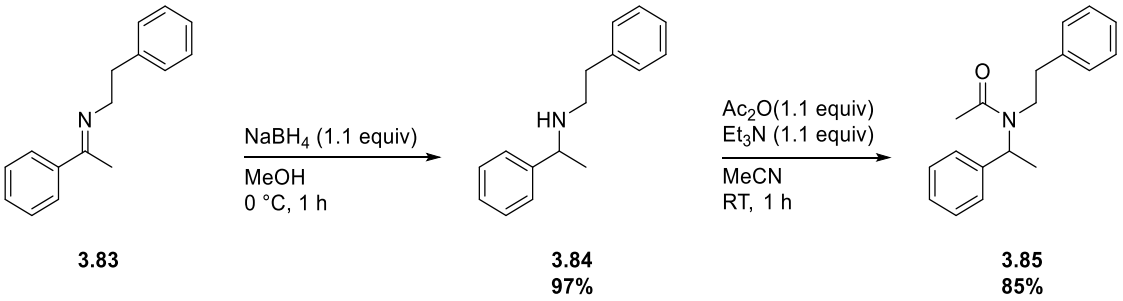

Scheme 3.10.4: Racemic reduction followed by acylation to afford amide **3.85** for HPLC reference.

The imine was then tested under the optimised conditions for the In(III)-catalysed hydrosilane reduction. HPLC/SFC analysis is ongoing.

To examine the effect of a *N*-alkyl-substituent *n*-butyl imine **3.86** was synthesised (**Scheme 3.10.5**).

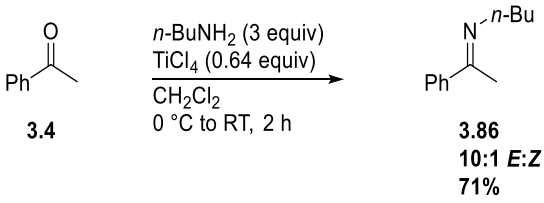

Scheme 3.10.5: Synthesis of *N*-butyl-(1-phenylethylidene)amine **3.86.**

This imine was reduced with $NaBH_4$ to afford amine **3.87**, to be used as racemic reference for HPLC analysis of the e.e. (**Scheme 3.10.6**).

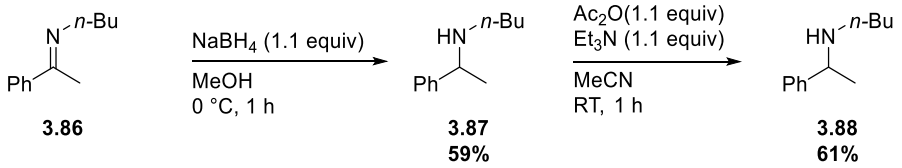

Scheme 3.10.6: Synthesis of two imines **3.42** and **3.43** with *N*-phenyl groups.

The imine was then tested under the optimised conditions for the In(III)-catalysed hydrosilane reduction. HPLC/SFC analysis is ongoing.

Plans were made to synthesise and test the influence of various substituents effect on the benzyl ring. However, as the importance hereof was realised too late, time constrains did not allow for this work to be carried out.

The imines planned to be synthesised are shown in **Figure 3.10.3**.

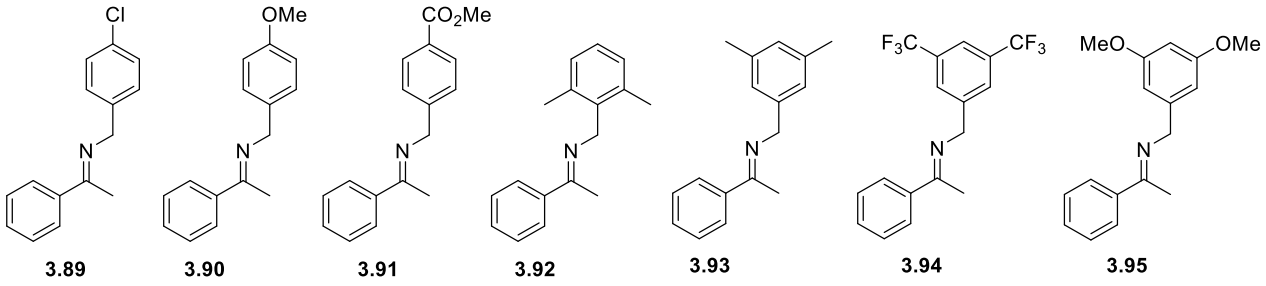

Figure 3.10.2: Imines planned synthesised to examine how varying steric and electronic effects on the *N*-Benzyl ring effects the e.e.

As will be discussed in Chapter 5 the computational mechanisms investigated suggest the R substituent in *N*-CH_2-R to be of little importance. If this is true the imines shown in **Figure 3.10.2** would have yielded amines in similar e.e. as the standard imine all the previous tests have been carried out on, under the optimised conditions.

Furthermore, it would have been interesting to examine the effect of the α-alkyl group e.g. examining the ethyl and propyl imines **3.96** and **3.97** (**Figure 3.10.3**), as well as increasing steric bulk on this position e.g. the effect of a *t*-Bu substituent at the α-position (**3.98**).

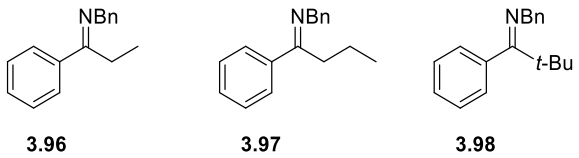

Figure 3.10.3: Imine with extended α-alkyl chains

3.12 Conclusion

An Indium(III)-catalysed hydrosilane reduction of imines was developed and optimised to afford 73% e.e. using (*R*)-3,3'-I_2-BINOL. The reaction provided promising e.e. only in polar protic solvents and the e.e. was dependent on the amount of MeOH present. The e.e. increased with premixing of the ligand and catalyst at elevated temperatures and with decreasing the concentration of the imine to 72 mM. The optimal solvent system was a mixture of *i*-PrOH and MeOH. Various reducing agents were screened; however, only $PhSiH_3$ efficiently reduced the imine. The addition of base had varying effects on the e.e. and ultimately did not result in higher e.e. than the 73% achieved without base. Of the many ligands screened, including both non-BINOL ligands and more than 50 BINOL-type ligands, only ligands with electronic effects directly in the 3,3'-positions yielded amines in moderate to good e.e. Aromatic *N*-substituents resulted in racemic amines, indicating that the alkyl position α to the nitrogen has mechanistic importance; the In(III) complex is likely to act as a LA. Optimisation examining the effects of varying the substituents on the *N*-benzyl ring along with extending the alkyl chain of the α-CH_3 group remain to be examined.

Chapter 4: Initial Investigations of Indium(III) Complexes

The experimental and computational mechanistic investigations described in this and the two following chapters were carried out alongside the methodology work described in Chapter 3 on optimising the reaction. This chapter describes the initial investigations carried out in the first year of this project.

4.1 BINOL-Metal Complexes

As described in Section 1.3, the initial choice of ligand for inducing chirality in the In(III)-catalysed hydrosilane reduction was BINOL-type ligands. These had already been used for obtaining excellent e.e. in In(III)-catalysed allylations and alkynylations of carbonyls.[82,83] Furthermore, the C_2-symmetric axis in the BINOL scaffold allows for computationally cheaper analysis. Oxophillic metals have been widely employed as LAs in combination with oxygen-containing ligands, such as BINOL. Through substitution, the versatile backbone in BINOL and its derivatives can be modified to affect not only the steric environment around the metal centre, but also the electronic properties of the oxygen atoms influencing the Lewis acidity of the metal centre and thus the reaction environment.[145] BINOL and its derivatives have been reported to bind well to many metals including main-group, transition-metal and lanthanide compounds. The catalysts-complexes formed often exhibit high levels of enantioselectivity and efficiency.[146–149] The skewed conformation of the BINOLate ligand results in a rigid chiral metallacycle.[150] Substituents at the 3,3'-position typically extend the direction of the substrate binding site, thus conveying asymmetry to the substrate (**Figure 4.1.1**). However, for the parent BINOLate, where the hydrogen atoms at the 3,3'-position are too small to protrude into the metal binding site, the discrimination between the enantiomers may be explained by electronic dissymmetry in the co-ordination sphere of the metal, arising from the skewed conformation of the BINOL scaffold.[151]

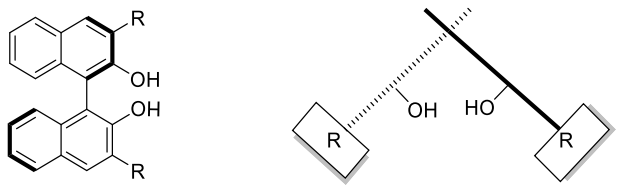

Figure 4.1.1: Left: 3,3'-substituted BINOL. Right: The Goodman projection of a 3,3'-substituted BINOL, which visualises the enclosure of the metal binding site by these substituents.

The reported examples of metal BINOLate complexes extend to include multimetallic catalyst complexes, which offer advantageous co-operative catalytic activity. One of the most famous

examples of this class of catalysts is Shibasaki's hetero-bimetallic rare-earth metal BINOLate complexes (**Figure 4.1.2**). In these complexes the rare-earth metal functions as a Lewis acid, while the alkali metal BINOLate acts as a Brønsted base.[152]

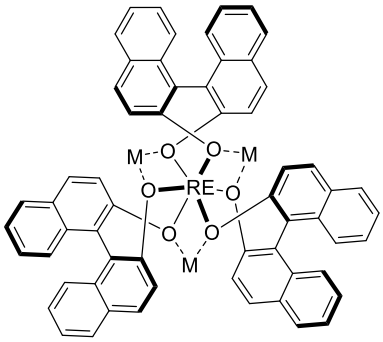

Figure 4.1.2: General representation of the Shibasaki catalysts. RE =rare-earth metal, M = alkali metal.

The first screenings performed (discussed in section 3.3) yielded racemic amines. For several of these, a grey substance had been observed, which could indicate formation of solid In(0). Metallic In(0) could be a result of the decomposition of InH_2, and as this hydride, being unbound to any chiral ligands, would yield racemic amines, complex formation was targeted. In the literature,[82,83] the In(III)-BINOL complex had not been characterised. However, both studies reported good enantioselectivity, which could only be explained by formation of some sort of chiral complex.

4.1.1 Crystal Field Theory and Geometry of Metal Complexes

Crystal field theory (CFT) is extensively used, especially within transition metal complexes, to explain a number of features of co-ordination complexes. In CFT the ligands in metal complexes are treated as point charges and the complex is considered to be held together by the electrostatic attraction between the metal ion, the LA, and the negative ligand point charges, the Lewis bases. Specifically, the interaction between the ligand point charges and the metal d-orbitals are considered. The electrostatic repulsion results in loss of degeneracy, since the interactions between the ligands and the d-orbitals are stabilising in some geometric orientation and destabilising in others. For example, the orbitals along the axis in an octahedral complex are directly aligned with the ligand and therefore destabilised through electrostatic repulsion, whereas the remaining three orbitals are stabilised. The energy gap between the set of stabilised orbitals and the set of destabilised orbitals is called the crystal field splitting energy (CFSE). The stabilised orbitals are lowered by the same amount of energy by which the destabilised orbitals are raised. CFSE is affected by the charge on the metal ion, the nature of the metal ion (e.g. the valence electron configuration) and the nature of the ligand. The

ligand can be either a strong field ligand, resulting in a large value of CFSE, or a weak field ligand, resulting in a small value of CFSE.[153]

4.2. Progress towards Characterising Indium-BINOL Complexes

Initially, isolation of the potential complex was attempted from the mixture of In(III) bromide, (*R*)-BINOL, dichloromethane and either DIPEA or THF. However, in both cases both the ^{1}H NMR and IR spectra were identical to BINOL. The initial ^{1}H NMR studies of the In(III)-BINOL-DIPEA solution had indicated complex formation as a change in chemical shift had been observed. However, this could be caused by indium co-ordinating DIPEA. Complex formation by refluxing a solution of (*R*)-BINOL and In(III) bromide in THF also proved unsuccessful.

Characterisation by mass spectrometry[vi] proved inconclusive; no mass corresponding to a compound consisting of both indium and BINOL could be detected. However, there are three possible explanations for this: either the complex does not exist, decomposes before detection or is not being ionised and therefore is not detected. In the literature,[154,155] examples of indium complexes with organic ligands characterised by mass spectrometry have several electronegative atoms co-ordinated to indium. If three BINOL molecules were co-ordinated to In(III), the In(III) metal centre would be surrounded by six oxygen atoms, which is expected to increase the probability of ionisation and detection of this complex by mass spectrometry. The majority of indium complexes with organic ligands reported (with characterisation) in the literature[155–158] have been synthesised employing irreversible deprotonation of the heteroatoms co-ordinating to the In(III) metal centre. One example, indium(III)-tris(dibenzyldithiocarbamato), $In(S_2CNBz_2)_3$, was synthesised from the sodium salt of the organic ligand and In(III) chloride.[155] Therefore, BINOL was deprotonated using sodium hydride and subsequently mixed with the indium salt. This was initially performed in THF. When adding In(III) bromide a white precipitate was observed. However, as the ^{1}H NMR of the resulting solution contained an increased number of different aromatic signals and no sign of hydroxyl protons, it was hypothesised that a mixture of In(III)-BINOL compounds was obtained, and to avoid further complication by THF co-ordination it was decided to use a non-co-ordinating solvent instead. As described in Section 3.3. the deprotonation proved of very limited success in dichloromethane, but successful in toluene. Formation of precipitate upon addition of In(III) bromide was not observed. The reaction proceeded with limited conversion and in the presence of (*R*)-BINOL it was inhibited. Thus, whatever complex formed was inactive.

[vi] Both ESI-MS and ASAP-MS was performed.

An entirely different approach was then investigated. Silver is known to be a Köenigs-Knorr promoter,[159] thus a silver salt e.g. silver carbonate can promote dehalogenation, which should increase the reactivity of In(III) towards BINOL (**Scheme 4.2.1**).

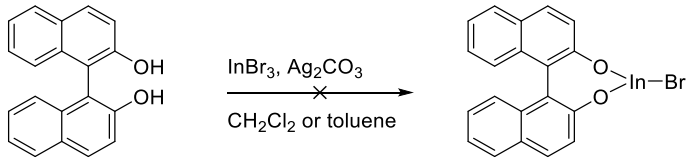

Scheme 4.2.1: Planned synthesis of an In(III)-BINOL complex by silver promoted dehalogenation of the $InBr_3$.

However, in only one out of eight attempts did silver carbonate seem to have an effect. In this case the greenish powder of the silver carbonate turned into solid chunks which could be silver bromide. The reaction mixture was filtered and crystallised from the solution. Both ^{1}H NMR and IR did not differ significantly from the spectra of BINOL. ASAP-MS only found BINOL and though the appearance of the crystals were visually different from those of BINOL (when recrystallised following the same procedure) an X-ray structure concluded that the crystals were indeed BINOL.

4.3. Multimetallic Complexes

It was of utmost importance to be able to form and characterise an In(III)-BINOL complex and the most promising indication of the formation of a such complex had been with sodium hydride and THF. THF had originally been abandoned as solvent as it is known to co-ordinate to In(III) and it was wished to avoid this additional complication. However, as the experiment was performed, indications of complex formation were observed: addition of In(III) bromide to the solution of deprotonated BINOL in THF resulted in formation of a white precipitate, potentially sodium bromide. Furthermore, significant changes in the ^{1}H NMR spectrum of the resulting solution were observed. Characterisation of a complex directly from the reaction mixture had not proven successful; thus, it was decided to attempt to crystallise a complex from the reaction mixture. If crystals could be obtained an X-ray study would reveal whether or not a complex was formed. Two reactions were performed, one with racemic BINOL and one with enantiomerically pure (*R*)-BINOL. Only 2.2 equiv of BINOL were employed, hoping to co-ordinate only two BINOL molecules to In(III) as this would allow for the possibility of a bromine atom also being attached to In(III). This is needed if the hydrosilane reduction is to proceed via a reactive In(III) hydride species according to the literature.[75,76] Sodium hydride was employed for deprotonation and overnight stirring with In(III) bromide (**Scheme 4.3.1**).

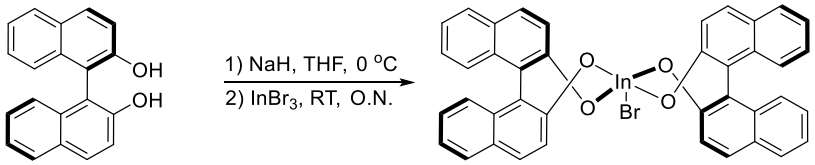

Scheme 4.3.1: Reaction with (*R*)-BINOL planning to co-ordinate two (*R*)-BINOL molecules to In(III).

Crystallisation of the supernatant from the reaction with (*R*)-BINOL resulted in colourless square crystals. A sample was removed for IR and ^{1}H NMR analysis. When removed from the THF solution these crystals seemed to dry out to give a yellow-beige solid. After being dried ^{1}H NMR indicated an average of 1.5 hydroxy protons per BINOL, which was less conclusive. However, the IR spectrum obtained differed significantly from the IR spectrum of BINOL, and the remaining crystals where submitted for X-Ray. An X-Ray of the crystals revealed a multimetallic complex of [{In((*R*)-BINOLate)$_3$}{Na(THF)$_2$}$_3$] (**Figure 4.3.1** & **Figure 4.3.2**) where sodium ions co-ordinate to the oxygen atoms of BINOL and THF co-ordinate to sodium.

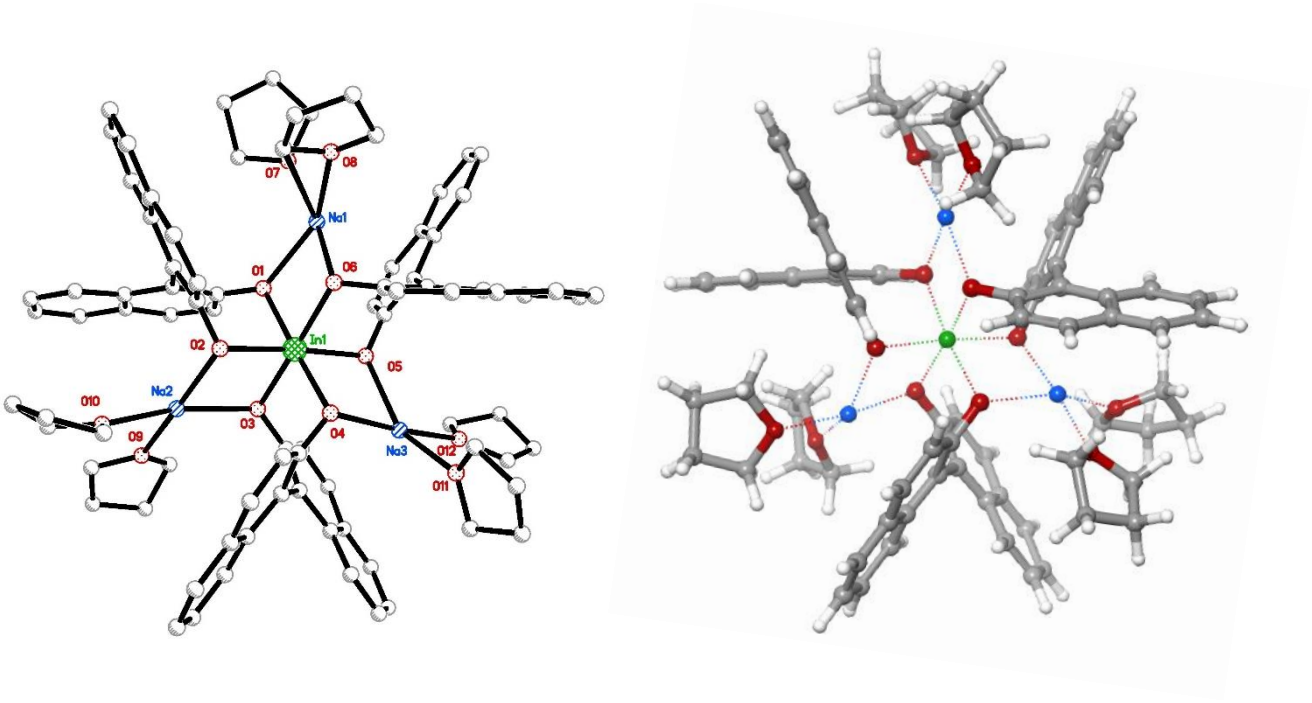

Figure 4.3.1: Left: The X-ray structure. Right: The Maestro model where hydrogen atoms are visible.

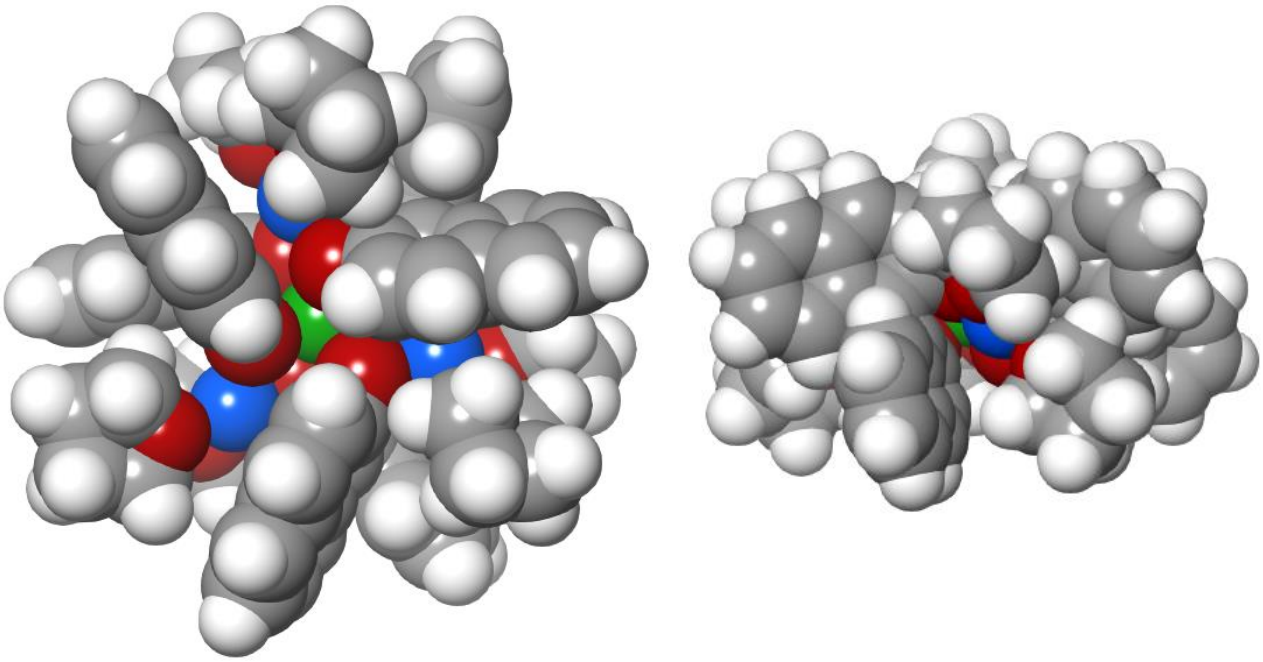

Figure 4.3.2: Space-filling model of the complex. Left: Top view as the X-ray structures. Right: Sideview.

This structure is very similar to Shibasaki's (RE-BINOL$_3$)M$_3$[vii] (section 1.2.) with the rare-earth metal replaced by In(III). Despite only 2.2 equiv of (*R*)-BINOL have been used, three (*R*)-BINOL molecules were co-ordinated to In(III) ion, which is not unexpected according to the literature.[155] Furthermore, irreversibly deprotonated BINOLs are expected to bind the In(III) ion stronger and thus cf. CFT it is not surprising they favour a different geometry around the In(III) metal centre, than the complexes that shall be presented in Chapter 5, where one or more deprotonated BINOL's have been replaced e.g. with solvent molecules

Interestingly, when racemic BINOL had been employed, otherwise following the exact same procedure, something different happened. Both the IR and ^{1}H NMR spectra exhibited close similarity but, it was not possible to crystallise and thus characterise the yellow-beige solid obtained.

The hydrosilane reduction of the imine was attempted with this sodium complex[viii] and catalytic activity, though limited, was observed. As the complex had been formed with only 2.2 equiv of (*R*)-BINOL, but each In(III) ion was co-ordinated to three (*R*)-BINOL molecules, another test reaction was performed, this time starting from 3.2 equiv of (*R*)-BINOL to ensure that all In(III) was fully co-ordinated to BINOL. In this reaction no trace of product was observed, indicating that the initially observed product formation was catalysed by In(III) in the solution which was not co-ordinated to

[vii] RE= rare-earth, M = alkali metal
[viii] With the rest of the dried solid from characterisation, while the crystals where submitted for X-ray.

BINOL. This would not lead to any enantioselectivity in the product. The space-filling model of the crystal structure (**Figure 2.5.2**) indicated a very inaccessible In(III) centre. Thus, it was not entirely surprising to find no catalytic activity. It was speculated if alterations of the alkali metal would result in less hindered access to the metal centre. The crystallographic database revealed that multimetallic complexes with In(III)-((*S*)-BINOL)$_3$ with lithium had already been synthesised with different co-ordinating solvents depending on the crystallisation method.[160,161] The literature procedures[160–162] where followed (with minor modifications) to synthesise an In(III)-(BINOLate)$_3$ complex with lithium and THF (**Scheme 4.3.2**).

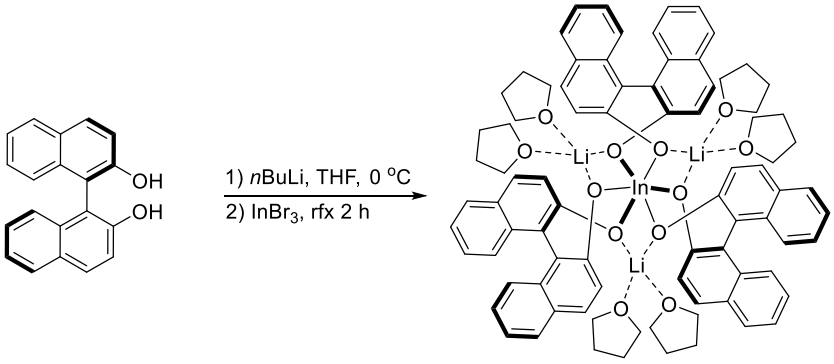

Scheme 4.3.2: Synthesis of [{In((*R*)-BINOLate)$_3$}{Li(THF)$_2$}{Li(THF)}$_2$]

Based on the In(III)-((*R*)-BINOLate)$_3$ complex with sodium and THF, it was hypothesised that each lithium ion would co-ordinate two THF molecules. However, according to X-ray crystallography this turned out not to be the case. In the literature,[163] this complex has been reported with either four or five THF molecules co-ordinating to lithium, thus the obtained crystal structure corresponds well hereto. The X-ray structure of the complex (**Figure 4.3.3**) differs from the sodium version of this In(III)-((*R*)-BINOLate)$_3$ complex in both the co-ordination of lithium, the crystallographic symmetry and the 3D geometrical outcome of the naphthalene rings.

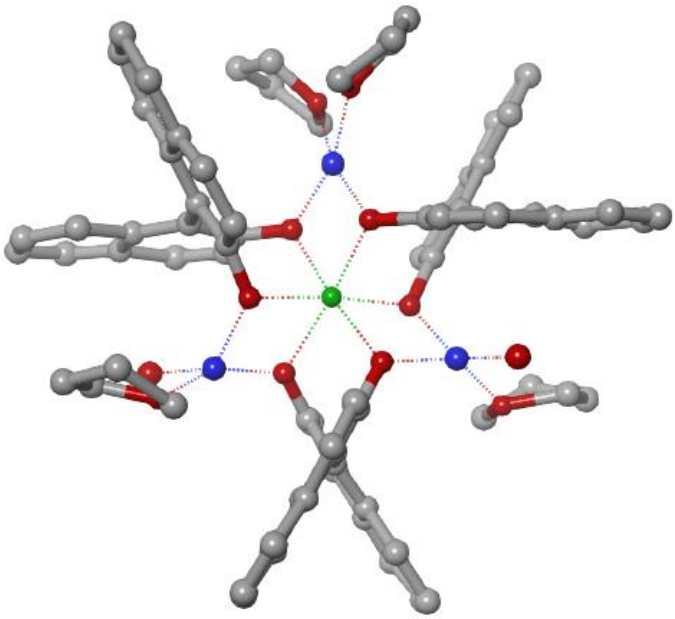

Figure 4.3.3: Maestro view of the X-ray structure.

The X-ray structure in **Figure 4.3.3** reveals a variation in the number of THF molecules co-ordinating to the lithium atoms. Crystallisation of this complex was not performed under strictly anaerobic conditions, as the reaction mixture was exposed to air during the filtration, which can explain what appears to be a co-ordinating water molecule at one of the lithium atoms. Similarly, crystallisation of the sodium version of this complex was not performed under strictly anaerobic conditions. However, two THF molecules are co-ordinated to each sodium atom. This may very well be the thermodynamically favoured structure, whereas for the smaller lithium atom sterically unfavourable interactions may occur when two THF molecules attempt to fit into this smaller available space. Thus, the presence of water may in this case lead to a ligand exchange equilibrium, which may be the cause of the problems refining the structure, resulting in what visually appears as distortion of the naphthalene rings (**Figure 4.3.4**).

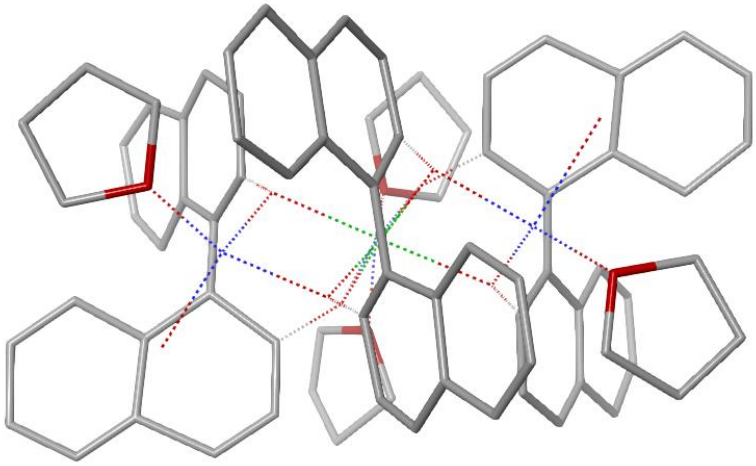

Figure 4.3.4: View of the naphthalene rings to show the distortion.

The R-factor[ix] for this structure is good (0.0834), but due to the distortion of the naphthalene rings this crystal structure in **Figure 4.3.3** must be interpreted with caution.

Crystal structures found in the literature[160] consist of two different structures (**Figure 4.3.5**), in which the amount of co-ordinating THF varies. Crystallisation was performed in THF and toluene after filtration. However, the reaction scale was significantly higher (40 times), thus enabling inert filtration.

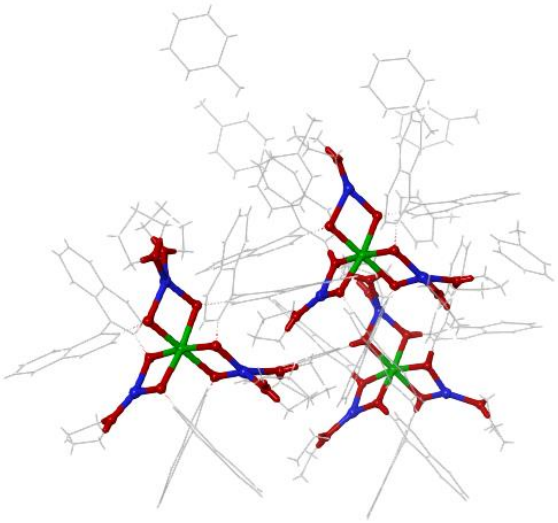

Figure 4.3.5: The X-ray structure (FUBFUD)[160] of similar complexes. The indium metal centres are highlighted along with the THF co-ordination sites, to show how the THF co-ordination varies: in the left structure two of the sodium atoms co-ordinate two THF molecules each, whereas in the two complexes shown to the right, only one sodium atom co-ordinates two THF, but those two complexes are rotated relative to each other.

[ix] The R-factor is a measure of how well the crystallographic model (the refined structure) predicts the experimental X-ray diffraction data.

Comparison of the geometry around indium in the sodium and the lithium complexes of In(III)-((*R*)-BINOLate)$_3$ indicates a large degree of similarity between these two structures (**Figure 4.3.6**).

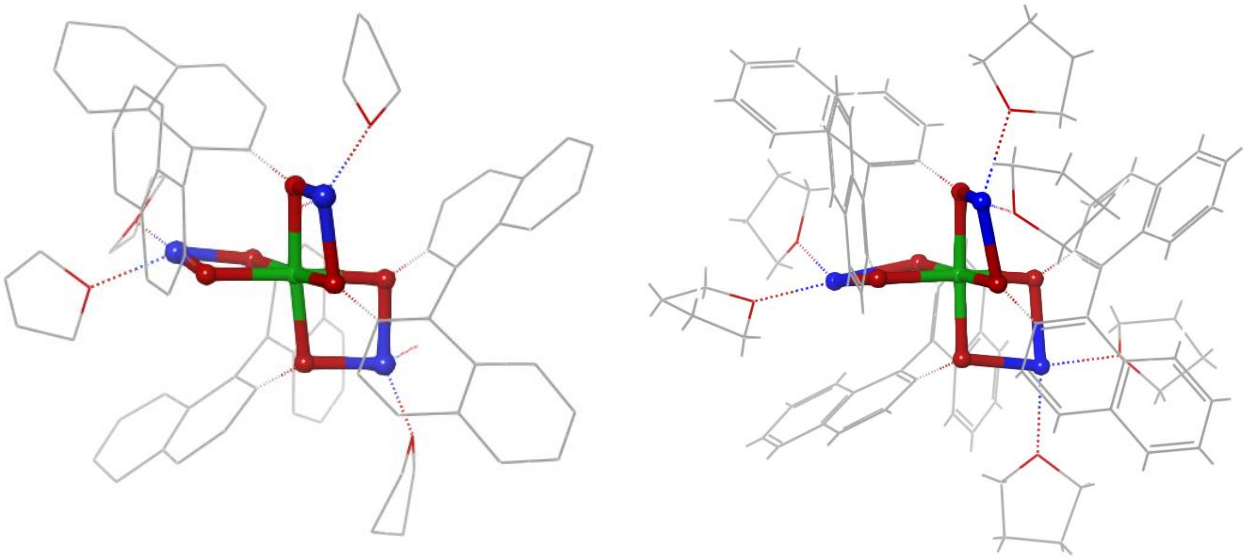

Figure 4.3.6: Comparison of the geometry around indium in the indium((*R*)-BINOLate)$_3$-lithium complex (left) and the In(III)-((*R*)-BINOLate)$_3$-sodium complex (right).

Though the crystal structure does not give exact information about the entire system for the lithium indium-BINOLate$_3$ complex, it does conclude that three BINOLate moieties are co-ordinated to indium, and, overall, shows a complex that is similar to the [{In((*R*)-BINOLate)$_3$}{Na(THF)$_2$}$_3$] complex (**Figure 4.3.1** and **Figure 4.3.2**).

The synthesis of an In(III)-(BINOL)$_2$-potassium complex (**Figure 4.3.7**) was reported from the Shibasaki group.[164] This complex had been synthesised and employed directly for enantioselective nitroaldol reaction. However, no characterisation of the complex was reported.

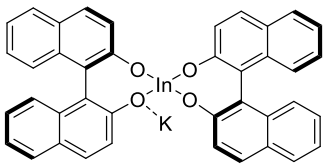

Figure 4.3.7: The suggested structure of the indium(III)-((*R*)-BINOL)$_2$-potassium complex.[164]

Interestingly, Arai *et al.*[164] examined the lithium, sodium and potassium versions of the bimetallic complex depicted in **Figure 4.3.7** and found that the enantioselectivity drastically increased with the size of the alkali metal; lithium gave an e.e. value close to zero, whereas the e.e. value obtained when employing the potassium complex was above 80%. Moreover, the reaction time also significantly

increased with the size of the alkali metal. Thus, for potassium a week more was needed for the reaction to go to completion.[164] For this specific nitroaldol reaction, the analogue gallium complex gave more promising results. However, even though gallium and indium are both main group 13 metals, indium is often superior when it comes to appealing properties such as stability towards air, water and alkaline conditions. This contributes to indium complexes being attractive to work with.[13]

Furthermore, this proposed In(III)-((*R*)-BINOLate)$_2$-potassium complex has co-ordination number four for In(III). Thus, there is a vacant co-ordination site, which could account for the catalytic ability and observed enantioselectivity induced by the complex.[161,164] However, examples (though fewer in number) have also been reported of metal centres with co-ordination number six that are still capable of performing enantioselective transfer.[161] The possibility of a fully co-ordinated complex still being catalytically active therefore remains. E.g. this complex could have partially bound BINOL's, only binding the In(III) through one out of its two oxygens, which would present another solution for lowering the sterical hindrance surrounding the In(III) metal centre.

The procedure for the formation of this complex[164] was followed and the imine and phenylsilane added. Product formation was observed, and further investigations revealed that the reaction rate improved when employing a solvent mixture of THF and dichloromethane, leading to 69% conversion at room temperature overnight, and 73% conversion after 48 hours (**Scheme 4.3.3**). The product was isolated in 61% yield.

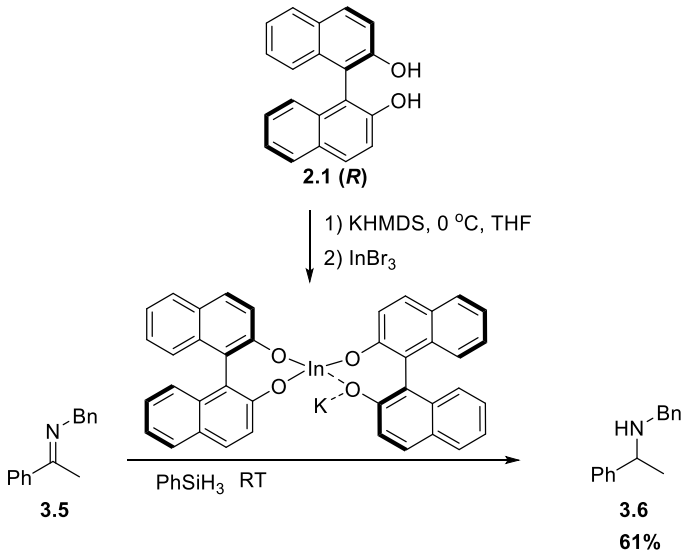

Scheme 4.3.3: Hydrosilane reduction of imine **3.5** using a potential complex of (*R*)-BINOL, indium and potassium.

It was attempted to isolate the complex by crystallisation. However, this proved to be even more troublesome than for the complexes already synthesised. Several different crystallisation methods

were attempted without success, and as the amine was found to be racemic further investigations were not performed. Alongside the investigations on In(III)-BINOL complexes made with potassium hexamethyl-disilazane it was attempted to form the In(III)-((*R*)-BINOLate)$_3$ complex with potassium instead of lithium or sodium by using potassium hydride for deprotonating (*R*)-BINOL (**Scheme 4.3.4**).

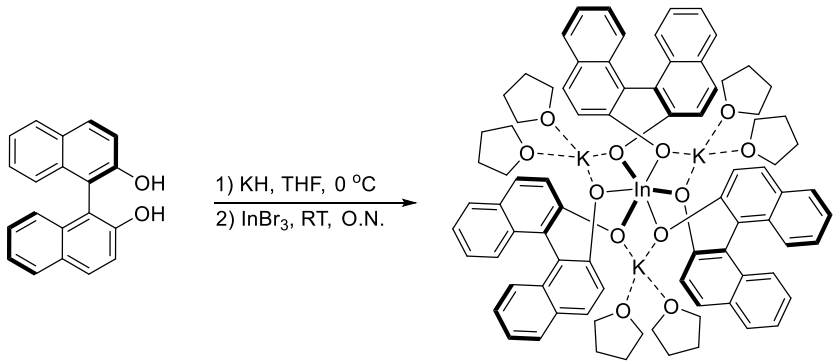

Scheme 4.3.4: Attempted synthesis of [{(K(THF)$_2$)$_3$}{In(*R*)-BINOLate)$_3$}]

By following the procedure employed for the formation of the sodium complex, a yellow solid was obtained. The ^{1}H NMR and IR spectra were similar to those of the sodium and lithium complexes, but the crystallisation proved troublesome and since the yellow solid facilitated a racemic reduction when employed as catalyst system for the amine reduction, no further effort was made towards crystallising this solid.

4.4. Computational Examination of an Indium-(BINOLate)$_2$ Complex

The computational theory is described in Chapter 5.

Alongside working towards the synthesis and characterisation of an In(III)-BINOL complex, computations were performed to examine the 3D structure of a potential complex containing indium, two BINOLs and a chlorine atom. The computations were based on a structure from the X-ray data base which looked similar. This complex[127] (**Figure 4.4.1**) contained two BINOL analogues, 2-hydroxy-2'-mercapto-1,1-binaphthyl, co-ordinated to an In(III) atom with a chlorine atom. Furthermore, the two oxygen atoms each co-ordinate a lithium ion, which co-ordinates three THF molecules or two THF molecules and the chlorine atom.

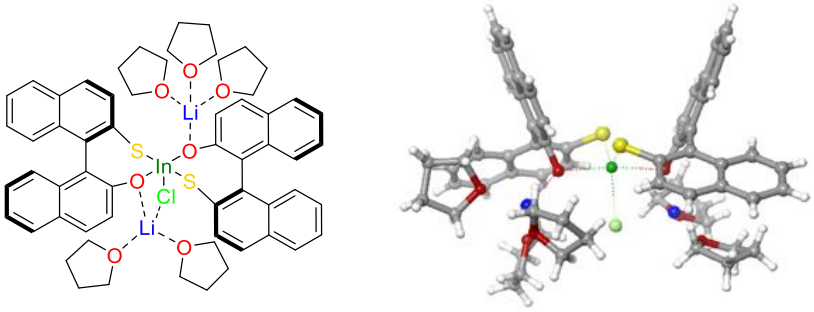

Figure 4.4.1: Left: Structure of the In(III)-complex with (*R*)-2-hydroxy-2'-mercapto-1,1-binaphthyl. Right: X-ray structure (Maestro view) LOSMEL.[127]

The sulfur atoms were replaced with oxygen, thus changing the ligand to (*R*)-BINOL, and lithium and THF were removed to simplify the system.[x] The resulting complex corresponds to the complex suggested in the literature,[88] but with an extra BINOL molecule co-ordinated to In(III). The structure of this complex was optimised using LACVP* and B3LYP. The structure of this complex was optimised using LACVP* and B3LYP, as B3LYP is computationally cheaper (less time consuming) than M06.[xi] In the optimised structure (**Figure 4.4.2**) the space between the two BINOL molecules is more condensed than the complex in **Figure 4.4.1**.

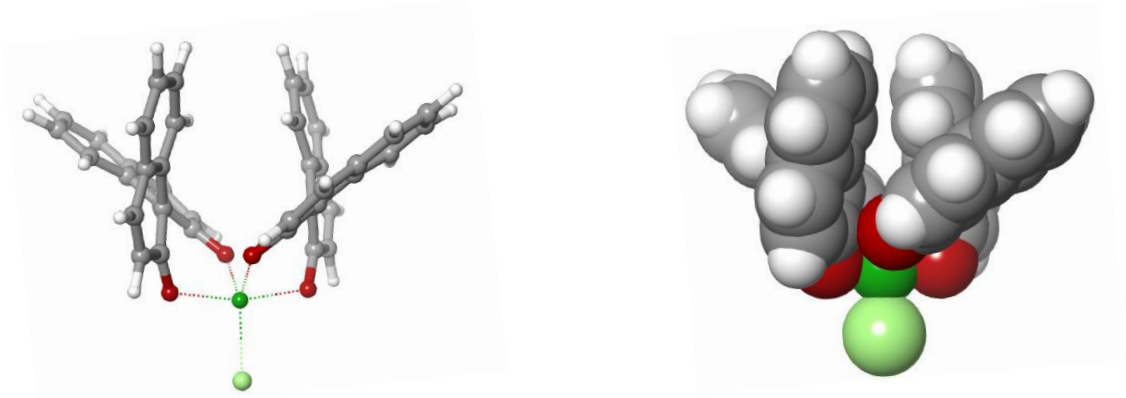

Figure 4.4.2: The (B3LYP, LACVP*) optimised structure of (*R*)-In(III)-(BINOL)$_2$ chloride.

This results in an expansion in the space around the chlorine atom. If this is the catalytically active site, a lack of enantioselectivity in the reaction could simply be caused by the lack of a cavity for the substrate to fit into. Thus, stereoselectivity could potentially be induced simply by adding bulk to the 3,3'-positions of the BINOL molecules. An example is the addition of a phenyl substituent to the 3,3'-positions (**Figure 4.4.3**), which seems to create a little cavity around the chloride atom.

[x] At this point there was also no intention of having either lithium or THF present in the system.
[xi] Later calculation with M06 resulted in the same geometry but higher energy.

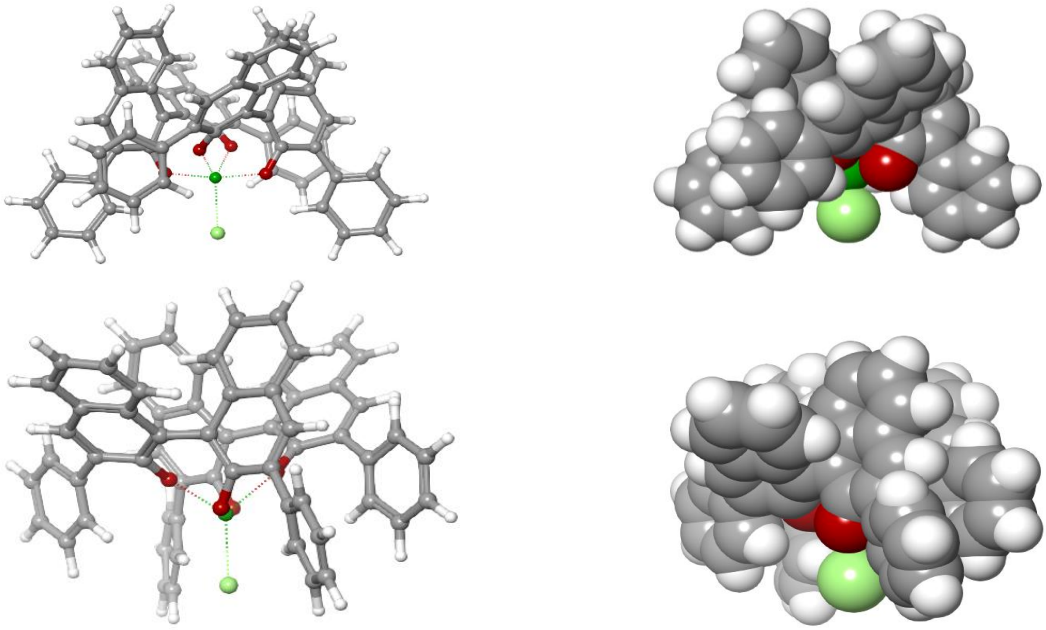

Figure 4.4.3: Optimised structure (B3LYP, LACVP*) of indium-(3,3'-phenyl-1,1'-binaphthyl)$_2$ chloride. Upper: front view. Lower: sideview.

If the complex in **Figure 4.4.3** showed some degree of enantioselectivity, this could be improved by even bulkier 3,3'-substituents such as triisopropylphenyl, as indium is significantly more enclosed in the cavity created by these substituents (**Figure 4.4.4**). Even when the model is slightly tilted, indium is not visible as it was in the case with only phenyl substituents (**Figure 4.4.3**). When viewing this complex from the bottom, In(III) is glimpsed behind the chloride atom. This overall seems to be promising for achieving enantioselectivity.

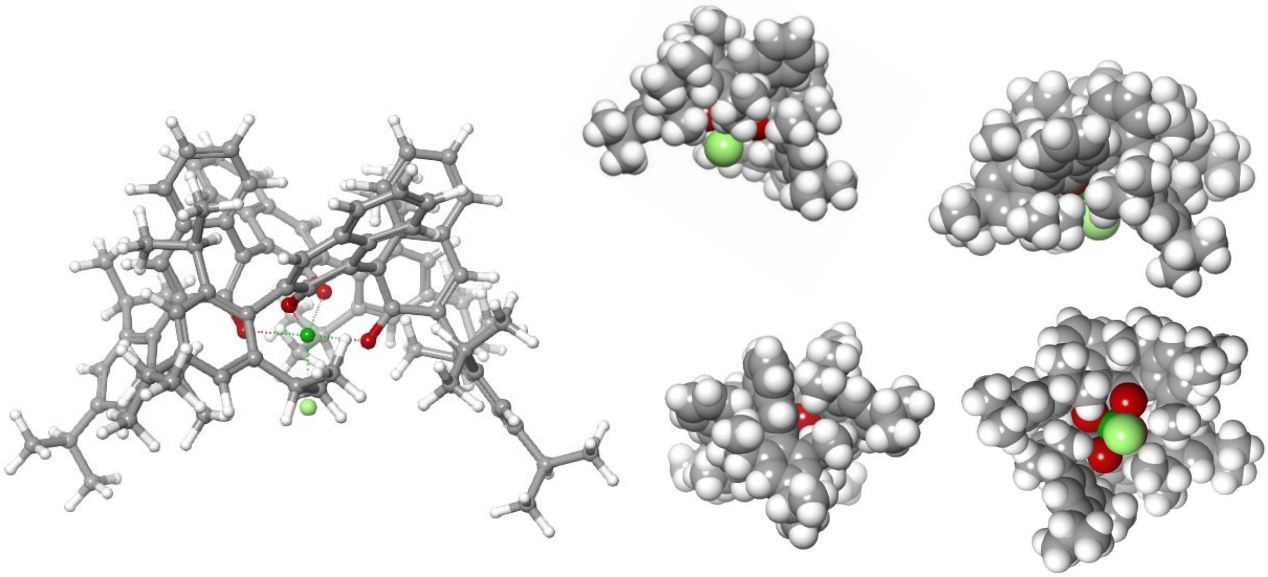

Figure 4.4.4: Optimised structure (B3LYP, LACVP*) of (3,3'-Bis(2,4,6-triisopropylphenyl)-1,1'-binaphthyl)$_2$-In(III) chloride.

It is important to note at this point, that these initial calculations (all calculations presented in this chapter) were carried out prior to realising the importance of the D3-correction in the B3LYP, which shall be presented in Chapter 5, and is especially important when calculating on systems consisting of several molecules which are interacting with each other, and intermolecular forces are likely to contribute significantly to both the geometric outcome and the energy of the resulting complex. Especially, the complex in **Figure 4.4.2** shows indications of pi-stacking interactions between the two BINOL scaffolds. Furthermore, no solvation has been taken into consideration at this point. Finally, and most importantly, none of the calculated complexes in this chapter has been thermodynamically evaluated, that is, as shall be presented in Chapter 5, evaluated against more stable configurations to examine whether it is energetically possible to form these complexes. All calculated complexes in this chapter exhibits similar bond length between In(III) on the BINOL oxygens, but further than that no comparisons have been made.

While waiting for the crystal structure of the crystals made by the sodium hydride approach (**Scheme 4.3.1**), computational investigations inspired by Shibasaki's catalysts[152] were made. The starting point of the investigations was based on the optimised structure of the indium-$(BINOL)_2$chloride with two lithium atoms added. As previously B3LYP and LACVP* were used for the energy optimisation. The ground state in this way (**Figure 4.4.5**) was flattened out compared to the original structure.

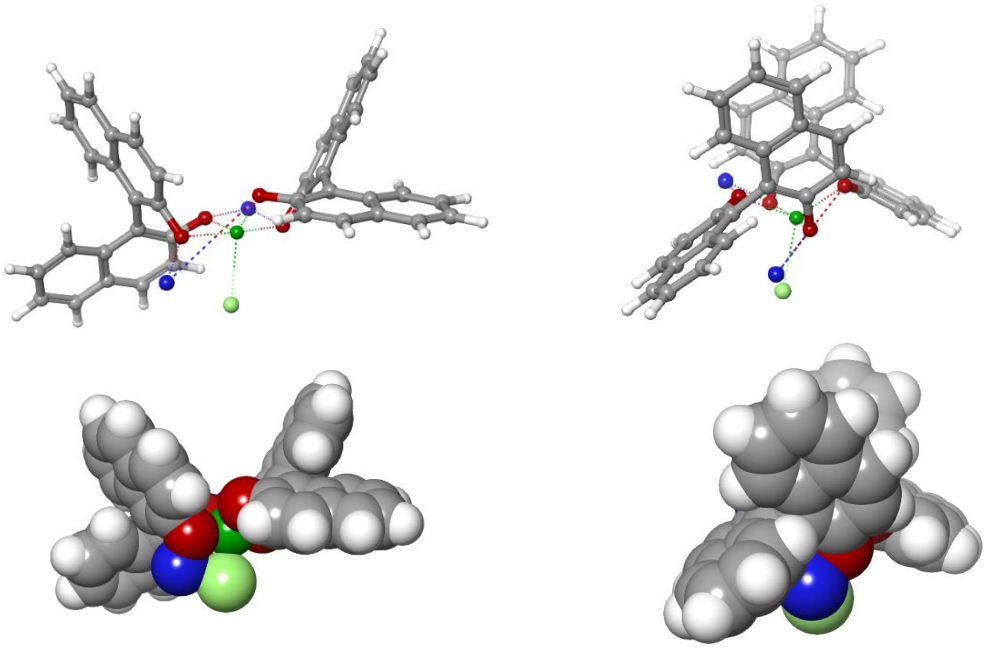

Figure 4.4.5: Optimised (B3LYP, LACVP*) structure of an In(III)-$BINOL_2$ complex with lithium and chlorine atoms.

This flattening of the structure could potentially enable better control of the stereochemistry. However, as the crystal structure revealed, if there are alkali metals present it is likely that solvent molecules will also be present. Nonetheless, it is an interesting observation, as it might also present a solution for co-ordinating only two ligands to the metal; if lithium flattens the structure and substituents are present at the 3,3'-positions, steric bulk could prevent the third BINOL molecule from co-ordinating. However, it is not known which will have the strongest influence – the lithium atom or the steric hindrance from 3,3'-substituents. Furthermore, flattening of the structure also results in the indium atom being more accessible from the top face (**Figure 4.4.6**), which should also be taken into account.

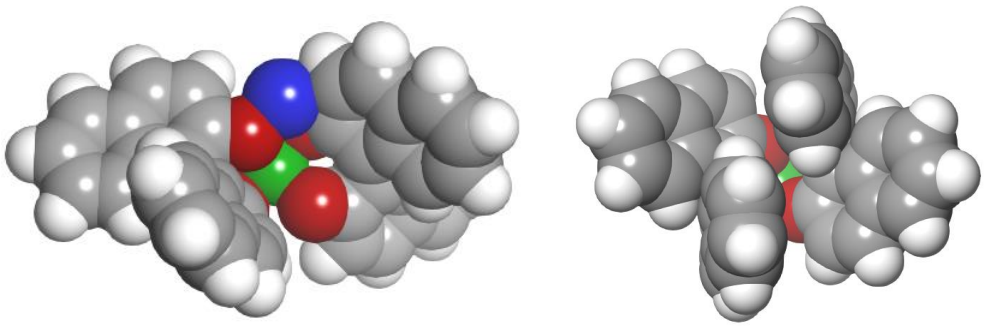

Figure 4.4.6: Top view (left) and bottom view (right) of In(III)-((*R*)-BINOL)$_2$-chloride-lithium$_2$.

As the crystal structures (**Figure 4.3.1**, **Figure 4.3.2** and **Figure 4.3.3**) also revealed absences of halogens, the optimisation was repeated without any halogen, and, as suggested in the literature,[164] only one alkali metal was included in the structure. In the ground state (B3LYP, LACVP*) of this complex [{In((*R*)-BINOLate)$_2$}{Li}] (**Figure 4.4.7**) the angle between the two BINOL molecules is approximately the same on both sides of the C_2-axis, which is significantly different from complex with two lithium atoms and one chlorine atom (**Figure 4.4.5**). Furthermore, the position of the lithium atom has changed, resulting in the lithium atom blocking the access to the In(III) metal centre from one side.

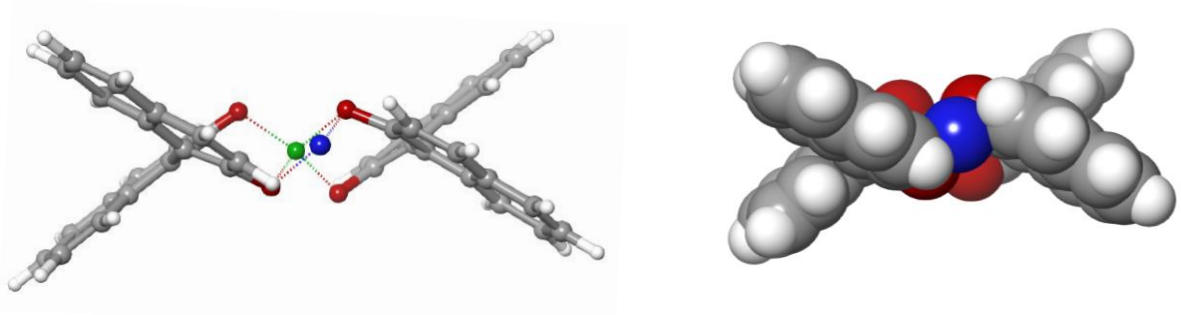

Figure 4.4.7: Sideview of the optimised (B3LYP, LACVP*) structure of indium-(BINOLate)$_2$-chloride-lithium complex.

The synthesised complexes seemed to be catalytically inactive in the initial experimental investigations. This could be accounted for by the 3D models of these In(III)-BINOL complexes (**Figure 4.3.1**, **Figure 4.3.2** and **Figure 4.3.3**), which suggest an inaccessible indium metal centre. Even without solvent molecules and the alkali metals indium seems inaccessible (**Figure 4.4.8**).

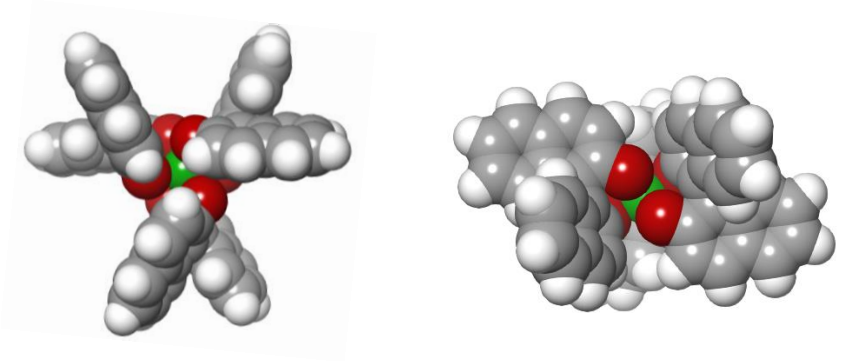

Figure 4.4.8: The synthesised indium-BINOL complex without solvent molecules and alkali metals.

In the literature, it was suggested that a vacant co-ordination site on In(III) is needed for effective catalysis. Another option for achieving this is by using linked BINOL. Matsunaga *et al.* developed a hetero bimetallic complex with gallium, lithium and an ether-linked BINOL (**Figure 4.4.9**), which showed improved stability in comparison to a the complex without the ether linkage.[165]

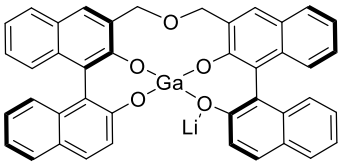

Figure 4.4.9: The gallium complex with an ether-linked BINOL. Adapted from Matsunaga et al.[165]

Thus, is possible that two BINOL molecules could be selectively bound to indium if they come in pairs, as it should not be possible to fit four BINOL molecules around the indium metal centre. Calculations were performed on the complex in **Figure 4.4.9** where gallium was replaced by indium. The B3LYP, LACVP* optimised structure (**Figure 4.4.10**) is similar to the In(III)-$(BINOLate)_2$-chloride-lithium complex (**Figure 4.4.5**), albeit the top angle between the BINOL moieties decreased and the lithium atom moved closer to In(III). Moreover, the ether linkage is blocking indium opposite to the lithium atom.

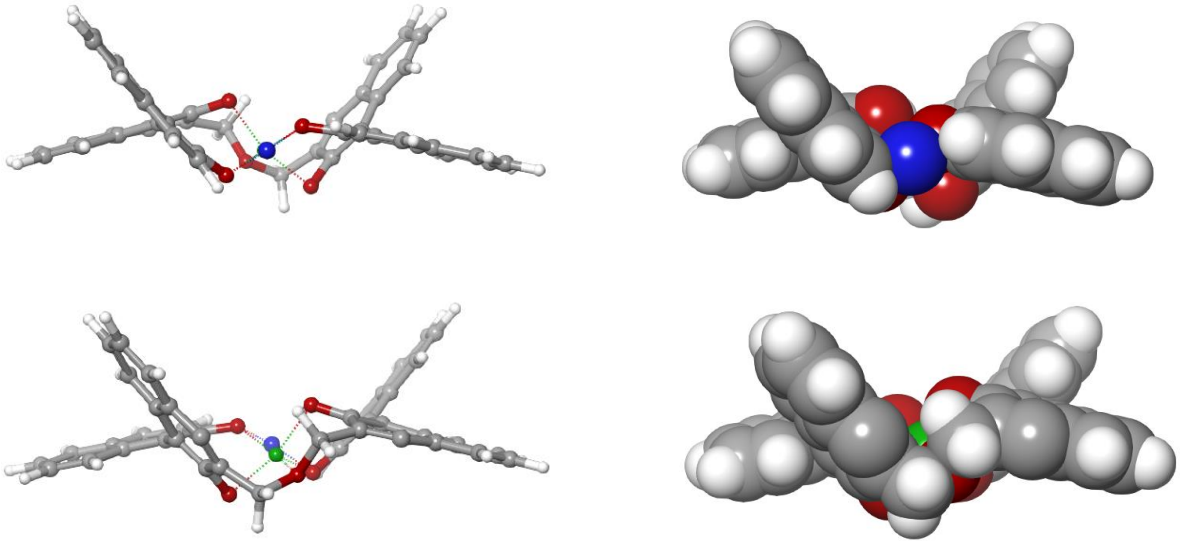

Figure 4.4.10: Optimised structure (B3LYP, LACVP*) of a linked (*R*)-BINOL complex with In(III) and lithium.

The In(III)-BINOL complexes synthesised have three BINOL molecules co-ordinated to indium. However, it is plausible that 3,3'-substituents on the BINOL scaffold will induce enough steric hindrance to prevent co-ordination from more than two BINOL molecules. Modifications of the crystal structure of [{In((*R*)-BINOLate)$_3$}{Na(THF)$_2$}$_3$] with 3,3'-triisopropylphenyl substituents on BINOL appears to cause lengthening of both the oxygen-indium bonds and the oxygen-lithium bonds, together with changes in the geometry of the In(III) metal centre (**Figure 4.4.11**). Therefore, if two 3,3'-triisopropylphenyl substituted BINOL molecules are already co-ordinated to In(III), it may be possible that the third modified BINOL simply cannot reach the indium atom.

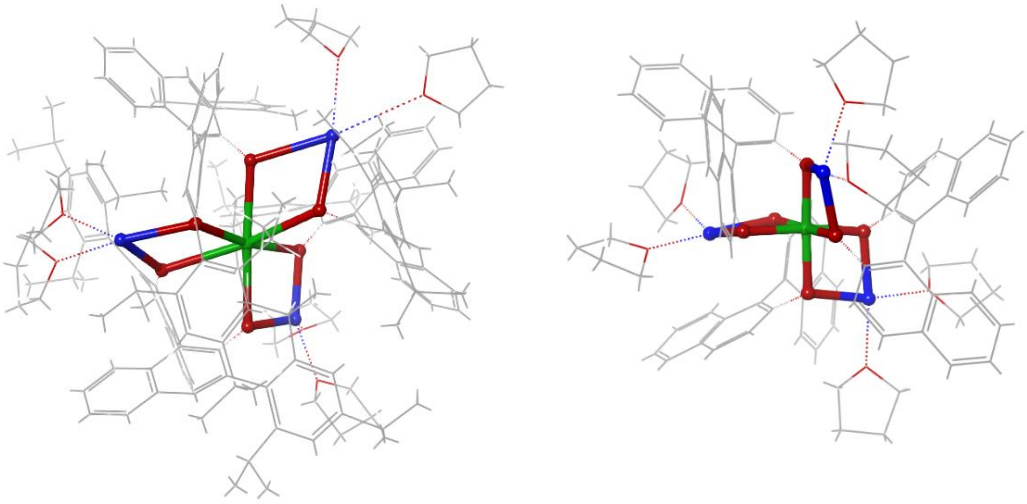

Figure 4.4.11: Left: Non-optimised Maestro model of [{In(3,3'-bis(2,4,6-triisopropylphenyl)-(*R*)-BINOLate)$_3$}{Na(THF)$_2$}$_3$]. Right: X-ray structure of [{In((*R*)-BINOLate)$_3$}{Na(THF)$_2$}$_3$].

Alternative complexes could be examined, e.g. the use of bridged BINOL scaffolds appears to have promising potential for ensuring only two BINOL molecules attach to the In(III) metal centre.

Another option is to synthesise an indium complex with the *S*-*O*-chelate as in the complex used for starting computational investigations (**Figure 4.4.1**). Viewing the space-filling model of this structure (**Figure 4.4.12**) from below the chlorine atom reveals a little cavity with free access to the chlorine atom. As the indium atom in this complex is only co-ordinated to two oxygens, two sulfurs and one chlorine atom, it has a vacant co-ordination site; hence, the chances of catalytically activity are higher. Furthermore, if the catalytically active centre is inside a cavity, chances of obtaining enantioselectivity are also higher.

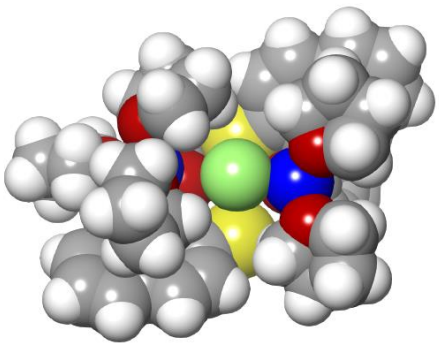

Figure 4.4.12: Bottom view of the space-filling model of LOSMEL[127] reveals a cavity surrounding the chlorine atom.

4.5 Conclusion

Initial investigations targeting formation and characterisation of an In(III)-BINOL complex successfully yielded two complexes for which crystal structures were obtained. These complexes were comprised of *hexa*-co-ordinated In(III) ions surrounded by three BINOL ligands with alkali metals and solvent molecules in between. At this point in the project, experimental work had revealed that steric bulk in the 3,3'-position did not increase the e.e.; rather, 3,3'-halogen substituted BINOL ligands had proven promising, suggesting greater influence from electronic effects.

After optimising the reaction to 73% e.e. (Chapter 3), computational mechanistic investigations were carried out. These are described in Chapter 5.

Chapter 5: Computational Mechanistic Investigations

This chapter describes computational mechanistic investigations of complex solvation and four plausible reaction pathways. The work presented in the chapter was carried out in Uppsala under the guidance of Peter Brandt.

Computational methods for modelling molecules are useful tools which can provide insight into the reaction mechanisms of catalytic processes and their selectivity for various products. These theoretical processes may be faster than experimental ones and are often the only way of obtaining the desired level of detailed mechanistic insight that chemists seek.[166]

5.1 Reactivity and Energy

In accordance with fundamental thermodynamics, chemical reactions will proceed spontaneously if they are associated with a decrease in the free energy of the system, which can be measured as Gibbs free energy.

The rate of a reaction is determined by the activation energy E_a as defined in the Arrhenius equation:

$$k = Ae^{-\frac{E_a}{(RT)}}$$

where k is the reaction rate coefficient, A is the reaction-specific frequency factor, R is the gas constant, and T is the temperature.

5.1.1 Potential Energy Surface

The Born-Oppenheimer approximation separates electronic and nuclear motion based on the assumption that the electrons rapidly adjust to any change in the nuclear position. The electronic energy U is a function of the nuclear co-ordinates and thus includes internuclear repulsion. The function U gives the potential energy of nuclear motion in the Schrödinger equation and gives rise to a multidimensional potential energy surface (PES).[167] Each point on the PES represents the potential energy of a single conformation of a molecule; thus, the PES is describing the relationship between molecular geometry and potential energy. Conformational changes, e.g. changes in torsion angle, can be regarded as movements along this multidimensional surface.[168] Stationary points along the PES that have zero gradient are of particular interest: stable conformations of a molecule are found in the local minima on the PES, while a saddle point along the path separating two minima represents a transition state (TS).[169] The PES of a system restricted to only two degrees of freedom, e.g. two bond lengths during a reaction, can be visualised as in **Figure 5.1**.

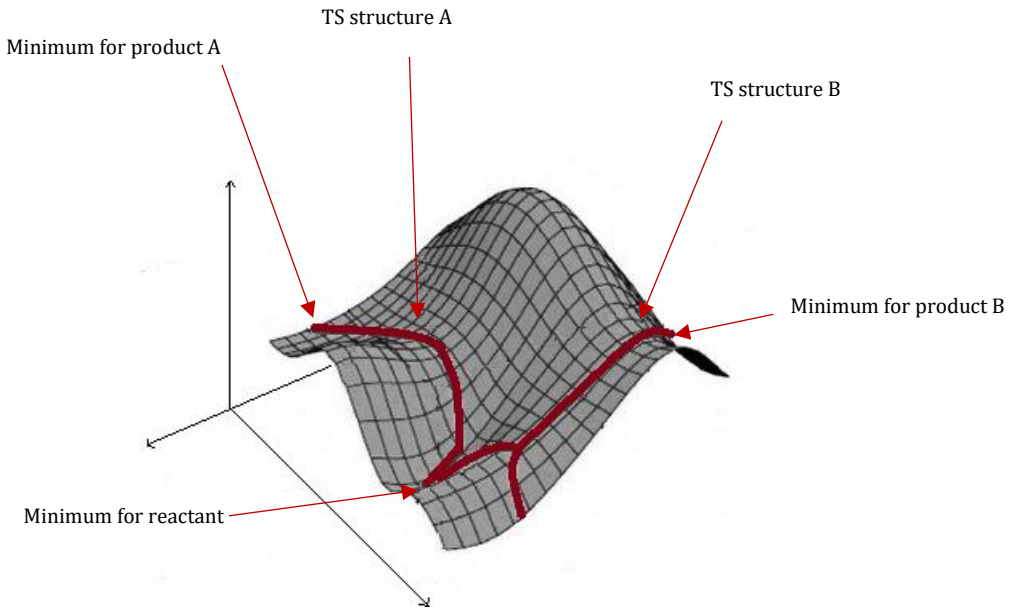

Figure 5.1: Model PES showing minima, reaction paths (in red) from reactant to two different products A and B through their correspondent TS. Adapted from Schlegel.[170]

The relative energies to the saddle point from the minimum on each side represent the minimal amount of energy required for the transition to take place in the forward and backward directions. From an arbitrary point on the PES, minimisation methods can be employed to locate the closest local minimum by following the local energy gradient. Once located, a single-point energy (SPE) calculation can be performed to give *U* for this particular arrangement of nuclei. This is calculated from the Hessian matrix (the force constant matrix) of the potential energy function and will give information about the local curvature of the PES. Force constants of the harmonic vibrations in a molecular system can also be calculated from the Hessian matrix, and these are of particular interest as local minima have only real frequencies, whereas one calculated frequency for a saddle point is imaginary.[167]

5.1.2 Transition State Theory

Transition state theory was introduced by Eyring in 1935 and links the reaction rate from the Arrhenius equation to the movement across the PES, thus adding mechanistic considerations to the rate law:[171]

$$k = \kappa \frac{k_B T}{h} e^{-\frac{\Delta G^{\ddagger}}{RT}}$$

κ is the transmission coefficient, which specifies the fraction of trajectories crossing the TS that will eventually proceed onwards to become product, k_B is Boltzmann's constant, h is Planck's constant, $\Delta G^{\ddagger}$ is the free energy of activation, T is the temperature and R is the gas constant.[167]

$\Delta G^{\ddagger}$ is the energy difference between the two enantiomeric transition states is therefore of particular interest to the thesis in hand. $\Delta G^{\ddagger}$ can be expressed from the ratio between the two enantiomers E:

$$\Delta G^{\ddagger} = -RT \cdot Ln(E)$$

The e.e. can be expressed from one of the enantiomers only:

$$\text{e.e.} = \frac{[\text{R}] - 1 + [\text{R}]}{1} \cdot 100$$

which through rearrangement it follows:

$$[\text{R}] = \frac{\frac{\text{e.e.} + 1}{100}}{2}$$

Therefore, E is given from:

$$E = \frac{[R]}{[S]} = \frac{\frac{\frac{\text{e.e.} + 1}{100}}{2}}{1 - \frac{\frac{\text{e.e.} + 1}{100}}{2}}$$

And from this the e.e. can be determined from $\Delta G^{\ddagger}$ or e.e. converted to $\Delta G^{\ddagger}$.

5.1.3 Molecular mechanics

Molecular mechanics (MM), introduced in 1946 by Hill[172] and Westheimer and Mayer,[173] applies classical mechanics to describe molecular systems. In MM, an atom is represented as a single particle and bonds linking atoms are treated like springs. The potential energy of such systems can be calculated using a set of parameterised functions called a force field (FF). Different FFs include various terms; generally, terms describing bond length, torsion, angle and non-bonding interactions, e.g. van der Waals, are considered.[168] MM FF energy calculations are relatively simple and thus computationally cheap, allowing for efficient optimisation of the conformational geometry. However, the electronic structure is not considered in the standard FF parameterisation and therefore does not allow for modelling of chemical reactions.

5.1.4 Quantum Mechanics

The basis of quantum mechanics (QM) is the wave function (ψ). The wave function constitutes the most complete description of a physical system; ψ characterises a particle's motion and from ψ various properties of the system under examination can be derived. The Hamiltonian operator ($\widehat{H}$) is the operator that returns a system's energy (E), which can be determined as:

$$\widehat{H}\psi = E\psi$$

QM calculations are not parameterised and are for that reason occasionally referred to as *ab initio*, "from first principles". Classic QM methods explicitly consider the electron wave function and thus are capable of accurately modelling a chemical reaction. However, in these cases the method depends on $4N$ co-ordinates (N is the number of electrons), $3N$ spatial coordinates and N spin coordinates, which makes this a very time-consuming method.[167]

The variational principle states that, for any normalised wave function, the computed energy will be the upper boundary of the true energy. The wave function itself is not observable; however, an N-electron function can be related to the electron probability density ρ(r) of the system through:

$$\rho(\mathrm{r}) = N \int \dots \int |\psi(r_1, s_1, r_2, s_2, \dots., r_N, s_N|^2 \, ds_1 dr_2 ds_2 \dots.. dr_N ds_N$$

where r_n are the spatial co-ordinates and s_n are the spin co-ordinates. This (strictly speaking) probability density is usually referred to as electron density.[167]

5.1.4.1 DFT

In 1964, Hohenberg and Kohn proved that the electron density of a system completely determines the electronic energy, and thus the fundamental of density functional theory (DFT) was established.[174] DFT relates the system's properties to the electron density function and depends on only three spatial co-ordinates. Therefore, DFT provides a much simpler and faster way of calculating the properties of a system.[175] In 1965, a practical method for finding the ground state energy from the ground state density was devised by Kohn and Sham, which employs the local density approximation.[xii] The Kohn-Sham (KS) method contains an unknown functional (the density functional), which must first be approximated. The better this approximation is, the closer the DFT result is to the true energy. The KS-DFT calculations start with an initial guess for the density of the

[xii] The local density approximation states that the local electron density of electrons is approximately the same.

system and from this an initial exchange correlation potential is estimated. Together with KS orbitals (linear combinations of one-electron basis functions which span the molecular orbitals), this initial exchange correlation potential is used to solve the KS equation, which finds the orbitals that minimise the molecular ground state energy.[167]

5.1.4.2 Level of Theory

The foundations of any computational study employing DFT are the chosen functional and the chosen basis set (the set of one-electron basis functions spanning the MOs). Hybrid functionals, such as B3LYP (Becke, 3-parameter, Lee-Yang-Parr)[176,177] or M06 (Minnesota 06),[178] incorporate a portion of exact exchange from Hartree-Fock theory and provide simple and accurate descriptions of the atomisation energies, bond lengths and vibrational frequencies of most molecules.[179] When performing DFT studies on indium compounds, the LANL2DZ (Los Alamos National Laboratory 2 Double Z) basis set is often chosen for Gaussian[180–182] and the LACVP (Los Alamos national laboratory, outermost Core orbital, Valence only, Pople)[183] basis set for Jaguar[182,184,185] (this employs LAV3P (Los Alamos national laboratory, Valence only, Pople))[183,186,187] on indium[188]). In Jaguar, LACVP is generally recommended for non-lanthanide molecules containing atoms beyond argon in the periodic table.[188] The basis set can be expanded by including polarisation functions, denoted * when added to all atoms excluding transition metals, hydrogen and helium, and by ** when also added to H and He. The purpose of these polarisation functions is to expand the space available for orbitals to allow for polarisation in a certain direction. Further expansion of the orbital radius can be achieved through addition of diffuse functions (+ or ++) which increases the accuracy when anions or highly electronegative atoms are under consideration. All DFT calculations presented in this thesis have been calculated with LACVP* for geometry optimisations and vibrational frequencies, whereas LACV3P**+ was used for SPE calculations with a solvation model to allow for calculations of free energies. For all DFT calculations, besides choosing the level of theory and the initial atomic configuration, the co-ordinates to be optimised, the convergence criteria and an initial guess for the Hessian (normally the Schlegel guess) must be defined. In this thesis all DFT calculations have been carried out with Jaguar in Maestro using default convergence criteria and with the Schlegel guess for the initial Hessian for geometry optimisations and SPE calculations, while QM-Hessian was used for TS searches.

5.1.4.2.1 Dispersion

Dispersion refers to attractive long-range intermolecular forces resulting from electron correlation. An accurate description of these electron-electron interactions is essential for modelling systems,

especially those with several molecules interacting in the stationary points under investigation.[189] However, they are not well modelled in most DFT functionals.[190] In the DFT calculations presented in this chapter, dispersion has been accounted for by using the DFT-D3 protocol.[191]

5.1.4.2.2 Solvation

Standard QM calculations take place in the gas phase. However, most chemical reactions proceed in solution, where solvent molecules constantly interact with the reaction system. This alters the properties of the reaction system which is why accurate models have to take the solvent into consideration. Explicit solvent models are the most accurate, though very time-consuming as they drastically increase the size of the system and the conformational freedoms. Therefore, continuum solvent models simulating the average electrostatic effect, through use of the radius and the solvent's dielectric constant (ε), are normally used. In this thesis, a finite continuum Poisson-Boltzmann model[192,193] (PBF/MeOH) has been applied for all free energy calculations in the DFT studies.

5.1.4.2.3 Free Energy Profiles

With help of DFT, the free energy-profile of a chemical reaction can be calculated.[169] The final free energies reported for the DFT studies in this thesis were derived by adding the electronic energy from the gas phase SPE calculation to the solvation energy, the calculated dispersion correction, the zero point energy and the harmonic contribution at the investigated temperature. The free-energy profiles can be thought of as schematic intersections of the free-energy surface of a reaction. A hypothetical free-energy profile in shown in **Figure 5.1.4.2.3**.

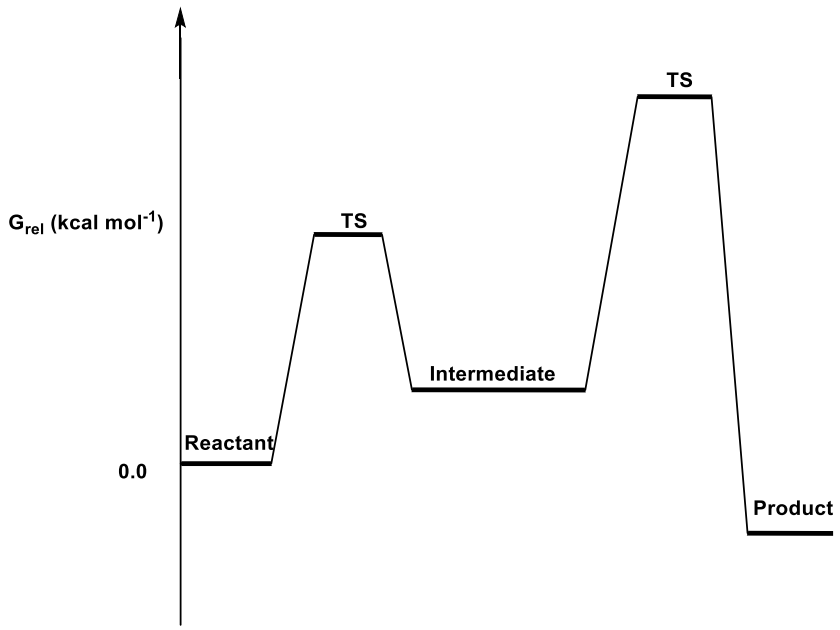

Figure 5.1.4.2.3: Hypothetical free-energy profile of a reaction.

Only the relative energies are of interest; therefore, the starting point is denoted as zero energy. From the free-energy profile it can be determined whether the reaction is endergonic or exergonic by comparing the energies of the reactant and the product, thus determining the thermodynamic properties of the reaction. The amount of energy required for the reaction to take place, the highest TS barriers, can be calculated, and these are related to the rate of the reaction.

5.2 The Model System

Invariably, computational chemistry involves considering the balance between chemical accuracy and computational cost. To lower computational costs, allowing for faster analysis, all calculations were first performed with a model system (**Figure 5.2.1a**). The model system is a smaller representation of the system but still contains all the atoms taking part in the reaction. In relevant cases, which will be presented in the coming sections, the output calculations for the model system were repeated with the whole system (**Figure 5.2.1b**) for more precise results. Furthermore, this allowed the accuracy of the abbreviated system compared to the whole system to be evaluated.

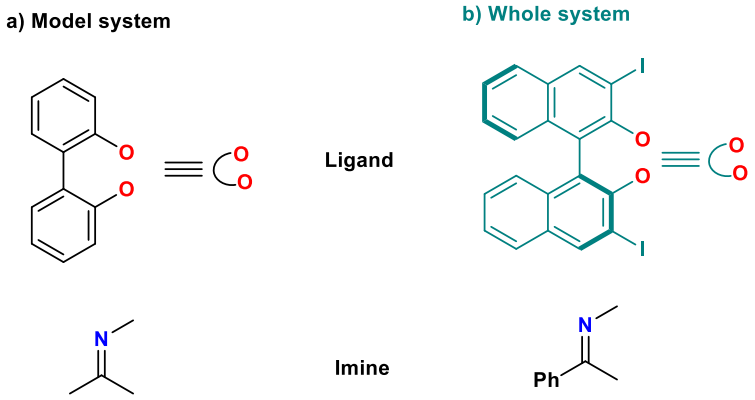

Figure 5.2.1: a) Model system b) the whole system. NB: Calculations were performed with the (*S*)-enantiomer of the BINOL scaffold, however, the two enantiomers would yield the exact same result.

Note that the whole system continues to model the imine as a *N*-Me imine, as the difference between *N*-Me and *N*-Bn is suggested to be minimal due to the flexibility on the adjacent carbon. Once a plausible mechanism has been established, the benzyl substituent should be included for the final calculations. Moreover, if further optimisation finds electronic or steric effects from the substituent on the benzyl ring to be important or if changes in the bulk on the benzylic position affect the e.e., the entire *N*-substituent needs to be included earlier in the calculations.

5.3 Examination of In(III)-Co-ordination

In(III) is reported in the literature[194,195] to have between 4 and 6 co-ordination sites occupied during steps of active catalysis. In the system under investigation – the In(III)-catalysed hydrosilane reduction of an imine – multiple compounds are capable of co-ordinating to In(III) metal-centre:

- The two polar protic solvents in the solution
- One or two oxygens of the BINOL ligand
    - If co-ordinating through one oxygen only, two BINOL ligands can co-ordinate
- The imine could co-ordinate through the nitrogen lone pair
- The amine product could co-ordinate through the nitrogen lone pair

As an initial examination, the energies of all possible complexes of In(III) with MeOH were evaluated. The results are shown in **Diagram 5.3.1.**

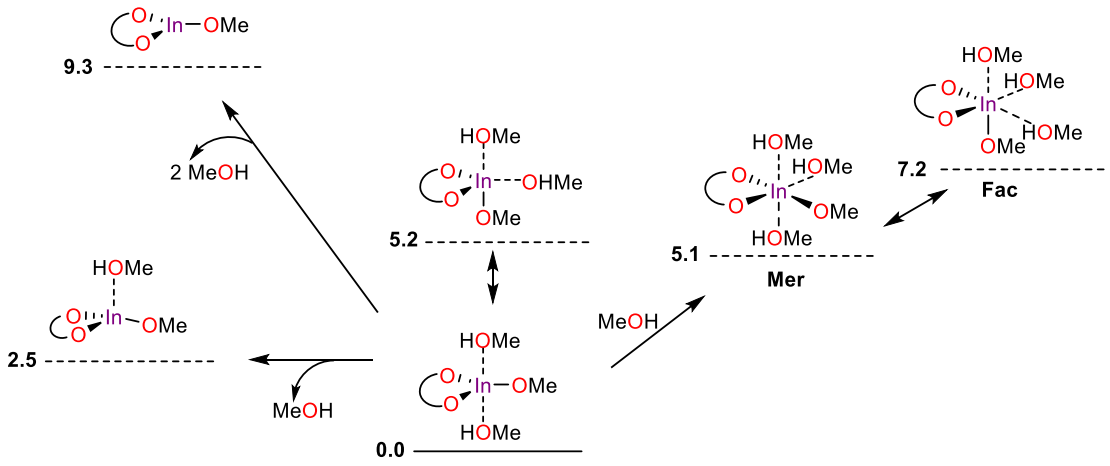

Diagram 5.3.1: Relative energies of various In(III) complexes with biphenol in MeOH.

The *penta*-co-ordinated In(III)-complex was found to be the most stable and the *tri*-co-ordinated complex (having no co-ordinated MeOH) was found to be the least stable. As expected, the *penta*-co-ordinated complex with an equatorial methoxy substituent was lower in energy than when the methoxy group was axial, and for the *hexa*-co-ordinated complex the meridional isomer was lower in energy than the facial isomer. For onwards calculations only the most stable *penta*- and *hexa*-co-ordinated complex was examined. The calculations were also performed using *i*-PrOH instead of MeOH for co-ordination (**Diagram 5.3.2**).

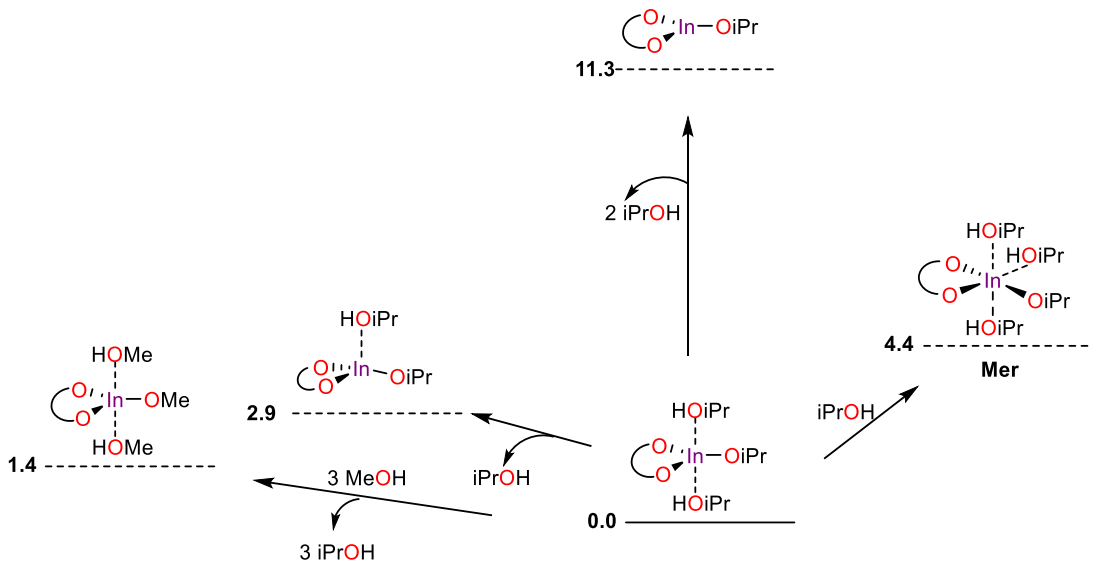

Free energies in kcal mol^{-1} calculated by B3LYP-D3/LACV3P^{+} (PBM/MeOH)//B3LYP-D3/LACVP***

Diagram 5.3.2: Relative energies of various In(III) complexes with biphenol in *i*-PrOH. The penta co-ordinated complex in MeOH is added for comparation.

The isopropanol versions of the complexes were lower in energy. However, the same trends were followed between the different co-ordination levels and isomers, and, on this basis, it was decided to employ MeOH as the co-ordinating solvent in all remaining calculations, to simplify the system under investigation and lower the computational costs.

The energies of all these MeOH-co-ordinated complexes were also calculated for the full system (**Diagram 5.3.3**) and these were found to overall follow the same trend as observed for the model system.

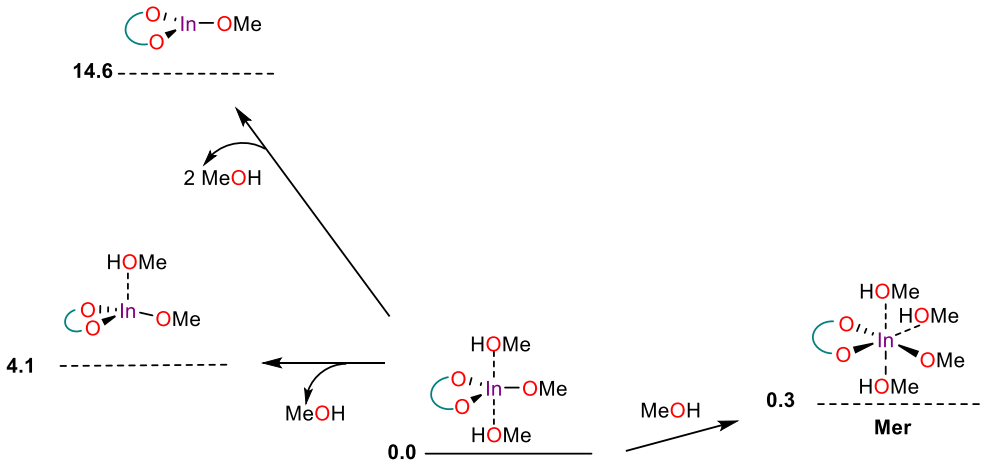

Free energies in kcal mol^{-1} calculated by B3LYP-D3/LACV3P^{+} (PBM/MeOH)//B3LYP-D3/LACVP***

Diagram 5.3.3: Relative energies of various In(III) complexes with 3,3'-I_2-BINOL in MeOH.

As noted from **Diagram 5.3.3** the *hexa*-co-ordinated complex is more stable than the *tetra*-co-ordinated complex when the energies of the complexes with the bisiodine ligand is considered, which is contrary to the results obtained for the model system. This can reflect a difference in CFSE caused by two different ligands, which is expected to vary as a result of the 3,3'-iodine substituents. However, the change in the energy difference between these two compounds is but 2.3 kcal, which is rather small. Furthermore, the most stable configuration continues to be the *penta*-co-ordinated.

The effect of co-ordinating the imine was investigated (**Diagram 5.3.4**) and found to be favourable in all cases except the case of the *hexa*-co-ordinated facial isomer. Notably, in the case of co-ordinating the imine, the most stable compound formed does not co-ordinate additional MeOH but is a *tetra*-co-ordinated In(III)-complex. The same trend was found when calculating the energies with the whole system, where the tetra-co-ordinated complex was found to be significantly more stable than the complexes with higher co-ordination numbers.

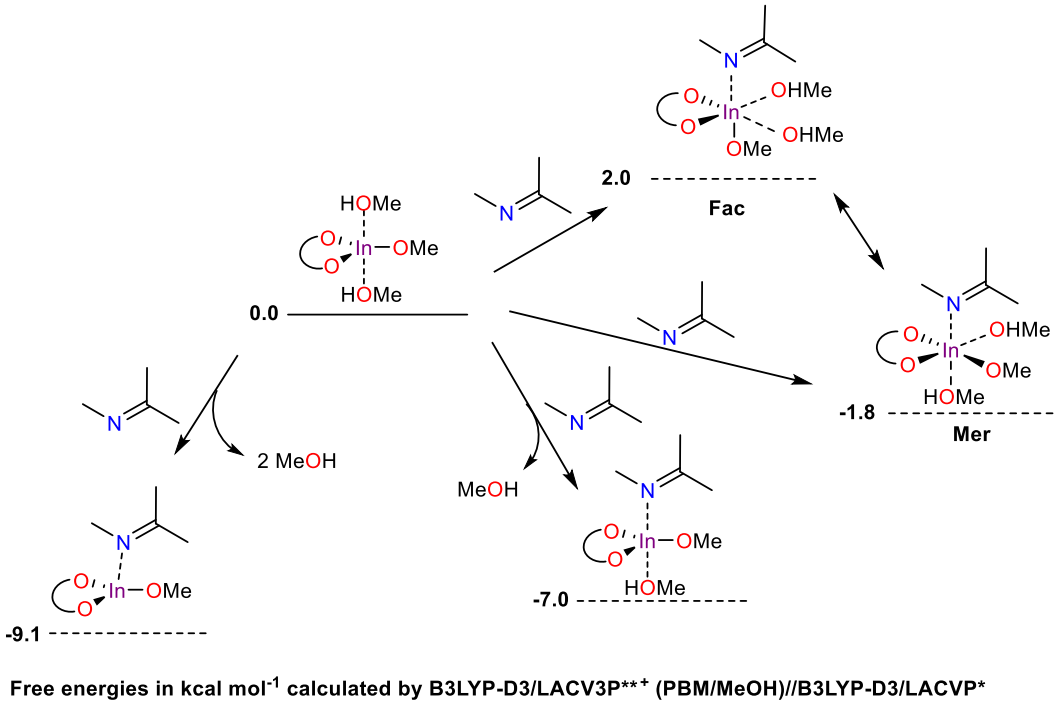

Diagram 5.3.4: Calculated energies for imine co-ordination.

Energies of various In(III)-hydride complexes where investigated (**Diagram 5.3.5**) and found to be favourable in the case of *tri-*, *tetra-* and *penta*-co-ordinated In(III). Notably, in this case the most stable compound was also the *tetra*-co-ordinated In(III); thus, the beginning of a potential trend was observed.

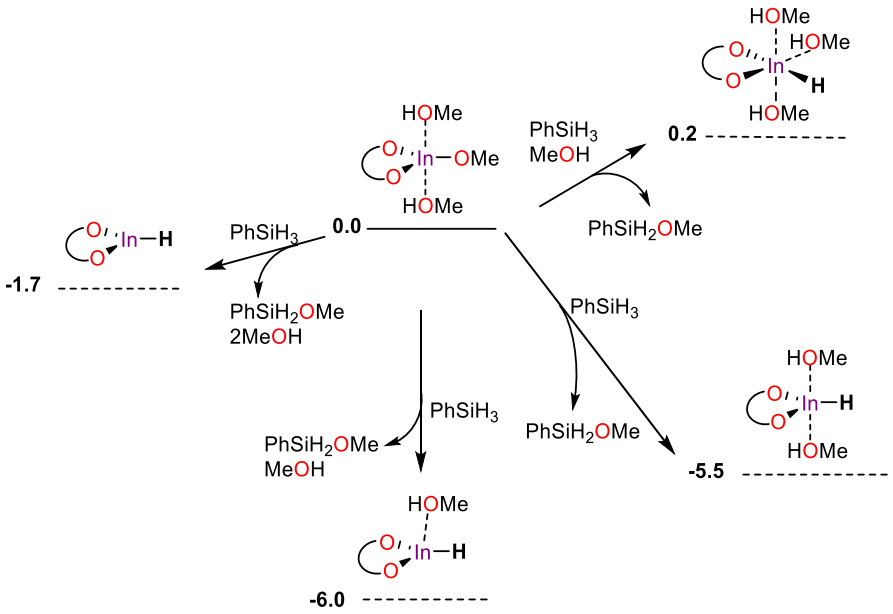

Free energies in kcal mol^{-1} calculated by B3LYP-D3/LACV3P^{+} (PBM/MeOH)//B3LYP-D3/LACVP***

Diagram 5.3.5: Relative energies for formation of various In(III)-biphenol hydride complexes in MeOH.

Formation of imine-co-ordinated In(III) hydrides was in all cases very thermodynamically favourable process (**Diagram 5.3.6**).

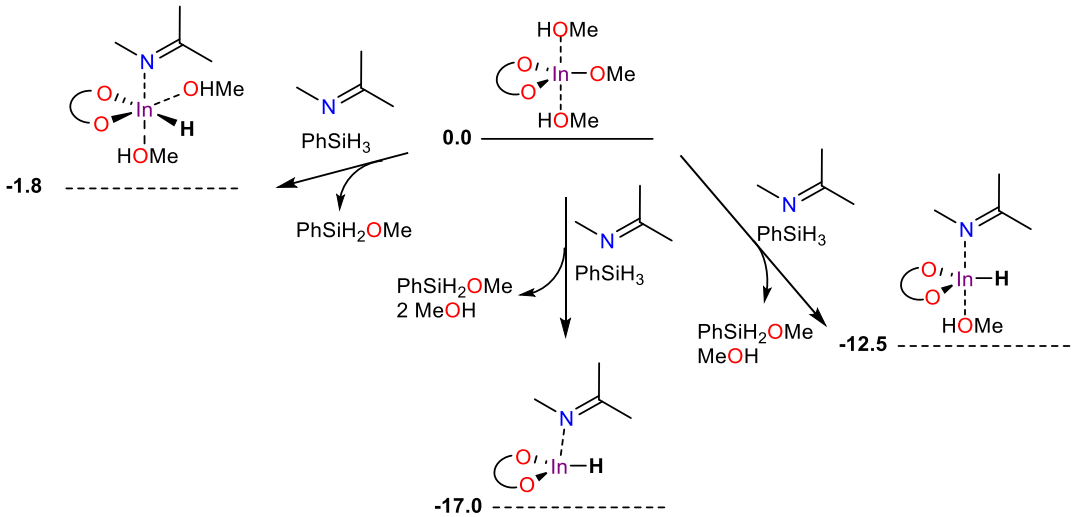

Free energies in kcal mol^{-1} calculated by B3LYP-D3/LACV3P^{+} (PBM/MeOH)//B3LYP-D3/LACVP***

Diagram 5.3.6: Relative energies for formation of various imine co-ordinated In(III)-biphenol hydride complexes in MeOH.

Finally, the energies of imine reduction and subsequent product release were calculated (**Diagram 5.3.7**) and found to all be thermodynamically favourable.

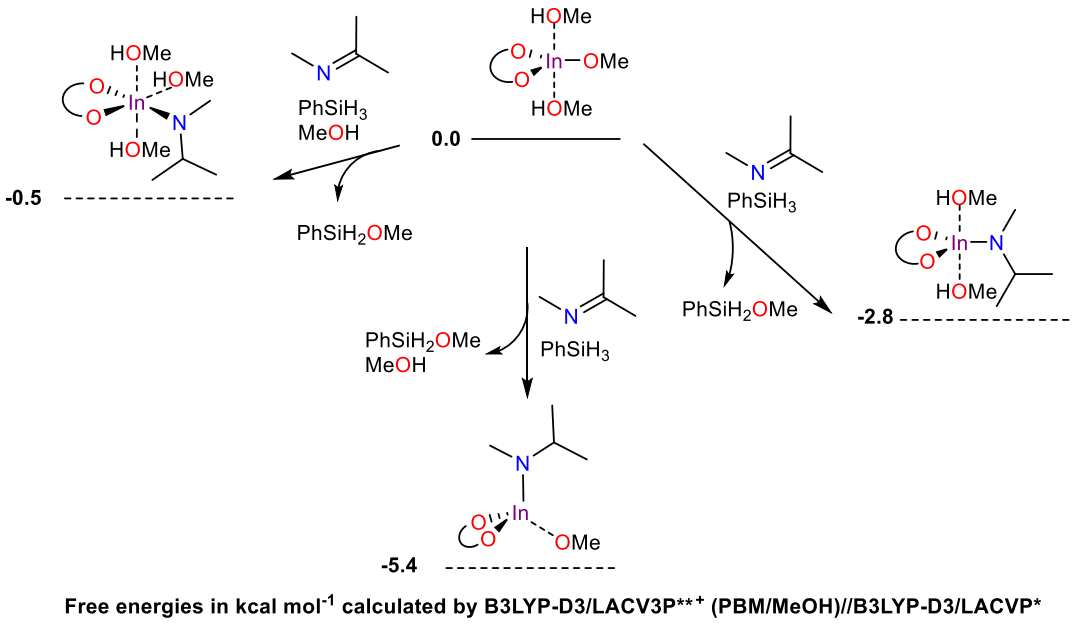

Diagram 5.3.7: Relative energies for the imine reduction in MeOH. The most stable amine complex is *tetra*-co-ordinated.

5.4 Investigation of various potential reaction pathways

The examination of various In(III) complexes in the section above indicates that the In(III) complexes found were likely to be *tetra*-co-ordinated when anything other than the BINOL ligand and MeOH solvent molecules co-ordinated. The calculated energies also suggested that the reaction pathway could proceed through an active In(III) hydride species. Along with investigation of a pathway via an In(III) hydride, two other pathways were investigated: Meerwein-Ponndorf-Verley (MPV) reduction and reduction via oxidative insertion. To investigate these three different mechanisms, energies for the intermediates along the reaction pathways were calculated and transition states found.

5.4.1: Investigation of a Meerwein-Ponndorf-Verley reduction mechanism

The possibility of the reaction pathway proceeding through an MPV-type mechanism was investigated first since formation of acetone was experimentally observed when *i*-PrOH was used as solvent for the reaction. The free-energy profile for this pathway and the TS found for each enantiomer are shown in **Diagram 5.4.1**.

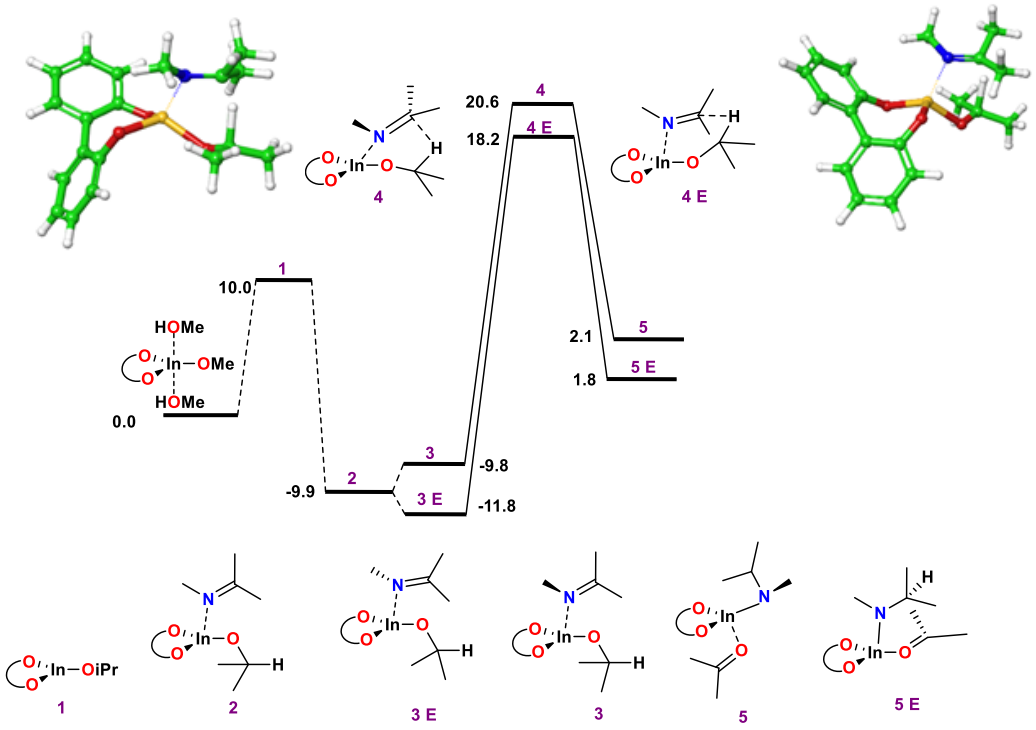

Diagram 5.4.1: Free-energy profile for MPV mechanism. Maestro models of the two enantiomeric transition states shown. Dotted lines correspond to conformational changes and changes in co-ordination around the In(III) metal-centre. Full lines connect the TS with the reactant and the product obtained by following the intrinsic reaction co-ordinates from the TS, thus validating the found TS.

As the binding of acetone is significantly more favourable than binding *i*-PrOH, the reaction is unlikely to proceed. Furthermore, the TS barrier of 30-30.4 kcal mol^{-1} is very high suggesting this pathway is less likely to proceed at room temperature.

5.4.2 Reduction via oxidative insertion

Another plausible pathway is reduction via oxidative insertion. Here In(III) acts as an LA activating the imine, which then receives a hydrogen from the silane (**Diagram 5.4.2**).

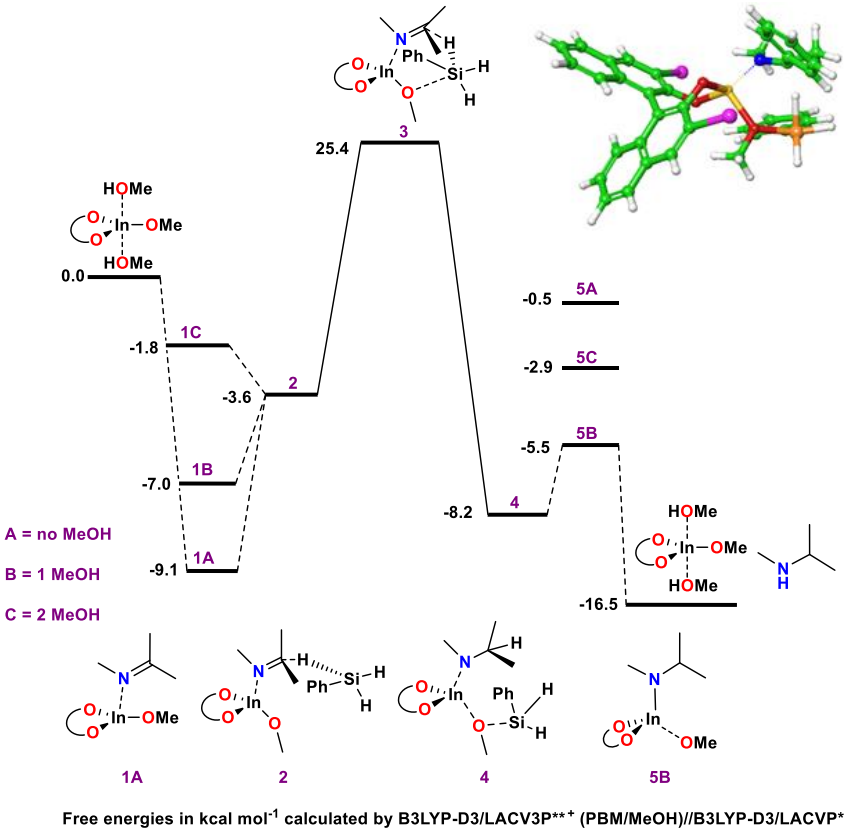

Diagram 5.4.2: Free-energy profile for a reduction via oxidative insertion mechanism with the In(III) complex acting as an LA. The TS shown is for the full system, as these calculations were repeated for the TS step only, validating the accuracy of the model system. Dotted lines correspond to conformational changes and changes in co-ordination. Full lines connect the reactant and product obtained by following the intrinsic reaction co-ordinates from the TS to validate this TS.

The TS barrier of 34.5 kcal mol^{-1} was very high, suggesting this pathway is also not the most likely pathway for the hydride transfer at room temperature.

5.4.3 Investigation of pathways involving In(III) hydrides

The co-ordination examination suggested that the formation of In(III) hydrides was thermodynamically favourable. The path to forming In(III) hydrides was investigated (**Diagram 5.4.3.1**).

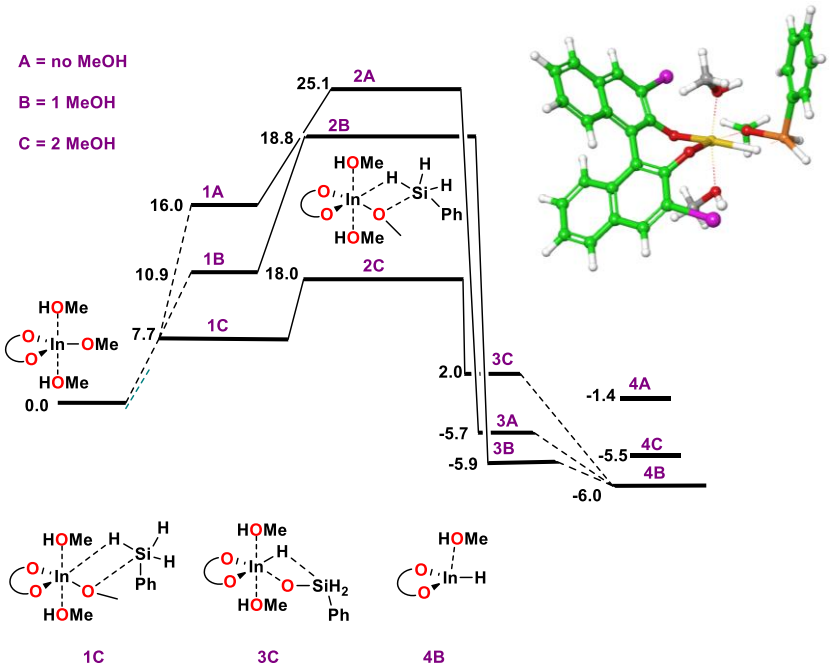

Diagram 5.4.3.1: Free-energy profile for formation of various In(III) hydride complexes. Dotted lines correspond to conformational changes and changes in co-ordination around the In(III) metal-centre. Full lines connect the TS with the reactant and the product obtained by following the intrinsic reaction co-ordinates from the TS, thus validating the found TS.

The TS barrier of 18 kcal mol^{-1} and the gain of 6.0 kcal mol^{-1} in the formation of the *tetra*-co-ordinated In(III) hydride demonstrate this pathway is likely to proceed at room temperature.

Subsequently, the co-ordination of the imine to the In(III) hydride complexes, followed by transfer of the hydrogen from these In(III) hydrides to the imine via oxidative insertion, was investigated. (**Diagram 5.4.3.2**).

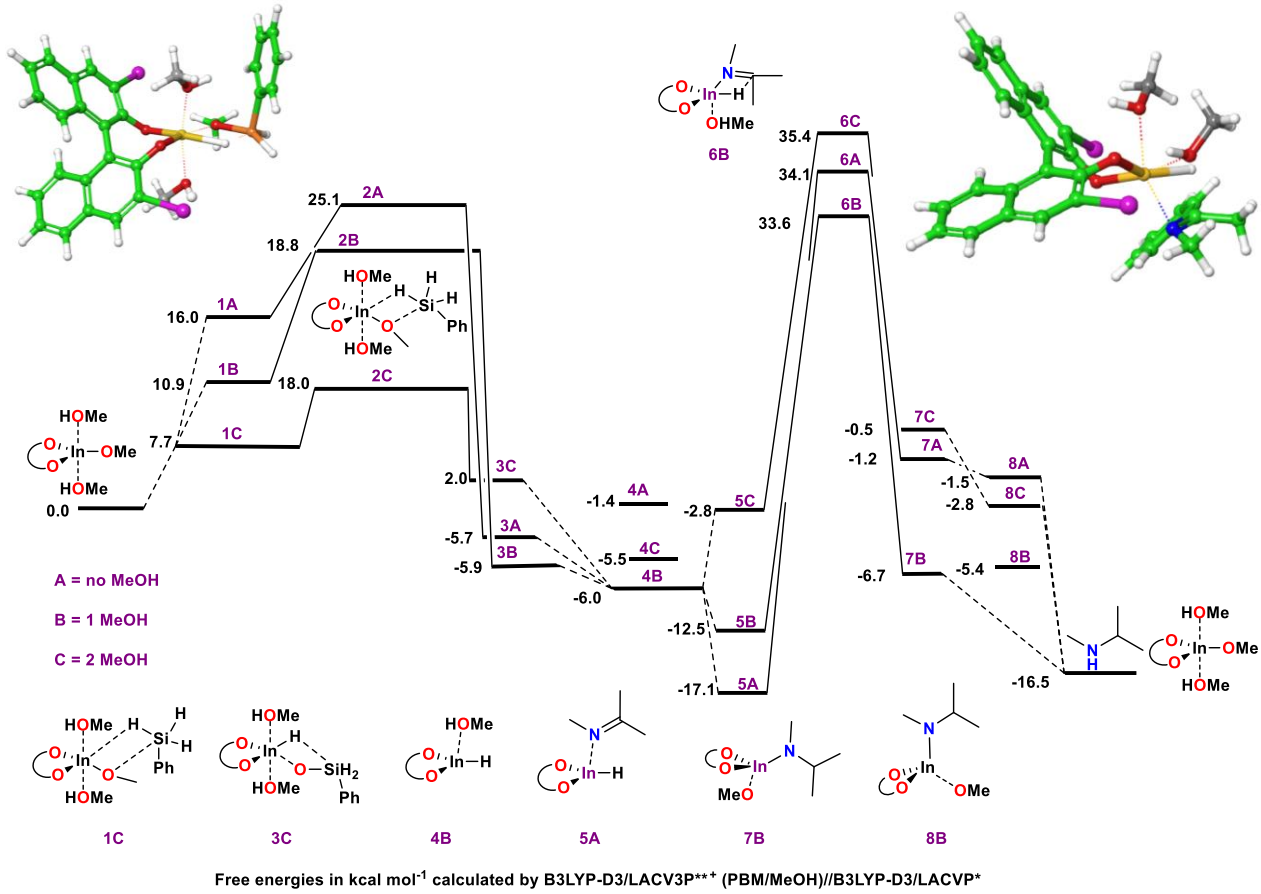

Diagram 5.4.3.2: Free-energy profile for formation of various In(III) hydride complexes and subsequent oxidation insertion and reduction of the imine. The transition states shown are for the whole system. Dotted lines correspond to conformational changes and changes in co-ordination around the In(III) metal-centre. Full lines connect each TS with the reactant and the product obtained by following the intrinsic reaction co-ordinates from the TS, thus validating the found TS.

The TS barrier for this step was found to be extremely high (50.7 kcal mol^{-1}), indicating that is an In(III) hydride is formed the hydrogen, is not likely to be delivered to the imine via this pathway.

A different mechanism has been observed for ruthenium hydrides.[196,197] Based hereon, the hydrogen could be delivered though a six-membered TS, where a MeOH molecule co-ordinated to the In(III) hydride activates the imine through a hydrogen bond to the nitrogen lone pair. This mechanism was examined and found to be energetically favourable. The free-energy profile for this reduction is shown in **Diagram 5.4.3.3**, including the free-energy profile for the formation of the In(III) hydride complex for the whole system. Formation of the In(III) hydride is only shown for the lowest energy configuration arising from the *penta*-co-ordinated In(III)-OMe-BINOL complex with two co-ordinating MeOH molecules. The whole system followed the trend of the model system, for which the profiles for the remaining In(III) hydride complexes are shown.

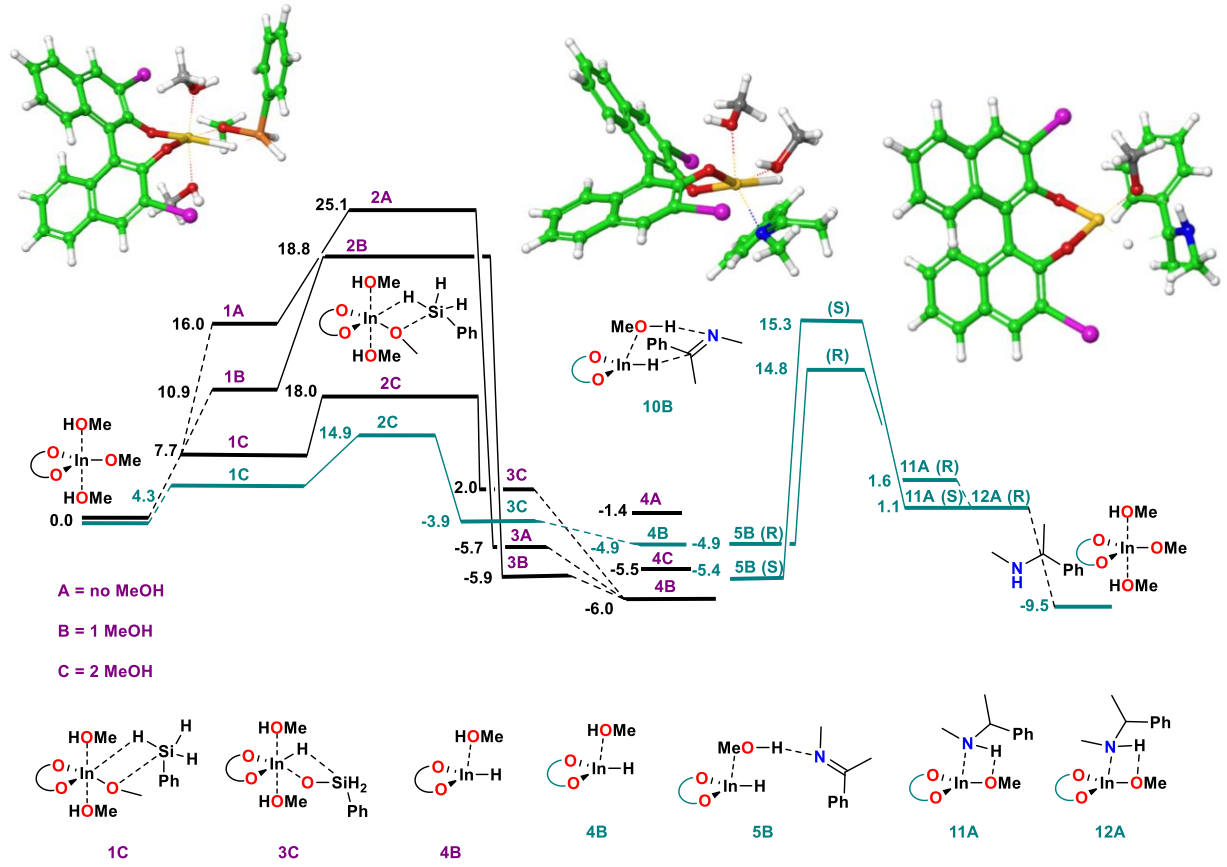

Diagram 5.4.3.3: Free-energy profile for formation of various In(III) hydride complexes and subsequent ruthenium-like reduction. The green lines are for the whole system while relevant model system free energies are depicted in black. The transition states are shown for the whole system. Dotted lines correspond to conformational changes and changes in co-ordination around the In(III) metal-centre. Full lines connect each TS with the reactant and the product obtained by following the intrinsic reaction co-ordinates from the TS, thus validating the found TS. The calculations for the reduction step were first performed with the model system, which followed the same trends.

The TS barrier for this step for the ruthenium-like imine reduction, was found to be 20.2 kcal mol^{-1}, which is the lowest TS barrier for the hydride transfer calculated in this thesis. Therefore, of the mechanistic pathways the most promising pathway evaluated computationally in this thesis. Both enantiomeric TS barriers were calculated, and the difference was found to be 0.5 kcal mol^{-1}, corresponding to 40% e.e. Experimentally it was observed that the (*R*)-3,3'-I_2-BINOL ligand favoured the (*R*)-amine and (*S*)-3,3'-I_2-BINOL ligand favoured the (*S*)-amine. Therefore, these computational results, which suggest that the (*R*)-amine will be favoured with (*S*)-3,3'-I_2-BINOL and vice versa, presents a much larger computational error.

5.4.4 Further computational investigations of plausible mechanistic pathways

A factor not yet discussed, which might, however, prove to be of significant importance, is potential isomerisation of the imine. All calculations have been performed employing the *E*-isomer of the

imine. However, in the optimised reaction conditions the imine is added to the preformed In(III) complex at 60 °C, and since the source of In(III) is $In(OTf)_3$, which is expected to ligand-exchange with the substituted BINOL ligand and co-ordinate MeOH, small amounts (up to 1.5 mol%) of TfOH are expected to be present in the reaction mixture. These two factors may both enable isomerisation of the imine. Thus, it could have been interesting to evaluate the *Z*-enantiomer of the imine in the reaction along with experimental investigation of isomerisation of the imine under various conditions.

As the pathway which proceeded via a reactive In(III) hydride complex had until this point proved most promising despite favouring the opposite enantiomer, experimental investigations targeting characterisation of an active In(III) hydride complex were carried out, which are described in Chapter 6.

Alongside further computational investigations into bisligated complexes, potential activation of the silane by the imine nitrogen lone pair and control through halogen bonds were carried out. This work is on-going and the obtained results are far too inconclusive and unfinished to be included. Some obtained structures are shown in **Figure 5.4.4.1**.

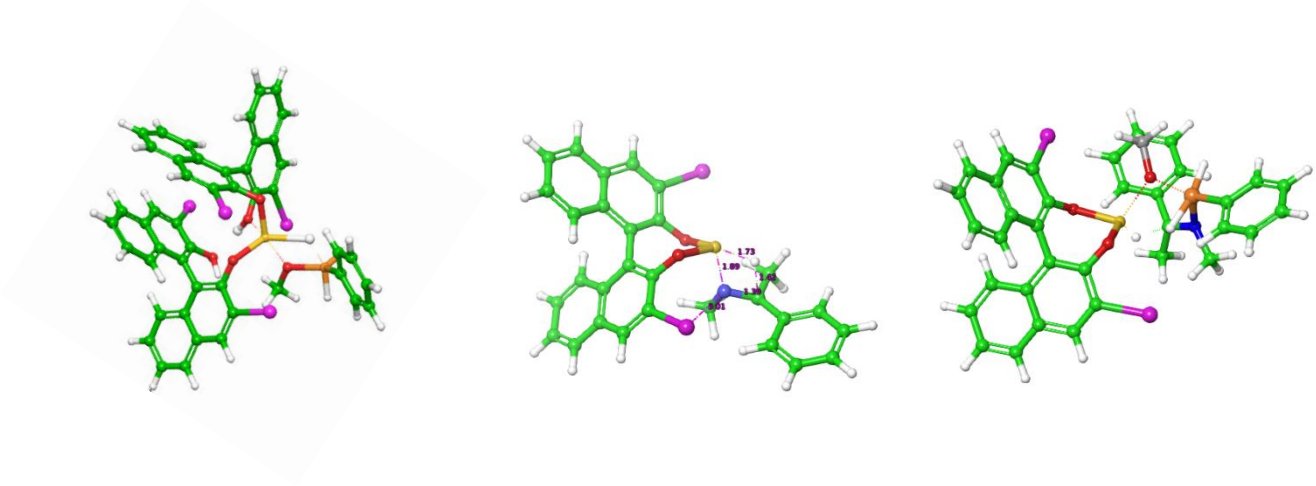

Figure 5.4.4.1: Further computational investigations from left to right: bisligated complex? (picture of located TS), halogen bonds? (picture of hypothesised TS); silane activation of the imines? (picture of located TS).

Based on the conclusions of the second part of Chapter 6, the work on elucidating the mechanism returned to hypothesising that the In(III) was acting just as a LA as was the case in several previous examples presented in Chapter 1 (for example see **Scheme 1.2.3.2**). However, as reduction through oxidative insertion (**Diagram 5.4.2**) revealed a very high TS barrier, the focus was shifted to the possibility of an active In-In dimer complex. Though this work is on-going, preliminary results are promising; the formation of a very simple In-In dimeric complex is very energetically favourable (**Diagram 5.4.4.1**).

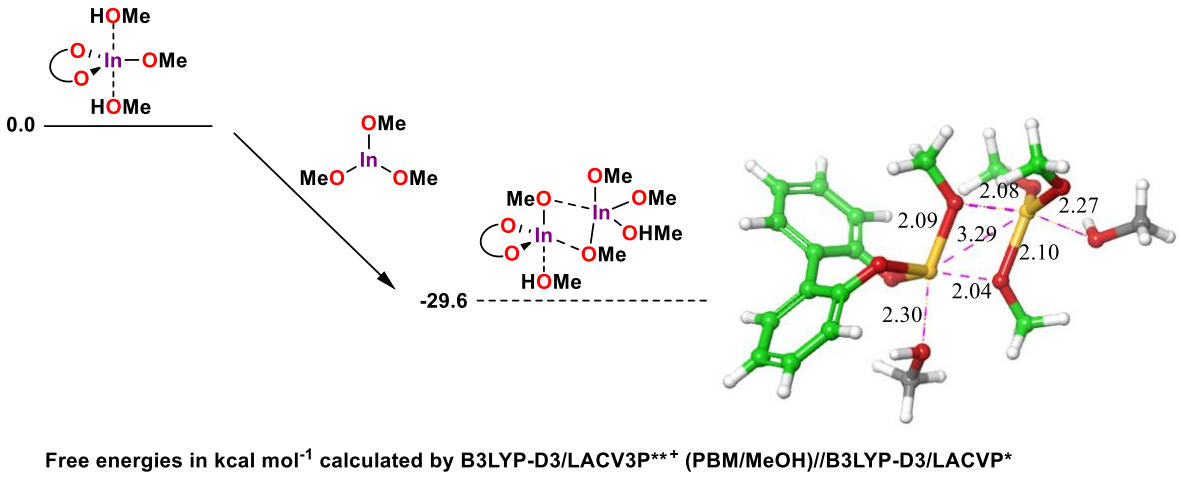

Diagram 5.4.4.1 Relative energies for the formation of a simple In(III)-In(III) dimeric complex with a In(III)-In(III) distance on 3.29 Å.

The cause of the racemic background reaction remains to be established. A fully complexed In(III)-In(III) dimeric complex, such as the complex in **Diagram 5.4.4.1** but with both In(III) ions co-ordinating a substituted BINOL ligand, could be the active species in the In(III) catalysed hydrosilane reduction, accounting for the observed e.e. and establishing a plausible reaction pathway. Alternatively, mixed dimeric complexes such as the complex presented in **Diagram 5.4.4.1** could be the cause.

5.5 Conclusion

The co-ordination around the In(III) metal centre was examined computationally in both MeOH and *i*-PrOH for a model system and the whole system. When the only other co-ordinating molecules were solvent molecules, In(III) with one ligand was found to be most stable as the *penta*-co-ordinated complex. Conversely, the *tetra*-co-ordinated complexes were lower in energy when imine, amine or silane molecules co-ordinated to the In(III) metal centre. All hydride complexes were likewise most stable as *tetra*-co-ordinated complexes. Four different plausible reaction pathways were examined. At room temperature both an MPV mechanism and a direct reduction mechanism was, under the chosen computational parameters, found to have very high TS barriers for the hydride transfer compared to the TS barrier for transferring the hydride from and In(III) hydride complex through a six-membered chair TS with one of the In(III)-co-ordinating MeOH molecules activating the imine through hydrogen donation. The energy difference between the two enantiomeric transition states corresponds to 40% e.e. but favoured the opposite enantiomer than what was observed experimentally. Further investigations are on-going and formation of In(III)-In(III) dimeric complexes have proven promising to date.

Chapter 6: Experimental Mechanistic Investigations

Alongside optimising the reaction, efforts were made to elucidate the reaction mechanism by examining the kinetics of the reaction and the structure of the active catalyst complex. The first part of the chapter focuses on kinetic experiments and the second part investigates the possibility of a non-linear effect, while the third section focuses on experimental work targeting the isolation and characterisation of an active In(III) complex.

6.1 Kinetics

In the following sections, the initial investigations of the kinetics in MeOD-d_4 will first be described and compared with the kinetics in *i*-PrOD-d_8. Then, extensive kinetic experiments examining how each component in the reaction mixture affects the rate of the imine reduction will be presented and discussed. The latter experiments were carried out with a system closely resembling the optimised system where up to 73% e.e. had been obtained, as described in Section 3.4. For all kinetics experiments the change in volume resulting from varying the paraments under examination (ligand addition, catalyst loading, silane stoichiometry and addition of additive) was hypothesised to be negligible compared to the total volume and thus not considered further.

For all graphs presented in this section time zero refers to addition of the silane.

6.1.1 Kinetic experiments in MeOD- d_4

Prior to the realisation that a pronounced increase in the e.e. could be achieved by changing the solvent system from MeOH to a mixture of *i*-PrOH and MeOH, kinetic experiments were carried out investigating the influence that the In(III) source, the ligand type and the ligand stoichiometry had on the rate of the imine reduction. With exception of the variable under examination in the given section, the conditions are the optimised reaction condition from Chapter 3 (**Scheme 6.1.1**).

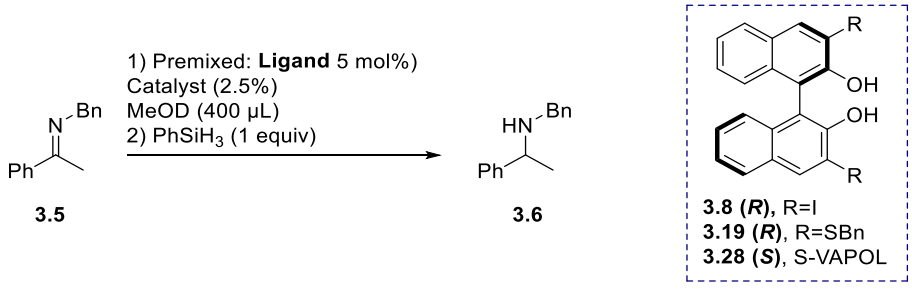

Scheme 6.1.1: Initial reaction conditions for the In(III)-catalysed hydrosilane reduction under investigation. All kinetic experiments in the following sections was performed according to these conditions; 143 µmol imine was used for each experiment and unless otherwise noted the ligand employed was the bis-iodide **3.8 (*R*)**.

Graph 6.1.1.1 shows the conversion for the imine reduction as a function of time for three different sources of In(III), both with and without (*R*)-3,3'-I_2-BINOL **3.8 (*R*)**.

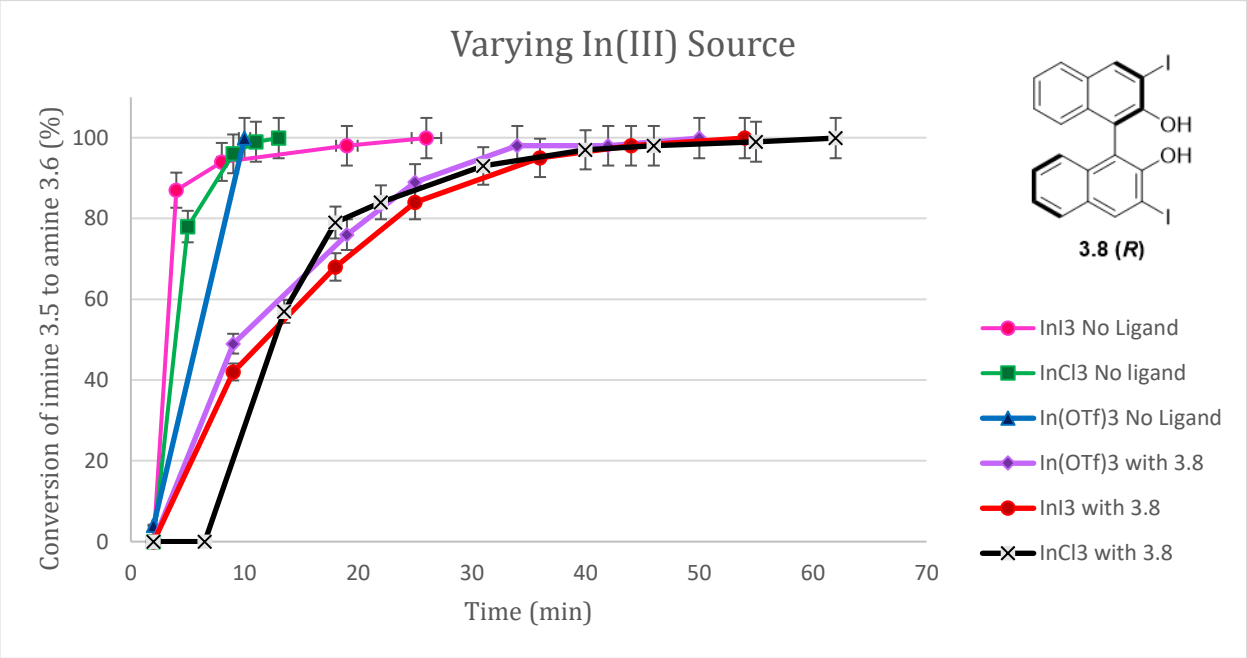

Graph 6.1.1.1: Conversion of imine as a function of time for different In(III)-sources (2.5 mol%) with and without ligand **3.8 (*R*)** (5 mol%). Conditions in accordance with **Scheme 6.1.1** using 143 µmol imine. At t=0 min silane was added. Conversion determined using 1,3,5-trimethoxybenzene as internal standard. Each datapoint represents a single measurement.

From **Graph 6.1.1.1**, it can be noted that the racemic background reaction was faster than the ligated reduction, independent of the source of In(III) employed. As mention in Chapter 3 a racemic background reaction could be outcompeted by a significant LAE. On the contrary, having a faster racemic background reaction means that the even a fraction of unligated In(III) would pose a significant competition. However, at the point these kinetic experiments were carried out, optimisation of the reaction was ongoing and the possibility of finding a better ligand potentially exhibiting a LAE remained.

As also observed in the screening reactions described in Chapter 3, formation of grey precipitate was observed in all reactions where no ligand was present.

The stoichiometry of the ligand ((*R*)-3,3'-I_2-BINOL) was investigated next (**Graph 6.1.1.2**) and it did not appear to influence the kinetics to any significant degree, with all results displaying similar reaction kinetics.

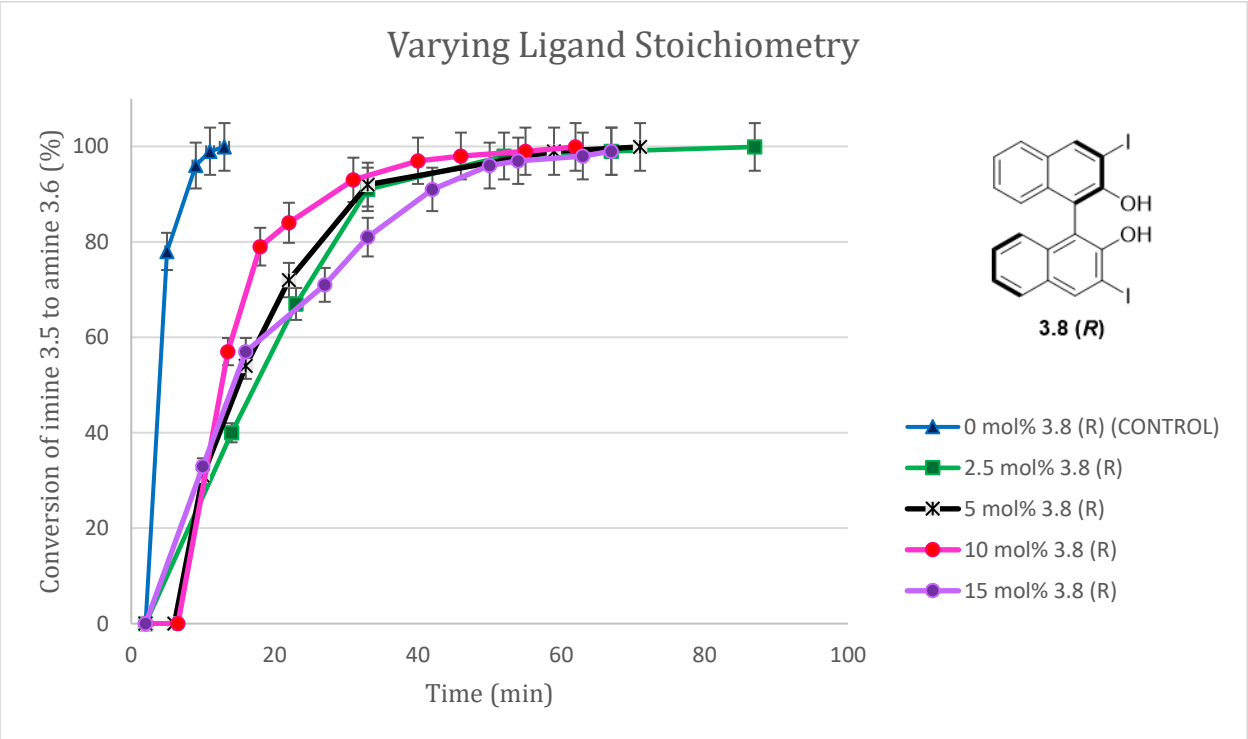

Graph 6.1.1.2 Conversion of imine as a function of time for varying ligand ((*R*)-3,3'-I_2-BINOL) to In(III) stoichiometry. Reactions conditions in accordance with **Scheme 6.1.1** using 2.5 mol% $InCl_3$ and 143 µmol imine. At t=0 min silane was added. Conversion determined using 1,3,5-trimethoxybenzene as internal standard. Each datapoint represents a single measurement.

The effect of varying the 3,3'-substituents on the ligand was also examined (**Graph 6.1.1.3**).

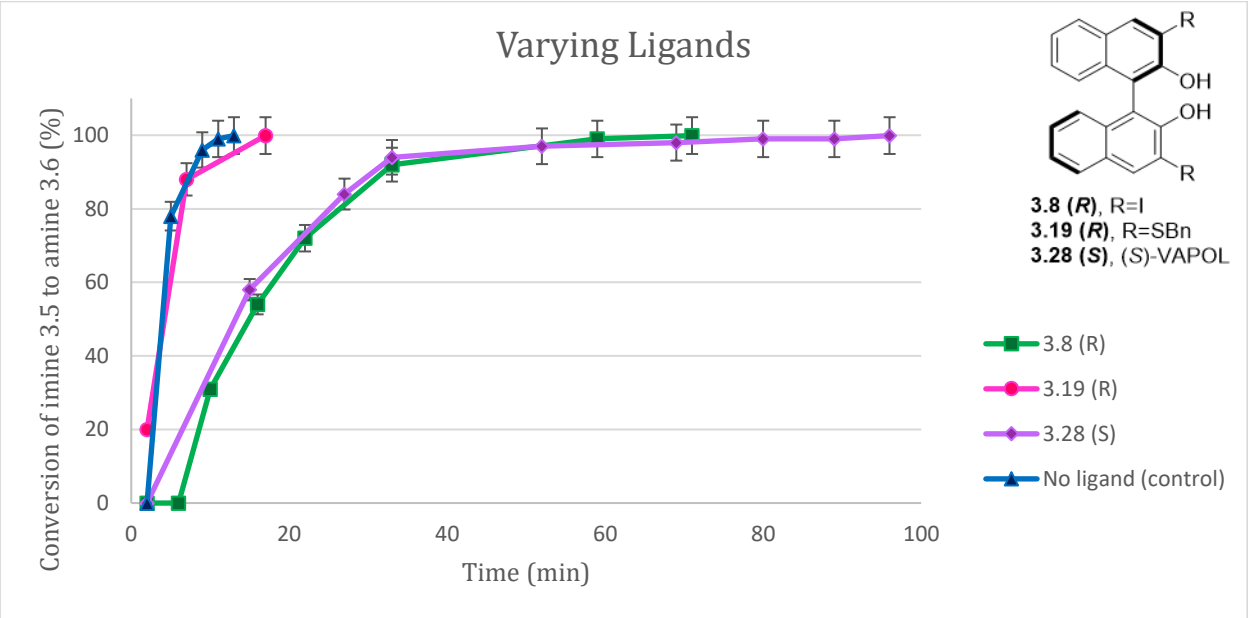

Graph 6.1.1.3 Conversion of imine as a function of time for three different ligands. Reactions conditions in accordance with **Scheme 6.1.2** using 2.5 mol% $InCl_3$ and 143 µmol imine. At t=0 min silane was added. Conversion determined using 1,3,5-trimethoxybenzene as internal standard. Each datapoint represents a single measurement.

Surprisingly, (R)-3,3'-$(SBn)_2$-BINOL was found to catalyse the reaction with a rate that was comparable with that of the background reaction, thus resulting in a significantly faster imine reduction than in the presence of either (R)-3,3'-I_2-BINOL or (S)-VAPOL. As described in Chapter 3, up to 24% e.e. could be obtained for the imine reduction when (R)-3,3'-$(SBn)_2$-BINOL was used as the ligand in MeOH; thus, some degree to binding of In(III) must happen. However, insufficient binding of this ligand to In(III) could be the cause of both the similarity of the rate with the background reaction and the fact that the e.e. could not be increased to more than 36% with this ligand. Further discussion of this ligand will follow in **Section 6.1.7** when the rate for this ligand is investigated in an *i*-PrOH-based solvent system.

As the experiment with added toluene described in Section 3.3 (**Table 3.3.1.4**) showed a decrease in the conversion when toluene was added, the rate of the imine reduction in the presence of added toluene was examined (**Graph 6.1.1.4**).

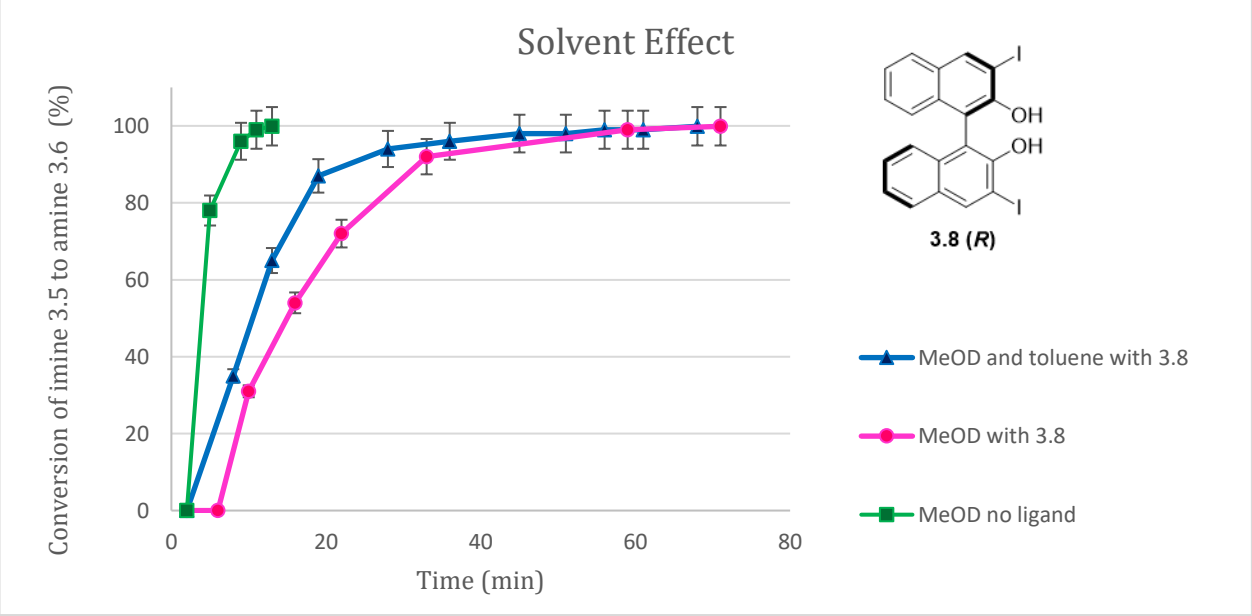

Graph 6.1.1.4 Conversion of imine as a function of time for solvent composition. The background reaction is plotted for comparation. Reactions conditions in accordance with **Scheme 6.1.1** using 2.5 mol% $InCl_3$ and 143 µmol imine. At t=0 min silane was added. 10 µL toluene was added to examine the effect of toluene on the kinetics. Conversion determined using 1,3,5-trimethoxybenzene as internal standard. Each datapoint represents a single measurement.

The addition of toluene resulted in a slight increase in the rate of the imine reduction. The experiment with toluene described here was performed with 10 µL toluene added to 400 µL MeOD, whereas the reaction system at this point was carried out with 10 µL toluene added to 100 µL MeOH. In the latter case, the conversion of the imine decreased. Before further kinetic studies were performed, examining the rate of the reaction with an increasing concentration of toluene, the promising

increase in e.e. in mixed MeOH/*i*-PrOH solvent systems was discovered. Therefore, examination of the rate of the reduction in *i*-PrOH was prioritised. Kinetic experiments with *i*-PrOD-d_8 were compared with the rate of the imine reduction in MeOD (**Graph 6.1.1.5**).

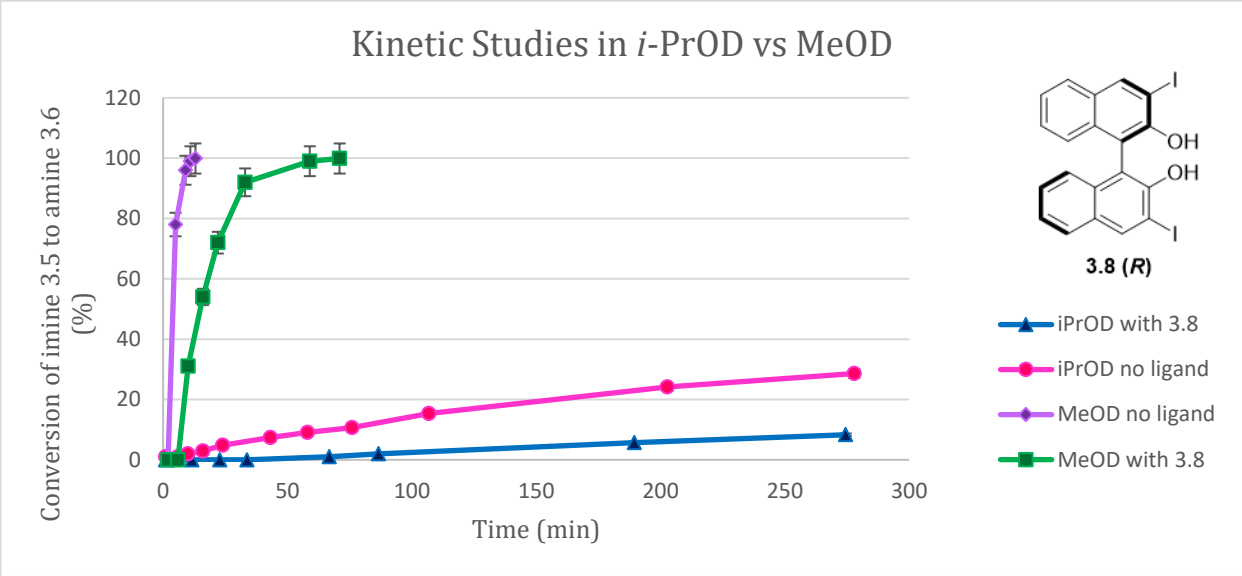

Graph 6.1.1.5 Conversion of imine as a function of time for the reaction in MeOD and *i*-PrOD with and without ligand. Reactions conditions in accordance with **Scheme 6.1.1** for the meassurements carried out in MeOD (2.5 mol% $InCl_3$, 143 µmol imine, 400 µL MeOD), whereas the kinetic experiments in *i*-PrOD reflects the optimised are closer to the optimised reactions conditions; 0.5 mol% $In(OTf)_3$, 1 mol% 3.8, 72 µmol imine, 675 µL *i*-PrOD. For reactions in *i*-PrOD this replaced MeOD as solvent. At t=0 min silane was added. Conversion determined using 1,3,5-trimethoxybenzene as internal standard. Each datapoint represents a single measurement.

It is evident from **Graph 6.1.1.5** that the reaction in *i*-PrOD is significantly slower, which is partly expected due to the lowered catalyst loading. Unfortunately, the imine reduction was found to proceed to no more than 40% after 24 hours both with and without ligand (datapoint excluded in graph to allow for comparison with the MeOD experiments). Whether the remaining almost 60% imine eventually would be reduced remains unknown; further measurements on this system were not performed as it was concluded to be a poor representation of the actual reaction system: imine reductions carried out in *i*-PrOH all went to completion. Several factors, which will be described in the following sections, decrease the rate of the imine reduction and result in an extended reaction time being required for achieving full conversion. It is hypothesised that the slow conversion could be caused by water in the deuterated solvent or the deuterated solvent itself. The effect of either would have a significantly more pronounced effect on a system where the reaction goes to full conversion in 12-18 hours than in reactions completed in less than 2 hours.

For kinetic studies described in the following sections, the reaction was carried out in NMR tubes with *i*-PrOH as a solvent. A melting point tube filled with *i*-PrOD was placed inside the NMR tube along with 50 µL *i*-PrOD being added directly into the reaction mixture. This was found to be a

reliable method of ensuring sufficient *i*-PrOD to allow the NMR spectrometer to lock and shim on the sample, while minimising the effect on the outcome of the reaction (rate, conversion, e.e.) caused by the deuterated solvent.

Several kinetic experiments were carried to evaluate the influence on the reaction rate of each component present in the reaction mixture. With exception of the variable under examination in the given section, the conditions are the optimised reaction condition from Chapter 3 (**Scheme 6.1.2**).

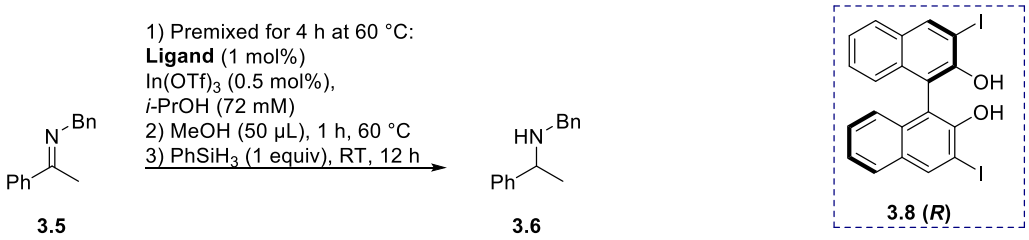

3.5 **3.6** **3.8 (*R*)**

Scheme 6.1.2: Optimised reaction conditions for the In(III)-catalysed hydrosilane reduction under investigation. All kinetic experiments in the following sections was performed according to these conditions; 72 µmol imine was used for each experiment and unless otherwise noted the ligand employed was the bis-iodide **3.8 (*R*)**.

The graphs shown in the following section show conversion as a function of time. Time zero refers to the when silane was added. For each dataset, attempts to determine the reaction order for the component under investigation were made. Unfortunately, the racemic background reaction continued to be significantly faster and has not been included in the graphs in the following section.

6.1.2 Examining the effect on reaction rate with varying ligand stoichiometry

Varying the stoichiometry of the ligand proved the reaction to be ligand decelerated as also previously observed. The reaction was fastest with only 0.5 mol% ligand and slowest with 2 mol%; however, 1 mol% and 1.5 mol% proceeded with similar rates (**Graph 6.1.2.1**).

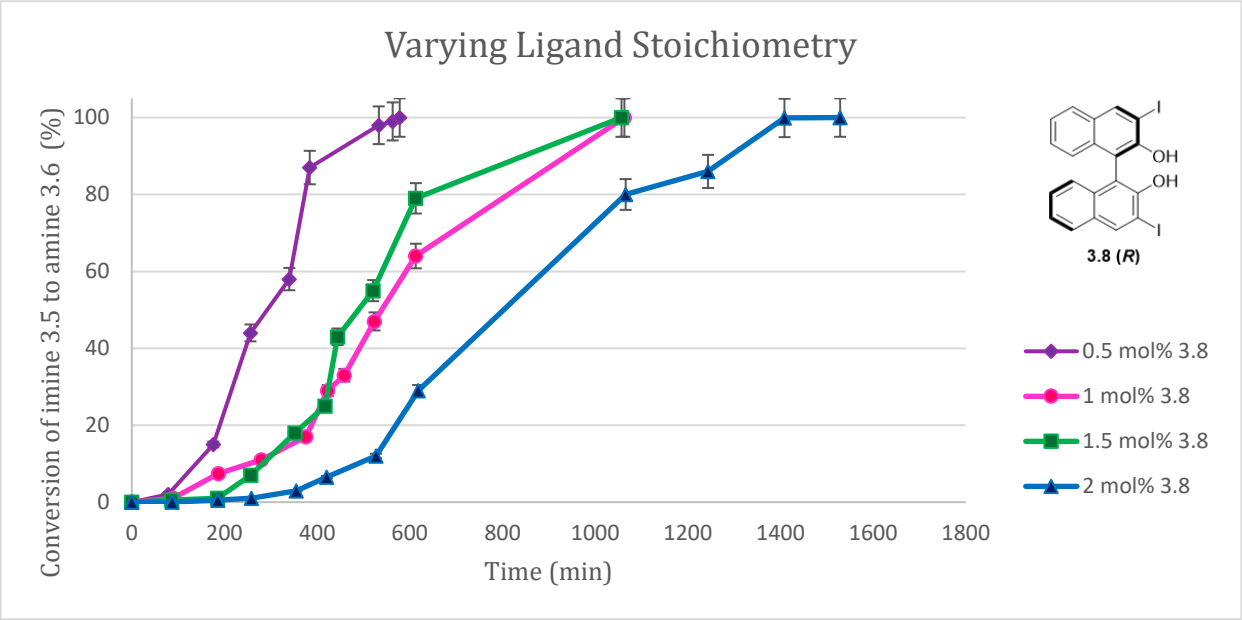

Graph 6.1.2.1 Conversion of imine as a function of time with varying the stoichiometry of the bis-iodide ligand **3.8 (*R*)**. Conversion determined using 1,3,5-trimethoxybenzene as internal standard. Reaction conditions in accordance with **Scheme 6.1.2** using 72 µmol imine. At t=0 min silane was added. Each datapoint represents a single measurement.

An induction period is observed before the reduction of the imine commences, at which point an acceleration in the rate is observed. The presence of an induction period suggests that a catalytically active complex capable of reducing the imine must form first. This corresponds well with the mechanism suggested based on the computational work presented in Chapter 5, which goes through the formation of an active In(III) hydride species. The In(III) hydride complex, which will reduce the imine, must first form from a hydride transfer from the silane. This step was computationally found to be rate determining, which also corresponds well with the acceleration observed once the imine reduction initiated.

Closer investigation of the initial rate during this induction period (**Graph 6.1.2.2**) shows an earlier onset of the reaction in the presence of only 0.5 and 1 mol% ligand. For 1.5 and 2 mol% ligand, the initial rate of the reaction appears similar. Whether this similarity is also true for 0.5 and 1 mol% cannot be verified due to an insufficient number of datapoints recorded in the first 100 minutes of the reaction.

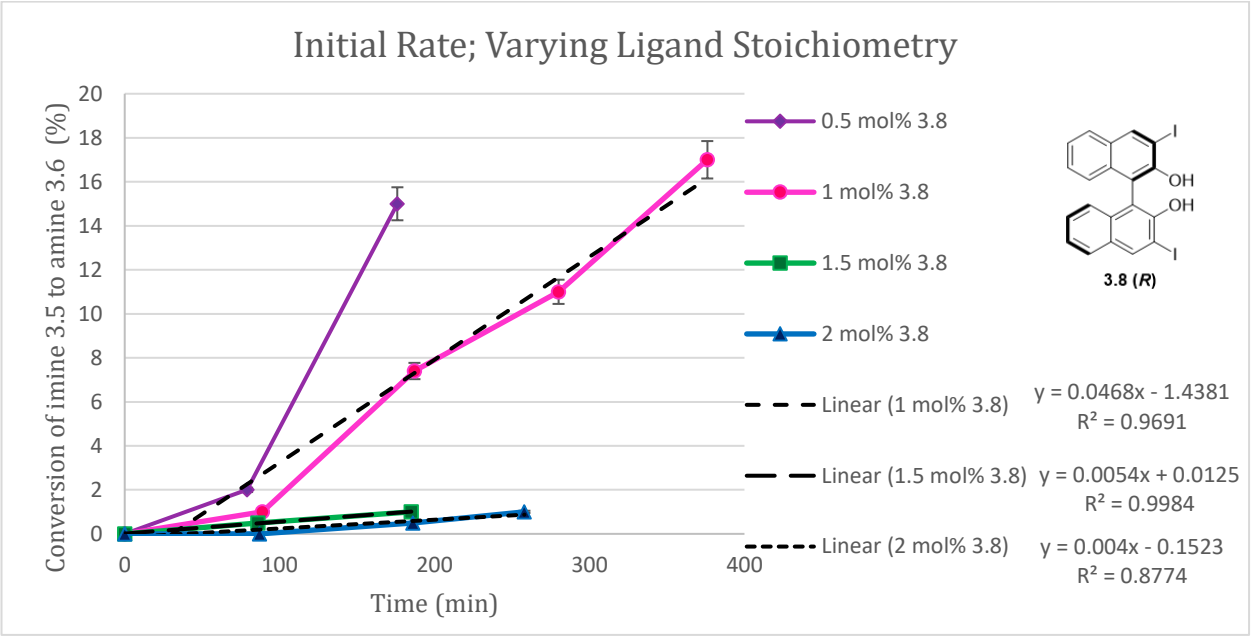

Graph 6.1.2.2 (Enlargement of Graph 6.1.2.1): Examining variation in initial rate for varying concentration of bisiodide ligand **3.8 (*R*)**. Conversion determined using 1,3,5-trimethoxybenzene as internal standard. Reaction conditions in accordance with **Scheme 6.1.2** using 72 µmol imine. At t=0 min silane was added. Each datapoint represents a single measurement.

The rate of the imine reduction is ligand decelerated (**Graph 6.1.2.3**). The e.e. was generally found to increase when more than 1 equiv of ligand was used. The catalyst turnover of In(III) for the imine reduction is not known; thus, it may be that traces of non-ligated In(III) catalyse a number of catalytic cycles before being reduced to metallic In(0). It is hypothesised that the use of more than 1 equiv of In(III) along with the extended premix at elevated temperatures could result in higher e.e., as a result of minimising a such background reaction.

The decrease in rate with further increase in the ligand concentration could be caused by ligand blocking the catalytic sites through co-ordinating to the In(III) metal-centre. Investigations of mechanisms with two ligands coordinated the In(III) are ongoing. Preliminary result indicate formation of an In(III) hydride complex with two ligands co-ordinated is thermodynamically plausible. However, to date a possible route to subsequent imine reduction has not been established: the steric bulk arising from the presence of two ligands has so far hindered co-ordination to the imine. Furthermore, as described towards the end of Chapter 5, the possibility of the active catalyst being an In(III)-In(III) dimer is thermodynamically plausible, and this implies the possibility of the existence of many different complexes with e.g. a mix of bis – and mono-ligated In(III) metal centres. In(III) ions with various numbers of ligands are likely to catalyse the reaction in different rates; or, alternatively, reactivity might be blocked by binding of another ligand. These factors could be important for explaining the ligand-decelerated effect observed.

The reaction order for the imine reduction with varying ligand concentration cannot be determined, as the graphs for 1 and 1.5 mol% seem to follow the same datapoints. It is not known whether this is caused by an experimental error or if both 1 and 1.5 mol% ligand lie in an interval in which the rate of the reaction is unaffected by the ligand concentration. Outside this interval the reaction rate increases with decreased ligand concentration.

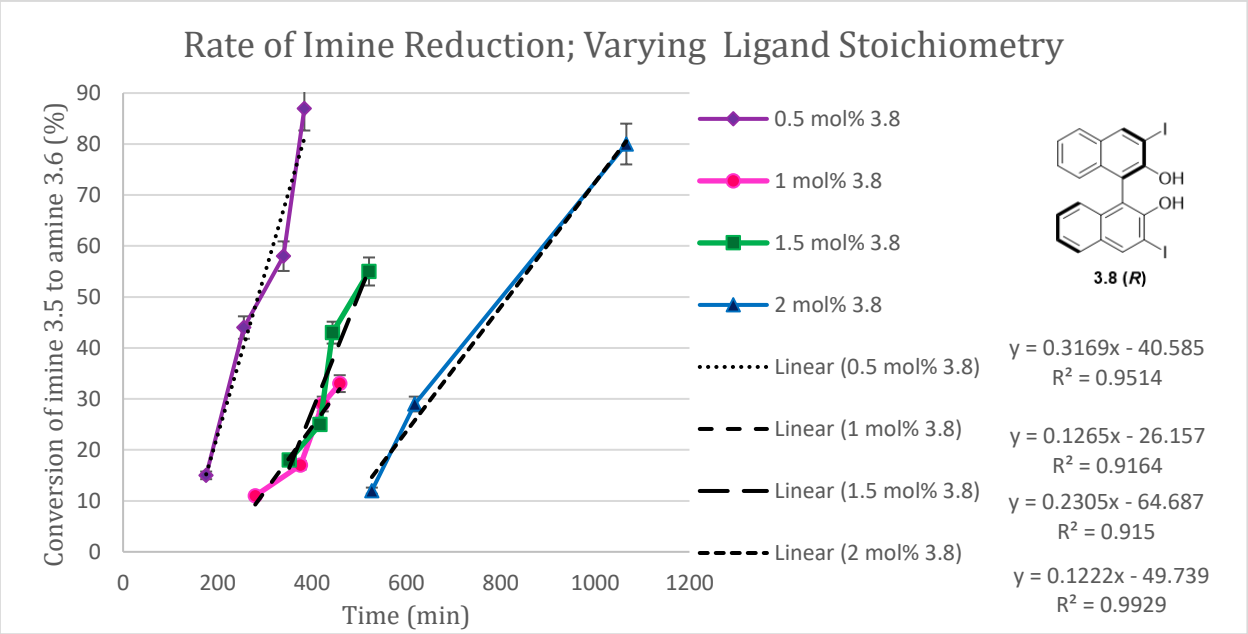

Graph 6.1.2.3 (Enlargement of Graph 6.1.2.1): Examining variation in rate of the imine reduction with varying concentration of bisiodide ligand **3.8 (*R*)**. Conversion determined using 1,3,5-trimethoxybenzene as internal standard. Reaction conditions in accordance with **Scheme 6.1.2** using 72 µmol imine. At t=0 min silane was added. Each datapoint represents a single measurement.

6.1.3 Varying the concentration of In(III)

Increasing the catalyst loading resulted in an increase in rate (**Graph 6.1.3.1**).

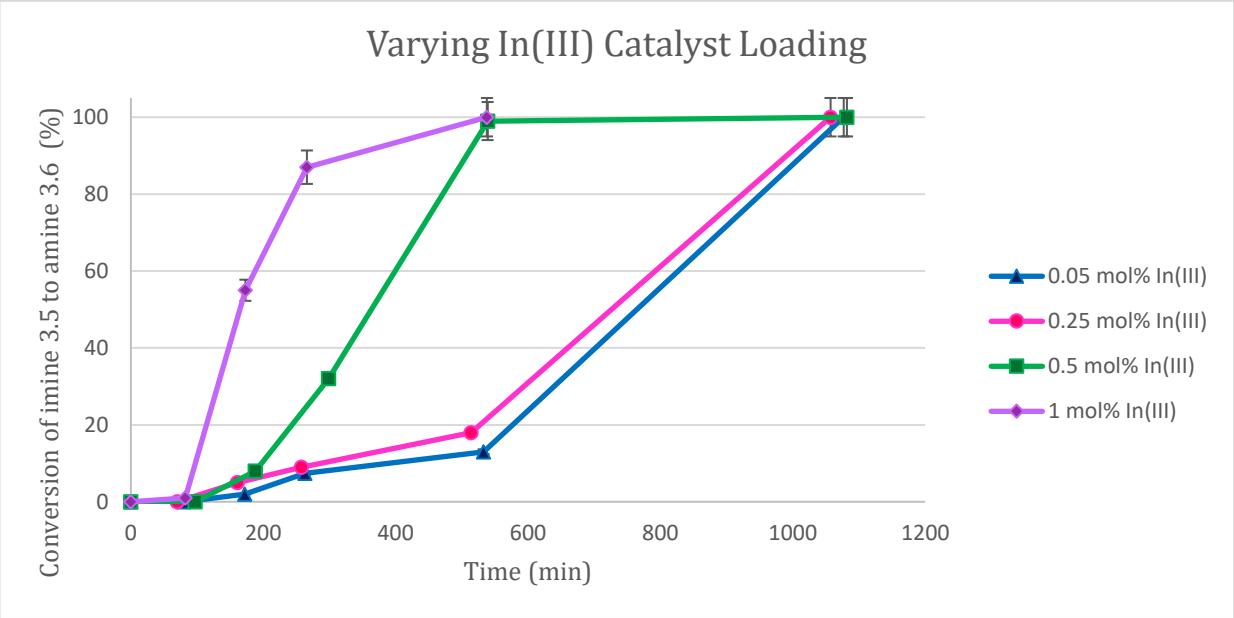

Graph 6.1.3.1 Conversion of imine as a function of time with varying In(III) catalyst loading. Conversion determined using 1,3,5-trimethoxybenzene as internal standard. Reaction conditions in accordance with **Scheme 6.1.2** using 72 µmol imine. At t=0 min silane was added. Each datapoint represents a single measurement.

The reaction is very slow in the beginning and then the rate increases significantly. Again, this indicates an induction period. The quality of the data could be significantly improved by recording more frequent measurements during the induction period for 1 and 0.5 mol% of In(III) as well as during the imine reduction for the reactions with 0.05 and 0.25 mol% In(III). A closer examination of the initial rate (**Graph 6.1.3.2**) highlights the difference in the transition from induction period to imine reduction for 0.5 and 1 mol% of In(III) compared to 0.05 and 0.25 mol%. For the lower In(III) loadings, the imine reduction is initiated prior to the more significant rate acceleration (**Graph 6.1.3.2**). However, even though there is a 5 times difference in the two lowest loadings they appear fairly similar in rate.

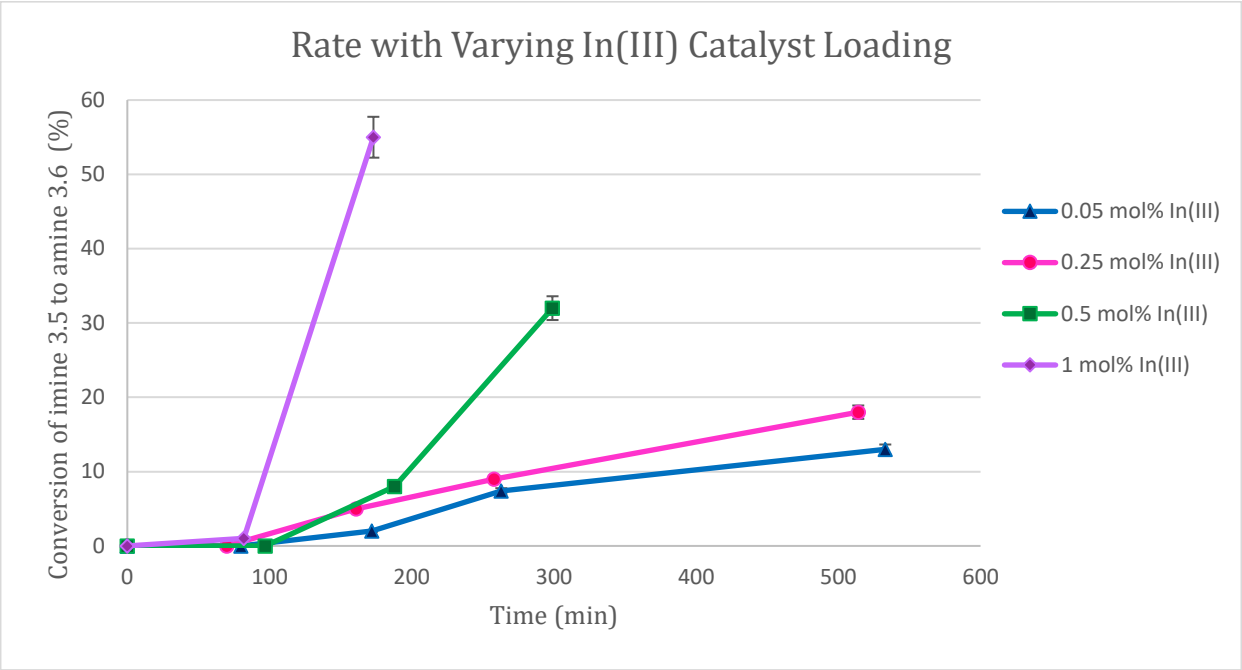

Graph 6.1.3.2 (Enlargement of Graph 6.1.3.1): Conversion of imine as a function of time with varying In(III) catalyst loading. Conversion determined using 1,3,5-trimethoxybenzene as internal standard. Reaction conditions in accordance with **Scheme 6.1.2** using 72 µmol imine. At t=0 min silane was added. Each datapoint represents a single measurement.

Closer examination of the rates for the imine reduction (**Graph 6.1.3.3**) suggests that the rate of the imine reduction is approximately proportional to the In(III) concentration; 1 mol% In(III) catalyses the reaction with approximately twice the rate of 0.5 mol% In(III). Unfortunately, the lack of data points between 600 and 1000 minutes for the two lower In(III) concentrations prevents comparison with the rate here, though it seems strikingly alike, indicating that there might be a threshold under which the In(III) concentration does not influence the rate.

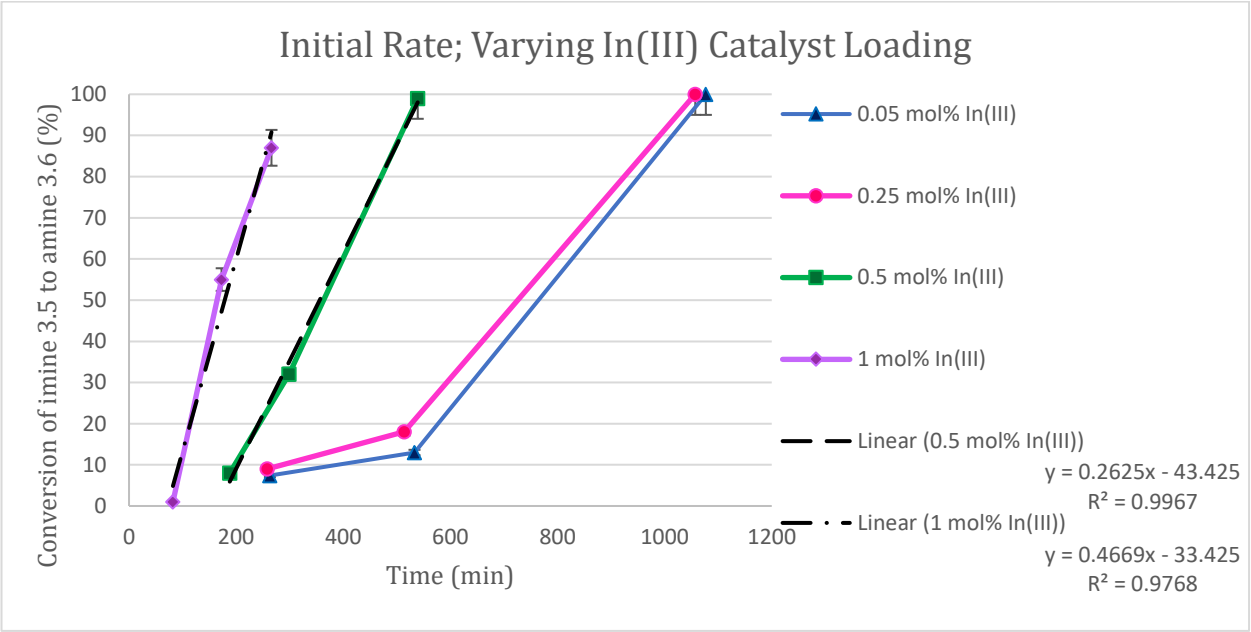

Graph 6.1.3.3 (Enlargement of Graph 6.1.3.1): Conversion of imine as a function of time with varying In(III) concentration, focusing on the rate of the imine reduction. Conversion determined using 1,3,5-trimethoxybenzene as internal standard. Reaction conditions in accordance with **Scheme 6.1.2** using 72 µmol imine**.** At t=0 min silane was added. Each datapoint represents a single measurement.

6.1.4 The effect of dilution

The effect of overall dilution was examined through varying the concentration of imine with respect to the total volume of *i*-PrOH and MeOH combined. As the ratio of MeOH to imine effects the rate of the reaction, the MeOH to imine ratio was kept constant. Likewise, the ligand to In(III) ratio, the catalyst loading and the silane stoichiometry was kept the same with respect to the imine (**Scheme 6.1.1**).

Increasing the concentration of the imine by decreasing the added volume of *i*-PrOH resulted in a faster conversion (**Graph 6.1.2.3**). With both 0.13M and 0.076 M there is an interesting decrease in the rate after 30-40 % conversion, for which the cause has not been found.

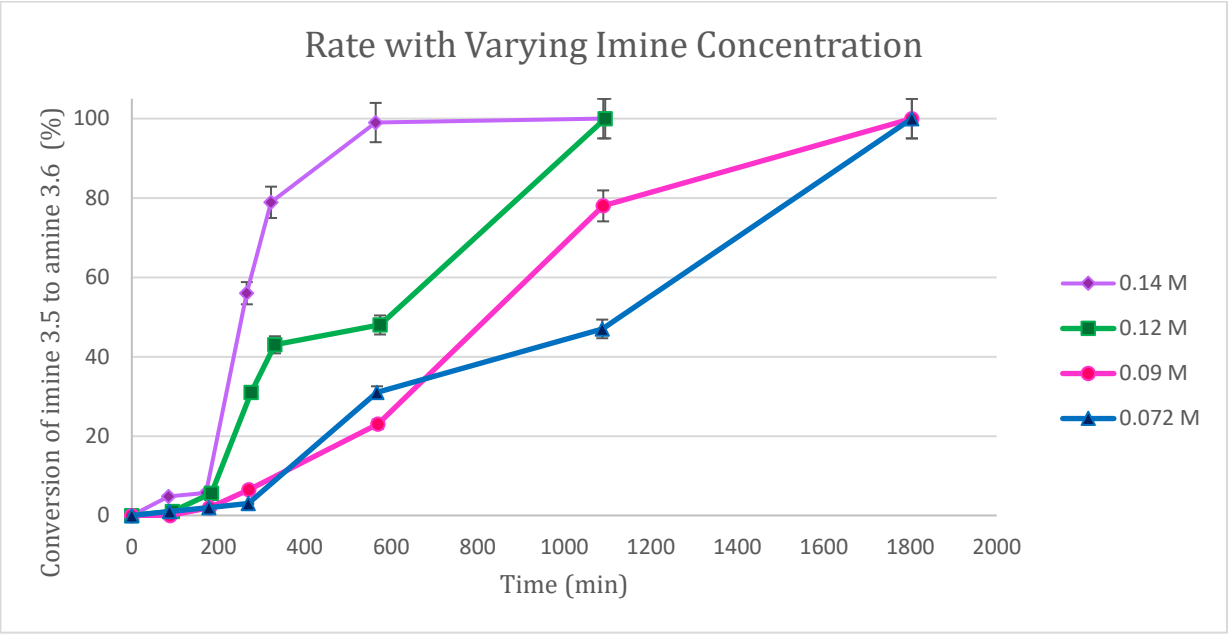

Graph 6.1.4.1: Conversion of imine as a function of time with varying the amount of *i*-PrOH. Conversion determined using 1,3,5-trimethoxybenzene as internal standard. Reaction conditions in accordance with **Scheme 6.1.2** using 72 µmol imine. At t=0 min silane was added. Each datapoint represents a single measurement.

Again, a pronounced induction period is observed; almost no imine reduction is observed in the first 200 minutes, after which an acceleration in rate is observed once the imine reduction properly starts. As seen in **Graph 6.1.4.2,** it is not possible to draw any conclusions regarding the effect of dilution on initial rate without repeating the experiment with more frequent measurements in the first 200 minutes of the reaction.

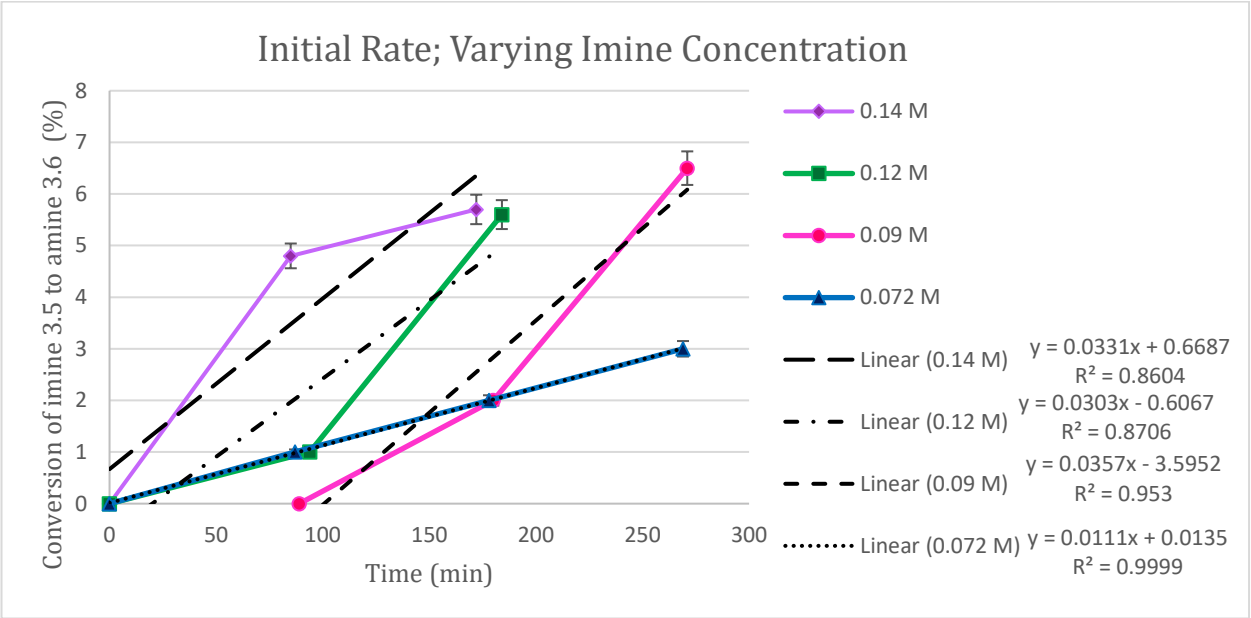

Graph 6.1.4.2 (Enlargement of Graph 6.1.4.1): Conversion of imine as a function of time with varying the amount of *i*-PrOH, attempts on determining initial rates. Conversion determined using 1,3,5-trimethoxybenzene as internal standard. Reaction conditions in accordance with **Scheme 6.1.2** using 72 µmol imine. At t=0 min silane was added. Each datapoint represents a single measurement.

The rate of the imine reduction with imine concentration is shown in **Graph 6.1.4.3.** For 0.072 M an extra data point is included to enable linear regression. For 0.12 M it must be noted that the regression shown in the graph below is prior to the sudden decrease in rate, the cause for which is unknown.

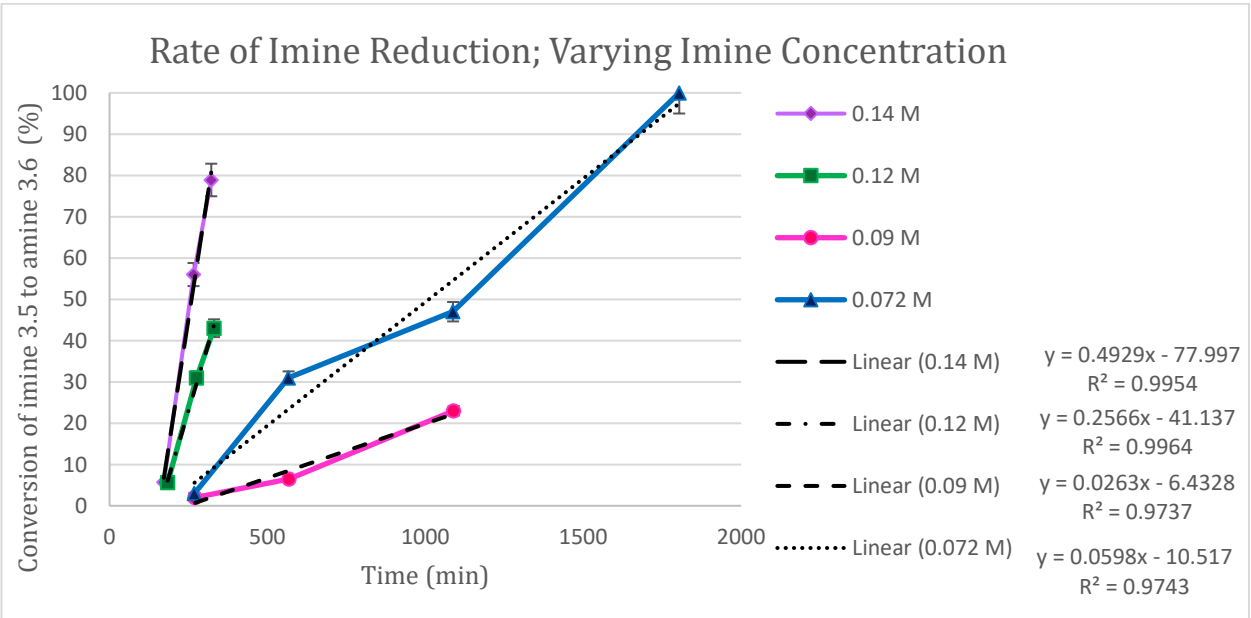

Graph 6.1.4.3 (Enlargement of Graph 6.1.4.1): Conversion of imine as a function of time with varying imine concentration, attempts on determining the rate of the imine reduction. Conversion determined using 1,3,5-trimethoxybenzene as internal standard. Reaction conditions in accordance with **Scheme 6.1.2** using 72 µmol imine. At t=0 min silane was added. Each datapoint represents a single measurement.

Since the reaction rate is lower for 0.09 M than 0.072 M, no conclusions can be drawn from the data obtained regarding the order of the reaction with respect to the concentration of the imine.

6.1.5 Varying the silane concentration

Increasing the amount of silane used was found to increase the rate of the reaction (**Graph 6.1.5.1**), which is consistent with a previously observed decrease in e.e. with increased silane concentration and increase in e.e. with decreased reaction rate.

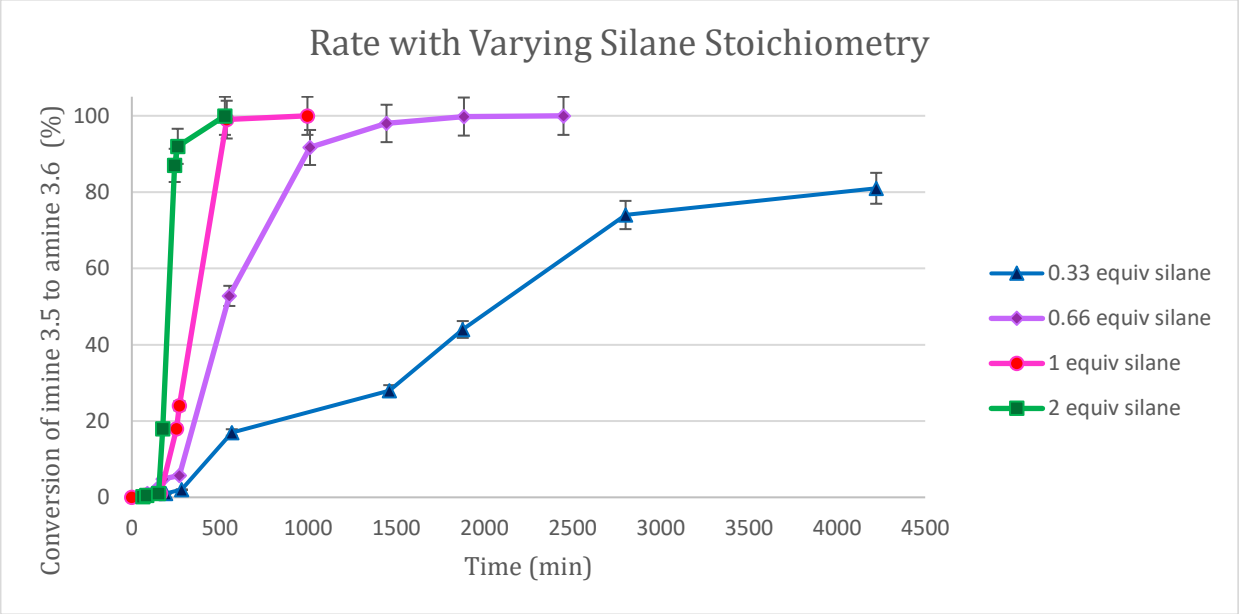

Graph 6.1.5.1: Conversion of imine as a function of time with varying silane stoichiometry. Conversion determined using 1,3,5-trimethoxybenzene as internal standard. Reaction conditions in accordance with **Scheme 6.1.2** using 72 µmol imine. At t=0 min silane was added. Each datapoint represents a single measurement.

From a closer examination of the rate during the induction period in **Graph 6.1.5.1** (**Graph 6.1.5.2**), indications of two different processes are found: an incubation period followed by the imine reduction. Analysis of the incubation period for initial rates of the reaction under the four different silane concentrations suggests that the silane concentration has a minimal influence on the reaction rate (**Graph 6.1.5.2**). However, it is to be noted that, of the experiments presented here, the lowest concentration of silane (0.33 equiv), in the case of all three hydrogen atoms being transferred from the silane, corresponds to stoichiometric hydride concentration. Further experiments with sub-stoichiometric hydride concentrations would be interesting to conduct. In Chapter 3, $PhSiH_3$ was found to be the only efficient reducing agent of the silanes examined. As $PhSiH_3$ is the only of the silane examines with the ability to transfer all three hydrogen atoms, this further indicates that the transfer of all three hydrogen atoms takes place.

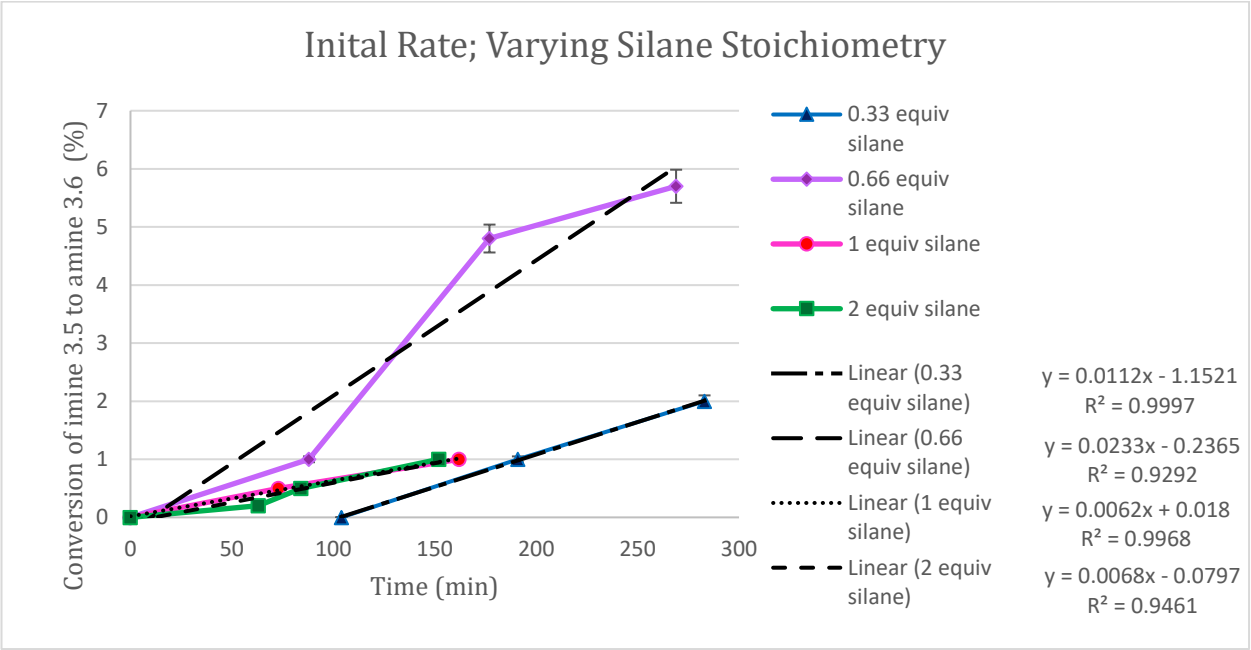

Graph 6.1.5.2 (Enlargement of Graph 6.1.5.1): Conversion of imine as a function of time with varying silane stoichiometry, focusing on initial rates. Conversion determined using 1,3,5-trimethoxybenzene as internal standard. At t=0 min silane was added. Reaction conditions in accordance with **Scheme 6.1.2** using 72 µmol imine. Each datapoint represents a single measurement.

Examining these initial rates with respect to reaction order, it is noted that the rate seems to be proportional to the silane concentration between 0.33 and 1 equiv. However, the rate increase from 1 and 2 equiv is insignificant, indicating an upper threshold over which the rate is no longer affected by the silane concentration.

If the second part of the steep slope of **Graph 6.1.5.1** is examined instead (**Graph 6.1.5.3**), the silane concentration exhibits strong influence on the rate. This step corresponds to the imine reduction.

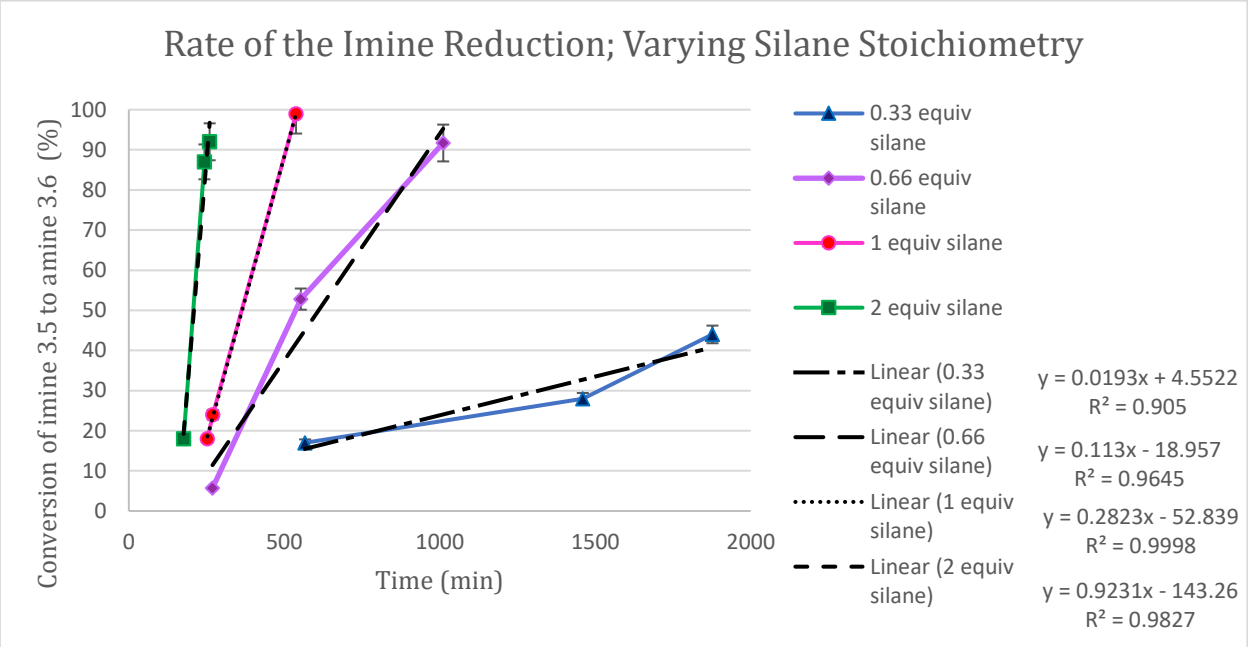

Graph 6.1.5.3 (Enlargement of Graph 6.1.5.1): Conversion of imine as a function of time with varying silane stoichiometry, focusing on initial rates. Conversion determined using 1,3,5-trimethoxybenzene as internal standard. Reaction conditions in accordance with **Scheme 6.1.2** using 72 µmol imine. At t=0 min silane was added. Each datapoint represents a single measurement.

From the rate expressions, the following relationship between the rate constants is found (**Graph 6.1.5.4**), indicating that the imine reduction is of 9th order with respect to the silane concentration.

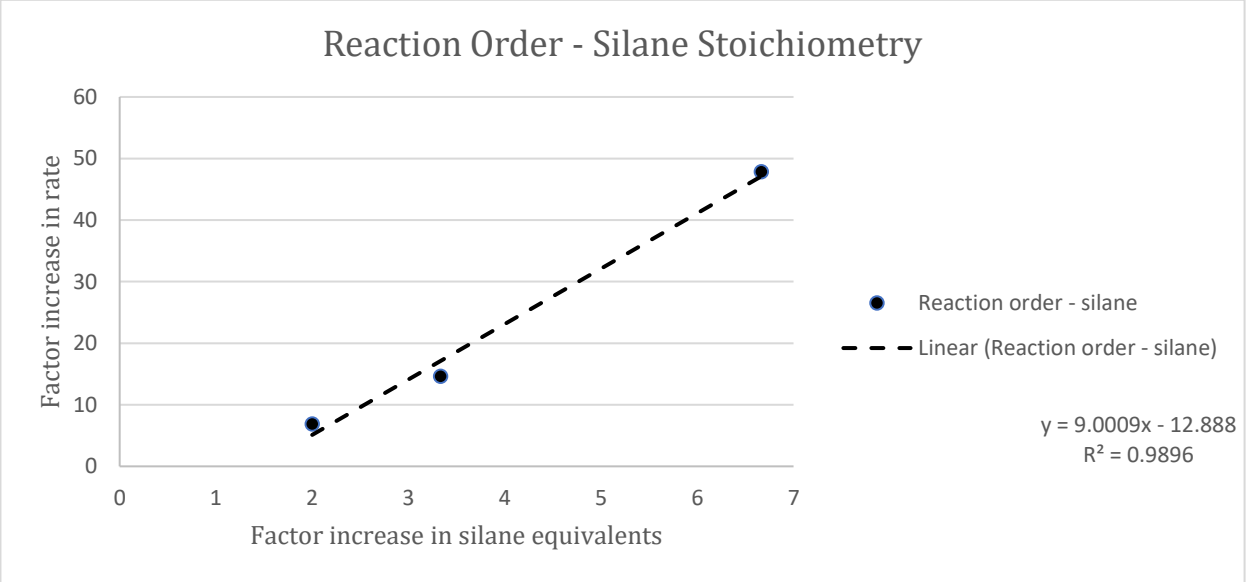

Graph 6.1.5.4: Determining the reaction order with respect to the silane stoichiometry.

The pronounced effect of the silane stoichiometry on the rate of the imine reduction might suggest the silane is transferring all three hydrogen atoms, as each equivalent of the silane corresponds to a three-fold increase in the hydrogen atoms available. The reaction order would thus be a 3rd order reaction with respect to the hydrogen atoms available for transfer. Furthermore, the silane could be participating in both the reduction of the imine and the regeneration of the active catalyst. For future work, when repeating these experiments, the rate with less than 0.33 equiv of the silane should also be examined.

6.1.6 Examining the effect of varying the MeOH concentration

Increasing the added amount of MeOH increases the rate (**Graph 6.1.6.1**), which may indicate MeOH has a positive influence on assembly of the active catalyst complex, whether this comes from aiding formation of or breaking of e.g. an In(III)-In(III) dimeric complex.

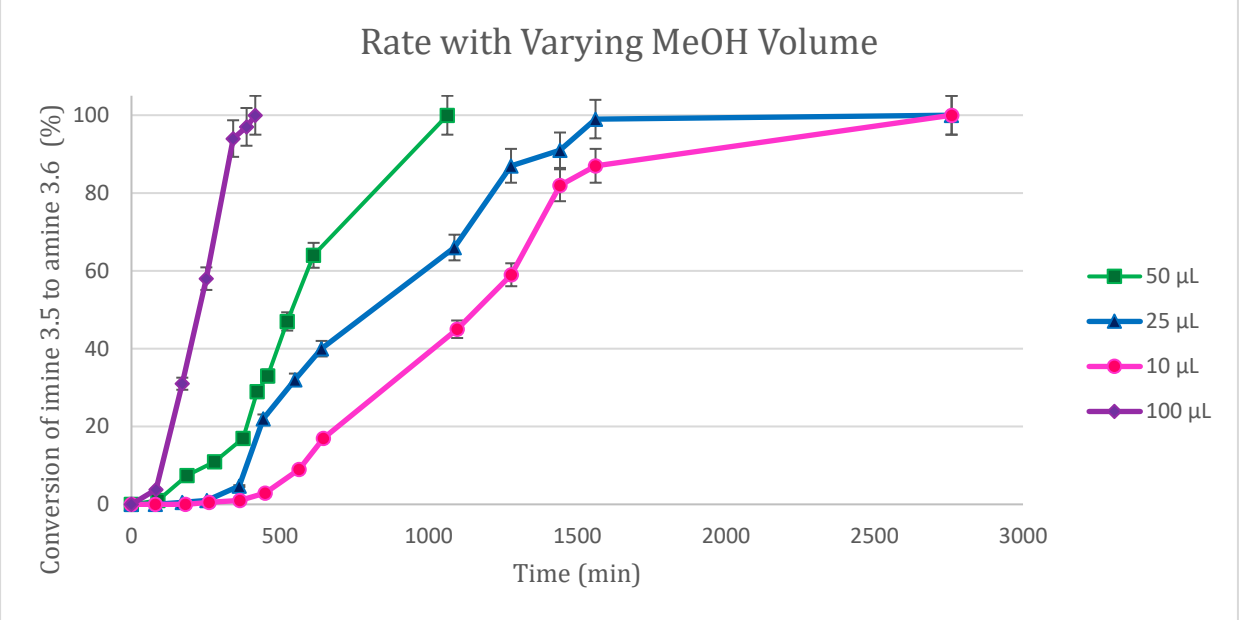

Graph 6.1.6.1: Conversion of imine as a function of time with varying amounts of MeOH. Conversion determined using 1,3,5-trimethoxybenzene as internal standard. Reaction conditions in accordance with **Scheme 6.1.2** using 72 µmol imine. At t=0 min silane was added. Each datapoint represents a single measurement.

A closer examination of the first hours of the reaction reveals a pronounced effect on the length of the incubation time with varying concentration of MeOH (**Graph 6.1.6.2**).

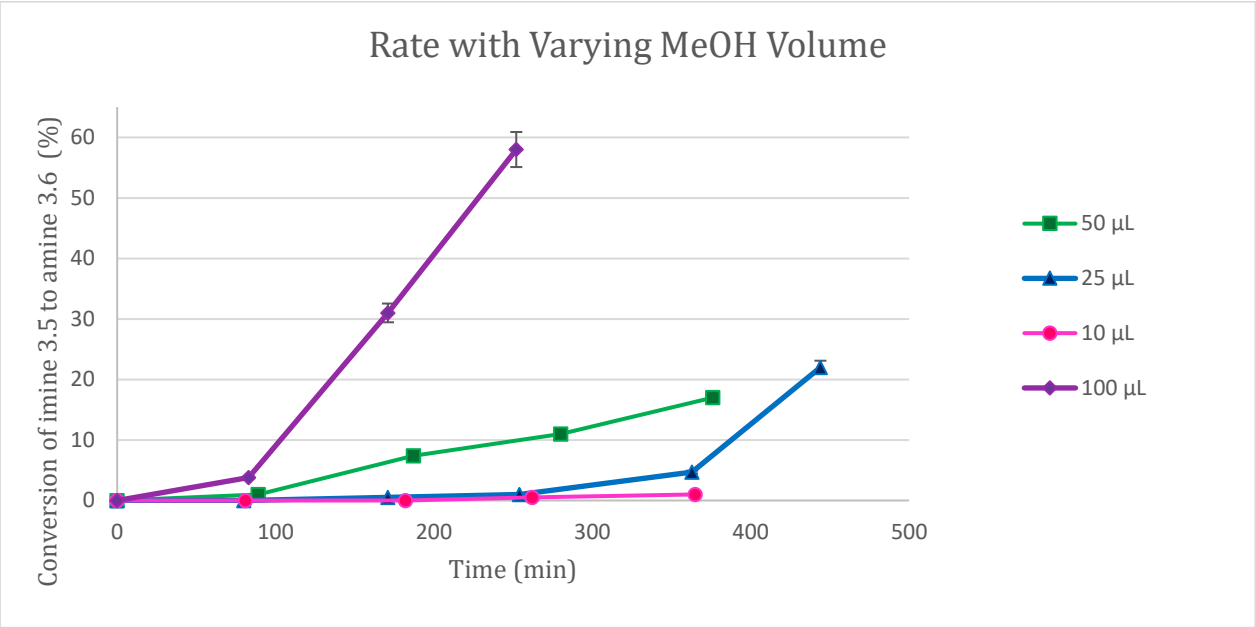

Graph 6.1.6.2 (Enlargement of Graph 6.1.6.1): Conversion of imine as a function of time with varying amount of MeOH. Conversion determined using 1,3,5-trimethoxybenzene as internal standard. Conditions in accordance with **Scheme 6.1.1.** At t=0 min silane was added. Each datapoint represents a single measurement.

Attempts to investigate the initial rate (**Graph 6.1.6.3**) are only possible for 10 and 25 µL of MeOH added due to lack of more frequent data points for 50 and 100 µL in the first 100 minutes of the reaction.

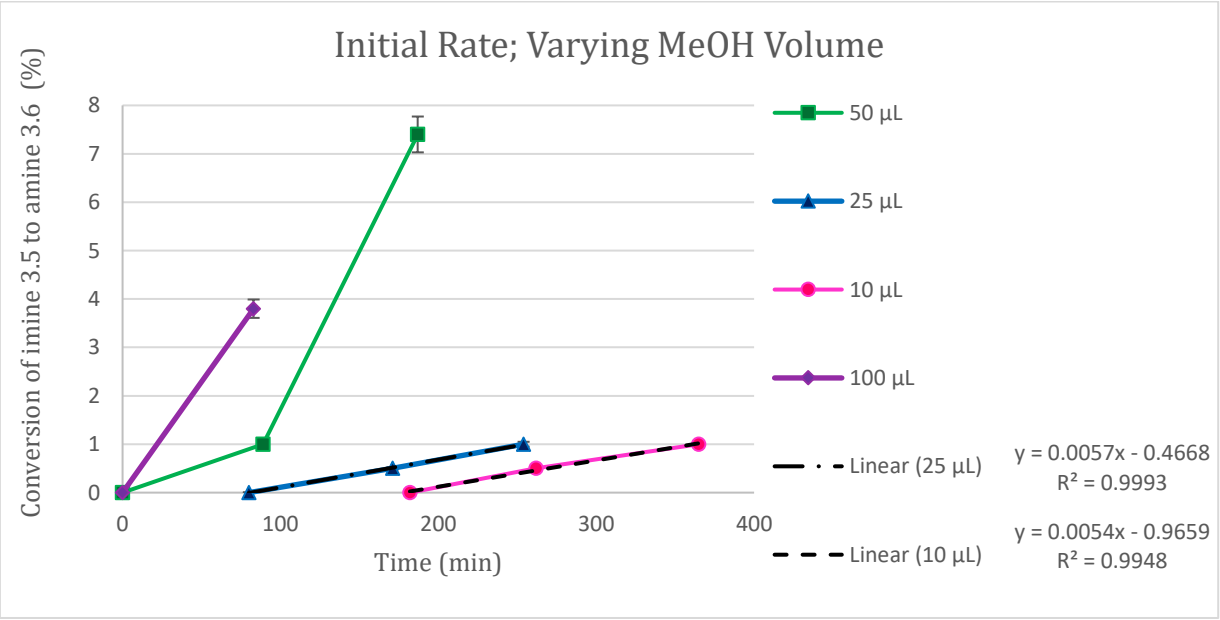

Graph 6.1.6.3 (Enlargement of Graph 6.1.6.1): Conversion of imine as a function of time with varying amount of MeOH; initial rates. Conversion determined using 1,3,5-trimethoxybenzene as internal standard. Reaction conditions in accordance with **Scheme 6.1.2** using 72 µmol imine. At t=0 min silane was added. Each datapoint represents a single measurement.

Measuring from the onset of conversion of imine, the initial rate for 10 and 25µL is very similar. However, it is striking how much the concentration of MeOH affects the onset of the reaction and it would have been very interesting to have more data points for the first 100 minutes of the reaction. This pronounced effect on when the imine reduction accelerates again indicate MeOH influence formation of the active catalyst complex. Closer examination of the rate of the imine reduction once the reaction has started suggests that the rate of imine conversion is proportional to the concentration of MeOH (**Graph 6.1.6.4**).

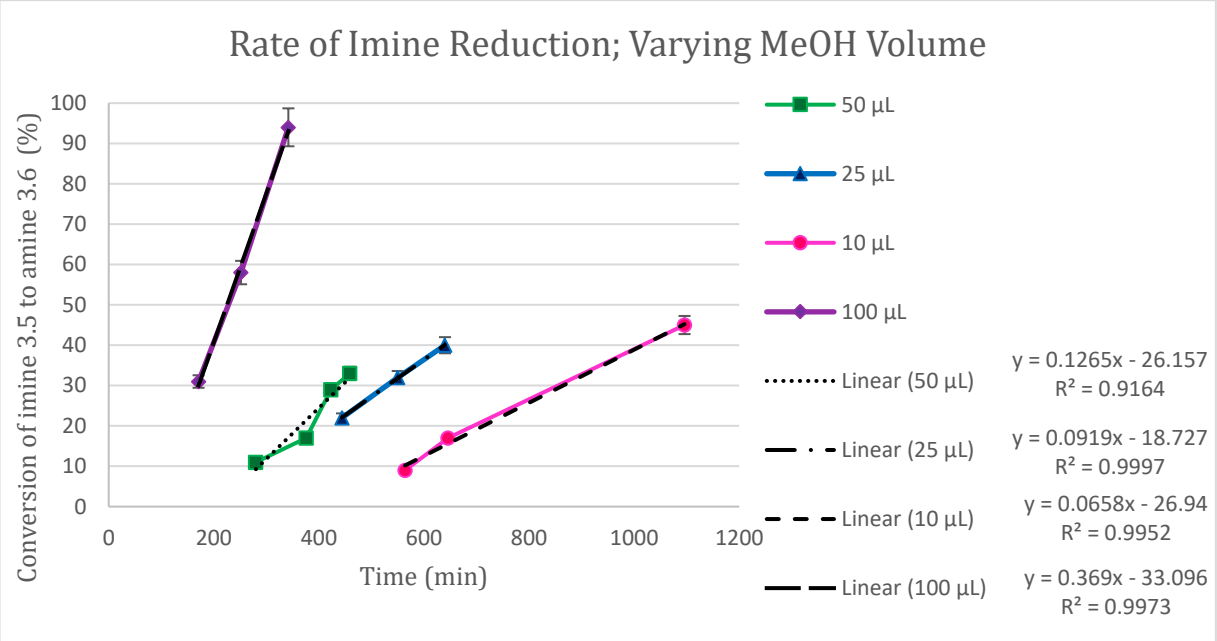

Graph 6.1.6.4 (Enlargement of Graph 6.1.6.1): Conversion of imine as a function of time with varying amount of MeOH; initial rates. Conversion determined using 1,3,5-trimethoxybenzene as internal standard. Reaction conditions in accordance with **Scheme 6.1.2** using 72 µmol imine. At t=0 min silane was added. Each datapoint represents a single measurement.

When plotting the increase in rate as a function of the increase in the MeOH concentration (**Graph 6.1.6.5**), a reasonable regression is found, suggesting that the rate increases by a factor of 0.6 when the concentration is doubled. A fractional rate order is not unexpected considering the highly complex nature of the system.

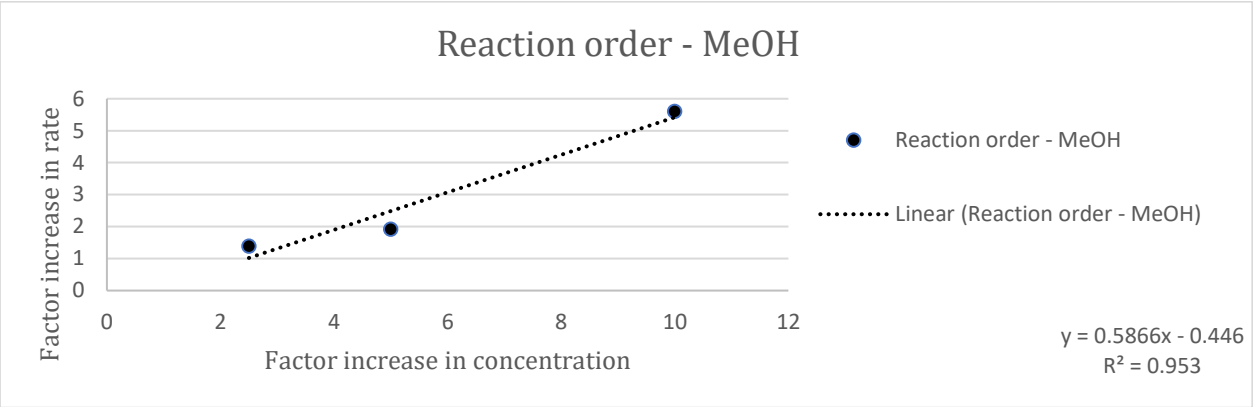

Graph 6.1.6.4: Reaction order for the reduction of the imine with respect to the increase in the methanol concentration.

6.1.7 The effect of changing the 3,3'-substituent

The effect of varying the 3,3'-substituent was less obvious (**Graph 6.1.2.4**). Unlike in pure MeOH, where the reaction with (*R*)-3,3'-$(SBn)_2$-BINOL as the ligand was significantly faster than the reaction with (*R*)-3,3'-I_2-BINOL, this was not observed in *i*-PrOH. On the contrary, the reaction took far longer to go to completion in the case of (*R*)-3,3'-$(SBn)_2$-BINOL. It appears that there are different onset times for the different ligands, but there does not seem to be a trend between the rate of the reaction and the e.e. observed with different ligands, *i.e.* the ligand resulting in the fastest conversion ((*R*)-3,3'-$(CF_3)_2$-BINOL) is not the one leading to highest e.e.

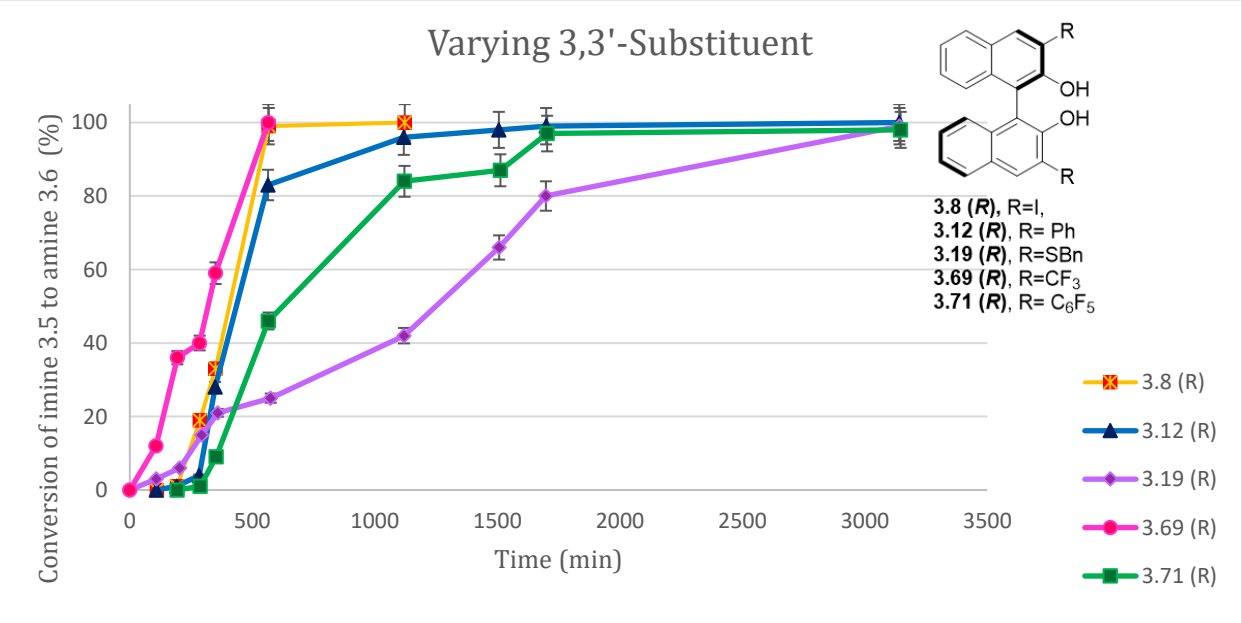

Graph 6.1.7.1 Conversion of imine as a function of time with varying 3,3'-substituent on the BINOL ligand. Conversion determined using 1,3,5-trimethoxybenzene as internal standard. Reaction conditions in accordance with **Scheme 6.1.2** using 72 µmol imine. At t=0 min silane was added. Each datapoint represents a single measurement.

Changes in the rate over time are observed. (*R*)-3,3'-$(SBn)_2$-BINOL in particular yields an interesting rate graph. The reaction seems to be fast in the beginning, then slows down and finally speeds up again, in contrast with the general behaviour of the rate with the other ligands: fast once the reduction is initiated and then slow towards the end. The highest e.e. obtained using 3,3'-$(SBn)_2$-BINOL was 36% in a mixed solvent system with 250 μL *i*-PrOH and 50 μL MeOH. When the amount of *i*-PrOH was increased to 1 mL, the e.e. dropped to 19%. As mentioned previously, the rate of the imine reduction with the ligand was similar to the rate of the background reaction when the reaction was carried out in MeOH. The e.e. could not be further optimised with this ligand, and whether the drop in e.e. with this ligand when the overall concentration is decreased is results from a combination of incomplete In(III) binding and no longer reacting in a rate comparable to the background reaction has not yet been investigated further. In the case of (*R*)-3,3'-I_2-BINOL, the e.e. increased with the decreased concentration and decreased rate of the imine reduction. The could suggest strong but slow binding of the In(III) by this ligand; the background reaction is out-competed by allowing the ligand time to binding In(III) prior to the addition of the imine. Furthermore, the increased temperature for the premixing greatly enhanced both the e.e. and the solubility of the (*R*)-3,3'-I_2-BINOL, further emphasising the potential for the increase in e.e. to have been caused by enhanced ligand binding through the creation of a homogenous system.

Towards the end of the reaction a deceleration in the rate is observed. The last phase is likely to correspond to a protonation of the amine.

A closer examination of the first 600 minutes reveals the 3 and 3'- substituents influence both the rate of imine conversion and the length of incubation time.

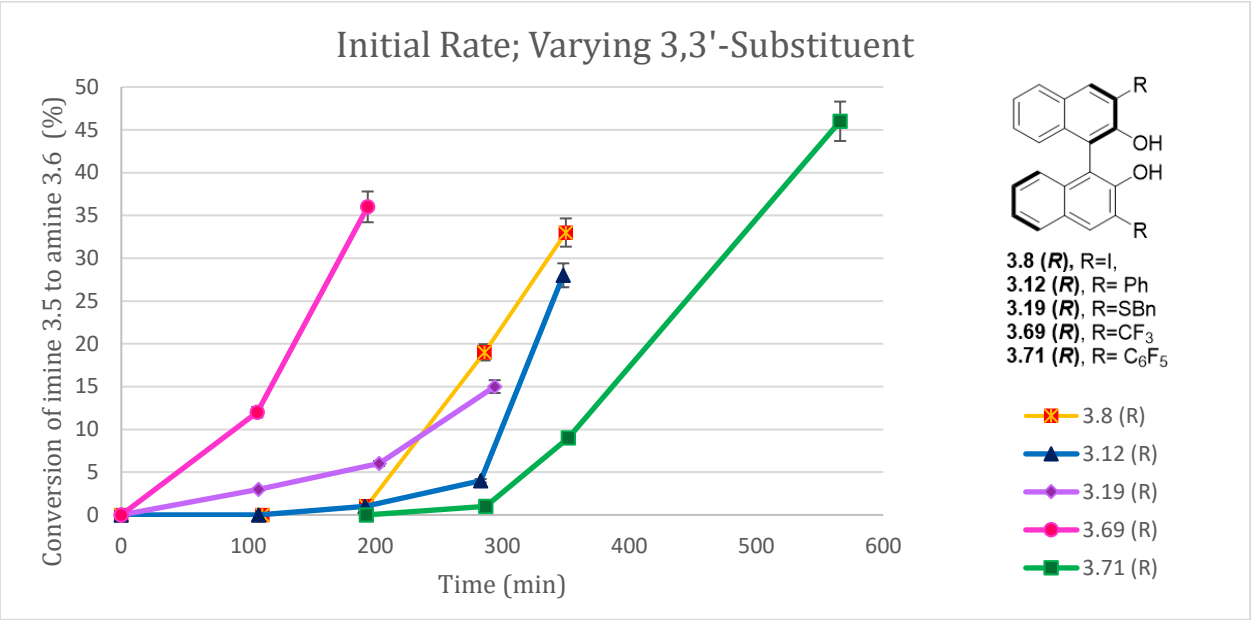

Graph 6.1.7.2 (Enlargement of Graph 6.1.7.1): Conversion of imine as a function of time with varying ligands. Conversion determined using 1,3,5-trimethoxybenzene as internal standard. Reaction conditions in accordance with **Scheme 6.1.2** using 72 µmol imine. At t=0 min silane was added. Each datapoint represents a single measurement.

The infrequency of the measurements prevents the determination of the initial rate for 3,3'-$(CF_3)_2$-BINOL (**Graph 6.1.7.3**). It is observed that this ligand, along with 3,3'-$(SBn)_2$-BINOL, enables the reaction to initiate much faster than the other ligands; thus, the induction period time is significantly shorter for these ligands.

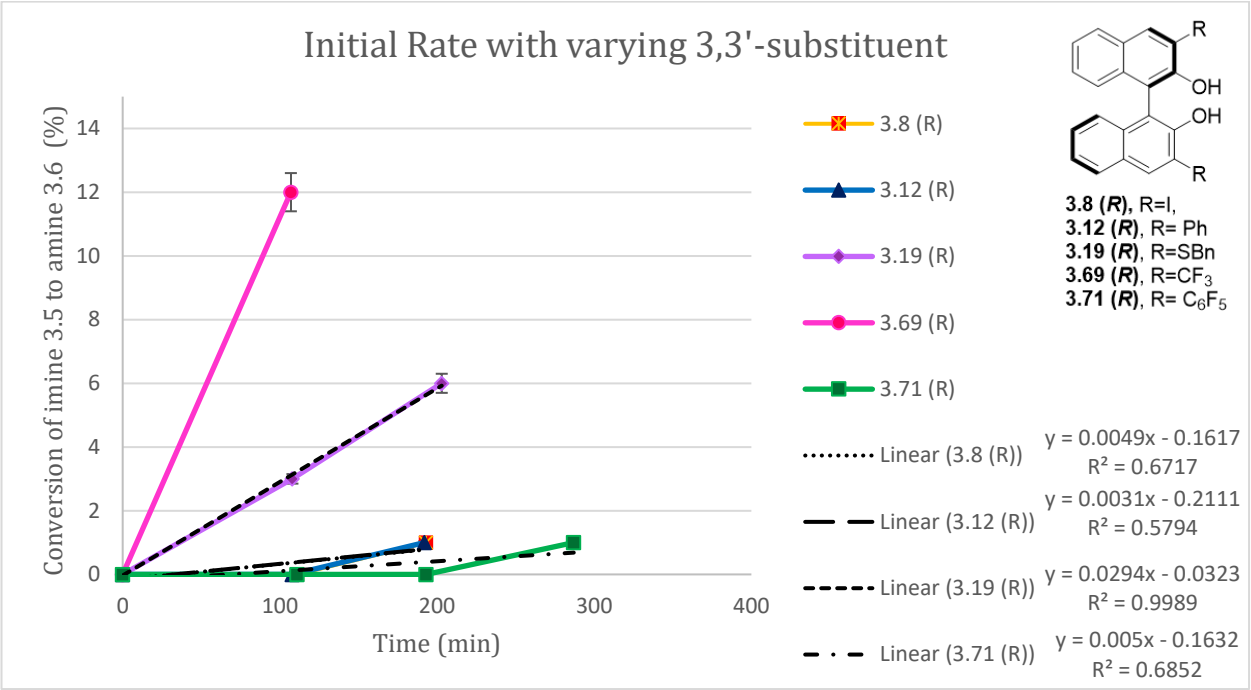

Graph 6.1.7.3 (Enlargement of Graph 6.1.7.1): Conversion of imine as a function of time with varying ligands, with attempts to determine initial rate. Conversion determined using 1,3,5-trimethoxybenzene as internal standard. Reaction conditions in accordance with **Scheme 6.1.2** using 72 µmol imine. At t=0 min silane was added. Each datapoint represents a single measurement.

The 3,3'-substituents also affect the rate of the imine reduction (**Graph 6.1.7.4**).

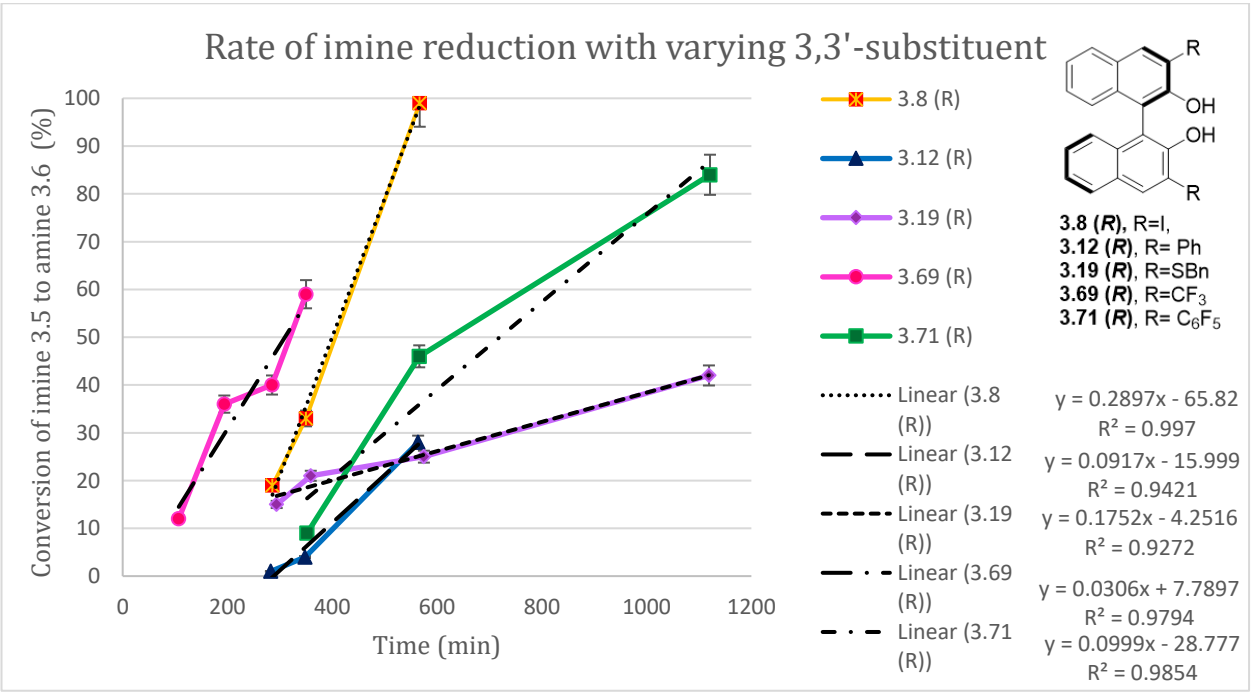

Graph 6.1.7.3 (Enlargement of Graph 6.1.7.1): Conversion of imine as a function of time with varying ligands, with attempts to determine initial rate. Conversion determined using 1,3,5-trimethoxybenzene as internal standard. Reaction conditions in accordance with **Scheme 6.1.2** using 72 µmol imine. At t=0 min silane was added. Each datapoint represents a single measurement.

The 3,3'-I_2-BINOL is the fastest followed by 3,3'-$(CF_3)_2$-BINOL, 3,3'-Ph_2-BINOL, 3,3'-$(C_6F_5)_2$-BINOL and 3,3'-$(SBn)_2$-BINOL as the slowest.

6.1.8 Discussion of the kinetic data

It is evident from the data presented in the last 7 subsections that repeating all the measurements would significantly improve the results. For each variable, the length of incubation, the onset of the imine reduction, the initial rate, the rate of the imine reduction and the time it takes to achieve full conversion are all affected. With the data presented in hand, it is possible to decide in which timeframe and how frequently NMR spectra should be recorded to obtain high quality data for each of the concentrations for each of the 7 variables examined. Another parameter that would be very useful to examine is the influence of temperature. The rate of the reaction increases with increased temperature. It was noted that the standard reaction (0.5 mol% In(III), 1 mol% 3,3'-I_2-BINOL, 1 mL *i*-PrOH, 50 µL MeOH, 1 equiv silane) went to completion in approximately 500 min in the reactions investigating the effect of varying the In(III) concentration, whereas the same reaction had only gone to 60% conversion in this time when the MeOH concentration was being varied. All experiments examining one variable have been carried out on the same day with the same ambient temperature; thus, they are comparable, and the only variable is the one under examination. However, as ambient room temperature in our laboratory varies between 10 °C and 34 °C, carrying out all experiments at e.g. 30 °C would allow comparison of the data between the graphs in the seven previous sections. The effect of the variable room temperature was realised during data processing and if time had allowed for the repetition of the experiments they would have been carried out with controlled temperature, and a set of reactions examining the rate at different temperatures would have been added.

The e.e. for the kinetic experiments varied significantly. Numbers between 40 and 70% were recorded. As no clear trends were observed this data is not included in this thesis.

6.1.9 Gas evolution

During the recording of these kinetic experiments, product was observed in the spectra in good correspondence with the observed onset of gas evolution and therefore initiated with the initiation of the imine reduction. This is in good correspondence with the expectation of observing liberation of hydrogen gas from the imine reduction. However, gas evolution did not cease to exist until long after full conversion was observed.

6.2 No Non-Linear effect

From the crystal structure in Chapter 4, it is known that In(III) can have up to 6 co-ordination sites saturated. In the interest of determining the stoichiometry of In(III)-ligand in the reaction, the e.e. of the amine was examined as a function of the e.e. of the ligand. A Non-Linear effect was not observed (**Graph 6.2**).

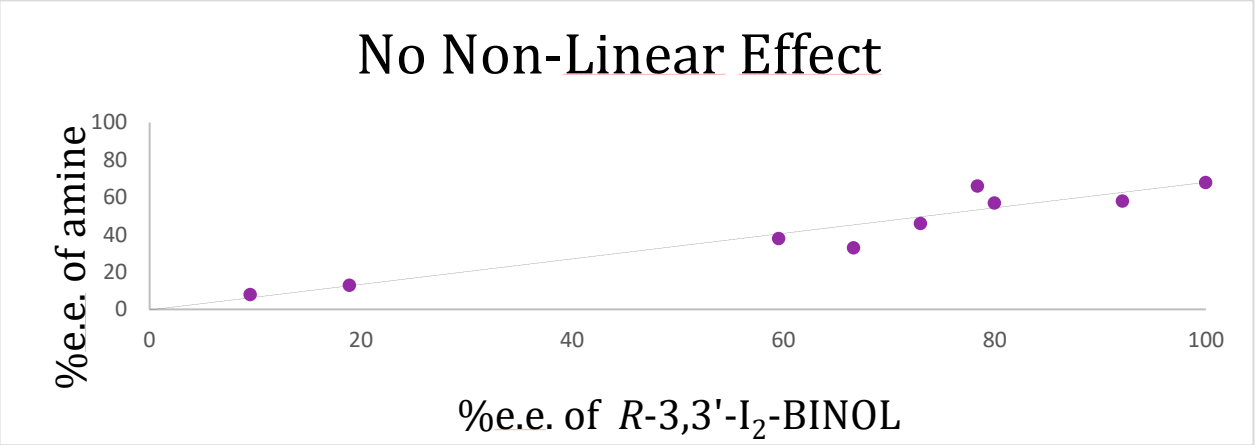

Graph 6.2 No non-linear effect observed.

However, this does not eliminate the possibility that the active catalyst might still have more than one ligand attached to In(III). Furthermore, as previously mentioned, the active catalyst is likely to be an In(III)-In(III) dimer and it is very plausible that a number of different complexes with e.g. different co-ordination numbers may exist in the reaction mixture.

6.3 Attempts towards isolation and characterisation of an active In(III) complex

Following the computational mechanistic results described in Chapter 5, the isolation and characterisation of an In(III) hydride complex was of particular interest.

The experiments described below were carried out with (*R*)- or (*S*)-3,3'-I_2-BINOL as the ligands, unless otherwise stated.

Based on the computational investigations described in Chapter 5, several attempts towards isolating and characterising an In(III) hydride complex were made. From the suggested thermodynamically plausible pathway in **Diagram 5.4.3.3**, it was hypothesised that the optimal way of forming this In(III)-H complex would be by the addition of the silane to the pre-formed In(III) ligand mix. This had previously been found to decrease the e.e. which is why the addition order is different for the experiments carried out to improve the e.e. However, as addition of the imine prior to the silane

would result in consumption of the potentially formed In(III) hydride in imine reduction, it was thought best to avoid adding this imine – even though the pre-reduction complex would be stabilised in energy by the imine.

Various experiments were carried out with ratio of In(III):ligand:silane. These were carried out on a larger scale and with increased concentration the hope that this would ease the characterisation, though still considerably diluted since concentrating the mixtures too much had resulted in formation of grey metallic solids, suggesting In(0). As mentioned in Chapter 3, formation of grey precipitate followed in all reactions yielding racemic amines.

Several characterisation methods were attempted. ^{1}H NMR spectra were recorded down to -90 ppm, investigating the appearance of a hydride signal; however, no signals at negative ppm values were observed. Changes was observed in the aromatic region over time, though it has not yet been possible to identify any structures from these signals. In ^{29}Si-NMR two signals were observed; a sharp signal at -60 ppm and a broad signal at -100 to -130 ppm. Both signals disappeared as the reaction imine was fully reduced. ^{115}In NMR was recorded; however, pure $In(NO_3)_3$ was the only In(III)-containing compound whose recorded ^{115}In NMR spectrum was of a suitable quality with a decent appearing peak (about 200 ppm broad). (*R*)-3,3'-$(CF_3)_2$-BINOL was used as a ligand examining the effect of In(III)-binding on the fluorine atoms, but only the ligand and the triflate counterion was observed by NMR. In the literature it is stated that the ^{115}In quadrupole hinders the detection of the In(III) hydride ^{1}H signal. However, detection of this hydride was reported using IR, where a sharp signal was be observed in the IR at 1801 cm^{-1}.[198] IR spectra of various samples containing the In(III)-BINOL-silane system was recorded, without the detection of such signal. As the samples were very dilute this could be the course of the signal not being observed; thus, further investigations must be conducted. MS was recorded with various ionisation methods on samples both directly after addition of silane and approximately 30 min after. Unfortunately, no reasonable structures were identified from the output data. However, in light of the kinetic data described in section 6.1.2 it is likely, that different In(III) complexes exists in the solution over time and if an In(III) hydride is indeed the active catalyst for the imine reduction this may be found in the solution later than 30 min where the MS spectra were recorded. Further NMR analysis during the imine reduction did however, not reveal any indications of a hydride being present. To increase concentration the premixed mixtures were evaporated. As the samples were concentrated, red solids started forming and it was decided to evaporate to dryness to examine these solids. When adding the silane to the premixed In(III)-ligand system, this red colour had been previously observed in solution and was therefore of high interest. The dried red solids changed colour to yellow when re-dissolved in MeOD to allow for NMR analysis. No hydride was observed, or any other compound structure identified. MS analysis of this red complex was likewise

inconclusive. The solids formed were not crystalline and could not be used for X-Ray. A mixture of different types of red as well as grey solids was observed. To examine if the red colour was caused by the iodine in the 3- and 3'-positions, other ligands were exposed to same procedure of premixing at elevated temperature, silane addition at RT and then evaporation to dryness. This resulted in different colours (**Picture 6.3**) and thus this colour is thought to be caused by the ligand, since this is the only variable connected with the change of colour. The (*R*)-H_8-I_2-BINOL was included, to be sure the colour was not caused by generation of elementary iodine from loss of the 3,3'-iodine atoms. In this case, a white compound was formed.

Picture 6.3: From left to right: 3,3'-Br_2-BINOL , 3,3'-I_2-BINOL, 3-CF_3-3'-I-BINOL, 3,3'-$(CF_3)_2$-BINOL and 3,3'-I_2-H_8-BINOL

The crystallisation of the complex with 3-CF_3-3'-I-BINOL was attempted from both MeOH, $PhSiH_3$ and a mix of MeOH and $PhSiH_3$ without success.

These red compounds were also tested as catalyst for the reaction. Without further addition of silane, no conversion was observed; however, with addition of silane the reduction went to completion. The e.e. of the amine was, in this case, lower than under optimised conditions. Since the composition of this red solid remains unknown, the exact mol% In(III) and ligand added through addition of 0.60 mg of this red solid is unknown, and thus the e.e. was expected to vary.

Despite extensive attempts to characterise / isolate an In(III) hydride complex, so proof of a hydride being present in during the reaction was found. In light of the last computational studies described in Chapter 5, revealing thermodynamically plausible formation of In(III)-In(III) dimeric complexes, other pathways such as oxidative insertion may be favourable with a such catalyst system. Thus, In(III) may afterall just act as a LA. One way to elucidate this experimentally is titration studies examining changes in the chemical shift for the imine carbon with varying concentrations of complex present. Unfortunately, time did not allow for completion of this.

6.4 Conclusion and further perspectives

Several kinetic experiments were carried out to investigate the reaction. The reaction was found to be ligand-decelerated for all ligands yielding high e.e. values (above 50%). Thus, the racemic background reaction continues to be a likely explanation for not achieving more than 73% e.e. under the optimised reaction conditions. The reaction rate was found to be independent of the source of In(III) and the reaction was faster in MeOD than *i*-PrOD. The rate of the imine reduction was found to increase with: increasing concentration of MeOH, decreasing overall concentration (decreasing amount of *i*-PrOH), increasing In(III) concentration and increasing silane concentration. The reaction was found to have an incubation time. The suggested mechanism in Chapter 5 goes through two steps, of which the first (the formation of the In(III) hydride) is the rate-determining step. The delay in onset of the imine reduction indicates an active catalyst complex needs to form prior to the reduction can be facilitated. This may be an In(III) hydride complex or a In(III)-In(III) dimer as computationally found to be thermodynamically plausible in Chapter 5. Increasing overall concentration, the ligand concentration or In(III) concentration decreased this incubation period, whereas the induction period appeared fairly unaffected by the silane stoichiometry. However, the effect of using less than 0.33 equiv of silane (thus less than 1 equiv of hydride) has not yet been examined. Increasing the MeOH concentration prominently decreased the induction period. The kinetics of the reaction proved to be very complicated and since almost every parameter affected both the induction period and the rate of the imine reduction, the data points have not been obtained with high enough frequency in the appropriate time frame for each of the examined parameters. If time had allowed the repetition of these experiments, higher quality data could have been obtained based on the insight gained from the first sets of experiments. From the kinetic data obtained, some cautious conclusions can be drawn with regards to the reaction order: the rate of the imine reduction appears to be 9th order for the silane stoichiometry, corresponding to 3rd order with each available hydride; the rate of the imine reduction is proportional to the concentration of In(III) after a threshold is passed; and the initial rate is of 0.6 order with respect to the MeOH concentration. Varying the 3 and 3' substituents affected both the incubation time and the rate of the imine reduction.

No non-linear effect was found when examining the e.e. of the amine as a function of the e.e. of the 3,3'-I_2-BINOL.

Extensive experimental work was carried out targeting the formation, isolation and characterisation of an In(III) hydride complex; however, characterisation by ^{1}H NMR, ^{19}F NMR, ^{29}Si NMR, ^{115}In NMR, IR, MS and X-Ray was inconclusive for both the resulting mixtures and the solid coloured complexes

obtained. As mentioned in Chapter 3, $LiBHEt_3$ was tested as reducing agent, as it is known to form metal hydrides. No reaction was observed in this case, which could be caused by either the $LiBHEt_3$ solution being outdated or an In(III) hydride complex not being formed. Further investigations with the super-hydride should be conducted. A possible solution for spectroscopic investigations of a hydride complex would be the use of deuterated silane to allow for the detection of In(III)-D, which potentially could be easier than the detection of In(III)-H. The catalytic abilities of the coloured complexes remain to be examined while they are still in solution and also on a stoichiometric scale.

Though a better understanding of the kinetics of the reaction was reached, more experiments need to be carried out. The fact that a non-linear effect was not observed does not rule it out and as no In(III) complex has yet been characterised from the reaction mixtures, work remain to be carried out in order to understand the mechanism of the reaction. Finally, the fact that In(III)-In(III) dimers are likely to form, extensive mechanistic work is yet to be done to elucidate the reaction pathway of the In(III) catalysed hydrosilane reduction described in this thesis. A key element herein is affinities studies to evaluate if In(III), in whatever type of complex it may be found active, is just acting as a LA.

Chapter 7: Scoping the reaction

7.1 Synthesis of acetophenone based imines

Various acetophenone based *N*-benzyl imines were synthesised to examine the substrate scope of the reaction (**Scheme 7.1.1**).

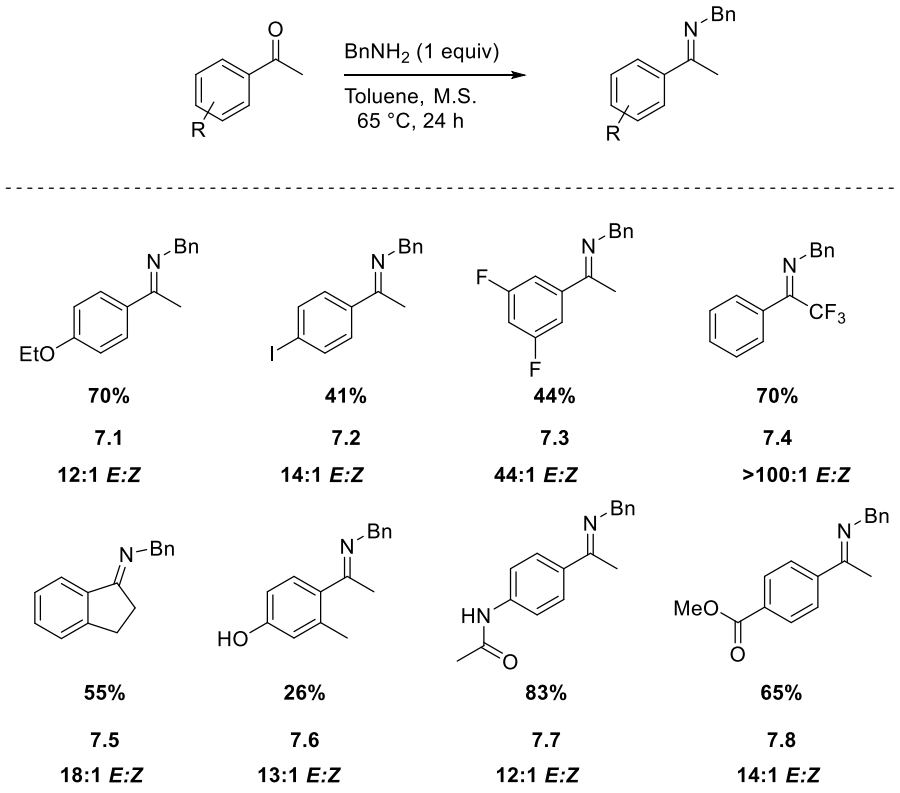

Scheme 7.2.1: Synthesis of acetophenone-based imines. Imines **7.1**-**7.4** and **7.6**-**7.8** were synthesised by Eilidh Bodfish, summerstudent in the Goodman Group 2018.

The ketone starting materials were chosen to cover EWG and electron donating effects on the *para*, *meta* and *ortho*-positions, effect of increased steric bulk from an anthracene ketone, the effect of an α-alkyl cyclic substituents along with functional group tolerance; ester, amide, free alcohol, nitrile, ether and halides. Several other acetophenone-based imines synthesis was planned (**Figure 7.1**); however, these have not yet been completed due to the time constrain.

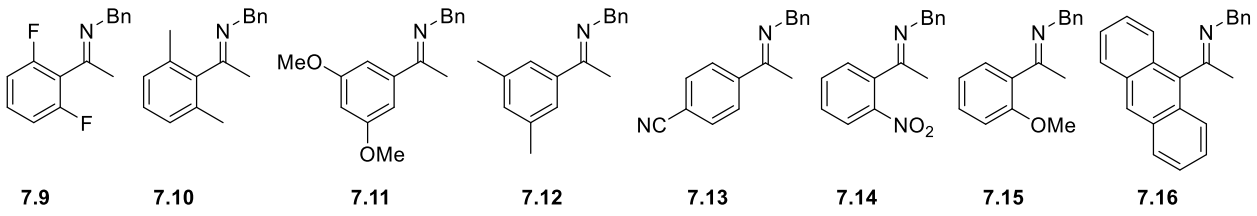

Figure 7.1: Acetophenone imines attempted / planned synthesised.

Two alkyl imines **7.18** and **7.20** were synthesised (**Scheme 7.1**) to examine the difference between aromatic and alkyl imines, however, both degraded upon purification attempts, and it was decided to carry on with acetophenone-based imines only.

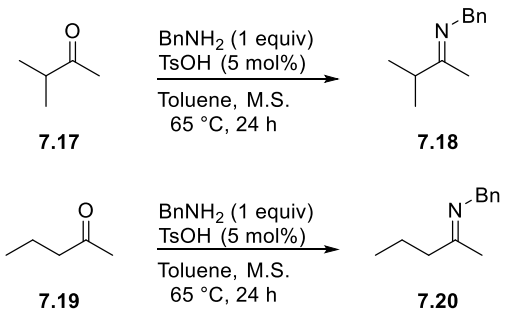

Scheme 7.2: Synthesis of alkylimines **7.18** and **7.20**.

As mentioned in Chapter 3, acetophenone based imines with extended alkyl chain would also have been interesting to synthesise and examine how these would behave in the In(III)-catalysed reduction.

7.2 Synthesis of racemic reference amides

As described in Chapter 3 the amines from the In(III) reduction was acetylated and the e.e. of the corresponding amides examined, since this gave more robust results from HPLC analysis. Each of the synthesised acetophenone-based imines were therefore subjected to racemic reduction with $NaBH_4$ (**Scheme 7.2.1**).

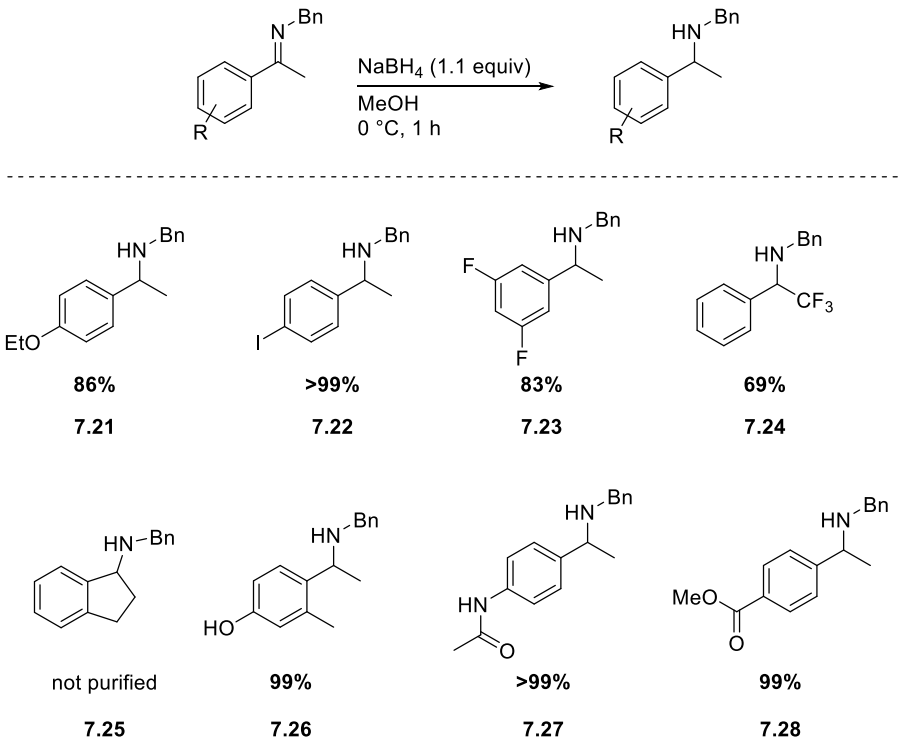

Scheme 7.2.1: Racemic reduction of acetophenone-based imines. Amines **7.21**-**7.24** and **7.26**-**7.28** were synthesised by Eilidh Bodfish.

Following the racemic reduction, the obtained amines were acetylated with acetic anhydride and triethylamine (**Scheme 7.2.2**).

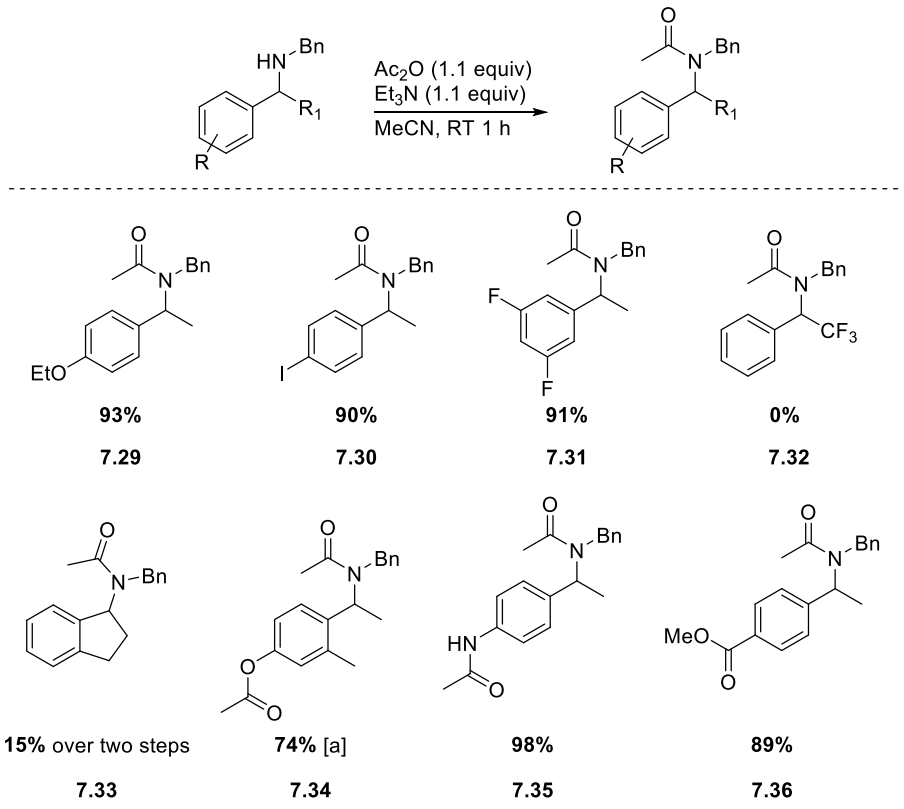

Scheme 7.2.2: Acylation of racemic reference amines. [a] 2.2 equiv of Et_3N and Ac_2O.

Amine **7.24** was attempted acylated both using Ac_2O and Et_3N and using AcCl. Unfortunately, no product was obtained in with Ac_2O and only trace of product was observed when AcCl was used. HPLC and SCF analysis of **7.24** is ongoing.

7.3 Scoping the reaction with the synthesised imines

The successfully synthesised imines were used as substrates for the In(III)-catalysed hydrosilane reduction under the optimised conditions (**Table 7.3.1**).

Table 7.3.1: Examining the acetophenone-based imines as substrates for the In(III)-catalysed hydrosilane reduction.

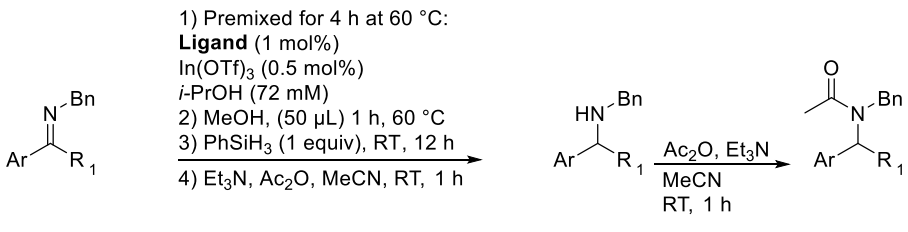

Entry	Imine	E:Z	Amine	NMR Yield[a] [%]	Amide		e.e. [b] [%]
1	**7.1**	12:1	**7.21**	>99	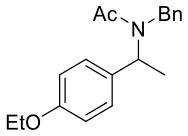	**7.29**	67 %
2	**7.2**	14:1	**7.22**	75	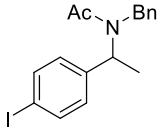	**7.30**	- [c]
3	**7.3**	44:1	**7.23**	92	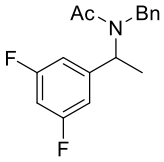	**7.31**	50%
4	**7.4**	>100:1	**7.24**	84	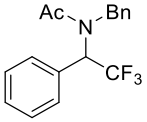	**7.32**	0%[d]
5	**7.5**	18:1	**7.25**	72	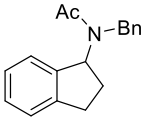	**7.33**	-[c]
6	**7.6**	13:1	**7.26**	99	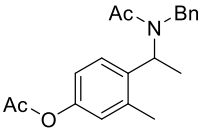	**7.34**	0%
7	**7.7**	12:1	**7.27**	93	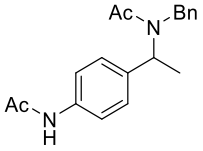	**7.35**	-[c]
8	**7.8**	14:1	**7.28**	75	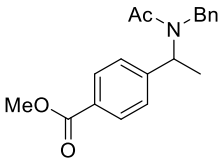	**7.36**	39%

All reactions carried out with 72 µmol imine. [a] Yield of amine determined by quantitative NMR. [b] e.e. of amide determined by chiral stationary phase SFC analysis. [c] Chiral stationary phase SFC analysis is ongoing. [d] e.e. of the amine determined by chiral stationary phase SFC analysis.

Amide **7.34** was found to be racemic under the optimised conditions (entry 6). If the aromatic hydroxyl groups in **7.6** binds as strongly to the In(III)-metal centre as the ligand hydroxy groups, a ligand exchange can take place, and thus the chiral environment on the In(III)-metal centre is lost. However, as the reaction proceeds affords good e.e. in alcoholic solvents a such ligand exchange is not significant in the case of aliphatic hydroxyl groups.

Both ether (entry 1), ester (entry 8) and halides (entry 3) was tolerated in the developed In(III)-catalysed hydrosilane reduction. The highest obtained e.e. continues to be 73% with imine **3.5**.

7.4 Conclusion

Several acetophenone based imines was synthesised, reduced until racemic conditions and acylated for HPLC references. The imines were then tested as substrates for the developed In(III)-catalysed hydrosilane reduction and both ester, ether and halides found to be tolerated. The highest e.e. continues to be 73%. Hydroxy groups in the imine was found to result in a the In(III)-catalysed hydrosilane reducing affording racemic products. Analysis of the remaining substrates is ongoing.

Due to time constrains a limited number of imines was successfully synthesised. If time had allowed for carrying out investigations to scale up the reaction and recovering the catalyst system, this would have been an interesting aspect of the project.

Chapter 8: Conclusions, future work and further perspectives

8.1 Conclusions

An indium(III)-catalysed hydrosilane reduction of imines was developed and optimised to yield 73% e.e. using (*R*)-3,3'-I_2-BINOL. The reaction provided promising e.e. only in polar protic solvents and the e.e. was dependent on the amount of MeOH additive present. The e.e. increased with decreasing concentration and premixing of the ligand and catalyst was found to be important for higher levels of enantio-induction. The optimal solvent system was found to be a mixture of *i*-PrOH and MeOH. Various reducing agents were screened; however, only $PhSiH_3$ efficiently reduced the imine. The addition of base had varying effect on the e.e. and ultimately did not result in higher e.e. than the 73% achieved without base. Of the many ligands screened, including both non-BINOL ligands and more than 50 BINOL-type ligands, only ligands with electronic effects directly in the 3,3'-positions yielded amines in moderate to good e.e. Aromatic *N*-substituents resulted in racemic amines, indicating that the alkyl position α to the nitrogen has mechanistic importance, which strongly suggest this is an important binding site for the active catalyst (LA activity). Due to time constraints, the effects of varying the substituents on the *N*-benzyl ring along with extending the alkyl chain of the α-CH_3 group remain to be examined (**Figure 8.2.1**).

In the side project described in Chapter 2, a C_1-CPA was successfully synthesised in 33% overall yield in eight steps from commercially available (*R*)-BINOL. This C_1-CPA had been predicted to outperform commercially available CPAs, and although this this not translate well experimentally, a hypothesis to explain the observed outcome was made. The intermediates from the synthesis of this C_1-CPA were deprotected to yield a range of BINOL ligands with different 3 and 3' substituents, which were then used in the main project of this thesis: the development of an enantioselective In(III)-catalysed reaction.

As part of the experimental mechanistic investigations, two In(III)-BINOL complexes were successfully synthesised and characterised. These complexes consisted of *hexa*-co-ordinated In(III) ions surrounded by three BINOL ligands with alkali metals and solvent molecules in between.

The co-ordination around the In(III) metal-centre was examined computationally in both MeOH and *i*-PrOH for a model system and the whole system. When the only other co-ordinating molecules were solvent molecules, In(III) with one ligand was found to be most stable as the *penta*-co-ordinated complex. Conversely, the *tetra*-co-ordinated complexes were lower in energy when imine, amine or silane molecules co-ordinated to the In(III) metal-centre. All hydride complexes were likewise most stable as *tetra*-co-ordinated complexes. Four different plausible reaction pathways were examined. At room temperature both an MPV mechanism and a direct reduction mechanism was, under the chosen computational parameters, found to have very high TS barriers for the hydride transfer

compared to the TS barrier for transferring the hydride from and In(III) hydride complex through a six-membered chair TS with one of the In(III)-co-ordinating MeOH molecules activating the imine through hydrogen donation. The energy difference between the two enantiomeric transition states corresponds to 40% e.e. but favoured the opposite enantiomer than what was observed experimentally. Further investigations are on-going and formation of In(III)-In(III) dimeric complexes have proven promising to date.

Several kinetic experiments were carried out to investigate the reaction. The reaction was found to be ligand-decelerated. The rate of the imine reduction was found to increase with: increasing concentration of MeOH, decreasing overall concentration (decreasing amount of *i*-PrOH), increasing In(III) concentration and increasing silane concentration. The reaction was found to have an incubation time. The suggested mechanism in Chapter 5 goes through two steps, of which the first (the formation of the In(III)-hydride) is the rate-determining step. Formation of an active hydride complex prior to the reduction of the imine could explain the delay in the onset of this reduction. Increasing overall concentration, the ligand concentration or In(III)-concentration decreased this incubation period, whereas the induction period appeared fairly unaffected by the silane stoichiometry. However, the effect of using less than 0.33 equiv of silane (thus less than 1 equiv of hydride) has not yet been examined. Increasing the MeOH concentration prominently decreased the incubation time, suggesting MeOH is important for the formation of the reactive catalytic complex. The kinetics of the reaction proved to be very complicated and since almost every parameter affected both the incubation time and the rate of the imine reduction, the datapoints have not been obtained with high enough frequency in the appropriate timeframe for each of the examined parameters. If time had allowed the repetition of these experiments, higher quality data could have been obtained based on the insight gained from the first sets of experiments. From the kinetic data obtained, some cautious conclusions can be drawn with regards to the reaction order: the rate of the imine reduction appears to be 9^{th} order for the silane stoichiometry, corresponding to 3^{rd} order with each available hydride; the rate of the imine reduction is proportional to the concentration of In(III) after a threshold is passed; the initial rate is of 0.6 order with respect to the MeOH concentration. Varying the 3 and 3' substituents affected both the incubation time and the rate of the imine reduction.

No non-linear effect was found when examining the e.e. of the amine as a function of the e.e. of the 3,3'-I_2-BINOL.

Extensive experimental work was carried out targeting the formation, isolation and characterisation of an In(III)-hydride complex; however, characterisation by ^{1}H NMR, ^{19}F NMR, ^{29}Si NMR, ^{115}In NMR,

IR, MS and X-Ray was unsuccessful for both the resulting mixtures and the solid coloured complexes obtained.

Though a better understanding of the kinetics of the reaction was reached, more experiments need to be carried out. The fact that a non-linear effect was not observed does not rule it out and as no In(III)-complex has yet been characterised from the reaction mixtures, work remains to be carried out in order to understand the mechanism of the reaction.

The first investigations of the substrate scope of the reaction were carried out after successful synthesis of eight acetophenone-based imines. These imines were tested under the optimised conditions and the e.e. examined through comparison with the synthesised racemic reference amides. The imines were then tested as substrates for the developed In(III)-catalysed hydrosilane reduction and both ester, ether and halides found to be tolerated. The highest e.e. continues to be 73%. Hydroxy groups in the imine was found to result in a the In(III)-catalysed hydrosilane reducing affording racemic products, which is consistent with the racemic results obtained when reducing ketones. Analysis of the remaining substrates is ongoing.

Though a better understanding of the kinetics of the reaction was reached, more experiments need to be carried out. The fact that a non-linear effect was not observed does not rule it out and as no In(III) complex has yet been characterised from the reaction mixtures, work remain to be carried out in order to understand the mechanism of the reaction. Finally, the fact that In(III)-In(III) dimers are likely to form, extensive mechanistic work is yet to be done to elucidate the reaction pathway of the In(III) catalysed hydrosilane reduction described in this thesis. A key element herein is affinities studies to evaluate if In(III), in whatever type of complex it may be found active, is just acting as a LA.

8.2 Future work

Due to the three-year time constraint of this PhD project a number of aspects (highlighted in **Figure 8.2.1**) of the developed In(III)-catalysed hydrosilane reduction of imines remain to be fully examined.

The effect of varying the substituents on the *N*-benzyl ring (red) constitutes an unoptimized parameter. Further investigation into the effect of extending the alkyl group in the α-position (purple) and varying the bulk on the *N*-CH_2 position (blue) would add valuable mechanistic information to the project. Further synthesis of acetophenone-based imines to expand the substrate scope and examination of the functional group tolerance of the reaction, along with investigations into scaling up and the catalyst recovery are yet to be carried out.

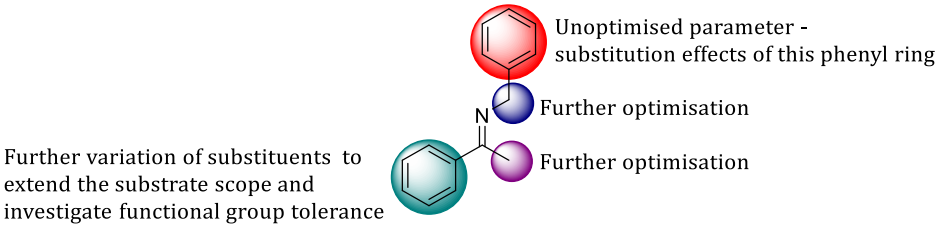

Figure 8.2.1: Remaining optimisation and investigation points.

Identification, isolation and characterisation of the active catalyst complex remains a challenge. Establishing a correlation between the computational mechanistic results and the experimental work is crucial for determining the reaction mechanism. Along with further kinetic studies, titration studies examining whether the In(III) complex acts simply as a LA is of utmost importance to elucidate the mechanism. Furthermore, computational investigation of the dimeric In(III)-In(III) complexes described in Chapter 5 (**Figure 8.2.2, Diagram 5.4.4.1**) could be the key for establishing a thermodynamically plausible pathway in agreement with the experimentally obtained e.e. values, and hopefully establishing both a plausible mechanism for the reaction along with understanding of how to improve the e.e. of the reaction.

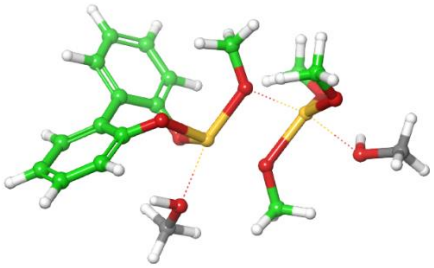

Figure 8.2.2: A simple In(III)-In(III) dimeric complex .

Further computational investigations to rule out other plausible pathways include: a bisligated complex, halogen bonds or a reduction through silane activated imines, and would be interesting to examine. Investigations of these parameters are under examination; however, at the submission point of this thesis, the obtained results are far too inconclusive and unfinished to be included. Some obtained structures are shown in **Figure 8.2.3**.

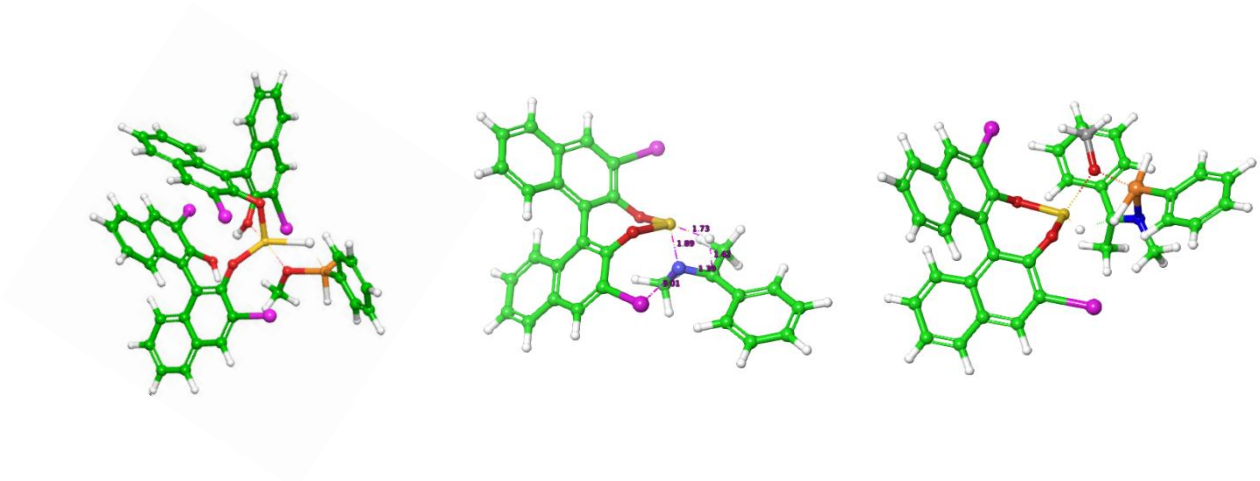

Figure 8.2.3 (Figure 5.4.4.1 reprinted): Further computational investigations from left to right: bisligated complex? (picture of located TS), halogen bonds? (picture of hypothesised TS); silane activation of the imines? (picture of located TS).

8.3 Further perspectives

Although many methods exist for enantioselective reduction of imines, the development of an In(III)-catalysed hydrosilane reaction is valuable from a mechanistic point of view, as In(III) is not commonly used in these transformation, and therefore its mechanism of action not extensively studied and understood in this context.

Thus, the most valuable contribution from this project is the progress made towards understanding enantioselective In(III)-catalysis, with the overall goal being to develop suitable ligands for successfully establishing enantioselective versions of other In(III)-catalysed reactions. One of these, which was under brief examination in this project, is an $In(OTf)_3$-catalysed spiroiminolactonisation.[71] The results are not included in this thesis, as only the non-ligated process was carried out and time did not allow for investigations of the ligated reaction. The suggested mechanism is shown in **Scheme 8.3.1**.

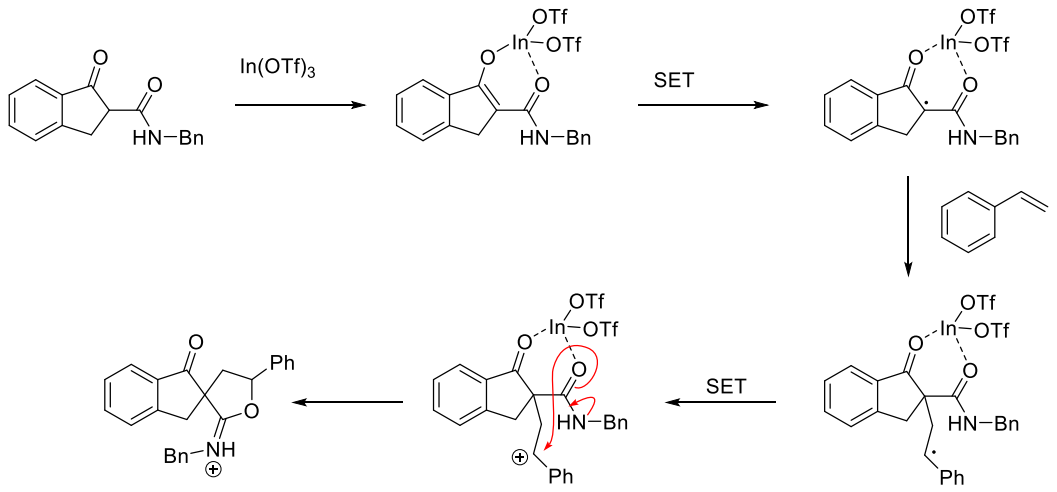

Scheme 8.3.1: Suggested mechanism for the $In(OTf)_3$-catalysed spiroiminolactonisation. Adapted from Ko et al.[71]

As In(III) acts as a LA for this transformation, by exchanging the triflate ions with a chiral ligand, this reaction would take place in a chiral environment, thus allowing enantioselectivity to be achieved. Several parameters would need investigation and optimisation, most importantly whether ligand exchange with the Cu(I) used for single-electron-transfer (SET) takes place. However, it would be an interesting reaction to examine and develop in high e.e.

9. References

(1) Pasteur, L. Mémoire Sur La Relation Qui Peut Exister Entre La Forme Cristal - Line et La Composition Chimique, et Sur La Cause de La Polarisation Rotatoire. *Comptes rendus Hebd. des séances l'Académie des Sci.* **1848**, *26*, 535–538.

(2) Caner, H.; Groner, E.; Levy, L.; Agranat, I. Trends in the Development of Chiral Drugs. *Drug Discov. Today* **2004**, *9*, 105–110.

(3) Agranat, I.; Caner, H.; Caldwell, J. Putting Chirality to Work: The Strategy of Chiral Switches. *Nat. Rev. Drug Discov.* **2002**, *1*, 753–768.

(4) Blaser, H.-U.; Federsel, H.-J. *Asymmetric Catalysis on Industrial Scale: Challenges, Approaches and Solutions*, 2nd ed.; Wiley-VCH Verlag GmbH & Co. KGaA, 2010.

(5) Nozaki, H.; Moriuti, S.; Takaya, H.; Noyori, R. Asymmetric Induction in Carbenoid Reaction by Means of a Dissymmetric Copper Chelate. *Tetrahedron Lett.* **1966**, *7*, 5239–5244.

(6) Ault, A. The Nobel Prize in Chemistry for 2001. *J. Chem. Educ.* **2002**, *79*, 572.

(7) Noyori, R. Centenary Lecture. Chemical Multiplication of Chirality: Science and Applications. *Chem. Soc. Rev.* **1989**, *18*, 187–208.

(8) Clayden, J.; Greeves, N.; Warren, S. Organic Chemistry. In *Oxford University Press*; 2012.

(9) Berrisford, D. J.; Bolm, C.; Sharpless, K. B. Ligand-Accelerated Catalysis. *Angew. Chemie Int. Ed. English* **1995**, *34* (10), 1059–1070.

(10) Katsuki, T.; Sharpless, K. B. The First Practical Method for Asymmetric Epoxidation. *J. Am. Chem. Soc.* **1980**, *102* (18), 5974–5976.

(11) Jacobsen, E. N.; Marko, I.; Mungall, W. S.; Schroeder, G.; Sharpless, K. B. Asymmetric Dihydroxylation via Ligand-Accelerated Catalysis. *J. Am. Chem. Soc.* **1988**, *110* (6), 1968–1970.

(12) Schroll, E. Indium: Element and Geochemistry. In *Geochemistry*; Kluwer Academic Publishers: Dordrecht, 1998; pp 339–340.

(13) Cintas, P. Synthetic Organoindium Chemistry. What Makes Indium so Appealing? *Synlett* **1995**, *11*, 1087–1096.

(14) Adolfsson, H.; Fleming 1935-, I. Science of Synthesis : Houben-Weyl Methods of Molecular Transformations. Category 1, Organometallics. Vol. 4, Compounds of Group 15 (As, Sb, Bi) and Silicon Compounds. Thieme,: Stuttgart p 1060p.

(15) Hamachi, Y.; Katano, M.; Ogiwara, Y.; Sakai, N. Production of Quaternary α-Aminonitriles by Means of Indium-Catalyzed Three-Component Reaction of Alkynes, Amines, and Trimethylsilyl Cyanide. *Org. Lett.* **2016**, *18*, 1634–1637.

(16) Ogiwara, Y.; Uchiyama, T.; Sakai, N. Reductive Amination/Cyclization of Keto Acids Using a Hydrosilane for Selective Production of Lactams versus Cyclic Amines by Switching of the Indium Catalyst. *Angew. Chem. Int. Ed.* **2016**, *55*, 1864–1867.

(17) Posevins, D.; Suta, K.; Turks, M. Indium-Triflate-Catalyzed Ritter Reaction in Liquid Sulfur Dioxide. *European J. Org. Chem.* **2016**, *2016*, 1414–1419.

(18) Babaoglu, E.; Harms, K.; Hilt, G. Indium-Mediated Blaise-Type Reaction of Bromomalonates with Nitriles and Isocyanates. *Synlett* **2016**, *27*, 1820–1823.

(19) Wu, S.; Li, Y.; Zhang, S. α-Regioselective Barbier Reaction of Carbonyl Compounds and Allyl Halides Mediated by Praseodymium. *J. Org. Chem.* **2016**, *81*, 8070–8076.

(20) Haddad, T. D.; Hirayama, L. C.; Singaram, B. Indium-Mediated Asymmetric Barbier-Type Allylations: Additions to Aldehydes and Ketones and Mechanistic Investigation of the Organoindium Reagents. *J. Org. Chem.* **2010**, *75*, 642–649.

(21) Babu, S. A.; Yasuda, M.; Okabe, Y.; Shibata, I.; Baba, A. High Chelation Control of Three Contiguous Stereogenic Centers in the Reformatsky Reactions of Indium Enolates with α-Hydroxy Ketones: Unexpected Stereochemistry of Lactone Formation. *Org. Lett.* **2006**, *8*, 3029–3032.

(22) Nomiyama, S.; Hondo, T.; Tsuchimoto, T. Easy Access to a Library of Alkylindoles: Reductive Alkylation of Indoles with Carbonyl Compounds and Hydrosilanes under Indium Catalysis. *Adv. Synth. Catal.* **2016**, *358*, 1136–1149.

(23) Miyazaki, T.; Katayama, M.; Yoshimoto, S.; Ogiwara, Y.; Sakai, N. Indium-Catalyzed Direct Preparation of Dibenzyl Sulfides from Benzyl Alcohols and Elemental Sulfur with a Hydrosilane and Its Application to the Preparation of Dibenzyl Selenide. *Tetrahedron Lett.* **2016**, *57*, 676–679.

(24) Chen, T.; Cai, C. Imidazolylpyridine-In$(OTf)_3$ Catalyzed Enantioselective Allylation of Ketimines Derived from Isatins. *Org. Biomol. Chem.* **2016**, *14*, 5019–5022.

(25) Mondal, S.; Roy, D.; Jaiswal, M. K.; Panda, G. A Green Synthesis of Unsymmetrical Triarylmethanes via Indium (III) Triflate Catalyzed Friedel Crafts Alkylation of o-Hydroxy

Bisbenzylic Alcohols under Solvent Free Conditions. *Tetrahedron Lett.* **2018**, *59* (2), 89–93.

(26) Hayashi, R.; Cook, G. R. Remarkably Mild and Efficient Intramolecular Friedel-Crafts Cyclization Catalyzed by In(III). *Org. Lett.* **2007**, *9* (7), 1311–1314.

(27) Shibata, I.; Kato, H.; Ishida, T.; Yasuda, M.; Baba, A. Catalytic Generation of Indium Hydride in a Highly Diastereoselective Reductive Aldol Reaction. *Angew. Chem. Int. Ed.* **2004**, *43*, 711–714.

(28) Ieki, R.; Miyamoto, S.; Tsunoi, S.; Shibata, I. Indium Hydride Catalyzed Chemo- and Diastereoselective Reductive Aldol Reactions. *J. Organomet. Chem.* **2014**, *751*, 471–474.

(29) Loh, T. P.; Pei, J.; Lin, M. Indium Trichloride ($InCl_3$) Catalysed Diels-Alder Reaction in Water. *Chem. Commun.* **1996**, *0* (20), 2315–2316.

(30) Wildermann, A.; Foricher, Y.; Netscher, T.; Bonrath, W. New Application of Indium Catalysts: A Novel and Green Concept in the Fine Chemicals Industry. *Pure Appl. Chem.* **2007**, *79* (11), 1839–1846.

(31) Augé, J.; Lubin-Germain, N.; Uziel, J. Recent Advances in Indium-Promoted Organic Reactions. *Synthesis (Stuttg).* **2007**, *2007* (12), 1739–1764.

(32) Lingaswamy, K.; Mohan, D.; Krishna, P.; Prapurna, Y. Indium(III) Chloride Promoted Highly Efficient Tandem Rearrangement–α-Addition Strategy towards the Synthesis of α-Hydroxyamides. *Synlett* **2016**, *27*, 1693–1698.

(33) Antoniotti, S.; Dalla, V.; Duñach, E. Metal Triflimidates: Better than Metal Triflates as Catalysts in Organic Synthesis-The Effect of a Highly Delocalized Counteranion. *Angew. Chemie Int. Ed.* **2010**, *49* (43), 7860–7888.

(34) Frost, C. G.; Hartley, J. P.; Griffin, D. Counterion Effects in Indium-Catalysed Aromatic Electrophilic Substitution Reactions. *Tetrahedron Lett.* **2002**, *43* (27), 4789–4791.

(35) Tsuchimoto, T.; Kanbara, M. Reductive Alkylation of Indoles with Alkynes and Hydrosilanes under Indium Catalysis. *Org. Lett.* **2011**, *13* (5), 912–915.

(36) Shen, L.; Zhao, K.; Doitomi, K.; Ganguly, R.; Li, Y.-X.; Shen, Z.-L.; Hirao, H.; Loh, T.-P. Lewis Acid-Catalyzed Selective [2 + 2]-Cycloaddition and Dearomatizing Cascade Reaction of Aryl Alkynes with Acrylates. *J. Am. Chem. Soc.* **2017**, *139* (38), 13570–13578.

(37) Onishi, Y.; Ito, T.; Yasuda, M.; Baba, A. Indium(III) Chloride/Chlorotrimethylsilane as a Highly

Active Lewis Acid Catalyst System for the Sakurai–Hosomi Reaction. *European J. Org. Chem.* **2002**, *2002* (9), 1578–1581.

(38) Saito, T.; Nishimoto, Y.; Yasuda, M.; Baba, A. Direct Coupling Reaction between Alcohols and Silyl Compounds: Enhancement of Lewis Acidity of Me3SiBr Using $InCl_3$. *J. Org. Chem.* **2006**, *71* (22), 8516–8522.

(39) Phil Ho Lee; Lee, K.; Sung, S. Y.; Chang, S. The Catalytic Sakurai Reaction. *J. Org. Chem.* **2001**, *66* (25), 8646–8649.

(40) Zhang, Q.-C.; Zhang, W.-W.; Shen, L.; Shen, Z.-L.; Loh, T.-P.; Zhang, Q.-C.; Zhang, W.-W.; Shen, L.; Shen, Z.-L.; Loh, T.-P. In(III)-TMSBr-Catalyzed Cascade Reaction of Diarylalkynes with Acrylates for the Synthesis of Aryldihydronaphthalene Derivatives. *Molecules* **2018**, *23* (4), 979.

(41) Licht, C.; Peiró, L. T.; Villalba, G. Global Substance Flow Analysis of Gallium, Germanium, and Indium: Quantification of Extraction, Uses, and Dissipative Losses within Their Anthropogenic Cycles. *J. Ind. Ecol.* **2015**, *19* (5), 890–903.

(42) Thiébaud, E.; Hilty, L.; Schluep, M.; Böni, H.; Faulstich, M.; Thiébaud, E.; Hilty, L. M.; Schluep, M.; Böni, H. W.; Faulstich, M. Where Do Our Resources Go? Indium, Neodymium, and Gold Flows Connected to the Use of Electronic Equipment in Switzerland. *Sustainability* **2018**, *10* (8), 2658.

(43) Yoshimura, A.; Daigo, I.; Matsuno, Y. Global Substance Flow Analysis of Indium. *Mater. Trans.* **2013**, *54* (1), 102–109.

(44) Ciacci, L.; Werner, T. T.; Vassura, I.; Passarini, F. Backlighting the European Indium Recycling Potentials. *J. Ind. Ecol.* **2018**.

(45) Gu, S.; Fu, B.; Dodbiba, G.; Fujita, T.; Fang, B. A Sustainable Approach to Separate and Recover Indium and Tin from Spent Indium–Tin Oxide Targets. *RSC Adv.* **2017**, *7* (82), 52017–52023.

(46) Werner, T. T.; Ciacci, L.; Mudd, G. M.; Reck, B. K.; Northey, S. A. Looking Down Under for a Circular Economy of Indium. *Environ. Sci. Technol.* **2018**, *52* (4), 2055–2062.

(47) Pradhan, D.; Panda, S.; Sukla, L. B. Recent Advances in Indium Metallurgy: A Review. *Miner. Process. Extr. Metall. Rev.* **2018**, *39* (3), 167–180.

(48) Kitanosono, T.; Masuda, K.; Xu, P.; Kobayashi, S. Catalytic Organic Reactions in Water toward Sustainable Society. *Chem. Rev.* **2018**, *118* (2), 679–746.

(49) Loh, T.-P.; Pei, J.; Koh, K. S.-V.; Cao, G.-Q.; Li, X.-R. Indium-Trichloride Catalyzed Mukaiyama-Aldol Reaction in Water: Solubility, Aggregation and Internal Pressure Effect. *Tetrahedron Lett.* **1997**, *38* (19), 3465–3468.

(50) Loh, T.-P.; Wei, L.-L. Novel One-Pot Mannich-Type Reaction in Water: Indium Trichloride-Catalyzed Condensation of Aldehydes, Amines and Silyl Enol Ethers for the Synthesis of β-Amino Ketones and Esters. *Tetrahedron Lett.* **1998**, *39* (3–4), 323–326.

(51) Li, C. J.; Chan, T. H. Organometallic Reactions in Aqueous Media with Indium. *Tetrahedron Lett.* **1991**, *32* (48), 7017–7020.

(52) Yi, X.-H.; Haberman, J. X.; Li, C.-J. Metal-Mediated Barbier-Type Carbonyl Allylation Under Solvent-Free Conditions. *Synth. Commun.* **1998**, *28* (16), 2999–3009.

(53) Lu, W.; Chan, T. H. Organometallic Reactions in Aqueous Media. Indium- and Zinc-Mediated Allylation of Sulfonimines. *J. Org. Chem.* **2000**, *65* (25), 8589–8594.

(54) Lu, W.; Tak Hang Chan. Indium-Mediated Organometallic Reactions in Aqueous Media. Stereoselectivity in the Crotylation of Sulfonimines Bearing a Proximal Chelating Group. *J. Org. Chem.* **2001**, *66* (10), 3467–3473.

(55) Nakamura, S.; Hara, Y.; Furukawa, T.; Hirashita, T. Enantioselective Barbier-Type Allylation of Ketones Using Allyl Halide and Indium in Water. *RSC Adv.* **2017**, *7* (25), 15582–15585.

(56) Wu, C.; Wang, Z.; Hu, Z.; Zeng, F.; Zhang, X.-Y.; Cao, Z.; Tang, Z.; He, W.-M.; Xu, X.-H. Direct Synthesis of Alkenyl Iodides *via* Indium-Catalyzed Iodoalkylation of Alkynes with Alcohols and Aqueous HI. *Org. Biomol. Chem.* **2018**, *16* (17), 3177–3180.

(57) David Amantini; Francesco Fringuelli; Ferdinando Pizzo, A.; Vaccaro, L. Bromolysis and Iodolysis of α,β-Epoxycarboxylic Acids in Water Catalyzed by Indium Halides. **2001**.

(58) Karami, B.; Khodabakhshi, S.; Karami, S. Indium(III) Trifluoromethanesulfonate: A Reusable Catalyst for the Sol-Vent-Free Synthesis of Some Quinazolinones/Thiones. *Croat. Chem. Acta* **2014**, *87* (1), 23–27.

(59) Koga, N.; Kimizu, T. Thermal Decomposition of Indium(III) Hydroxide Prepared by the Microwave-Assisted Hydrothermal Method. *J. Am. Ceram. Soc.* **2008**, *91* (12), 4052–4058.

(60) Lee, S.; Kim, G. H.; Ryu, S.-S.; Hong, H. S. Recovery of Indium Powders from Indium Chloride Solutions by Cementation A. *Can. Metall. Q.* **2014**, *53* (2), 232–239.

(61) Koshima, H.; Kubota, M. High-Throughput Synthesis of Alkylbenzophenones with Indium Triflate in the Absence of Solvents Using Microwave. *Synth. Commun.* **2003**, *33* (22), 3983–3988.

(62) Fujimoto, T.; Endo, K.; Nakamura, M.; Nakamura, E. Synthesis of Ethyl 2-Ethanoyl-2-Methyl-3-Phenylbut-3-Enoate. In *Organic Syntheses*; John Wiley & Sons, Inc.: Hoboken, NJ, USA, 2009; pp 325–332.

(63) Guo, H.; Ding, K. Indium Tribromide. In *Encyclopedia of Reagents for Organic Synthesis*; John Wiley & Sons, Ltd: Chichester, UK, 2011.

(64) Mensinger, Z. L.; Zakharov, L. N.; Johnson, D. W. Synthesis and Crystallization of Infinite Indium and Gallium Acetate 1D Chain Structures and Concomitant Ethyl Acetate Hydrolysis. *Inorg. Chem.* **2009**, *48* (8), 3505–3507.

(65) Pérez, I.; Sestelo, J. P.; Sarandeses, L. A. Atom-Efficient Metal-Catalyzed Cross-Coupling Reaction of Indium Organometallics with Organic Electrophiles. *J. Am. Chem. Soc.* **2001**, *123* (18), 4155–4160.

(66) Shen, Z.-L.; Wang, S.-Y.; Chok, Y.-K.; Xu, Y.-H.; Loh, T.-P. Organoindium Reagents: The Preparation and Application in Organic Synthesis. *Chem. Rev.* **2013**, *113*, 271–401.

(67) Riveiros, R.; Tato, R.; Pérez Sestelo, J.; Sarandeses, L. A. Rhodium-Catalyzed Allylic Substitution Reactions with Indium(III) Organometallics. *European J. Org. Chem.* **2012**, *2012* (15), 3018–3023.

(68) Alonso-Marañón, L.; Sarandeses, L. A.; Martínez, M. M.; Pérez Sestelo, J. Sequential In-Catalyzed Intramolecular Hydroarylation and Pd-Catalyzed Cross-Coupling Reactions Using Bromopropargyl Aryl Ethers and Amines. *Org. Chem. Front.* **2017**, *4* (4), 500–505.

(69) Gil-Negrete, J. M.; Sestelo, J. P.; Sarandeses, L. A. Transition-Metal-Free Cross-Coupling of Indium Organometallics with Chromene and Isochroman Acetals Mediated by $BF_3{\cdot}OEt_2$. *Org. Lett.* **2016**, *18* (17), 4316–4319.

(70) Alonso-Marañón, L.; Martínez, M. M.; Sarandeses, L. A.; Sestelo, J. P. Indium-Catalyzed Intramolecular Hydroarylation of Aryl Propargyl Ethers. *Org. Biomol. Chem.* **2015**, *13* (2), 379–387.

(71) Ko, T. Y.; Youn, S. W. Cooperative Indium(III)/Silver(I) System for Oxidative Coupling/Annulation of 1,3-Dicarbonyls and Styrenes: Construction of Five-Membered

Heterocycles. *Adv. Synth. Catal.* **2016**, *358* (12), 1934–1941.

(72) Wu, Z.; Fang, X.; Leng, Y.; Yao, H.; Lin, A. Indium-Mediated Palladium-Catalyzed Allylic Alkylation of Isatins with Alkynes. *Adv. Synth. Catal.* **2018**, *360* (6), 1289–1295.

(73) Yonekura, K.; Yoshimura, Y.; Akehi, M.; Tsuchimoto, T. A Heteroarylamine Library: Indium-Catalyzed Nucleophilic Aromatic Substitution of Alkoxyheteroarenes with Amines. *Adv. Synth. Catal.* **2018**, *360* (6), 1159–1181.

(74) Larson, G. L.; Fry, J. L. *Ionic and Organometallic-Catalyzed Organosilane Reductions*; Wiley,: Hoboken, N.J.

(75) Sakai, N.; Fujii, K.; Konakahara, T. One-Step Conversion to Tertiary Amines: $InBr_3/Et_3SiH$-Mediated Reductive Deoxygenation of Tertiary Amides. *Tetrahedron Lett.* **2008**, *49*, 6873–6875.

(76) Miura, K.; Yamada, Y.; Tomita, M.; Hosomi, A. Indium(III) Acetate-Catalyzed 1,4-Reduction and Reductive Aldol Reactions of α-Enones with Phenylsilane. *Synlett* **2004**, *11*, 1985–1989.

(77) Ieki, R.; Miyamoto, S.; Tsunoi, S.; Shibata, I. Indium Hydride Catalyzed Chemo- and Diastereoselective Reductive Aldol Reactions. *J. Organomet. Chem.* **2014**, *751*, 471–474.

(78) Sakai, N.; Takahashi, N.; Ogiwara, Y. Indium-Catalyzed Hydroamination/Hydrosilylation of Terminal Alkynes and Aromatic Amines through a One-Pot, Two-Step Protocol. *European J. Org. Chem.* **2014**, *2014*, 5078–5082.

(79) Ogiwara, Y.; Shimoda, W.; Ide, K.; Nakajima, T.; Sakai, N. Carboxamides as *N* -Alkylating Reagents of Secondary Amines in Indium-Catalyzed Reductive Amination with a Hydrosilane. *European J. Org. Chem.* **2017**, *2017* (20), 2866–2870.

(80) Teo, Y. C.; Goh, J. D.; Loh, T. P. Catalytic Enantioselective Allylation of Ketones via a Chiral Indium(III) Complex. *Org. Lett.* **2005**, *7* (13), 2743–2745.

(81) Lu, J.; Ji, S. J.; Teo, Y. C.; Loh, T. P. Highly Enantioselective Allylation of Aldehydes Catalyzed by Indium(III) - PYBOX Complex. *Org. Lett.* **2005**, *7* (1), 159–161.

(82) Lu, J.; Hong, M.-L.; Ji, S.-J.; Teo, Y.-C.; Loh, T.-P. Enantioselective Allylation of Ketones Catalyzed by Chiral In(Iii)-PYBOX Complexes. *Chem. Commun.* **2005**, *0* (33), 4217.

(83) Takita, R.; Yakura, K.; Ohshima, T.; Shibasaki, M. Asymmetric Alkynylation of Aldehydes Catalyzed by an In(III)/BINOL Complex. *J. Am. Chem. Soc.* **2005**, *127*, 13760–13761.

(84) Zhang, X.; Chen, D.; Liu, X.; Feng, X. Enantioselective Allylation of Ketones Catalyzed by N,N′-Dioxide and Indium(III) Complex. *J. Org. Chem.* **2007**, *72* (14), 5227–5233.

(85) Huang, J.; Wang, J.; Chen, X.; Wen, Y.; Liu, X.; Feng, X. Highly Enantioselective Allylation of Aromatic α-Keto Phosphonates Catalyzed by Chiral N, N′-Dioxide-Indium(III) Complexes. *Adv. Synth. Catal.* **2008**, *350* (2), 287–294.

(86) Cook, G. R.; Kargbo, R.; Maity, B. Catalytic Enantioselective Indium-Mediated Allylation of Hydrazones. *Org. Lett.* **2005**, *7*, 2767–2770.

(87) Kumar, D.; Vemula, S. R.; Balasubramanian, N.; Cook, G. R. Indium-Mediated Stereoselective Allylation. *Acc. Chem. Res.* **2016**, *49* (10), 2169–2178.

(88) Teo, Y. C.; Goh, J. D.; Loh, T. P. Catalytic Enantioselective Allylation of Ketones via a Chiral Indium(III) Complex. *Org. Lett.* **2005**, *7* (13), 2743–2745.

(89) Taft, R. W. Polar and Steric Substituent Constants for Aliphatic and o-Benzoate Groups from Rates of Esterification and Hydrolysis of Esters. *J. Am. Chem. Soc.* **1952**, *74* (12), 3120–3128.

(90) Taft, R. W. Linear Steric Energy Relationships. *J. Am. Chem. Soc.* **1953**, *75* (18), 4538–4539.

(91) Charton, M. Nature of the Ortho Effect. II. Composition of the Taft Steric Parameters. *J. Am. Chem. Soc.* **1969**, *91* (3), 615–618.

(92) Charton, M. Steric Effects. I. Esterification and Acid-Catalyzed Hydrolysis of Esters. *J. Am. Chem. Soc.* **1975**, *97* (6), 1552–1556.

(93) Charton, M. Steric Effects. II. Base-Catalyzed Ester Hydrolysis. *J. Am. Chem. Soc.* **1975**, *97* (13), 3691–3693.

(94) Charton, M. Steric Effects. III. Bimolecular Nucleophilic Substitution. *J. Am. Chem. Soc.* **1975**, *97* (13), 3694–3697.

(95) Charton, M. Steric Effects. 7. Additional V Constants. *J. Org. Chem.* **1976**, *41* (12), 2217–2220.

(96) Winstein, S.; Holness, N. J. Neighboring Carbon and Hydrogen. XIX. t-Butylcyclohexyl Derivatives. Quantitative Conformational Analysis. *J. Am. Chem. Soc.* **1955**, *77* (21), 5562–5578.

(97) Bott, G.; Field, L. D.; Sternhell, S. Steric Effects. A Study of a Rationally Designed System. *J. Am. Chem. Soc.* **1980**, *102* (17), 5618–5626.

(98) Adams, R.; Yuan, H. C. The Stereochemistry of Diphenyls and Analogous Compounds. *Chem.*

Rev. **1933**, *12* (2), 261–338.

(99) Tolman, C. A. Phosphorus Ligand Exchange Equilibriums on Zerovalent Nickel. Dominant Role for Steric Effects. *J. Am. Chem. Soc.* **1970**, *92* (10), 2956–2965.

(100) Tolman, C. A. Steric Effects of Phosphorus Ligands in Organometallic Chemistry and Homogeneous Catalysis. *Chem. Rev.* **1977**, *77* (3), 313–348.

(101) Hillier, A. C.; Sommer, W. J.; Yong, B. S.; Petersen, J. L.; Cavallo, L.; Nolan, S. P. A Combined Experimental and Theoretical Study Examining the Binding of N-Heterocyclic Carbenes (NHC) to the Cp*RuCl (Cp* = H5-C5Me5) Moiety: Insight into Stereoelectronic Differences between Unsaturated and Saturated NHC Ligands. *Organometallics* **2003**, *22* (21), 4322–4326.

(102) Sigman, M. S.; Harper, K. C.; Bess, E. N.; Milo, A. The Development of Multidimensional Analysis Tools for Asymmetric Catalysis and Beyond. *Acc. Chem. Res.* **2016**, *49* (6), 1292–1301.

(103) Akiyama, T. Stronger Brønsted Acids. *Chemical Reviews*. American Chemical Society 2007, pp 5744–5758.

(104) Terada, M. Chiral Phosphoric Acids as Versatile Catalysts for Enantioselective Transformations. *Synthesis*. Georg Thieme Verlag Stuttgart, 2010, pp 1929–1982.

(105) Parmar, D.; Sugiono, E.; Raja, S.; Rueping, M. Complete Field Guide to Asymmetric BINOL-Phosphate Derived Brønsted Acid and Metal Catalysis: History and Classification by Mode of Activation; Brønsted Acidity, Hydrogen Bonding, Ion Pairing, and Metal Phosphates. *Chem. Rev.* **2014**, *114* (18), 9047–9153.

(106) Mitsumori, S.; Zhang, H.; Cheong, P. H. Y.; Houk, K. N.; Tanaka, F.; Barbas, C. F. Direct Asymmetric Anti-Mannich-Type Reactions Catalyzed by a Designed Amino Acid. *J. Am. Chem. Soc.* **2006**, *128* (4), 1040–1041.

(107) Straker, R. N.; Peng, Q.; Mekareeya, A.; Paton, R. S.; Anderson, E. A. Computational Ligand Design in Enantio- and Diastereoselective Ynamide [5+2] Cycloisomerization. *Nat. Commun.* **2016**, *7*, 10109.

(108) Poree, C.; Schoenebeck, F. A Holy Grail in Chemistry: Computational Catalyst Design: Feasible or Fiction? *Acc. Chem. Res.* **2017**, *50* (3), 605–608.

(109) Reid, J. P.; Goodman, J. M. Goldilocks Catalysts: Computational Insights into the Role of the 3,3′ Substituents on the Selectivity of BINOL-Derived Phosphoric Acid Catalysts. *J. Am. Chem. Soc.* **2016**, *138* (25), 7910–7917.

(110) Reid, J. P.; Goodman, J. M. Selecting Chiral BINOL-Derived Phosphoric Acid Catalysts: General Model To Identify Steric Features Essential for Enantioselectivity. *Chem. - A Eur. J.* **2017**, *23* (57), 14248–14260.

(111) Reid, J. P. Development and Application of Computational Methods for the Prediction of Chiral Phosphoric Acid Catalyst Performance, University of Cambridge, 2017.

(112) Yang, F.; Wei, S.; Chen, C.-A.; Xi, P.; Yang, L.; Lan, J.; Gau, H.-M.; You, J. A New Strategy for Designing Non-C2-Symmetric Monometallic Bifunctional Catalysts and Their Application in Enantioselective Cyanation of Aldehydes. *Chem. - A Eur. J.* **2008**, *14* (7), 2223–2231.

(113) Zhang, Z.-G.; Dong, Z.-B.; Li, J.-S. Synthesis and Application of 3-Substituted (S)-BINOL as Chiral Ligands for the Asymmetric Ethylation of Aldehydes. *Chirality* **2010**, *22* (9), 820–826.

(114) Wu, T. R.; Shen, L.; Chong, J. M. Asymmetric Allylboration of Aldehydes and Ketones Using 3,3‘-Disubstitutedbinaphthol-Modified Boronates. *Org. Lett.* **2004**, *6* (16), 2701–2704.

(115) Synthesis of Alpha-Halo Ethers from Symmetric Acetals and in Situ Methoxymethylation of an Alcohol. *Org. Synth.* **2007**, *84*, 102.

(116) Hong, X.; Küçük, H. B.; Maji, M. S.; Yang, Y.-F.; Rueping, M.; Houk, K. N. Mechanism and Selectivity of *N* -Triflylphosphoramide Catalyzed (3 + + 2) Cycloaddition between Hydrazones and Alkenes. *J. Am. Chem. Soc.* **2014**, *136* (39), 13769–13780.

(117) Jin, J.; Zhao, Y.; Gouranourimi, A.; Ariafard, A.; Hong Chan, P. W. Chiral Brønsted Acid Catalyzed Enantioselective Dehydrative Nazarov-Type Electrocyclization of Aryl and 2-Thienyl Vinyl Alcohols. *J. Am. Chem. Soc.* **2018**, *140* (17), 5834–5841.

(118) Xie, Y.; Cheng, G.-J.; Lee, S.; Kaib, P. S. J.; Thiel, W.; List, B. Catalytic Asymmetric Vinylogous Prins Cyclization: A Highly Diastereo- and Enantioselective Entry to Tetrahydrofurans. *J. Am. Chem. Soc.* **2016**, *138* (44), 14538–14541.

(119) Doyle, M. P.; West, C. T. Silane Reductions in Acidic Media. VI. Mechanism of Organosilane Reductions of Carbonyl Compounds. Transition State Geometries of Hydride Transfer Reactions. *J. Org. Chem.* **1975**, *40*, 3835–3838.

(120) Brown, H. C.; Krishnamurthy, S. Forty Years of Hydride Reductions. *Tetrahedron* **1979**, *35*, 567–607.

(121) Wakchaure, V. N.; Kaib, P. S. J.; Leutzsch, M.; List, B. Disulfonimide-Catalyzed Asymmetric Reduction of *N* -Alkyl Imines. *Angew. Chemie Int. Ed.* **2015**, *54* (40), 11852–11856.

(122) Hermeke, J.; Mewald, M.; Oestreich, M. Experimental Analysis of the Catalytic Cycle of the Borane-Promoted Imine Reduction with Hydrosilanes: Spectroscopic Detection of Unexpected Intermediates and a Refined Mechanism. *J. Am. Chem. Soc.* **2013**, *135*, 17537–17546.

(123) Jiang, X.; Minnaard, A. J.; Hessen, B.; Feringa, B. L.; Duchateau, A. L. L.; Andrien, J. G. O.; Boogers, J. A. F.; de Vries, J. G. Application of Monodentate Secondary Phosphine Oxides, a New Class of Chiral Ligands, in Ir(I)-Catalyzed Asymmetric Imine Hydrogenation. *Org. Lett.* **2003**, *5*, 1503–1506.

(124) Whittlesey, B. R.; Ittycheriah, I. P. Trichlorobis(Tetrahydrofuran)Indium(III). *Acta Crystallogr. Sect. C Cryst. Struct. Commun.* **1994**, *50*, 693–695.

(125) Aldridge, S.; Downs, A. J. The Group 13 Metals Aluminium, Gallium, Indium and Thallium: Chemical Patterns and Peculiarities. Wiley & Sons 2011, pp 93–98.

(126) Cross, R. J.; Farrugia, L. J.; McArthur, D. R.; Peacock, R. D.; Taylor, D. S. C. Syntheses, Crystal Structures, and CD Spectra of Simple Heterobimetallic Transition Metal Binaphtholates. *Inorg. Chem.* **1999**, *38*, 5698–5702.

(127) Blake, A. J.; Cunningham, A.; Ford, A.; Teat, S. J.; Woodward, S. Enantioselective Reduction of Prochiral Ketones by Catecholborane Catalysed by Chiral Group 13 Complexes. *Chem. - A Eur. J.* **2000**, *6*, 3586–3594.

(128) Xu, Y.; Clarkson, G. C.; Docherty, G.; North, C. L.; Woodward, G.; Wills, M. Ruthenium(II) Complexes of Monodonor Ligands: Efficient Reagents for Asymmetric Ketone Hydrogenation. *J. Org. Chem.* **2005**, *70* (20), 8079–8087.

(129) Turner, H. M.; Patel, J.; Niljianskul, N.; Chong, J. M. Binaphthol-Catalyzed Asymmetric Conjugate Arylboration of Enones. *Org. Lett.* **2011**, *13* (21), 5796–5799.

(130) Zhang, Y.; Li, N.; Qu, B.; Ma, S.; Lee, H.; Gonnella, N. C.; Gao, J.; Li, W.; Tan, Z.; Reeves, J. T.; et al. Asymmetric Methallylation of Ketones Catalyzed by a Highly Active Organocatalyst 3,3′-F_2-BINOL. *Org. Lett.* **2013**, *15* (7), 1710–1713.

(131) Sephton, S. M.; Wang, C.; Zakharov, L. N.; Blakemore, P. R. Silylcyanation of Aldehydes, Ketones, and Imines Catalyzed by a 6,6′-Bis-Sulfonamide Derivative of 7,7′-Dihydroxy-8,8′-Biquinolyl (AzaBINOL). *European J. Org. Chem.* **2012**, *2012* (17), 3249–3260.

(132) Dar, A. A.; Enjamuri, N.; Shadab, M.; Ali, N.; Khan, A. T. Synthesis of Unsymmetrical Sulfides and

Their Oxidation to Sulfones to Discover Potent Antileishmanial Agents. *ACS Comb. Sci.* **2015**, *17* (11), 671–681.

(133) Charmant, J. P. H.; Dyke, A. M.; Lloyd-Jones, G. C. The Anionic Thia-Fries Rearrangement of Aryl Triflates. *Chem. Commun.* **2003**, *0* (3), 380–381.

(134) Kargbo, R.; Takahashi, Y.; Bhor, S.; Cook, G. R.; Lloyd-Jones, G. C.; Shepperson, I. R. Readily Accessible, Modular, and Tuneable BINOL 3,3′- Perfluoroalkylsulfones: Highly Efficient Catalysts for Enantioselective in-Mediated Imine Allylation. *J. Am. Chem. Soc.* **2007**, *129* (13), 3846–3847.

(135) Dyke, A. M.; Gill, D. M.; Harvey, J. N.; Hester, A. J.; Lloyd-Jones, G. C.; Muñoz, M. P.; Shepperson, I. R. Decoupling Deprotonation from Metalation: Thia-Fries Rearrangement. *Angew. Chemie Int. Ed.* **2008**, *47* (27), 5067–5070.

(136) Mosiashvili, L.; Chankvetadze, L.; Farkas, T.; Chankvetadze, B. On the Effect of Basic and Acidic Additives on the Separation of the Enantiomers of Some Basic Drugs with Polysaccharide-Based Chiral Selectors and Polar Organic Mobile Phases. *J. Chromatogr. A* **2013**, *1317*, 167–174.

(137) Ye, Y. K.; Lord, B.; Stringham, R. W. Memory Effect of Mobile Phase Additives in Chiral Separations on a Chiralpak AD Column. *J. Chromatogr. A* **2002**, *945* (1–2), 139–146.

(138) Forrester, J. D.; Zalkin, A.; Templeton, D. H. Crystal and Molecular Structure of Indium(III) Iodide (In_2I_6). *Inorg. Chem.* **1964**, *3* (1), 63–67.

(139) Verdaguer, X.; Lange, U. E. W.; Buchwald, S. L. Amine Additives Greatly Expand the Scope of Asymmetric Hydrosilylation of Imines. *Angew. Chemie Int. Ed.* **1998**, *37* (8), 1103–1107.

(140) Kremer, A. B.; Osten, K. M.; Yu, I.; Ebrahimi, T.; Aluthge, D. C.; Mehrkhodavandi, P. Dinucleating Ligand Platforms Supporting Indium and Zinc Catalysts for Cyclic Ester Polymerization. *Inorg. Chem.* **2016**, *55* (11), 5365–5374.

(141) Tai, Y.-X.; Ji, Y.-M.; Lu, Y.-L.; Li, M.-X.; Wu, Y.-Y.; Han, Q.-X. Cadmium(II) and Indium(III) Complexes Derived from 2-Benzoylpyridine N(4)-Cyclohexylthiosemicarbazone: Synthesis, Crystal Structures, Spectroscopic Characterization and Cytotoxicity. *Synth. Met.* **2016**, *219*, 109–114.

(142) Aluthge, D. C.; Yan, E. X.; Ahn, J. M.; Mehrkhodavandi, P. Role of Aggregation in the Synthesis and Polymerization Activity of SalBinap Indium Alkoxide Complexes. *Inorg. Chem.* **2014**, *53*

(13), 6828–6836.

(143) Le, P. Q.; Nguyen, T. S.; May, J. A. A General Method for the Enantioselective Synthesis of α-Chiral Heterocycles. *Org. Lett.* **2012**, *14* (23), 6104–6107.

(144) Pousse, G.; Devineau, A.; Dalla, V.; Humphreys, L.; Lasne, M.-C.; Rouden, J.; Blanchet, J. Synthesis of BINOL Derived Phosphorodithioic Acids as New Chiral Brønsted Acids and an Improved Synthesis of 3,3′-Disubstituted H8-BINOL Derivatives. *Tetrahedron* **2009**, *65* (51), 10617–10622.

(145) Chen, Y.; Yekta, S.; Yudin, A. K. Modified BINOL Ligands in Asymmetric Catalysis. *Chem. Rev.* **2003**, *103*, 3155–3212.

(146) Rosini, C.; Franzini, L.; Raffaelli, A.; Salvadori, P. Synthesis and Applications of Binaphthylic C_2 -Symmetry Derivatives as Chiral Auxiliaries in Enantioselective Reactions. *Synthesis (Stuttg).* **1992**, *1992*, 503–517.

(147) Pu, L. 1,1‘-Binaphthyl Dimers, Oligomers, and Polymers: Molecular Recognition, Asymmetric Catalysis, and New Materials. *Chem. Rev.* **1998**, *98*, 2405–2494.

(148) Shibasaki, M.; Yoshikawa, N. Lanthanide Complexes in Multifunctional Asymmetric Catalysis. *Chem. Rev.* **2002**, *102*, 2187–2210.

(149) Aspinall, H. C.; Greeves, N. Defining Effective Chiral Binding Sites at Lanthanides —Highly Enantioselective Reagents and Catalysts from Binaphtholate and Pybox Ligands. *J. Organomet. Chem.* **2002**, *647*, 151–157.

(150) Walsh, P. J.; Kozlowski, M. C. Fundamentals of Asymmetric Catalysis. University Science Books ; 2009, pp 118–126.

(151) Brown, S. N.; Chu, E. T.; Hull, M. W.; Noll, B. C. Electronic Dissymmetry in Chiral Recognition. *J. Am. Chem. Soc.* **2005**, *127*, 16010–16011.

(152) Kumagai, N.; Kanai, M.; Sasai, H. A Career in Catalysis: Masakatsu Shibasaki. *ACS Catal.* **2016**, *6*, 4699–4709.

(153) Bersuker, I. B. (Isaak B. *Electronic Structure and Properties of Transition Metal Compounds : Introduction to the Theory / by Isaac B. Bersuker.*; Wiley: New York ; Chichester, 1996.

(154) Charalambous, J.; Gossett, R. G.; Johri, M. H.; Kensett, M. J. Mass Spectra of Tris(β-Diketonato)Gallium(III) and -Indium(III). *Inorganica Chim. Acta* **1977**, *22*, 101–105.

(155) Hehemann, D. G.; Lau, J. E.; Harris, J. D.; Hoops, M. D.; Duffy, N. V.; Fanwick, P. E.; Khan, O.; Jin, M. H.-C.; Hepp, A. F. Synthesis, Characterization and Decomposition Studies of Tris(N,N-Dibenzyldithiocarbamato)Indium(III): Chemical Spray Deposition of Polycrystalline $CuInS_2$ on Copper Films. *Mater. Sci. Eng. B* **2005**, *116*, 381–389.

(156) Osten, K. M.; Aluthge, D. C.; Patrick, B. O.; Mehrkhodavandi, P. Probing the Role of Secondary versus Tertiary Amine Donor Ligands for Indium Catalysts in Lactide Polymerization. *Inorg. Chem.* **2014**, *53*, 9897–9906.

(157) Osten, K. M.; Aluthge, D. C.; Mehrkhodavandi, P.; Dechy-Cabaret, O.; Martin-Vaca, B.; Bourissou, D.; Drumright, R. E.; Gruber, P. R.; Henton, D. E.; Gupta, B.; et al. The Effect of Steric Changes on the Isoselectivity of Dinuclear Indium Catalysts for Lactide Polymerization. *Dalt. Trans.* **2015**, *44*, 6126–6139.

(158) Aluthge, D. C.; Yan, E. X.; Ahn, J. M.; Mehrkhodavandi, P. Role of Aggregation in the Synthesis and Polymerization Activity of SalBinap Indium Alkoxide Complexes. *Inorg. Chem.* **2014**, *53*, 6828–6836.

(159) Brito-Arias, M. Synthesis and Characterization of Glycosides. In *Synthesis and Characterization of Glycosides*; Springer, 2007; pp 73–76.

(160) Pauls, J.; Chitsaz, S.; Neumüller, B. Chirale Gallium- Und Indium-Alkoxometallate. *Z. Anorg. Allg. Chem.* **2000**, *626*, 2028–2034.

(161) Chitsaz, S.; Neumüller, B. BINOL Compounds of Group 13. *Organometallics* **2001**, *20*, 2338–2343.

(162) Aspinall, H. C.; Bickley, J. F.; Dwyer, J. L. M.; Greeves, N.; Steiner, A. Lithium Binaphtholates: Chiral Chains and Clusters. *Angew. Chem.* **2000**, *39*, 2858–2861.

(163) Werner, B.; Kräter, T.; Neumüller, B. Darstellung Und Eigenschaften von Organoindiumbromiden. *Z. Anorg. Allg. Chem.* **1995**, *621*, 346–358.

(164) Arai, T.; Yamada, Y. M. A.; Yamamoto, N.; Sasai, H.; Shibasaki, M. Self-Assembly of Heterobimetallic Complexes and Reactive Nucleophiles: A General Strategy for the Activation of Asymmetric Reactions Promoted by Heterobimetallic Catalysts. *Chem. Eur. J.* **1996**, *2*, 1368–1372.

(165) Matsunaga, S.; Ohshima, T.; Shibasaki, M. Linked-BINOL: An Approach towards Practical Asymmetric Multifunctional Catalysis. *Adv. Synth. Catal.* **2002**, *344*, 3–15.

(166) Houk, K. N.; Cheong, P. H.-Y. Computational Prediction of Small-Molecule Catalysts. *Nature* **2008**, *455*, 309–313.

(167) Levine, I. N. Quantum Chemistry. Seventh ed. Pearson 2014, pp 436–643.

(168) Höltje, Hans-Dieter; Sipple, Wolfgang; Rognan, Didier; Folkers, G. *Molecular Modeling: Basic Principles and Applications*, 2 nd.; Wiley-VCH Verlag GmbH & Co. KGaA, 2003.

(169) Leach, A. R. *Molecular Modelling : Principles and Applications / Andrew R. Leach.*, 2nd ed.; Prentice Hall: Harlow, 2001.

(170) Schlegel, H. B. *Modern Electronic Structure Theory. Part I and II / Editor, David R. Yarkony.*; World Scientific, 1995.

(171) Eyring, H. The Activated Complex in Chemical Reactions. *J. Chem. Phys.* **1935**, *3* (2), 107–115.

(172) Hill, T. L. On Steric Effects. *J. Chem. Phys.* **1946**, *14* (7), 465–465.

(173) Westheimer, F. H.; Mayer, J. E. The Theory of the Racemization of Optically Active Derivatives of Diphenyl. *J. Chem. Phys.* **1946**, *14* (12), 733–738.

(174) Hohenberg, P.; Kohn, W. Inhomogeneous Electron Gas. *Phys. Rev.* **1964**, *136*, B864–B871.

(175) Sholl, D. S.; Steckel, J. A. Density Functional Theory : A Practical Introduction. Wiley,: Hoboken, N.J. pp xii, 238 p.

(176) Becke, A. D. A New Mixing of Hartree–Fock and Local Density-Functional Theories. *J. Chem. Phys.* **1993**, *98*, 1372–1377.

(177) Lee, C.; Yang, W.; Parr, R. G. Development of the Colle-Salvetti Correlation-Energy Formula into a Functional of the Electron Density. *Phys. Rev. B* **1988**, *37*, 785–789.

(178) Zhao, Y.; Truhlar, D. G. Density Functionals with Broad Applicability in Chemistry. *Acc. Chem. Res.* **2008**, *41*, 157–167.

(179) Perdew, J. P.; Ernzerhof, M.; Burke, K. Rationale for Mixing Exact Exchange with Density Functional Approximations. *J. Chem. Phys.* **1996**, *105*, 9982–9985.

(180) Asadi, Z.; Asadi, M.; Shorkaei, M. R. Synthesis, Characterization and DFT Study of New Water-Soluble Aluminum(III), Gallium(III) and Indium(III) Schiff Base Complexes: Effect of Metal on the Binding Propensity with Bovine Serum Albumin in Water. *J. Iran. Chem. Soc.* **2016**, *13*, 429–442.

(181) Zhanpeisov, N. U.; Nakatani, H.; Fukumura, H. Theoretical DFT Study of the Structure and Chemical Activity of Small Indium(III) Oxide Clusters. *Res. Chem. Intermed.* **2011**, *37*, 647–658.

(182) Zhao, Q.; Xie, L.; Kulik, H. J. Discovering Amorphous Indium Phosphide Nanostructures with High-Temperature Ab Initio Molecular Dynamics. *J. Phys. Chem. C* **2015**, *119*, 23238–23249.

(183) Hay, P. J.; Wadt, W. R. Ab Initio Effective Core Potentials for Molecular Calculations. Potentials for K to Au Including the Outermost Core Orbitals. *J. Chem. Phys.* **1985**, *82*, 299–310.

(184) Rong, Y.; Palmer, J. H.; Parkin, G. Benzannulated Tris(2-Mercapto-1-Imidazolyl)Hydroborato Ligands: Tetradentate κ^4-S_3H Binding and Access to Monomeric Monovalent Thallium in an [S_3] Coordination Environment. *DaltonTrans.* **2014**, *43*, 1397–1407.

(185) Yurkerwich, K.; Rong, Y.; Parkin, G. Gallium Hydride and Monovalent Indium Compounds That Feature Tris(Pyrazolyl)Hydroborate Ligands. *Acta Crystallogr. Sect. C Cryst. Struct. Commun.* **2013**, *69*, 963–967.

(186) Wadt, W. R.; Hay, P. J. Ab Initio Effective Core Potentials for Molecular Calculations. Potentials for Main Group Elements Na to Bi. *J. Chem. Phys.* **1985**, *82*, 284–298.

(187) Hay, P. J.; Wadt, W. R. Ab Initio Effective Core Potentials for Molecular Calculations. Potentials for the Transition Metal Atoms Sc to Hg. *J. Chem. Phys.* **1985**, *82*, 270–283.

(188) Jaguar User Manual, Version 7.6. **2009**.

(189) Ahlquist, M. S. G.; Norrby, P.-O. Dispersion and Back-Donation Gives Tetracoordinate [Pd(PPh3)4]. *Angew. Chemie Int. Ed.* **2011**, *50* (49), 11794–11797.

(190) Grimme, S. Density Functional Theory with London Dispersion Corrections. *Wiley Interdiscip. Rev. Comput. Mol. Sci.* **2011**, *1* (2), 211–228.

(191) Grimme, S.; Antony, J.; Ehrlich, S.; Krieg, H. A Consistent and Accurate *Ab Initio* Parametrization of Density Functional Dispersion Correction (DFT-D) for the 94 Elements H-Pu. *J. Chem. Phys.* **2010**, *132* (15), 154104.

(192) Tannor, D. J.; Marten, B.; Murphy, R.; Friesner, R. A.; Sitkoff, D.; Nicholls, A.; Honig, B.; Ringnalda, M.; Goddard, W. A. Accurate First Principles Calculation of Molecular Charge Distributions and Solvation Energies from Ab Initio Quantum Mechanics and Continuum Dielectric Theory. *J. Am. Chem. Soc.* **1994**, *116* (26), 11875–11882.

(193) Marten, B.; Kim, K.; Cortis, C.; Friesner, R. A.; Murphy, R. B.; Ringnalda, M. N.; Sitkoff, D.; Honig,

B. New Model for Calculation of Solvation Free Energies: Correction of Self-Consistent Reaction Field Continuum Dielectric Theory for Short-Range Hydrogen-Bonding Effects. *J. Phys. Chem.* **1996**, *100* (28), 11775–11788.

(194) Cinar, M. E.; Schmittel, M. One-Pot Domino Aldol Reaction of Indium Enolates Affording 6-Deoxy-α-D,L-Altropyranose Derivatives: Synthesis, Mechanism, and Computational Results. *J. Org. Chem.* **2015**, *80* (16), 8175–8182.

(195) Lo Fiego, M. J.; Dorn, V. B.; Badajoz, M. A.; Lockhart, M. T.; Chopa, A. B. Experimental and DFT Study on the Indium-Mediated Synthesis of Benzophenones via Arylstannanes. *RSC Adv.* **2014**, *4* (90), 49079–49085.

(196) Noyori, R.; Hashiguchi, S. Asymmetric Transfer Hydrogenation Catalyzed by Chiral Ruthenium Complexes. *Acc. Chem. Res.* **1997**, *30* (2), 97–102.

(197) Hedberg, C.; Källström, K.; Arvidsson, P. I.; Brandt, P.; Andersson, P. G. Mechanistic Insights into the Phosphine-Free RuCp*-Diamine-Catalyzed Hydrogenation of Aryl Ketones: Experimental and Theoretical Evidence for an Alcohol-Mediated Dihydrogen Activation. *J. Am. Chem. Soc.* **2005**, *127* (43), 15083–15090.

(198) Miyai, T.; Inoue, K.; Yasuda, M.; Shibata, I.; Baba, A. Preparation of a Novel Indium Hydride and Application to Practical Organic Synthesis. *Tetrahedron Lett.* **1998**, *39* (14), 1929–1932.

(199) Simonsen, K. B.; Gothelf, K. V.; Jørgensen, K. A. A Simple Synthetic Approach to 3,3′-Diaryl BINOLs. *J. Org. Chem.* **1998**, *63* (21), 7536–7538.

(200) Yang, J.-F.; Wang, R.-H.; Wang, Y.-X.; Yao, W.-W.; Liu, Q.-S.; Ye, M. Ligand-Accelerated Direct C−H Arylation of BINOL: A Rapid One-Step Synthesis of Racemic 3,3′-Diaryl BINOLs. *Angew. Chemie Int. Ed.* **2016**, *55* (45), 14116–14120.

(201) Zhang, Y.; Lim, C.-S.; Sim, D. S. B.; Pan, H.-J.; Zhao, Y. Catalytic Enantioselective Amination of Alcohols by the Use of Borrowing Hydrogen Methodology: Cooperative Catalysis by Iridium and a Chiral Phosphoric Acid. *Angew. Chemie* **2014**, *126* (5), 1423–1427.

(202) Baudequin, C.; Zamfir, A.; Tsogoeva, S. B. Highly Enantioselective Organocatalytic Formation of a Quaternary Carbon Center via Chiral Brønsted Acid Catalyzed Self-Coupling of Enamides. *Chem. Commun.* **2008**, *0* (38), 4637.

(203) Klussmann, M.; Ratjen, L.; Hoffmann, S.; Wakchaure, V.; Goddard, R.; List, B. Synthesis of TRIP and Analysis of Phosphate Salt Impurities. *Synlett* **2010**, *2010* (14), 2189–2192.

(204) Egami, H.; Katsuki, T. Iron-Catalyzed Asymmetric Aerobic Oxidation: Oxidative Coupling of 2-Naphthols. *J. Am. Chem. Soc.* **2009**, *131* (17), 6082–6083.

(205) Singh, R.; Czekelius, C.; Schrock, R. R.; Peter Müller, A.; Hoveyda, A. H. Molybdenum Imido Alkylidene Metathesis Catalysts That Contain Electron-Withdrawing Biphenolates or Binaphtholates. **2007**.

(206) Lundy, B. J.; Jansone-Popova, S.; May, J. A. Enantioselective Conjugate Addition of Alkenylboronic Acids to Indole-Appended Enones. *Org. Lett.* **2011**, *13* (18), 4958–4961.

(207) Momiyama, N.; Nishimoto, H.; Terada, M. Chiral Brønsted Acid Catalysis for Enantioselective Hosomi−Sakurai Reaction of Imines with Allyltrimethylsilane. *Org. Lett.* **2011**, *13* (8), 2126–2129.

(208) Cram, D. J.; Helgeson, R. C.; Peacock, S. C.; Kaplan, L. J.; Domeier, L. A.; Moreau, P.; Koga, K.; Mayer, J. M.; Chao, Y.; Siegel, M. G.; et al. Host-Guest Complexation. 8. Macrocyclic Polyethers Shaped by Two Rigid Substituted Dinaphthyl or Ditetralyl Units. *J. Org. Chem.* **1978**, *43* (10), 1930–1946.

(209) Wakchaure, V. N.; Kaib, P. S. J.; Leutzsch, M.; List, B. Disulfonimide-Catalyzed Asymmetric Reduction of N -Alkyl Imines. *Angew. Chem. Int. Ed.* **2015**, *54*, 11852–11856.

(210) Berbasov, D. O.; Ojemaye, I. D.; Soloshonok, V. A. Synthesis of Highly 1,3-Proton Shift Transferable N-Benzyl Imines of Trifluoroacetophenone under the “Low-Basicity” Reaction Conditions. *J. Fluor. Chem.* **2004**, *125* (4), 603–607.

(211) Soetens, M.; Drouet, F.; Riant, O. (η^5 -Pentamethylcyclopentadienyl)Iridium Complex Catalyzed Imine Reductions Utilizing the Biomimetic 1,4-NAD(P)H Cofactor and *N* -Benzyl-1,4-Dihydronicotinamide as the Hydride-Transfer Agent. *ChemCatChem* **2017**, *9* (6), 929–933.

(212) Shirai, S.; Nara, H.; Kayaki, Y.; Ikariya, T. Remarkable Positive Effect of Silver Salts on Asymmetric Hydrogenation of Acyclic Imines with Cp*Ir Complexes Bearing Chiral N-Sulfonylated Diamine Ligands. *Organometallics* **2009**, *28* (3), 802–809.

(213) Samec, J. S. M.; Éll, A. H.; Bäckvall, J.-E. Efficient Ruthenium-Catalyzed Aerobic Oxidation of Amines by Using a Biomimetic Coupled Catalytic System. *Chem. - A Eur. J.* **2005**, *11* (8), 2327–2334.

(214) Guizzetti, S.; Benaglia, M.; Cozzi, F.; Annunziata, R. Chiral Lewis Base Promoted Trichlorosilane Reduction of Ketimines. An Enantioselective Organocatalytic Synthesis of Chiral Amines.

Tetrahedron **2009**, *65* (32), 6354–6363.

(215) Chen, H.; Ye, J.-L.; Huang, P.-Q. Chemoselective Direct Reductive Trifluoromethylation of Amides: A Flexible Access to Functionalized α-Trifluoromethylamines. *Org. Chem. Front.* **2018**, *5* (6), 943–947.

(216) Bragg, R. A.; Clayden, J.; Morris, G. A.; Pink, J. H. Stereodynamics of Bond Rotation in Tertiary Aromatic Amides. *Chem. - A Eur. J.* **2002**, *8*, 1279–1289.

(217) Zhang, M.-N.; Zhao, M.-N.; Chen, M.; Ren, Z.-H.; Wang, Y.-Y.; Guan, Z.-H.; Liu, C.; Liu, D.; Lei, A.; Jeffrey, J.; et al. Copper-Catalyzed Radical Coupling of 1,3-Dicarbonyl Compounds with Terminal Alkenes for the Synthesis of Tetracarbonyl Compounds. *Chem. Commun.* **2016**, *52* (36), 6127–6130.

Experimental

Computational Details:

All computation work was performed using the Schrödinger suite of computational chemistry software, specifically Jaguar (Chapter 4: Schrödinger Release 2014-2: Jaguar. 2014; Chapter 5 Schrödinger Release 2018-3) and Maestro (Chapter 4: Schrödinger Release 2014-2: Maestro 2014; Chapter 5: Schrödinger Release 2018-3: Maestro 2018).

Computational supplementary data (input, output, log, mae) files for the calculations presented in Chapter 4, 5 and 8 is accessible in the Cambridge Repository: https://doi.org/10.17863/CAM.34949

General Experimental Details:

All experiments were performed under anhydrous conditions under an argon atmosphere in oven-dried glassware, employing standard techniques for handling air and moist sensitive materials, unless otherwise stated.

Reagents: CH_2Cl_2, MeOH, toluene and hexane were distilled from calcium hydride under an argon atmosphere; tetrahydrofuran (THF) was distilled from benzophenone ketyl radical and sodium wire under an argon atmosphere. EtOH was dried over 3 Å freshly activated molecular sieves and *i*-PrOH over 4 Å freshly activated molecular sieves (M.S.). All solvents employed for recrystallisation and storage of the indium-BINOL complexes were dry. Acetophenone was distilled from potassium carbonate and used fresh. DIPEA was distilled from CaH_2 and used fresh. Solvents employed in workup and column chromatography were distilled prior to use. Aqueous (aq.) solutions of NH_4Cl, $NaHCO_3$ and brine (NaCl) were saturated (sat.). All chemicals were used as received unless otherwise noted. KHMDS, $NiCl_2(PPh_3)_2$, $Pd(PPh_3)_4$, $GaBr_3$ and InI_3 were handled in the glovebox.

NMR spectra: NMR spectra were recorded on a 400 MHz Avance III HD Smart Probe Spectrometer. ^{1}H NMR spectra were recorded on at 400 MHz. Chemical shifts are reported in parts per million (ppm) and the spectra are calibrated to the resonance resulting from incomplete deuteration of the $CDCl_3$: 7.26 ppm; MeOD-d_4: 3.31 ppm quintet, Acetone-d_6: 2.09 ppm, quitet). ^{13}C NMR spectra were recorded at 101 MHz with complete proton decoupling. Chemical shifts are reported in ppm with the solvent resonance as the internal standard ($^{13}CDCl_3$: 77.16 ppm, t; sept; MeOD-d_4: 49.00 ppm, septet, Acetone- d_6:29.84 septet, 1.32 ppm septet). ^{19}F NMR spectra were recorded at 376 MHz with proton decoupling. ^{31}P NMR spectra were recorded at 162 MHz with proton decoupling. Data are reported as follows: chemical shift δ/ppm, integration (^{1}H only), multiplicity (s = singlet, d = doublet, t = triplet, q = quartet, br. = broad, m = multiplet or combinations thereof; ^{13}C signals are singlets unless

otherwise stated), coupling constants *J* in Hz, assignment. ^{1}H COSY, HSQC and HMBC were used where appropriate to facilitate structural assignment.

High Resolution Mass Spectrometry (HRMS): Some were recorded on a Waters Xevo G2-S, ThermoFinnigan Orbitrap Classic or Waters Vion IMS Qtof all with a ESI probe. Measured values are reported to 4 decimal places are within ±5 ppm of the calculated value. The calculated values are based on the most abundant isotope.

Chromatography: Analytical thin layer chromatography was performed using precoated Merck glass backed silica gel plates (Silicagel 60 F254). Visualisation was by ultraviolet fluorescence (λ = 254 nm) and/or staining with potassium permanganate, phosphomolybdic acid / $Ce_2(SO_4)_3$, ninhydrin / H_2SO_4 or anisaldehyde dips. Flash column chromatography (FCC) was performed using Merck Kieselgel 60 (230-400 mesh) silica gel under a positive pressure of regulated compressed air.

Optical rotations: Measured in THF on a Anton Paar MCP100 polarimeter using a sodium lamp (λ 589 nm, D-line). α_D values are reported at a given temperature (°C) in degrees cm^2g^{-1} with concentration in $mg.mL^{-1}$.

Chiral HPLC analysis: Performed on an Agilent Infinity 1260 using a Phenomenex Lux Amylose 1 with a mixed solvent system of water in MeCN or on an Agilent 1100 using a Diacel OD with a mixed solvent of *n*-hexane and *i*-PrOH.

Chiral SCF analysis: Performed on a Waters Acquity UPC^2 using Chiral-Art columns (SA, SB, SJ).

X-ray crystallography*:* Recorded on Bruker D8- QUEST PHOTON-100 diffractometer using CuKa radiation (lambda = 1.5418 Å) at the Cambridge University Chemistry X-Ray Laboratory. Data was collected at 180 K, with the crystal cooled in a stream of N_2 gas.

Melting points: Recorded on a Electrothermal 1A 9100 Digital Melting Point Apparatus.

Infrared spectra: Recorded on a Perkin-Elmer Spectrum One (FTIR) spectrometer. Absorbance frequencies (ν_{max}) for selected peaks are reported in wavenumbers (cm^{-1}) (s = strong, m = medium, w = weak, vw = very weak br. = broad).

BINOL Ligands:

General procedure A: MOM deprotection

A solution of MOM-PG diol (1 equiv) in 1,4-dioxane (0.11 M) and HCl (conc. 37%, 2 equiv) was stirred at 80 °C for 3 hours, allowed to cool to ambient temperature and quenched with $NaHCO_3$ (aq., sat.), resulting in gas evolution (H_2). The diol product was extracted with Et_2O, dried over Na_2SO_4 and concentrated *in vacuo*.

(*R*)-2,2'-Bis(methoxymethyl)-1-1'-bi-2-naphthol [**2.2 (*R*)**][114]

MOMCl was prepared fresh following a reported procedure:[115] Acetyl chloride (6.25 mL, 87.9 mmol, 2.5 equiv) was added dropwise to a stirred solution of dimethoxymethane (7.78 mL, 87.9 mmol, 2.5 equiv) and $ZnBr_2$ (2.5 mg, 11.4 µmol) in toluene (1.2 M) . The flask was fitted with a reflux condenser and the reaction mixture was stirred at room temperature for 3 hours, during which time the reaction mixture slowly self-heated to approximately 40 °C, then allowed to cool to ambient temperature.

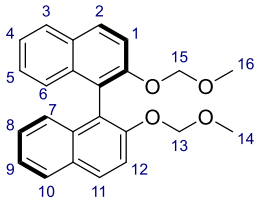

A solution of (*R*)-BINOL **2.1 (*R*)** (10.0 g, 34.9 mmol, 1 equiv) in THF (0.70 M) was added dropwise to a stirred suspension of NaH (4.19 g, 60% in mineral oil, 105 mmol, 3 equiv) in THF (0.70 M) at 0 °C. Gas evolution was observed. The resulting light yellow solution was stirred at 0 °C for 1 hour and allowed to warm to ambient temperature. The yellow reaction mixture was re-cooled to 0 °C and the freshly prepared MOMCl was added dropwise. Formation of white precipitate was observed. The resulting white suspension was stirred at ambient temperature for 16 hours. The reaction was cooled to 0 °C, then quenched with NH_4Cl (aq., sat.). The THF layer was separated and concentrated. The residue taken up in CH_2Cl_2, washed twice with water and then with brine. The organic layer was dried over Na_2SO_4, concentrated *in vacuo*. The product was precipitated with MeOH, collected by filtration and dried to yield a white amorphous solid in 98% yield (12.8 g, 34. 2 mmol). **^{1}H NMR** (400 MHz, $CDCl_3$) δ (ppm): δ 8.00 (d, J = 9.0 Hz, 2H, $H_{1,12}$), 7.92 (d, J = 8.2 Hz, 2H, $H_{3,10}$), 7.64 (d, J = 9.0 Hz, 2H, $H_{2,11}$), 7.42 – 7.38 (m, 2H, $H_{4,9}$), 7.31 – 7.18 (m, 4H, $H_{5,6,7,8}$), 5.14 (d, J = 6.8 Hz, 2H, $H_{13/15}$), 5.03 (d, J = 6.8 Hz, 2H, $H_{13/15}$), 3.20 (s, 6H, $H_{14,16}$). Spectroscopic data is in agreement with the literature.[114] **2.2 (*S*)** was prepared following the same procedure using **2.1 (*S*)** (3.71 g, 13.0 mmol) yielding **2.2 (*S*)** as a white amorphous solid in 92% yield (4.46 g, 11.9 mmol). Spectroscopic data equal to that of **2.2 (*R*)**.

(*R*)-3-Iodo-2,2'-bis(methoxymethyl)-1-1'-bi-2-naphthol [**2.8 (*R*)**][112]

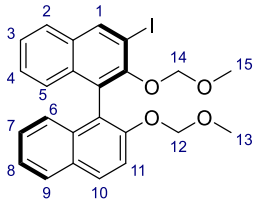

n-BuLi (7.68 mL, 1.6 M in hexane, 12.3 mmol, 1.15 equiv) was added dropwise to a stirred solution of **2.2 (*R*)** (4.00 g, 10.97 mmol, 1 equiv) at -78 °C. The pale yellow solution was stirred at -78 °C for 6 hours. Iodine (4.07 g, 16.0 mmol, 1.5 equiv) was added in one portion. The resulting solution was stirred at -78 °C for one hour then allowed to warm to ambient temperature and stirred for additional 13 hours. A change in colour from pale yellow to dark red was observed. The reaction mixture was cooled to 0 °C and quenched with $Na_2S_2O_3$ (aq., sat.). A pale yellow solid was precipitated from the yellow solution, collected by filtration and purified by FCC (1:1:23 CH_2Cl_2:EA:PE) to afford the product as a white amorphous solid in 74% yield (3.97g, 7.94 mmol). **^{1}H NMR** (400 MHz, $CDCl_3$) δ (ppm): δ 8.53 (s, 1H, H_1), 7.98 (d, *J* = 9.1 Hz, 1H, H_{11}), 7.87 (d, *J* = 8.1 Hz, 1H, $H_{2/9}$), 7.79 (d, *J* = 8.2 Hz, 1H, $H_{2/9}$), 7.59 (d, *J* = 9.1 Hz, 1H, H_{10}), 7.46 – 7.33 (m, 2H, $H_{3,8}$), 7.33 – 7.22 (m, 2H, $H_{4,7}$), 7.22 – 7.12 (m, 2H, $H_{5,6}$), 5.15 (d, *J* = 6.9 Hz, 1H, H_{12}), 5.05 (d, *J* = 6.9 Hz, 1H, H_{12}), 4.75 (d, *J* = 5.3 Hz, 1H, H_{14}), 4.71 (d, *J* = 5.3 Hz, 1H, H_{14}), 3.20 (s, 3H, H_{13}), 2.73 (s, 3H, H_{15}). Spectroscopic data is in accordance with the literature.[112]

(*R*)-3-Phenyl-2,2'-bis(methoxymethyl)-1-1'-bi-2-naphthol [**2.9 (*R*)**]

Suzuki cross coupling was carried out according to a reported procedure.[199]

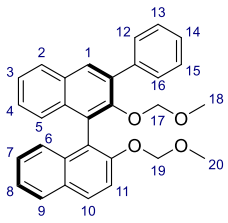

A suspension of $PhB(OH)_2$ (0.233 g, 1.91 mmol, 1.25 equiv), $Ba(OH)_2 \cdot 8\,H_2O$ (1.21 g, 3.82 mmol, 2.5 equiv), $Pd(PPh_3)_4$ (88.3 mg, 76.5 µmol, 0.05 equiv) and **2.8 (*R*)** (0.765 g, 1.53 mmol, 1 equiv) in a degassed solvent system of 16:5 1,4-dioxane: water (0.19 M) was stirred at 80 °C for 19 hours. The black suspension was concentrated, the organic residues taken into CH_2Cl_2, washed with HCl (1 N) and brine, then dried over Na_2SO_4 and concentrated *in vacuo*. The crude product was purified by FCC (1:1:8 CH_2Cl_2:EA:*n*-hexane) to afford the product as a white amorphous solid in 36% yield (249 mg, 0.553 mmol) over two steps. **^{1}H NMR** (400 MHz, $CDCl_3$) δ (ppm): 7.96 (t, *J* = 4.5 Hz, 2H, Ar), 7.89 (dd, *J* = 15.5, 8.1 Hz, 2H, Ar), 7.77 – 7.67 (m, 2H, Ar), 7.60 (d, *J* = 9.1 Hz, 1H, Ar), 7.54 – 7.32 (m, 5H, Ar), 7.32 – 7.19 (m, 4H, Ar), 5.18 (d, *J* = 6.9 Hz, 1H, H_{17}), 5.08 (d, *J* = 6.9 Hz, 1H, H_{17}), 4.35 (d, *J* = 5.8 Hz, 1H, H_{19}), 4.29 (d, *J* = 5.8 Hz, 1H, H_{19}), 3.23 (s, 3H, H_{20}), 2.29 (s, 3H, H_{18}). **^{13}C NMR** (101 MHz, $CDCl_3$) δ (ppm): 153.0, 151.2, 139.2, 135.7, 134.2, 133.5, 131.1, 130.4, 129.9, 129.8, 129.8, 128.4, 128.1, 127.9, 127.3, 126.7, 126.4, 126.3, 126.0, 126.0, 125.3, 124.2, 121.4, 116.9, 98.8, 95.3, 56.1. **FTIR**: (neat)

v_{max} (cm^{-1}): 2955 (w), 2937 (w), 2899 (w), 2824 (w), 1616 (w), 1594 (m), 1509 (m). **HRMS-ESI$^+$** calc. for $[C_{30}H_{26}O_4Na]^+$ expect 473.1723, found 473.1729.

(*R*)-3-(2,4,6-triisopropylphenyl)-2,2'-bis(methoxymethyl)-1-1'-bi-2-naphthol [**2.4 (*R*)**]

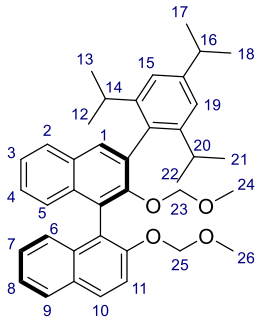

Grignard formation: To a solution of 2-bromo-1,3,5-triisopropylbenzene (4.86 g, 17.2 mmol, 2.2 equiv) in Et_2O (0.59 M) was added magnesium turnings (0.616 g, 25.3 mmol, 3.25 equiv), 1,2-dibromoethane (0.101 mL, 1.17 mmol, 0.15 equiv) and iodine (9.89 mg, 39.0 µmol, 0.005 equiv). The resulting suspension was stirred at 60 °C for 20 hours.

Kumada cross coupling: The Grignard solution was added dropwise to a stirred suspension of $NiCl_2(PPh_3)_2$ (255 mg, 0.390 mmol, 0.05 equiv) and bisiodide **3.7 (*R*)** (3.90 g, 1.79 mmol, 1 equiv) in degassed Et_2O (0.16 M). The resulting suspension was stirred at 55 °C for 20 hours, then quenched with NH_4Cl (aq., sat.) at 0 °C. The organic residues were extracted with Et_2O, washed with brine, dried over Na_2SO_4 and concentrated *in vacuo*. The crude product was purified by FCC (5:5:240 EA:CH_2Cl_2:PE) to afford the product as a white amorphous solid in 88% yield (3.95 g, 6.85 mmol). **^{1}H NMR** (400 MHz, $CDCl_3$) δ 8.02 (d, *J* = 9.1 Hz, 1H, Ar), 7.93 (dd, *J* = 17.0, 8.7 Hz, 3H, Ar), 7.70 (d, *J* = 9.1 Hz, 1H, Ar), 7.50 – 7.32 (m, 6H, Ar), 7.19 (s, 2H, $H_{15,19}$), 5.23 (d, *J* = 6.9 Hz, 1H, H_{25}), 5.16 (d, *J* = 6.9 Hz, 1H, H_{25}), 4.38 (d, *J* = 5.2 Hz, 1H, H_{23}), 4.30 (d, *J* = 5.2 Hz, 1H, H_{23}), 3.33 (s, 3H, H_{26}), 3.09 – 2.82 (m, 3H, $H_{14,16,20}$), 2.33 (s, 3H, H_{26}), 1.38 (d, *J* = 6.9 Hz, 3H, $H_{21/22}$), 1.36 – 1.26 (m, 12H, $H_{12,13,17,18}$), 1.23 (d, *J* = 6.8 Hz, 3H, $H_{21/22}$).

(*R*)-3-(2,4,6'triisopropylphenyl)-[1,1'-binaphthalene]-2,2'-diol [**2.17 (*R*)**][200]

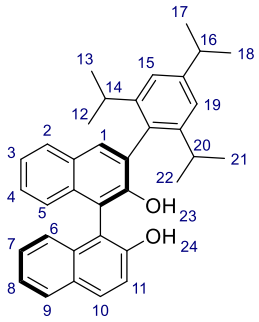

2.4 (*R*) (0.250 g, 0.433 g) was MOM-deprotected following *general procedure A* and purified by FCC (1:1:8 EA:CH_2Cl_2:PE) to afford the diol as an amorphous white solid in quantitative yield (0.211 g, 0.432 mmol). **^{1}H NMR** (400 MHz, Acetone) δ (ppm): 8.04 (s, 1H, $H_{23/34}$), 7.91 (dd, *J* = 13.0, 7.6 Hz, 3H, Ar), 7.72 (s, 1H, $H_{23/24}$), 7.42 – 7.04 (m, 10H, Ar), 3.11 – 2.79 (m, 3H, $H_{14,16,20}$), 1.31 (d, *J* = 6.9 Hz, 6H, $H_{21,22}$), 1.22 – 1.08 (m, 12H, $H_{12,13,17,18}$). **^{13}C NMR** (101 MHz, Acetone) δ 154.9, 153.2, 148.8, 148.2, 148.0, 135.5, 134.9, 134.0, 131.2, 131.1, 130.8, 130.1, 129.9, 129.0, 128.9, 127.2, 126.7, 125.3, 125.2, 123.8, 123.8, 121.3, 121.2, 119.5, 115.0, 114.5, 35.1, 31.6, 31.3, 25.0, 24.6, 24.5, 24.4, 24.3. Spectroscopic data reported in $CDCl_3$ in the literature[200] are in reasonable correspondence. Spectra were recorded in acetone due to the significantly higher solubility and improved resolution.

(*R*)-3-(2,4,6-triisopropylphenyl)-3'-iodo-2,2'-bis(methoxymethyl)- 1-1'-bi-naphthalene [**2.5 (*R*)**]

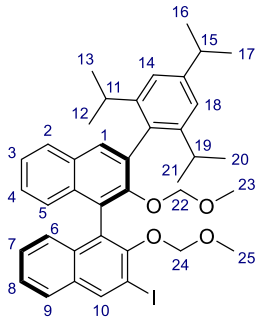

n-Buli (5.24 mL, 1.6 M in hexane, 8.38 mmol, 1.3 equiv) was added dropwise to a stirred solution of **2.2 (*R*)** (3.72 g, 6.45 mmol, 1 equiv) in THF (0.09 M) at 0 °C. The resulting yellow solution was allowed to warm to ambient temperature and stirred for one additional hour. The red-brown reaction mixture was cooled to -78 °C and iodine (2.86 g, 11.3 mmol, 1.75 eq.) was added in one portion. After 20 min the reaction mixture was allowed to warm to ambient temperature and stirred for further 1 hour. Unreacted iodine was quenched with $Na_2S_2O_3$ (aq., sat.). The THF layer was separated and concentrated. The residue was taken into EA and extracted with EA. The combined organic layers were washed with water, then brine, dried over $MgSO_4$ and concentrated *in vacuo*. The crude product was purified by FCC (5:5:240 CH_2Cl_2:EA:PE) to afford the product as a white amorphous solid in 90 % yield (4.09 g, 5.82 mmol). **^{1}H NMR** (400 MHz, $CDCl_3$) δ (ppm) 8.51 (s, 1H, H_{10}), 7.84 (d, *J* = 8.1 Hz, 1H, $H_{2/9}$), 7.80 (s, 1H, H_1), 7.76 (d, *J* = 8.2 Hz, 1H, $H_{2/9}$), 7.41 (dt, *J* = 9.8, 4.3 Hz, 2H, Ar), 7.35 – 7.19 (m, 4H, Ar), 7.08 (d, *J* = 3.2 Hz, 2H, $H_{5,6}$), 4.80 (d, *J* = 5.4 Hz, 1H, $H_{22/24}$), 4.77 (d, *J* = 5.4 Hz, 1H, $H_{22/24}$), 4.29 (d, *J* = 5.3 Hz, 1H, $H_{22/24}$), 4.23 (d, *J* = 5.3 Hz, 1H, $H_{22/24}$), 3.02 – 2.68 (m, 2H, $H_{11,15}$), 2.84 (s, 3H, $H_{23/25}$), 2.87 – 2.81 (m, 1H, H_{19}), 2.25 (s, 3H, $H_{23/25}$), 1.29 (d, *J* = 6.9 Hz, 6H, $H_{20,21}$), 1.25 – 1.06 (m, 12H, $H_{12,13,16,17}$).

(*R*)-3-iodo-3'-(2,4,6'triisopropylphenyl)-[1,1'-binaphthalene]-2,2'-diol [**2.18 (*R*)**]

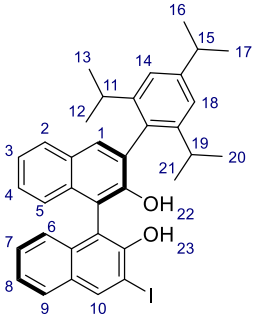

2.5 (*R*) (0.200 g, 0.285 g) was MOM-deprotected following *general procedure A* and purified by FCC (1:1:8 EA:CH_2Cl_2:PE) to afford the diol as an amorphous white solid in 94% yield (0.164 g, 0.267 mmol).

^{1}H NMR (400 MHz, Acetone) δ 8.58 (s, 1H, H_{10}), 8.27 (s, br. 1H, $H_{22/23}$), 7.92 (d, *J* = 8.0 Hz, 1H, $H_{2/9}$), 7.87 (d, *J* = 7.5 Hz, 1H, $H_{2/9}$), 7.76 (s, 1H, H_1), 7.54 (s, br. 1H, $H_{22/23}$), 7.39 – 7.02 (m, 8H, Ar), 3.16 (dt, *J* = 13.6, 6.8 Hz, 1H, $H_{11/15}$), 2.99 (dt, *J* = 13.8, 6.9 Hz, 1H, $H_{11/15}$), 2.91 – 2.71 (m, 1H, H_{19}), 1.33 (d, *J* = 6.9 Hz, 6H, $H_{21,20}$), 1.27 – 1.08 (m, 12H, $H_{12,13,16,17}$). **^{13}C NMR** (101 MHz, Acetone) δ 153.8, 152.9, 148.9, 148.3, 148.1, 140.4, 135.1, 134.7, 133.6, 131.9, 131.5, 131.5, 123.0, 129.0, 127.9, 127.7, 127.1, 125.3, 124.8, 124.6, 124.1, 121.4, 121.2, 114.9, 113.6, 88.6, 67.5, 25.2, 24.6, 24.6, 24.5, 24.3. **FTIR** (neat) ν_{max} (cm^{-1}): 3519 (w), 2958 (s), 2920 (m), 2869 (m), 1615 (w), 1601 (w), 1570 (m). **HRMS-ESI$^+$** calc. for $[C_{35}H_{36}IO_2]^+$ expect 615.1754, found 615.1754. $[\boldsymbol{\alpha}]_{\boldsymbol{D}}^{\mathbf{25.0}}$= +128.4 (c=1.00, THF).

(*R*)-3-phenyl-3'-(2,4,6-triisopropylphenyl)-[1-1'-bi-naphthalene]-2,2'-diol [**2.11 (*R*)**]

Suzuki cross coupling was carried out according to a reported procedure.[199]

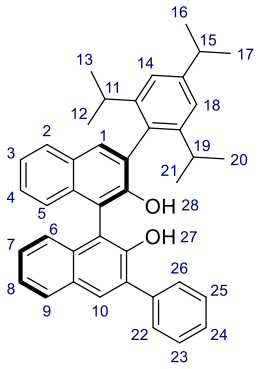

A suspension of $PhB(OH)_2$ (26.3 mg, 0.431 mmol, 1.25 equiv), $Ba(OH)_2 \cdot 8\ H_2O$ (0.136 g, 0.431 mmol, 2.5 equiv), $Pd(PPh_3)_4$ (19.9 mg, 17.2 µmol, 0.1 equiv) and **2.5 (R)** (0.121 g, 0.172 mmol, 1 equiv) in a degassed solvent system of 16:5 1,4-dioxane: water (0.19 M) was stirred at 80 °C for 23 hours. The black suspension was concentrated, the organic residues taken into CH_2Cl_2, washed with HCl (1 N) and brine, then dried over Na_2SO_4 and concentrated *in vacuo*. The crude product (128 mg) was submitted for MOM-deprotection following *general procedure A*. The crude diol was purified by FCC (1:1 CH_2Cl_2:PE) to afford the product as a white amorphous solid in 82% yield (80.2 mg, 0.142 mmol) over two steps. **^{1}H NMR** (400 MHz, $CDCl_3$) δ 7.98 (s, 1H, $H_{1/10}$), 7.89 (t, *J* = 7.4 Hz, 2H, Ar), 7.81 (s, 1H, $H_{1/10}$), 7.78 – 7.71 (m, 2H, Ar), 7.55 – 7.27 (m, 8H, Ar), 7.19 (d, *J* = 8.3 Hz, 1H, Ar), 7.14 (s, 2H, $H_{14,18}$), 5.29 (s, 1H, $H_{27/28}$), 4.99 (s, 1H, $H_{27/28}$), 2.96 (dt, *J* = 13.9, 6.8 Hz, 1H, H_{19}), 2.78 – 2.71 (m, 2H, $H_{11,17}$), 1.31 (d, *J* = 6.9 Hz, 6H, $H_{20,21}$), 1.22 – 1.09 (m, 12H, $H_{12,13,16,17}$). **^{13}C NMR** (101 MHz, $CDCl_3$) δ (ppm): 151.3, 149.7, 149.5, 148.0, 147.9, 138.0, 133.5, 133.1, 131.5, 131.0, 130.7, 130.1, 129.8, 129.5, 129.4, 129.3, 128.5, 128.5, 127.7, 127.3, 127.0, 124.6, 124.4, 124.2, 124.1, 121.4, 121.4, 113.9, 112.0, 34.5, 31.1, 31.0, 24.6, 24.6, 24.2, 24.1, 24.1. **FTIR**: (neat) ν_{max} (cm^{-1}): 3518 (w), 2958 (m), 2919 (m), 2850 (w), 1621 (w), 1602 (w). **HRMS-ESI$^+$** calc. for $[C_{41}H_{40}O_2Na]^+$ expect 587.2921, found 587.2922. $[\boldsymbol{\alpha}]_{\boldsymbol{D}}^{\mathbf{25.0}}$ = +119.3 (c=1.00, THF).

(*R*)-3-(2,4,6-triisopropylphenyl)-3'-phenyl-1-1'-bi-2-naphthyl-2,2'-diyl hydrogenphosphate [**2.7 (*R*)**]

Prepared according to a reported procedure.[201]

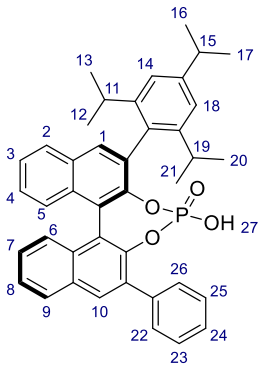

$POCl_3$ (39.7 µL, 0.425 mmol, 3 equiv) was added to a solution of **2.11 (*R*)** (80.0 mg, 0.142 mmol, 1 equiv) in pyridine (0.14 M). The reaction mixture was stirred under reflux for 17 hours, then allowed to cool to ambient temperature. Water (1 mL) was added and the reaction stirred under reflux for additional 3 hours. After allowing the resulting mixture to cool to ambient temperature, the organic residue was taken up in CH_2Cl_2 and thoroughly washed with HCl (1 N) until the aqueous layer remained acidic (pH=1). The combined organic layers were washed with brine, dried over Na_2SO_4 and concentrated. The crude product was purified by FCC (10% MeOH in CH_2Cl_2) to afford the product as a white amorphous solid in 79% yield (70.0 mg, 0.112 mmol).**^{1}H NMR** (400 MHz, $CDCl_3$) δ (ppm): 9.18 (s, 1H, H_{27}), 7.99 (s, 1H, $H_{1/10}$), 7.90 (t, *J* = 7.9 Hz, 2H, Ar), 7.85 (s, 1H, $H_{1/10}$), 7.54 – 7.35 (m, 5H, Ar), 7.34 – 7.19 (m, 3H, Ar), 7.14 (s, 2H, $H_{14,18}$), 6.99 – 6.79 (m, 3H, Ar), 2.92 (dt, *J* = 13.4, 6.6 Hz, 1H, $H_{11/15}$), 2.75 (dt, *J* = 12.9, 6.2 Hz, 1H, H_{19}), 2.57 (dt, *J* = 13.4, 6.6 Hz, 1H, $H_{11/15}$), 1.35 – 1.21 (m, 6H, $H_{12,13/16,17}$), 1.18 (t, *J* = 6.0 Hz, 6H, $H_{12,13/16,17}$), 1.11 (d, *J* = 5.7 Hz, 3H, $H_{20/21}$), 1.01 (d, *J* = 6.6 Hz, 3H, $H_{20/21}$). **^{13}C NMR** (101 MHz, $CDCl_3$) δ (ppm): 148.9, 148.2, 147.4, 146.2 (d, $^2J_{C\text{-}P}$ = 8.9 Hz), 144.6 (d, $^2J_{C\text{-}P}$ = 9.6 Hz), 136.2, 134.2, 134.2, 132.8, 132.6 (d, $^3J_{C\text{-}P}$ = 3.6 Hz), 132.4, 132.3, 132.1, 131.7, 131.2, 131.0, 129.6, 128.7, 128.4, 128.3, 128.0, 127.6, 126.9, 126.6, 126.5, 126.0 (d, $^3J_{C\text{-}P}$ = 3.1 Hz), 122.7, 122.7, 122.1, 122.1, 121.4, 120.6, 34.5, 31.4, 31.2, 26.6, 24.9, 24.3, 23.9, 23.1. **^{31}P NMR** (162 MHz, $CDCl_3$) δ (ppm): 3.68. **FTIR**: (neat) ν_{max} (cm^{-1}): 3059 (w), 2959 (m), 2928 (w), 2869 (w), 1604 (w), 1565 (w). **HRMS-ESI$^+$** calc. for $[C_{41}H_{40}O_4P]^+$ expect 627.2659, found 627.2643. $[\boldsymbol{\alpha}]_{\boldsymbol{D}}^{\mathbf{25.0}}$= -145.8 (c=0.62, THF).

(*E*)-*N,N'*-(1,3-diphenylbut-1-ene-1,3-diyl)diacetamide [**2.13**][202]

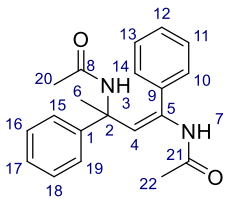

2.7 (*R*) (19.4 mg, 31.1 µmol, 0.1 equiv) and enamide **2.12** (50.0 mg, 0.310 mmol, 1 equiv) in toluene (0.1 M) was stirred at room temperature for 3 days. The reaction mixture was quenched with $NaHCO_3$ (aq., sat.), extracted with CH_2Cl_2, dried over $MgSO_4$ and concentrated *in vacuo*. The crude product was purified by FCC (1:1 EA:PE) to afford the product as a white amorphous solid in 58 % yield (28.8 mg, 89.3 µmol). ^{1}H NMR (400 MHz, MeOD-d_4) δ (ppm): 7.45 – 7.08 (m, 10H, Ar), 5.59 (s, 1H, H_4), 2.10 (s, 3H, $H_{20/22}$), 1.66 (s, 3H, $H_{20/22}$), 1.33 (s, 3H, H_6). **^{13}C NMR** (101 MHz, MeOD-d_4) δ (ppm): 173.5, 171.4, 144.0, 139.3,

138.9, 129.4, 129.1, 129.1, 127.6, 127.3, 126.7, 125.0, 59.6, 35.0, 23.0, 22.5. Spectroscopic data was recorded in MeOD-d_4 due to the significantly improved solubility. With the exception of the exchangeable protons which do not appear in MeOD-d_4 the ^{1}H NMR is in correspondence with the literature. ^{13}C NMR was not reported.[202] **HPLC Analysis**: Diacel OD (*n*-hexane:*i*-PrOH = 90:10, 1 mL min^{-1}, 25 °C) t_R = 16.40 (major), 23.04 (minor) minutes. The e.e. was determined to 9%.

(*R*)-3,3'-Bisiodo-2,2'-bis(methoxymethyl)-1-1'-bi-naphthalene [**3.7 (*R*)**][114]

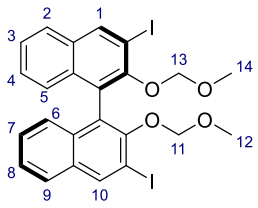

n-Buli (25.0 mL, 1.6 M in hexane, 40.1 mmol, 3 equiv) was added dropwise to a stirred solution of **2.2 (*R*)** (5.00 g, 13.4 mmol, 1 equiv) in THF (0.13 M) at 0 °C. The resulting yellow solution was allowed to warm to ambient temperature and stirred for additional 1 hour. The redbrown reaction mixture was cooled to -78 °C and iodine (11.9 g, 46.7 mmol, 3.5 eq.) was added in one portion. After 20 min the reaction mixture was allowed to warm to ambient temperature and stirred for further 1 hour. Unreacted iodine was quenched with $Na_2S_2O_3$ (aq., sat.). The THF layer was separated and concentrated. The residue was taken into EA and extracted with EA. The combined organic layers were washed with water, then brine, dried over $MgSO_4$ and concentrated *in vacuo*. The crude product was purified by FCC (3:1 CH_2Cl_2:PE) to afford the product as a white amorphous solid in 69% yield (5.78 g, 9.23 mmol). **^{1}H NMR** (400 MHz, $CDCl_3$) δ (ppm): 8.54 (s, 2H, $H_{1,10}$), 7.78 (d, *J* = 8.2 Hz, 2H, $H_{2,9}$), 7.45 – 7.41 (m, 2H, $H_{3,8}$), 7.32 – 7.27 (m, 2H, $H_{4,7}$), 7.17 (d, *J* = 7.9 Hz, 2H, $H_{5,6}$), 4.81 (d, *J* = 5.7 Hz, 2H, $H_{11/13}$), 4.69 (d, *J* = 5.7 Hz, 2H, $H_{11/13}$), 2.60 (s, 6H, $H_{12,14}$). Spectroscopic data is in accordance with the literature.[114] **2.8 (*S*)** was prepared following the same procedure using **2.2 (*S*)** (2.00 g, 5.34 mmol) yielding **2.8 (*S*)** as a white amorphous solid in 75% yield (2.52 g, 4.02 mmol). Spectroscopic data of **2.8 (*S*)** was equal to that of **2.8 (*R*)**.

(*R*)-3,3'-Diiodo-[1,1'-binaphthalene]-2,2'-diol [**3.8 (*R*)**][114]

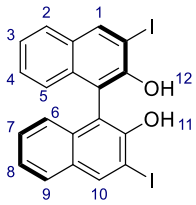

3.7 (*R*) (1.85 g, 2.95mmol) was MOM-deprotected following *general procedure A* and purified from the 1,4-dioxane mixture by titration with Et_2O to afford the diol as an amorphous white solid in 98 % yield (1.56 g, 2.90 mmol). **^{1}H NMR** (400 MHz, $CDCl_3$) δ (ppm): 8.52 (s, 2H, $H_{1,10}$), 7.79 (d, *J* = 8.0 Hz, 2H, $H_{2,9}$), 7.45 – 7.28 (m, 4H, $H_{3,4,7,8}$), 7.07 (d, *J* = 8.4 Hz, 2H, $H_{5,6}$), 5.33 (s, br. 1H, $H_{11,12}$). **^{13}C NMR** (101 MHz, $CDCl_3$) δ (ppm): 150.3, 140.5, 133.4, 130.8, 128.1, 127.4, 124.9, 124.6, 112.8. Spectroscopic data is in accordance with the literature.[114] **2.2 (*S*)** (1.00 g, 1.60 mmol) yielding **2.7 (*S*)** was MOM-deprotected following *general*

procedure A and purified by FCC (20% Et_2O in Pe) to afford the product **2.8 (*S*)** as a white amorphous solid in 99% yield (0.850 g, 1.58 mmol). Spectroscopic data identical to **2.8 (*R*)**.

(*R*)-3,3'-bis(2,4,6-triisopropylphenyl)-[1,1'-binaphthalene]-2,2'-diol [**3.10 (*R*)**][203]

Grignard formation: To a solution of 2-bromo-1,3,5-triisopropylbenzene (1.25 g, 4.43 mmol, 4.40 equiv) in Et_2O (0.59 M) was added magnesium turnings (0.159 g, 6.54 mmol, 6.50 equiv), 1,2-dibromoethane (26.1 µL, 0.302 mmol, 0.30 equiv) and iodine (1.53 mg, 6.04 µmol, 0.01 equiv). The resulting suspension was stirred at 60 °C for 20 hours.

Kumada cross coupling: The Grignard solution was added dropwise to a stirred suspension of

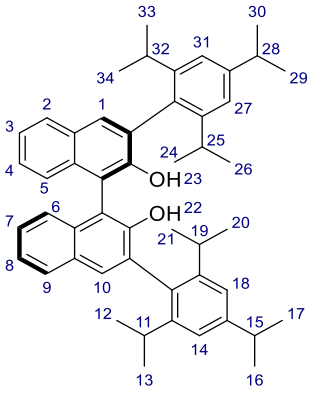

$NiCl_2(PPh_3)_2$ (65.8 mg, 0.101 mmol, 0.1 equiv) and bisiodide **3.7 (*R*)** (0.630 g, 1.01 mmol, 1 equiv) in degassed Et_2O (0.16 M). The resulting suspension was stirred at 55 °C for 20 hours, then quenched with NH_4Cl (aq., sat.) at 0 °C. The organic residues were extracted with Et_2O, washed with brine, dried over Na_2SO_4 and concentrated *in vacuo*. The crude product (784 mg) was submitted for MOM-deprotection following *general procedure A*. After the crude product was concentrated the residual 1,4-dioxane was removed by triturating the product with Et_2O to afford a white amorphous solid afford in 89% yield (0.617 g, 0.893 mmol) over two steps.

^{1}H NMR (400 MHz, $CDCl_3$) δ (ppm): 7.88 (d, *J* = 8.0 Hz, 2H, Ar), 7.78 (s, 2H, Ar), 7.43 – 7.28 (m, 6H, Ar), 7.15 (dd, *J* = 7.7, 1.4 Hz, 4H, Ar), 4.93 (s, 2H, $H_{22,23}$), 2.97 (dq, *J* = 13.8, 6.9 Hz, 2H, $H_{11,15/19,25/28,32}$), 2.92 – 2.77 (m, 2H, $H_{11,15/19,25/28,32}$), 2.77 – 2.62 (m, 2H, $H_{11,15/19,25/28,32}$), 1.33 (d, *J* = 6.9 Hz, 12H, $H_{12,13,16,17/29,30,33,34}$), 1.22 (d, *J* = 6.8 Hz, 6H, $H_{24,26/20,21}$), 1.12 (dd, *J* = 9.4, 6.9 Hz, 12H, $H_{12,13,16,17/29,30,33,34}$), 1.05 (d, *J* = 6.9 Hz, 6H, $H_{24,26/20,21}$). **^{13}C NMR** (101 MHz, $CDCl_3$) δ 150.6, 149.1, 147.8, 147.7, 133.4, 130.6, 130.3, 129.1, 129.0, 128.2, 126.6, 124.5, 123.7, 121.2, 121.2, 113.1, 34.3, 30.9, 30.8, 24.3, 24.3, 24.1, 24.0, 23.9, 23.7). Spectroscopic data is in agreement with the literature.[203]

(*R*)-3,3'-Diphenyl-[1,1'-binaphthalene]-2,2'-diol [**3.12 (*R*)**][199]

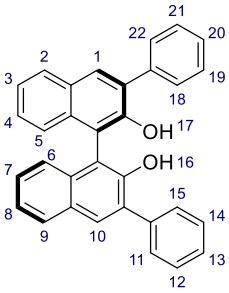

A suspension of $PhB(OH)_2$ (0.122 g, 0.998 mmol, 2.5 equiv), $Ba(OH)_2 \cdot 8\ H_2O$ (0.630 g, 2.00 mmol, 5 equiv), $Pd(PPh_3)_4$ (46.1 mg, 39.9 µmol, 0.1 equiv) and **3.7 (*R*)** (0.250 g, 0.399 mmol, 1 equiv) in a degassed solvent system of 16:5 1,4-dioxane: water (0.19 M) was stirred at 80 °C for 18 hours. The black suspension was concentrated, the organic residues taken into CH_2Cl_2, washed with HCl (1 N) and brine, then dried over Na_2SO_4 and concentrated *in vacuo*. The crude product (290 mg) was submitted for MOM-deprotection following *general procedure A.* The crude diol was purified by FCC (1:1 CH_2Cl_2:PE) to afford the product as a white amorphous solid in 90% yield (0.190 g, 0.361 mmol) over two steps. **^{1}H NMR** (400 MHz, $CDCl_3$) δ (ppm): 8.02 (s, 2H, $H_{1,10}$), 7.92 (d, *J* = 8.0 Hz, 2H), 7.73 (dt, *J* = 8.2, 1.7 Hz, 4H), 7.71 – 7.63 (m, 2H), 7.63 – 7.29 (m, 8H), 7.23 (d, *J* = 8.4 Hz, 2H), 5.38 (s, 2H, $H_{16,17}$). **^{13}C NMR** (101 MHz, $CDCl_3$) δ (ppm): 150.3, 137.6, 133.1, 131.5, 130.8, 129.8, 129.6, 128.6, 128.6, 127.9, 127.5, 124.5, 124.4, 112.6. Spectroscopic data is in accordance with the literature.[199]

(*R*)-3,3'-Dibromo-[1,1'-binaphthalene]-2,2'-diol [**3.13 (*R*)**][114,128]

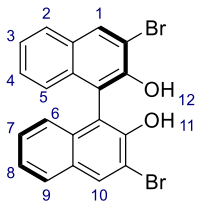

n-Buli (1.04 mL, 1.67 mmol, 1.60 M in hexane, 2.5 equiv) was added dropwise to a stirred solution of (*R*)-MOM-BINOL **2.2 (*R*)** (250 mg, 0.668 mmol, 1 equiv) in THF (0.13 M) at 0 °C. A change in colour from colourless to yellow was observed. The reaction mixture was allowed to warm to ambient temperature. After being stirred for additional 2 hours the reaction mixture was cooled to -78 °C, then a solution of bromine (103 µL, 2.00 mmol, 3 equiv) in pentane (2.5 M) was added dropwise. The resulting yellow reaction mixture was allowed to warm to ambient temperature for further 20 hours. The reaction mixture was then poured into Na_2SO_3 (aq., sat.), extracted with EA, the combined organic layers washed with brine, dried over Na_2SO_4 and concentrated *in vacuo*. The crude product was purified by FCC (3:1 CH_2Cl_2:PE) to afford the product as an off-white in 91% yield (271 mg, 0.610 mmol). **^{1}H NMR** (400 MHz, Acetone) δ (ppm): 8.41 (s, 2H, $H_{11,12}$), 8.33 (s, 2H, $H_{1,10}$), 7.91 (d, *J* = 8.1 Hz, 2H, $H_{2,9}$), 7.44 – 7.33 (m, 2H, $H_{3,8}$), 7.33 – 7.23 (m, 2H, $H_{4,7}$), 7.00 (d, *J* = 8.4 Hz, 2H, $H_{5,6}$). **^{13}C NMR** (101 MHz, Acetone) δ (ppm): 151.3, 134.3, 133.8, 130.6, 128.2, 127.9, 125.2, 125.0, 115.9, 114.1. Spectroscopic data reported in $CDCl_3$ in the literature[114] are in reasonable correspondence. Spectra were recorded in acetone due to the significantly higher solubility and improved resolution.

(*R*)-3,3'-Dichloro-[1,1'-binaphthalene]-2,2'-diol [**3.15 (*R*)**][129,204]

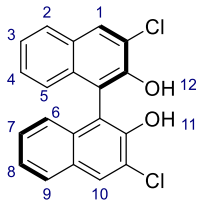

n-Buli (1.00 mL, 1.60 mmol, 1.60 M in hexane, 3 equiv) was added dropwise to a stirred solution of (*R*)-MOM-BINOL **2.2 (*R*)** (200 mg, 0.534 mmol, 1 equiv) in Et_2O (0.07M) at 0 °C. A change in colour from colourless to yellow was observed. The reaction mixture was allowed to warm up to ambient temperature. After being stirred for additional 3 hours the reaction mixture was cooled to 0 °C, then a solution of hexachloroethane (380 mg, 1.60 mmol, 3 equiv) in THF (0.27 M) was added dropwise. A change of colour to black and then yellow was observed. The reaction mixture was allowed to warm to ambient temperature for further 16 hours. The reaction was quenched with NH_4Cl (aq., sat.), extracted with CH_2Cl_2, the combined organic layers dried over Na_2SO_4 and concentrated *in vacuo*. The crude product (292 mg) was submitted for MOM-deprotection following *general procedure A*. The crude diol was purified by FCC (10% EA in PE) to afford the product as a pale yellow amorphous solid in 80% yield (152 mg, 0.428 mmol) over two steps. **^{1}H NMR** (400 MHz, Acetone) δ (ppm): 8.43 (s, 2H, $H_{11,12}$), 8.16 (s, 2H, $H_{1,10}$), 7.92 (d, *J* = 8.2 Hz, 2H, $H_{2,9}$), 7.37 (td, *J* = 8.2, 1.1 Hz, 2H, $H_{3,8}$), 7. 27 (dt, *J* = 8.3, 1.1 Hz, 2H, $H_{4,7}$), 7.04 (d, *J* = 8.4 Hz, 2H, $H_{5,6}$). **^{13}C NMR** (101 MHz, Acetone) δ (ppm): 150.4, 133.8, 129.9, 129.9, 128.2, 127.7, 125.2, 125.0, 124.2, 116.5. Spectroscopic data reported in $CDCl_3$ in the literature[204] are in reasonable correspondence. Spectra were recorded in acetone due to the significantly higher solubility and improved resolution.

(*R*)-3,3'-Difluoro-[1,1'-binaphthalene]-2,2'-diol [**3.17 (*R*)**][130]

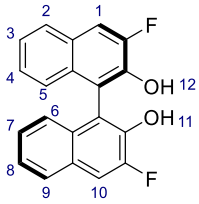

n-Buli (1.00 mL, 1.60 mmol, 1.60 M in hexane, 3 equiv) was added dropwise to a stirred solution of (*R*)-MOM-BINOL **2.2 (*R*)** (200 mg, 0.534 mmol, 1 equiv) in THF (0.13M) at 0 °C. A change in colour from colourless to yellow was observed. The reaction mixture was allowed to warm to ambient temperature. After being stirred for additional 1 hour the reaction mixture was cooled to -78 °C, then a solution of *N*-fluorobenzenesulfonimide (505 mg, 1.60 mmol, 3 equiv) in THF (0.4 M) was added dropwise. A change of colour to yellow and then red was observed. The reaction mixture was stirred at -78 °C for additional 30 min, allowed to warm to ambient temperature and quenched with H_2O. The resulting orange solution was extracted with EA, the combined organic layers washed with $NaHCO_3$ (aq., sat.), H_2O and brine, then dried over Na_2SO_4 and concentrated *in vacuo*. The crude product (223 mg, red liquid) was submitted for MOM-deprotection following *general procedure A*. The crude diol was purified by FCC (20% EA in PE) to afford the product as an off-white amorphous solid in 75% yield (129 mg, 0.400 mmol) over two steps. **^{1}H NMR** (400 MHz, Acetone) δ (ppm): 8.67 (s, 1H, $H_{11/12}$), 8.64

(s, 1H, $H_{11/12}$), 7.92 (d, *J* = 8.1 Hz, 2H,$H_{2,9}$), 7.83 (d, *J* = 4.8 Hz, 1H $H_{1/10}$), 7.80 (d, *J* = 4.8 Hz, 1H $H_{1/10}$), 7.38 (d, *J* = 7.3 Hz, 1H, $H_{5/6}$), 7.36 (d 8.0 Hz, $H_{3/8}$) 7.25 (d, *J* = 8.0, $H_{3/8}$), 7.23, (d, *J*= 7.3Hz, 1H, $H_{5/6}$), 7.18 – 7.04 (m, 2H, $H_{4,7}$). **^{13}C NMR** (101 MHz, Acetone) δ (ppm): 153.2 (dd, $^{1}J_{C\text{-}F}$ = 245.2, $^{6}J_{C\text{-}F}$ = 2.3 Hz), 144.6 (d, $^{2}J_{C\text{-}F}$ = 15.8 Hz), 131.9 (d, $^{6}J_{C\text{-}F}$ = 1.5 Hz), 129.3 (d, $^{3}J_{C\text{-}F}$ = 8.8 Hz), 128.3 (dd, $^{3}J_{C\text{-}F}$ = 5.2, $^{4}J_{C\text{-}F}$ = 3.5 Hz), 126.6 (dd, $^{5}J_{C\text{-}F}$ = 3.8, $^{6}J_{C\text{-}F}$ 2.5 Hz), 125.3 (d, $^{5}J_{C\text{-}F}$ = 1.8 Hz), 125.1 (d, $^{4}J_{C\text{-}F}$ = 4.3 Hz), 118.0 (dd, $^{4}J_{C\text{-}F}$ = 5.6, $^{5}J_{C\text{-}F}$ 3.3 Hz), 113.0 (dd, $^{2}J_{C\text{-}F}$ = 18.0, $^{5}J_{C\text{-}F}$= 4.0 Hz). Spectroscopic data reported literature was reported in DMSO at 150.92 MHz and no reports of the fluorine couplings were made.[130] Spectra were recorded in acetone due to the significantly higher solubility and improved resolution.

(*R*)-3,3'-Dithiobenzyl-[1,1'-binaphthalene]-2,2'-diol **3.19 (*R*)** NNP-03-264

Thiobenzylation of the 3,3'-position was carried out following a reported procedure.[131]

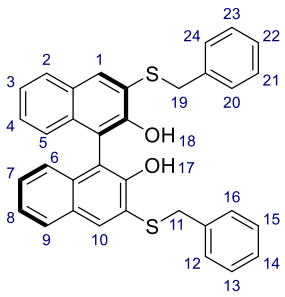

n-Buli (1.25 mL, 2.00 mmol, 1.60 M in hexane, 3 equiv) was added dropwise to a stirred solution of (*R*)-MOM-BINOL **2.2 (*R*)** (250 mg, 0.668 mmol, 1 equiv) in Et_2O (0.03M) at 0 °C. A change in colour from colourless to yellow was observed. The reaction mixture was allowed to warm to ambient temperature. After being stirred for additional 2 hours the reaction mixture was cooled to -78 °C, then a solution of benzyl disulfide (576 mg, 2.34 mmol, 3.5 equiv) in Et_2O (0.20 M) was added dropwise. A change of colour to brown was observed. The reaction mixture was allowed to warm to ambient temperature for further 5 hours. The resulting yellow reaction mixture was quenched with NH_4Cl (aq., sat.), extracted with CH_2Cl_2, the combined organic layers dried over Na_2SO_4 and concentrated *in vacuo*. The crude product (299 mg) was submitted for MOM-deprotection following *general procedure A*. The crude diol was purified by FCC (3:1 CH_2Cl_2:PE) to afford the product as a yellow amorphous solid in 64% yield (226 mg, 0.426 mmol) over two steps. **^{1}H NMR** (400 MHz, Acetone) δ 7.97 (s, br. 1H,[a] $H_{17,18}$), 7.95 (s, 2H, $H_{1,10}$), 7.81 (d, *J* = 8.0 Hz, 2H, $H_{2,9}$), 7.45 (d, *J* = 7.3 Hz, 4H, Ar), 7.35 – 7.16 (m, 10H, Ar), 6.93 (d, *J* = 8.4 Hz, 2H, $H_{5,6}$), 4.35 (d, *J* = 12.6 Hz, 2H, $H_{11/19}$), 4.28 (d, *J* = 12.7 Hz, 2H, $H_{11/19}$). **^{13}C NMR** (101 MHz, $CDCl_3$) δ (ppm): 151.1, 137.3, 135.4, 134.2, 129.1, 129.1, 128.8, 128.0, 127.6, 127.5, 124.9, 124.1, 122.5, 114.1, 40.7. **FTIR** (neat) ν_{max} (cm^{-1}): 3574 (vw), 3265 (w), 2971 (m), 2893 (w), 1577 (m). **HRMS-ESI^{+}** calc. for $[C_{34}H_{26}O_2S_2Na]^+$ expect 553.1266, found 553.1263. [a] Exchangeable proton, should integrate to 2H.

(*R*)-3,3'-Bis(benzylsulfonyl) -[1,1'-binaphthalene]-2,2'-diol [**3.20 (*R*)**]

Oxidation carried out in accordance with a reported procedure.[132]

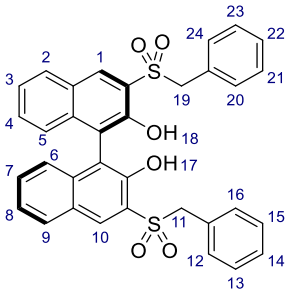

A solution of *m*-CPBA (181 mg, 1.05 mmol, 3 equiv) in CH_2Cl_2 (0.53 M) was added dropwise to a stirred solution of **3.19 (*R*)** (186 mg, 0.350 mmol, 1 equiv) in CH_2Cl_2 (0.18 M) at 0 °C. Formation of white precipitate was observed. The reaction mixture was stirred at 0 °C for 1 h, then allowed to warm to ambient temperature and stirred for additional 3 hours. The sulfone-product was the extracted with EA, washed with $NaHCO_3$ (aq., sat.) and brine, dried over Na_2SO_4 and concentrated *in vacuo*. The crude product was purified by FCC (1:1 EA:PE) to afford the product as a yellow amorphous solid in 52% yield (108 mg, 0.182 mmol). **^{1}H NMR** (400 MHz, Acetone) δ (ppm): 8.44 (s, 2H, $H_{17,18}$), 8.05 (d, *J* = 7.9 Hz, 2H, $H_{1,10}$), 7.70 – 7.11 (m, 16 H, Ar), 7.01 (d, *J* = 8.3 Hz, 2H, Ar), 4.92 (d, *J* = 13.8 Hz, 2H, $H_{11/19}$), 4.79 (d, *J* = 13.8 Hz, 2H, $H_{11/19}$). **^{13}C NMR** (101 MHz, Acetone) δ (ppm): 137.8, 134.0, 131.8, 130.7, 130.6, 129.7, 129.4, 129.3, 128.2, 127.3, 125.6, 125.1, 61.7. **FTIR** (neat) ν_{max} (cm^{-1}): 3314 (vw), 2920 (vw), 2341 (vw), 2107 (w), 1995 (w), 1621 (m), 1586 (m). **HRMS-ESI$^+$:** calc. for $[C_{34}H_{26}O_6NaS_2]^+$ expect 617.1063, found 617.1085. $[\boldsymbol{\alpha}]_{\boldsymbol{D}}^{\mathbf{25.0}}$ = -58.7 (c=1.00, THF).

(*R*)-[1,1'-binaphthalene]-2,2'-diyl bis(trifluoromethanesulfonate) [**3.21 (*R*)**][134]

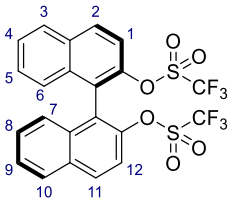

Triethylamine (0.729 mL, 7.33 mmol, 4.2 equiv) was added to a stirred suspension of (*R*)-BINOL **2.1 (*R*)** (0.500 g, 1.75 mmol, 1 equiv) in CH_2Cl_2 (1.8 M). The resulting yellow solution was cooled to -78 °C and triflic anhydride (0.644 mL, 3.81 mmol, 2.18 equiv) was added dropwise. The reaction mixture was allowed to warm to 0 °C and stirred for 1 hour. The brown solution was concentrated and purified by FCC (1:5 EA:PE) to afford the product as a white amorphous solid in 99% yield (0.953 mg, 1.73 mmol). **^{1}H NMR** (400 MHz, $CDCl_3$) δ 8.14 (d, *J* = 9.1 Hz, 2H, $H_{1,12}$), 8.01 (d, *J* = 8.3 Hz, 2H, $H_{2,11}$), 7.69 – 7.50 (m, 4H, $H_{3,4,10,9}$), 7.49 – 7.32 (m, 2H, $H_{5,8}$), 7.26 (t, *J* = 4.2 Hz, 2H, $H_{6,7}$). **^{13}C NMR** (101 MHz, $CDCl_3$) δ (ppm): 145.6, 133.3, 132.5, 132.2, 128.5, 128.1, 127.5, 126.9, 123.6, 119.5, 118.3 (q, $^1J_{C\text{-}F}$ = 320.1 Hz).**^{19}F NMR** (376 MHz, $CDCl_3$) δ (ppm): -74.6. Spectroscopic data is in accordance with the literature.[134]

(*R*)-3-iodo-3'-(trifluoromethyl)-[1,1'-binaphthalene]-2,2'-diol [**3.68 (R)**]

Prepared following a reported procedure.[114]

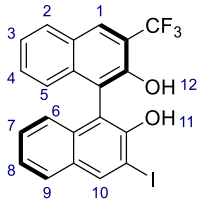

A mixture of **2.2 (*R*)** (1.00 g, 1.60 mmol, 1 equiv) in DMF (0.08 M) was added $FSO_2CF_2CO_2Me$ (0.813 mL, 6.39 mmol, 4 equiv), CuI (0.729 g, 3.83 mmol, 2.4 equiv) and HMPA (1.11 mL, 6.39 mmol, 4 equiv) was stirred at 70 °C for 7 hours. The reaction mixture was then allowed to cool to ambient temperature, diluted with CH_2Cl_2 (200 mL), washed with water, dried over Na_2SO_4 and concentrated to afford an orange syrup. The crude product was purified by FCC (5:5:240 EA:CH_2Cl_2:PE). The major product was **3.66 (*R*)** which was obtained in 44% yield (361 mg, 0.633 mmol, 62% BRSM). **^{1}H NMR** (400 MHz, $CDCl_3$) δ (ppm): 8.57 (s, 1H, $H_{1/10}$), 8.32 (s, 1H, $H_{1/10}$), 7.97 (d, *J* = 8.1 Hz, 1H, $H_{2/9}$), 7.80 (d, *J* = 8.2 Hz, 1H, $H_{2/9}$), 7.61 – 7.09 (m, 6H, Ar), 4.78 (dd, *J* = 50.6, 5.6 Hz, 2H, CH_2(MOM)), 4.61 (dd, *J* = 63.9, 5.6 Hz, 2H CH_2(MOM)), 2.77 (s, 3H, CH_3(MOM)), 2.55 (s, 3H CH_3(MOM)). **3.66 (*R*)** (290 mg, 0.510 mmol) was submitted to MOM-deprotection following *general procedure A*. The crude product was purified by FCC (1:4 Et_2O:PE) to afford the product **3.68 (*R*)** as a pale yellow amorphous solid in quantitative yield (244 mg, 0.508 mmol). **^{1}H NMR** (400 MHz, Acetone) δ (ppm): 8.68 (d, *J* = 17.7 Hz, 3H, $H_{11,12,1/10}$), 8.48 (d, *J* = 11.6 Hz, 1H, $H_{1/10}$), 8.13 (d, *J* = 8.0 Hz, 1H, $H_{2/9}$), 7.92 (d, *J* = 8.0 Hz, 1H, $H_{2/9}$), 7.56 – 7.21 (m, 4H, $H_{3,4,7,8}$), 7.20 – 6.94 (m, 2H, $H_{5,6}$). **^{13}C NMR** (101 MHz, Acetone) δ 153.4, 151.9, 141.2, 136.7, 135.0, 131.4, 130.2, 129.9 (q, $^3J_{C\text{-}F}$=5.6 Hz), 128.2, 128.2, 128.0, 125.0 (q, $^1J_{C\text{-}F}$ = 217.9 Hz), 124.9, 124.9, 120.0 (q, $^2J_{C\text{-}F}$ = 30.3 Hz), 116.3, 112.9, 89.2. ^{19}F NMR (376 MHz, Acetone) δ (ppm): -62.6 – -62.8 (m). **FTIR** (neat) ν_{max} (cm^{-1}): 3533 (w), 3059 (vw), 2917 (vw), 1628 (m), 1607 (w), 1575 (w), 1502 (w). **HRMS-ESI$^+$** calc. for $[C_{21}H_{13}F_3IO_2]^+$ expect 480.9907, found 480.9912. $[\boldsymbol{\alpha}]_{\boldsymbol{D}}^{\mathbf{25.0}}$= +116.7 (c=1.00, THF).

(*R*)-3,3'-Bis(trifluoromethyl)-[1,1'-binaphthalene]-2,2'-diol [**3.69 (*R*)**][114]

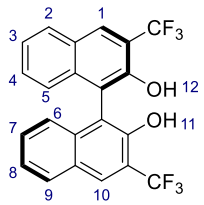

A mixture of **2.2 (*R*)** (1.00 g, 1.60 mmol, 1 equiv) in DMF (0.08 M) was added $FSO_2CF_2CO_2Me$ (0.813 mL, 6.39 mmol, 4 equiv), CuI (0.729 g, 3.83 mmol, 2.4 equiv) and HMPA (1.11 mL, 6.39 mmol, 4 equiv) was stirred at 70 °C for 20 hours. The reaction mixture was then allowed to cool to ambient temperature, diluted with CH_2Cl_2 (200 mL), washed with water and then brine. The combined organic layers were dried over Na_2SO_4 and concentrated to afford a yellow syrup. The crude product was purified by FCC (5:5:290 EA:CH_2Cl_2:PE). The major product was **3.67 (*R*)** which was obtained in 44% yield (396 mg, 0.697 mmol). **3.66 (*R*)** was the minor product and obtained in 29% yield (263 mg, 0.463 mmol). **^{1}H NMR** (400 MHz, $CDCl_3$) δ (ppm): 8.34 (s, 2H, $H_{1,10}$), 7.99 (d, *J* = 8.2 Hz, 2H, $H_{2,9}$), 7.52 (t, *J* =

7.1 Hz, 2H, $H_{3,8}$), 7.42 (t, *J* = 7.2 Hz, 2H, $H_{4,7}$), 7.31 – 7.13 (m, 2H, $H_{5,6}$), 4.76 (d, *J* = 5.5 Hz, 2H, CH_2(MOM)), 4.52 (d, *J* = 5.5 Hz, 2H, CH_2(MOM)), 2.71 (s, 6H, CH_3(MOM)). **3.67 (*R*)** (340 mg, 0.598 mmol) was submitted to MOM-deprotection following *general procedure A*. The crude product was purified by FCC (1:4 Et_2O:PE) to afford the product **3.69 (*R*)** as a yellow amorphous solid in 97% yield (280 mg, 0.583 mmol). **^{1}H NMR** (400 MHz, Acetone) δ (ppm): 8.88 (s, 2H, $H_{11,12}$), 8.55 (s, 2H, $H_{1,10}$), 8.20 (d, *J* = 7.7 Hz, 2H, $H_{2,9}$), 7.50 (tt, *J* = 13.7, 6.7 Hz, 4H, $H_{3,4,7,8}$), 7.20 (d, *J* = 8.2 Hz, 2H, $H_{5,6}$). **^{13}C NMR** (101 MHz, Acetone) δ (ppm): 152.4, 136.9, 130.4, 130.3 (q, *J* = 5.7 Hz), 130.1, 128.5, 125.1, (q, $^1J_{C\text{-}F}$ = 272.1), 120.34 (q, $^2J_{C\text{-}F}$ = 30.5 Hz), 115.3. **^{19}F NMR** (376 MHz, Acetone) δ (ppm): -62.8. Spectroscopic data reported in $CDCl_3$ in the literature[114] are in reasonable correspondence. Spectra were recorded in acetone due to the significantly higher solubility and improved resolution.

(*R*)-3,3'-Bis(perfluorophenyl)-[1,1'-binaphthalene]-2,2'-diol [**3.71 (*R*)**] [143,205–207]

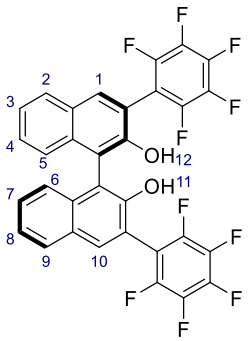

n-Buli (5.01 mL, 8.01 mmol, 1.60 M in hexane, 3 equiv) was added dropwise to a stirred solution of (*R*)-MOM-BINOL **2.2 (*R*)** (1.00 g, 2.67 mmol, 1 equiv) in THF (0.17 M) at 0 °C. A change in colour from colourless to yellow was observed. The reaction mixture was allowed to warm to ambient temperature. After being stirred for additional 1 hour the reaction mixture was cooled to -78 °C and hexafluorobenzene (2.16 mL, 18.7 mmol, 7 equiv) was added dropwise. The reaction mixture was allowed to warm to ambient temperature for further 24 hours. The resulting brown reaction mixture was quenched with NH_4Cl (aq., sat.), extracted with Et_2O, the combined organic layers were washed with brine, dried over Na_2SO_4 and concentrated *in vacuo*. The crude product was purified by FCC (5% EA in PE) to afford the product as a white amorphous solid in 71% yield (1.35 g, 1.91 mmol). **^{1}H NMR** (400 MHz, $CDCl_3$) δ (ppm): 7.96 (s, 2H, $H_{1,10}$), 7.93 (d, *J* = 8.1 Hz, 2H, $H_{2,9}$), 7.55 – 7.45 (m, 2H, $H_{3,8}$), 7.45 – 7.36 (m, 2H, $H_{4,7}$), 7.33 (d, *J* = 8.4 Hz, 2H, $H_{5,6}$), 4.47 (d, *J* = 6.0 Hz, 2H, CH_2(MOM)), 4.42 (d, *J* = 6.0 Hz, 2H, CH_2(MOM)), 2.62 (s, 6H, CH_3(MOM)). **^{19}F NMR** (376 MHz, $CDCl_3$) δ (ppm): -139.2 (dd, *J* = 23.4, 8.1 Hz), -139.8 (dd, *J* = 23.2, 8.0 Hz), -154.8 (t, *J* = 20.9 Hz), -162.2 – -162.6 (m). **3.70 (*R*)** (1.00 g, 1.42 mmol) was submitted for MOM-deprotection following *general procedure A.* The crude diol was purified by FCC (15% Et_2O in PE) to afford the diol product **3.71 (*R*)** as a white amorphous solid in 99% yield (0.865 g, 1.40 mmol). **^{1}H NMR** (400 MHz, $CDCl_3$) δ (ppm): 8.03 (s, 2H, $H_{1,10}$), 7.99 – 7.86 (m, 2H, $H_{2,9}$), 7.53 – 7.37 (m, 4H, $H_{3,4,7,8}$), 7.27 – 7.19 (m, 2H, $H_{5,6}$), 5.24 (s, 2H, $H_{11,12}$). **^{19}F NMR** (376 MHz, $CDCl_3$) δ (ppm): -139.7 (dd, *J* = 23.2, 8.1 Hz), -134.0 (dd, *J* = 23.2, 8.1 Hz), -154.6 (t, *J* = 20.9 Hz), -162.2 – -162.9 (m). **^{13}C NMR** (101 MHz, $CDCl_3$) δ (ppm): 150.6, 146.42 – 145.80 (m), 143.85 – 143.33 (m), 142.69 – 142.13 (m), 139.65

– 138.76 (m), 136.90 – 136.32 (m), 134.2, 133.8, 129.1, 129.0, 129.0, 125.2, 124.2, 115.9, 112.08 (td, $^{2}J_{C\text{-}F}$ = 18.9, $^{3}J_{C\text{-}F}$ 3.8 Hz), 111.6. Spectroscopic data is in accordance with the literature.[205]

(*R*)-3,3'-diiodo-5,5',6,6',7,7',8,8'-octahydro-[1,1'-binaphthalene]-2,2'-diol [**3.73 (*R*)**][144]

Hydrogenation was carried out following a reported procedure, [208] followed by iodination in accordance with a reported procedure.[144]

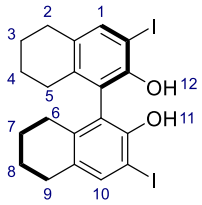

A suspension of Pt_2O (99.3 mg, 0.07 equiv) and (*R*) -BINOL **2.1 (*R*)** (1.00 g, 3.49 mmol, 1 equiv) in acetic acid (0.12 M) was stirred vigorously under a hydrogen atmosphere at room temperature for 18 hours. The grey suspension was filtered through celite, diluted with CH_3Cl, washed with water and then brine. The organic layer was dried over Na_2SO_4 and concentrated. The crude product was purified by FCC (20% EA in PE) to afford the product **3.72 (*R*)** as a white amorphous solid in 92% yield (0.950 g, 2.23 mmol). **^{1}H NMR** (400 MHz, $CDCl_3$) δ (ppm): 7.07 (d, *J* = 8.5 Hz, 2H, H_{ortho}), 6.83 (d, *J* = 8.3 Hz, 2H, $H_{1,10}$), 4.55 (s, br., 2H, $H_{11,12}$), 2.75 (t, *J* = 6.1 Hz, 4H, $H_{2,9}$), 2.39 – 1.89 (m, 8H, $H_{3,4,7,8}$) 1.79 – 1.62 (m, 4 H, $H_{5,6}$). Spectroscopic data in accordance with the literature.[208] To a solution of **3.72 (*R*)** (0.500 g, 1.70 mmol, 1 equiv) in CH_2Cl_2 (0.11 M) at room temperature was the added successively morpholine (0.879 mL, 10.2 mmol, 6 equiv) and iodine (0.862 g, 3.40 mmol, 2 equiv). The resulting red solution was stirred at room temperature for further 5 hours, diluted with CH_2Cl_2 and washed with HCl (1 N). The product was extracted with CH_2Cl_2 and washed thoroughly with $Na_2S_2O_3$ (aq., sat.). The organic layer was washed with brine, dried over Na_2SO_4 and concentrated *in vacuo* and purified by FCC (20% EA in PE) to afford the product as a white amorphous solid in¨95% yield (0.879 g, 1.61 mmol). **^{1}H NMR** (400 MHz, $CDCl_3$) δ (ppm) 7.51 (s, 2H, $H_{1,10}$), 4.97 (s, 2H, $H_{11,12}$), 2.73 (t, *J* = 5.9 Hz, 4H, $H_{2,9}$), 2.27 (dt, *J* = 17.5, 6.0 Hz, 2H, $H_{3/8}$), 2.10 (dt, *J* = 17.5, 5.9 Hz, 2H, $H_{3/8}$), 1.84 – 1.56 (m, 8H, $H_{4,5,6,7}$). **^{13}C NMR** (101 MHz, $CDCl_3$) δ (ppm): 149.9, 139.4, 137.9, 132.6, 120.8, 81.2, 29.0, 27.1, 22.89, 22.8. Spectroscopic data is in accordance with the literature.[144]

Imines:

N-methyl-1-phenylethan-1-imine [**3.3**][209]

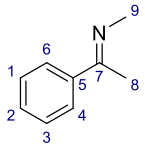

To a stirred solution of methyl amine (2.0 mL, 16.0 mmol, 33% in EtOH, 4 equiv) with freshly activated molecular sieves (3Å) acetophenone (0.48 mL, 4.0 mmol, 1 equiv) was added. The reaction mixture was stirred at room temperature for 3 days, filtered through celite and washed with CH_2Cl_2. The crude product was concentrated *in vacuo* to yield a yellow oil (0.485 g, 3.64 mmol, 91%), as a mixture 9:1 of E:Z isomers. The imine was used without further purification. **^{1}H NMR** (400 MHz, $CDCl_3$) δ (ppm): 7.82-7.69 (m, 2H, $H_{4,6}$), 7.45 – 7.37 (m, 3H, $H_{1\text{-}3}$), 3.38 (d, *J* = 0.7 Hz, 3H, H_9), 2.27 (d, *J* = 0.7 Hz, 3H, H_8). **^{13}C NMR** (100 MHz, $CDCl_3$) δ (ppm): 167.0, 141.1, 129.3, 128.1, 126.3, 39.4, 15.0. Spectroscopic data is in accordance with the literature.[209]

N-Butyl-1-phenylethan-1-imine [**3.86**][209]

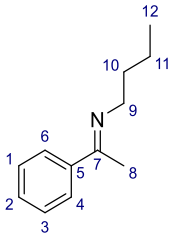

N-butylamine (3.0 mL, 30 mmol, 3 equiv.) was added to a stirred solution of acetophenone (1.2 mL, 10 mmol, 1 equiv.) at 0 °C. A solution of $TiCl_4$ (0.7 mL, 6.4 mmol, 0.64 equiv.) in CH_2Cl_2 (0.9 M) was added over 30 minutes. Formation of white precipitate was observed along with a change in colour of the solution from colourless to brown. The reaction mixture was stirred at room temperature for 2 hours, filtered through celite and washed with MTBE. The combined organic layers were washed with brine, dried over Na_2SO_4 and concentrated *in vacuo* to afford the product as a light brown oil in 71% yield (1.26 g, 7.19 mmol), as a 12/1 mixture of *E*/*Z* isomers. **^{1}H NMR** (400 MHz, $CDCl_3$) δ (ppm): 7.79 (dd, *J* = 6.7, 3.0 Hz, 2H, $H_{4,6}$), 7.43 – 7.30 (m, 3H, $H_{1\text{-}3}$), 3.50 (t, *J* = 7.1 Hz, 2H, H_9), 2.22 (s, 3H, H_8), 1.80 – 1.73 (m, 2H, H_{10}), 1.54 – 1.45 (m, 2H, H_{11}), 1.01 (t, *J* = 7.4 Hz, 3H, H_{12}). **^{13}C NMR** (101 MHz, $CDCl_3$) δ (ppm): 164.4, 141.3, 129.0, 127.9, 126.3, 51.7, 32.9, 20.6, 15.1, 13.9. Data is in accordance with the literature.[209]

General procedure B: Synthesis of imines in toluene

Amine (1 equiv) was added to a stirred solution of ketone (1 equiv) in toluene (1.2 M) with freshly activated molecular sieves (4 Å). The reaction mixture was heated to 65 °C and stirred for 24 hours. The resulting yellow cloudy solution was allowed to cool to ambient temperature, filtered through celite and washed with CH_2Cl_2. The crude product was concentrated *in vacuo*. The crude product was purified by recrystallisation.

N-Benzyl-1-phenylethan-1-imine **[3.5]**[122,123]

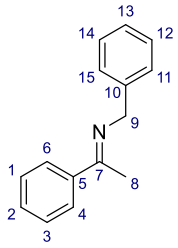

Synthesised from acetophenone (1.07 mL, 9.16 mmol) and benzylamine (1.00 mL, 9.16 mmol) according to *general procedure B* and recrystallised from cold hexane to afford pale yellow square crystals in 78% yield (1.49 g, 7.13 mmol) as a 11:1 mixture of E:Z isomers. **^{1}H NMR** (400 MHz, $CDCl_3$) δ (ppm): 7.94-7.85 (m, 2H, Ar), 7.49-7.34 (m, 7H, Ar), 7.30-7.26 (m, 1H, Ar) 4.77 (s, 2H, H_9), 2.35 (s, 3H, H_8). **^{13}C NMR** (101 MHz, $CDCl_3$) δ (ppm): 165.9, 141.0, 140.5, 129.6, 128.3, 128.2, 127.7, 126.7, 126.5, 55.7, 15.8. Data is in accordance with the literature.[122]

N-Benzyl-1-(4-ethoxyphenyl)ethan-1-imine [**7.1**]

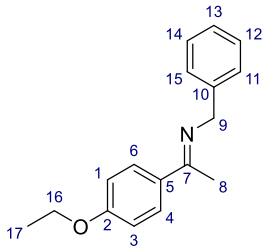

Synthesised from 4-ethoxyacetophenone (3.00 g, 18.3 mmol) and benzylamine (2.00 mL, 18.3 mmol) according to *general procedure B* and recrystallised from hexane to afford a white crystalline solid in 70% yield (3.26 g, 12.85 mmol) as a 12:1 mixture of E:Z isomers. **^{1}H NMR** (400 MHz, $CDCl_3$) δ (ppm): 7.78 – 7.67 (m, 2H, Ar), 7.65 – 7.54 (m, 2H, Ar), 7.52 – 7.29 (m, 4H, Ar), 7.29 – 7.11 (m, 1H, Ar), 4.72 (s, 2H, H_9), 2.30 (s, 3H, H_8). **^{13}C NMR** (101 MHz, $CDCl_3$) δ (ppm): 165.1, 160.2, 140.8, 133.5, 128.3, 128.2, 127.6, 126.4, 113.9, 63.4, 55.4, 15.4, 14.7. **FTIR** (neat) ν_{max} (cm^{-1}): 3087 (w), 3057 (w), 3031 (w), 2983 (w), 2927 (w), 2875 (w), 2894 (w), 1630 (m), 1601 (s), 1579 (m), 1513 (m). **HRMS-ESI^{+}**: calc. for $[C_{17}H_{20}NO]^{+}$ expect 254.1539, found 254.1541. **MP**: 72-74 °C.

N-Benzyl-1-(4-iodophenyl)ethan-1-imine, [**7.2**]

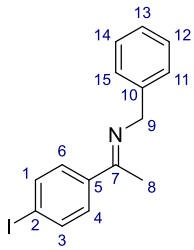

Synthesised from 4-iodoacetophenone (3.00 g, 12.2 mmol) and benzylamine (1.33 mL, 12.2 mmol) according to *general procedure B* and recrystallised from hexane and EtOAc to afford the product as a yellow crystalline solid in 41% (1.66 g, 4.95 mmol) as a 14:1 mixture of E:Z isomers. **^{1}H NMR** (400 MHz, $CDCl_3$) δ (ppm): 7.72 (d, J = 8.2 Hz, 2H, $H_{1,3}$), 7.61 (d, J = 8.3 Hz, 2H, $H_{4,6}$), 7.47 – 7.31 (m, 4H, $H_{11,12,14,15}$), 7.30 – 7.18 (m, 1H, H_{13}), 4.72 (s, 2H, H_9), 2.30 (s, 3H, H_8). **^{13}C NMR** (101 MHz, $CDCl_3$) δ (ppm): 164.9, 140.2, 137.8, 137.3, 128.5, 128.4, 127.6, 126.6, 96.2, 55.7, 15.5. **FTIR** (neat) ν_{max} (cm^{-1}): 3564 (w),

3029 (w), 2885 (w), 1684 (m), 1625 (s), 1603 (m), 1578 (s), 1550 (m). **HRMS-ESI**$^+$ calc. for $[C_{15}H_{15}IN]^+$ expect 336.0244, found 336.0238. MP: 52-53 °C

N-Benzyl-1-(3,5-difluorophenyl)ethan-1-imine, [**7.3**]

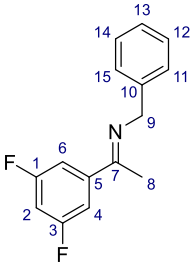

Synthesised from 3,5-difluoroacetophenone (3.00 g, 19.2 mmol) and benzylamine (2.1 mL, 19.2 mmol) according to *general procedure B* and recrystallised from hexane to afford the product as off-white crystals in 44% yield (2.09 g, 8.52 mmol) as a 44:1 mixture of E:Z isomers. **^{1}H NMR** (400 MHz, $CDCl_3$) δ (ppm): 7.49 – 7.32 (m, 5H, $H_{11\text{-}15}$), 7.32 – 7.16 (m, 2H, H, $H_{4,6}$), 6.84 (tt, J = 8.6, 2.4 Hz, 1H, H_2), 4.73 (s, 2H, H_9), 2.31 (s, 3H, H_8). **^{13}C NMR** (101 MHz, $CDCl_3$) δ (ppm): 163.5 (d, $^5J_{C\text{-}F}$ = 3.0 Hz), 163.1 (dd, $^1J_{C\text{-}F}$ = 247.8, $^3J_{C\text{-}F}$ = 12.5 Hz), 144.4 (t, $^4J_{C\text{-}F}$ = 8.5 Hz), 140.0, 128.6, 127.8, 126.9, 110.1 – 109.6 (m), 105.2, 104.9 104.93 (t, $^2J_{C\text{-}F}$ = 25.6 Hz), 104.7, 56.0, 15.9. **^{19}F NMR** (376 MHz, $CDCl_3$) δ (ppm) -109.89 – -110.08 (m). **FTIR** (neat) ν_{max} (cm^{-1}): 3083 (w), 3060 (w), 3023 (w), 2874 (w), 1635 (m), 1619 (m), 1603 (m), 1588 (s), 1519 (m). **HRMS-ESI**$^+$ calc. for $[C_{15}H_{14}F_2N]^+$ expect 246.1089, found 246.1085. **MP**: 47-49 °C.

N-Benzyl-2,2,2-trifluoro-1-phenylethan-1-imine, [**7.8**][210]

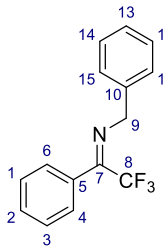

Synthesised from 2,2,2-trifluoroacetophenone (4.86 g, 27.9 mmol) and benzylamine (3.05 mL, 27.9 mmol) according to *general procedure B* and purified by FCC (20% EA in PE) to afford a colourless liquid in 70% yield (5.17 g, 19.6 mmol) as a >100:1 mixture of E:Z isomers. **^{1}H NMR** (400 MHz, $CDCl_3$) δ (ppm): 7.54 – 7.47 (m, 3H, Ar), 7.36 – 7.25 (m, 7H, Ar), 4.62 (s, 2H, H_9). **^{13}C NMR** (101 MHz, $CDCl_3$) δ (ppm): 159.1 (q, $^2J_{C\text{-}F}$ = 33.8 Hz), 138.1, 138.1, 130.4, 129.0, 128.7, 127.7, 127.7, 127.3, 119.9 (q, $^1J_{C\text{-}F}$ = 278.7 Hz), 56.9. Spectroscopic data is in accordance with the literature.[210]

N-Benzyl-2,3-dihydro-1*H*-inden-1-imine, [**7.5**]

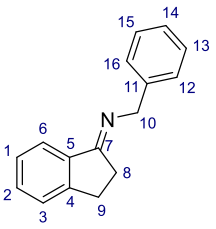

Synthesised from indanone (1.10 g, 8.32 mmol) and benzylamine (0.91 mL, 8.32 mmol) according to *general procedure B* and recrystallised from hexane to afford the product as a khaki-green crystalline solid in 55% yield (1.02 g, 4.61 mmol) as a 18:1 mixture of E:Z isomers. **^{1}H NMR** (400 MHz, $CDCl_3$) δ (ppm): 7.91 (d, J = 7.7 Hz, 1H, H_6), 7.65 – 7.08 (m, 8H, $H_{1\text{-}3,12\text{-}16}$), 4.72 (s, 2H, H_{10}), 3.26 – 3.06 (m, 2H, H_8),

2.95 – 2.72 (m, 2H, H_9). **^{13}C NMR** (101 MHz, $CDCl_3$) δ (ppm): 175.1, 149.6, 140.3, 139.8, 131.2, 128.4, 127.7, 126.9, 126.6, 125.5, 122.5, 57.2, 28.4, 28.1. **FTIR** (neat) ν_{max} (cm^{-1}): 3079 (w), 3051 (w), 3024 (w), 2926 (w), 2855 (w), 1649 (s), 1601 (m), 1580 (w). **HRMS-ESI$^+$** calc. for $[C_{16}H_{16}N]^+$ expect 222.1277, found 222.1277. **MP**: 66-68 °C.

4-(1-(benzylimino)ethyl)-3-methylphenol, [**7.6**]

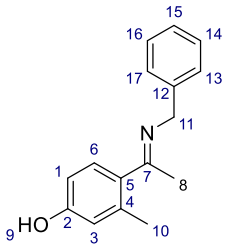

Synthesised according to *general procedure B* and recrystallised from hexane, Et_2O and MeOH to afford the product as a white crystalline solid in 26% yield (1.26 g, 5.26 mmol) as a 13:1 mixture of E:Z isomers. **^{1}H NMR** (400 MHz, MeOD-d_4) δ (ppm): 7.43 – 7.15 (m, 6H, Ar), 6.94 – 6.78 (m, 2H, Ar), 4.24 (s, 2H, H_{11}), 2.23 (s, 3H, H_{10}) 2.11 (s, 3H, H_8). **^{13}C NMR** (101 MHz, MeOD-d_4) δ (ppm): 174.9, 158.8, 140.6, 136.0, 129.5, 129.4, 129.1, 127.9, 127.8, 117.9, 114.2, 57.7, 22.8, 19.4. **FTIR** (neat) ν_{max} (cm^{-1}): 3083-2883 (br w), 1639 (m), 1614 (w), 1574 (m). **HRMS-ESI$^+$** calc. for $[C_{16}H_{18}NO]^+$ expect 240.1383, found 240.1384. **MP**: 127-129 °C.

N-(4-(1-(benzylimino)ethyl)phenyl)acetamide, [**7.7**]

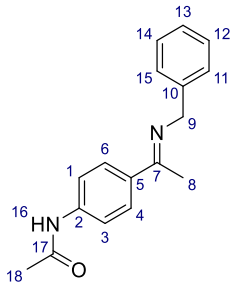

Synthesised from 4-acetamidoacetophenone (3.00 g, 16.9 mmol) and benzylamine (1.85 mL, 16.9 mmol) according to *general procedure B*. The product crystallised when concentrated from the work up mixture of CH_2Cl_2 and toluene to afford a pale yellow crystalline solid in 83% yield (3.76 g, 14.1 mmol) as a 12:1 mixture of E:Z isomers. **^{1}H NMR** (400 MHz, $CDCl_3$) δ (ppm): 7.84 (d, J = 8.7 Hz, 2H, $H_{1,3}$), 7.60 – 7.16 (m, 7H, $H_{4,6,11\text{-}15}$), 4.73 (s, 2H, H_9), 2.31 (s, 3H, H_{18}), 2.16 (s, 3H, H_8). **^{13}C NMR** (101 MHz, $CDCl_3$) δ (ppm): 168.3, 165.2, 140.5, 139.2, 136.8, 128.4, 127.7, 127.6, 126.6, 119.1, 55.6, 24.7, 15.6. **FTIR** (neat) ν_{max} (cm^{-1}): 3307 (m), 3262 (w), 3197 (w), 3123 (w), 3084(w), 3062 (w), 3062 (w), 3001 (w), 2897 (w), 2861 (w), 2801 (w), 1669 (s), 1632 (m), 1598 (s), 1532 (s), 1509 (s). **HRMS-ESI$^+$** calc. for $[C_{17}H_{19}N_2O]^+$ expect 267.1492, found 267.1487. **MP**: 157-159 °C.

Methyl 4-(benzylimino)ethyl)phenyl)benzoate, [**7.8**]

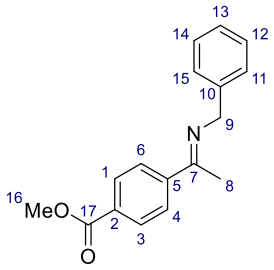

Synthesised from methyl 4-acetylbenzoate (2.00 g, 11.2 mmol) and benzylamine (1.23 mL, 11.2 mmol) according to *general procedure B* and recrystallised from hexane to afford a pale yellow needles in 65% yield (1.95 g, 7.29 mmol) as a 14:1 mixture of E:Z isomers. **^{1}H NMR** (400 MHz, $CDCl_3$) δ (ppm): 8.11 – 7.98 (m, 2H, $H_{1,3}$), 7.97 – 7.81 (m, 2H, $H_{4,6}$), 7.43 (d, *J* = 7.4 Hz, 2H, $H_{11,15}$), 7.37 (dd, *J* = 10.3, 4.8 Hz, 2H, $H_{12,14}$), 7.32 – 7.18 (m, 1H, H_{13}), 4.76 (s, 2H, H_9), 3.93 (s, 3H, H_{16}), 2.36 (s, 3H, H_8). **^{13}C NMR** (101 MHz, $CDCl_3$) δ (ppm): 166.8, 165.1, 144.9, 140.1, 130.8, 129.5, 128.4, 127.7, 126.7, 126.6, 55.9, 52.1, 15.9. **FTIR** (neat) ν_{max} (cm^{-1}): 3084 (w), 3061 (w), 3028 (w), 2957 (w), 2891 (w), 2842 (w), 1720 (s), 1626 (m), 1603 (m), 1506 (w). **HRMS-ESI$^+$** calc. for $[C_{17}H_{18}NO_2]^+$ expect 268.1332, found 268.1320. **MP**: 71-73 °C.

N-Phenylethyl-1-phenylethan-1-imine, [**3.83**][211]

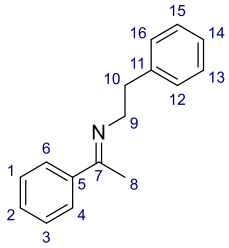

Synthesised from acetophenone (2.15 mL, 17.2 mmol) and 2-phenylethan-1-amine (2.00 mL, 17.2 mmol) according to *general procedure B* and recrystallised from hexane at -18 °C to afford a pale yellow product, liquid at RT, in 46% yield (1.81 g, 8.10 mmol) as a 8:1 mixture of E:Z isomers. **^{1}H NMR** (400 MHz, $CDCl_3$) δ (ppm): 7.80 (dd, *J* = 3.4, 1.9 Hz, 2H, H), 7.47 – 7.15 (m, 8H), 3.79 (t, *J* = 7.5 Hz, 2H, H_9), 3.13 (t, *J* = 7.5, 2H, H_{10}), 2.15 (s, 3H, H_8). **^{13}C NMR** (101 MHz, $CDCl_3$) δ (ppm): 165.5, 141.2, 140.6, 129.3, 128.9, 128.3, 128.1, 126.5, 126.0, 54.0, 37.4, 15.4. Data is in accordance with the literature.[211]

N-1-Diphenylethan-1-imine, [**3.76**][212]

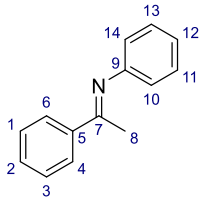

Synthesised from acetophenone (1.07 mL, 9.16 mmol) and aniline (0.84 mL, 9.16 mmol) according to *general procedure B* and recrystallised from cold hexane to afford the product as yellow crystals in 57% yield (1.02 g, 5.22 mmol) as a 13:1 mixture of E:Z isomers. **^{1}H NMR** (400 MHz, $CDCl_3$) δ (ppm): 8.05 – 7.90 (m, 2H, Ar), 7.59 – 7.41 (m, 3H, Ar), 7.41 – 7.30 (m, 2H, Ar), 7.14 – 7.05 (m, 1H, Ar), 6.91 – 6.71 (m, 2H, Ar), 2.24 (s, 3H, H_8). **^{13}C NMR** (101 MHz, $CDCl_3$) δ (ppm): 165.5, 151.7, 139.4, 130.5, 128.9, 128.4, 127.1, 123.2, 119.4, 17.4. Data is in accordance with the literature.[212]

N-(4-Methoxyphenyl)-1-phenylethan-1-imine, [**3.75**][213]

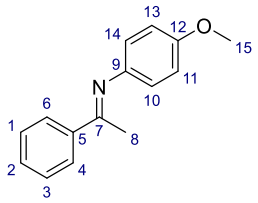

Synthesised from acetophenone (1.07 mL, 9.16 mmol) and 4-methoxyaniline (1.05 mL, 9.16 mmol) according to *general procedure B* and recrystallised from hexane to afford yellow crystals in 72% yield (1.47 g, 6.52 mmol) as a 52:1 mixture of E:Z isomers. **^{1}H NMR** (400 MHz, $CDCl_3$) δ (ppm): 7.98 – 7.96 (m, 2H, Ar), 7.48 – 7.42 (m, 3H, Ar), 6.93– 6.90 (m, 2H, Ar), 6.78 – 6.74 (m, 2H, Ar), 3.82 (s, 3H, H_{15}), 2.26 (s, 3H, H_8). **^{13}C NMR** (101 MHz, $CDCl_3$) δ (ppm): δ 165.9, 156.0, 144.9 139.9 130.5, 128.5, 127.2, 120.9, 114.3, 55.6, 17.5. Spectroscopic data is in accordance with the literature.[213]

Amines:

Screening Procedure 1:[a] CH_2Cl_2, DIPEA

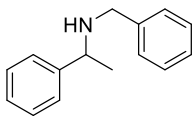

$InBr_3$ (17.8 mg, 0.05 mmol, 10 mol%) and (*R*)-BINOL (14.4 mg, 0.05 mmol, 10 mol%) was suspended in CH_2Cl_2 affording a slightly pink suspension with white solids. DIPEA (43.5 µL, 0.25 mmol, 50 mol%) was added dropwise and a change of colour from yellow to colourless was observed along with the white solids slowly going into solution. The reaction mixture was stirred for 90 min and added to *N*-benzyl-(1-phenylethylidene)amine **3.5** (105 mg, 0.5 mmol, 1 eq.) followed by additional stirring for 30 min. Phenylsilane (62 µL, 0.5 mmol, 1 eq.) was added dropwise resulting in slow gas release and the reaction mixture was refluxed for 24h, during which a grey solid chuck was formed. The reaction was quenched with NH_4Cl (0.5 mL) and extracted with EtOAc. The combined organic layers were washed with brine, dried over Na_2SO_4 and concentrated *in vacou*. The crude product was purified by flash column chromatography (2% acetone, 2 % Et_3N in CH_2Cl_2) to afford a yellow oil (72.7 mg, 0.34 mmol, 69%).

[a] This procedure was also used for the reductions of acetophenone and *N*-methyl-1-phenylethan-1-imine. As neither of these two compound were successfully reduced /isolated no further details are given hereon.

Screening Procedure 2: THF co-evaporation

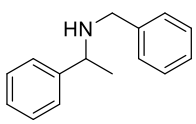

$InBr_3$ (17.8 mg, 0.05 mmol, 10 mol%) was co-evaporated with THF and dissolved in THF. (*R*)-BINOL (14.4 mg, 0.05 mmol, 10 mol%) and 4Å MS was added and the reaction mixture stirred for 2 h. *N*-benzyl-(1-phenylethylidene)amine **2.5** (105 mg, 0.5 mmol, 1 eq.) was added to afford a yellow solution, which was stirred at room temperature for

30 min. Phenylsilane (62 µL, 0.5 mmol, 1 eq.) was added dropwise resulting in heavy gas release. The reaction mixture was stirred at 30 °C. After the first hour the colour had changed to pink orange. After 18 hours small grey chucks had formed and ^{1}H-NMR analysis showed 79% conversion. The reaction went red when the suba seal was removed and the reaction exposed to air. The reaction mixture was quenched with NH_4Cl and extracted with EtOAc. The combined organic layers were washed with brine, dried over Na_2SO_4 and concentrated *in vacuo*. The yellow oil was redissolved in MeOH, which afforded light yellow precipitate. The supernatant was isolated by filtration, concentrated and the crude product purified by flash column chromatography (5% acetone, 1 % Et_3N in CH_2Cl_2) to afford the product as a yellow oil (62.3 mg, 0.3 mmol, 60%).

Screening Procedure 4: Potassium hexamethyldisilazane

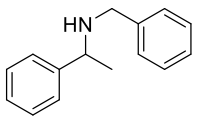

To a stirred solution of KHMDS (42.0 mg, 0.21 mmol, 40 mol%) in THF (0.5 mL) (*R*)-BINOL (30.2 mg, 0.11 mmol, 20 mol%) was added. The resulting yellow solution was stirred at room temperature for 1 hour and $InBr_3$ (18 mg, 0.05 mmol, 10 mol%) was added. Formation of a white precipitate was observed, and the solution turned colourless. The reaction mixture was stirred for additional 1 hour and *N*-benzyl-(1-phenylethylidene)amine **2.5** (105 mg, 0.5 mmol, 1 eq.) was added to afford a yellow solution. Phenylsilane (62 µL, 0.5 mmol, 1 eq.) was added dropwise. A change of colour to orange was observed after 1 hour. After 15 hours the solution had small grey chucks had formed and ^{1}H NMR analysis showed 69% conversion. Additional 24 hours stirring resulted in 73% conversion. The reaction mixture was quenched with NH_4Cl and extracted with EtOAc. The combined organic layers were washed with brine, dried over Na_2SO_4 and concentrated *in vacuo*. The yellow oil was redissolved in MeOH, which afforded light yellow precipitate. The supernatant was isolated by filtration, concentrated and the crude product purified by flash column chromatography (5% acetone, 1 % Et_3N in CH_2Cl_2) to afford the product as a yellow oil (65.0 mg, 0.31 mmol, 61%).

For Screening Procedures 5-6 In(III) was added from a stock solution and the conversion was examined by quantitative NMR after filtration of the reaction mixture using 1,3,5-trimethoxybenzene as internal standard.

Screening Procedure 5: NaH as base.

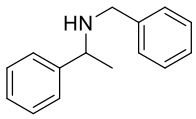

To a mixture of ligand in THF was added NaH at 0 °C. The reaction mixture was allowed to warm up to ambient temperature and further stirred for 1 h. The THF was removed through concentration by a nitrogen stream and solvent was added. The remaining procedure will follow procedure 6.

Screening Procedure 6: Screening reactions in vials

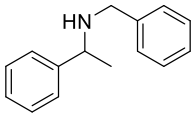

In(III) was added to a mixture of ligand in solvent at RT with or without additive added. The reaction mixture stirred for 15 minutes,[a] then imine was added and after additional 10 minutes[b] $PhSiH_3$ was added.

[a] unless otherwise noted in the given table. [b] If In(III) and ligand was premixes for 1 h or more, $PhSiH_3$ was added 30 minutes after addition of the imine at RT, and after 60 minutes if the imine was mixed with In(III) and ligand at 60 °C.

General procedure C: Racemic reduction of imines

$NaBH_4$ (1.1 equiv) was added to a stirred solution of imine (1 equiv) in MeOH (0.25 M) at 0 °C. The reaction mixture was stirred at 0 °C for 1 hour, quenched with NaOH (10%w/vol, 1 mL) and extracted with EtOAc. The combined organic layers were washed with brine, dried over Na_2SO_4 and concentrated *in vacuo* to yield the crude amine.

N-Benzyl-phenylethan-1-amine [**3.6**].[122]

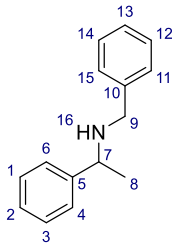

Synthesised from **3.5** (0.108 g, 0.516 mmol) using $NaBH_4$ (21.5 mg, 0.568 mmol) in accordance with *general procedure C* to afford the product as a colourless liquid 89 % (97.3 mg, 0.460 mmol). **^{1}H NMR** (400 MHz, $CDCl_3$) δ (ppm): 7.40-7.20 (m, 10H, $H_{1\text{-}4,6,11\text{-}15}$), 3.82 (q, *J* = 6.6 Hz, 1H, H_7), 3.67 (d, *J* = 13.2 Hz, 1H, H_9), 3.60 (d, *J* = 13.2 Hz, 1H, H_9), 1.61 (br. s, 1H, H_{16}), 1.38 (d, *J* = 6.6 Hz, 3H, H_8). **^{13}C NMR** (101 MHz, $CDCl_3$) δ (ppm): 145.6, 140.6, 128.5, 128.4, 128.1, 126.9, 126.8, 126.7, 57. 5, 51.7, 24.5. Data is in accordance with the literature.[122]

N-Phenylethyl-1-phenylethan-1-amine, [**3.83**][211]

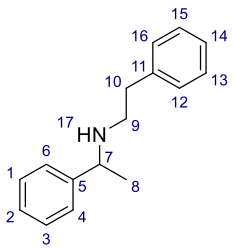

Synthesised from **3.83** (0.100 g, 0.571 mmol) using $NaBH_4$ (23.7 mg, 0.628 mmol) according to *general procedure C* to afford the product a colourless liquid in 97% yield (0.196 g, 0.928 mmol). **^{1}H NMR** (400 MHz, $CDCl_3$) δ (ppm): δ 7.48 – 7.07 (m, 10H, $H_{1\text{-}4,6,12\text{-}16}$), 3.83 (q, *J* = 6.6 Hz, 1H, H_7), 2.95 – 2.62 (m, 4H, $H_{9,10}$), 1.55 (br. s, 1 H, H_{17}), 1.39 (d, *J* = 6.6 Hz, 3H, H_8). **^{13}C NMR** (101 MHz, $CDCl_3$) δ (ppm): 145.4, 139.9, 128.5, 128.2, 128.2, 126.7, 126.4, 125.9, 58.0, 48.7, 36.2, 24.2. Data in accordance with the literature.[211]

N-(1-phenylethyl)butan-1-amine, [**3.87**][214]

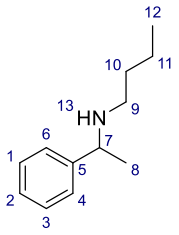

Synthesised from **3.83** (0.100 g, 0.57 mmol) using $NaBH_4$ (24.0 mg, 0.63 mmol) according to *general procedure C* to afford the product as a light brown liquid in 59% yield (60 mg, 0.337 mmol). **^{1}H NMR** (400 MHz, $CDCl_3$) δ (ppm): 7.43 – 7.28 (m, 4H, Ar), 7.28 – 7.19 (m, 1H, Ar), 3.76 (q, *J* = 6.6 Hz, 1H, H_7), 2.59 – 2.32 (m, 2H, H_9), 1.64 (br s,1H, H_{13}), 1.48 – 1.39 (m, 2H, H_{10}), 1.36 (d, *J* = 6.6 Hz, 3H, H_8), 1.34 – 1.22 (m, 2H, H_{11}), 0.88 (t, *J* = 7.3 Hz, 3H, H_{12}). **^{13}C NMR** (101 MHz, $CDCl_3$) δ (ppm): 145.8, 128.3, 126.8, 126.5, 58.4, 47.5, 32.4, 24.3, 20.4, 14.0. **FTIR** (neat) ν_{max} (cm^{-1}): 3086 (w), 3057 (w), 3032 (w), 2957 (m), 2955 (m), 2879 (m), 2857 (m). **HRMS-ESI$^+$** calc. for $[C_{12}H_{20}N]^+$ expect 178.1590, found 178.1598. ^{1}H NMR Data in accordance with the literature.[214]

N-Benzyl-1-(4-ethoxyphenyl)ethan-1-amine, [**7.21**]

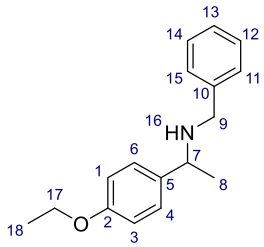

Synthesised from **7.1** (0.500 g, 1.97 mmol) using $NaBH_4$ (82.1 mg, 2.17 mmol) in accordance with *general procedure C* to afford the product as a pale yellow liquid in 86% yield (0.437 g, 1.70 mmol). **^{1}H NMR** (400 MHz, $CDCl_3$) δ (ppm): δ 7.40 – 7.14 (m, 7H, Ar), 6.95 – 6.81 (m, 2H, Ar), 4.04 (q, *J* = 7.0 Hz, 2H, H_{17}), 3.77 (q, *J* = 6.6 Hz, 1H, H_7), 3.66 (d, *J* = 13.2 Hz, 1H, H_9), 3.59 (d, *J* = 13.2 Hz, 1H, H_9), 1.58 (s, 1H, H_{16}), 1.42 (t, *J* = 7.0 Hz, 3H, H_{18}), 1.35 (d, *J* = 6.6 Hz, 3H, H_8). **^{13}C NMR** (101 MHz, $CDCl_3$) δ (ppm): 157.9, 140.7, 137.4, 128.3, 128.1, 127.7, 126.8, 114.4, 63.4, 56.8, 51.6, 24.4, 14.9. **FTIR** (neat) ν_{max} (cm^{-1}): 3314 (vw), 3059 (w), 3027 (w), 2977 (m), 2873 (w), 2833 (w), 1610 (m), 1584 (m), 1509 (s). **HRMS-ESI$^+$** (m/z): calc. for $[C_{17}H_{22}NO]^+$ expect 256.1696, found 256.1702.

N-Benzyl-1-(4-iodophenyl)ethan-1-amine, [**7.22**]

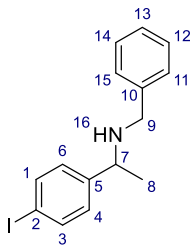

Synthesised from **7.2** (0.500 g, 1.49 mmol) using $NaBH_4$ (62.1 mg, 1.64 mmol) in accordance with *general procedure C* and purified by FCC (20% EA in PE) to afford the product as a yellow liquid in quantitative yield (0.501 g, 1.49 mmol). **^{1}H NMR** (400 MHz, $CDCl_3$) δ (ppm): 7.69 (d, *J* = 8.2 Hz, 2H, Ar), 7.40 – 7.21 (m, 5H, Ar), 7.13 (t, *J* = 7.4 Hz, 2H, Ar), 3.78 (q, *J* = 6.5 Hz, 1H, H_7), 3.66 (d, *J* = 13.2 Hz, 1H, H_9), 3.58 (d, *J* = 13.2 Hz, 1H, H_9), 1.61 (br s, 1H, H_{16}), 1.35 (d, *J* = 6.6 Hz, 3H, H_8). **^{13}C NMR** (101 MHz, $CDCl_3$) δ (ppm): 145.3, 140.3, 137.5, 128.8, 128.4, 128.0, 126.9, 92.0, 57.0, 51.6, 24.5. **FTIR** (neat) ν_{max} (cm^{-1}): 3564 (w), 3029 (w), 2885 (w), 1869 (w), 1819 (w), 1684 (w), 1625 (s), 1603 (m), 1578 (s), 1550 (m). **HRMS-ESI$^+$** (m/z): calc. for $[C_{16}H_{17}IN]^+$ expect 338.0400, found 338.0406.

N-Benzyl-1-(3,5-diflourophenyl)ethan-1-amine, [**7.23**]

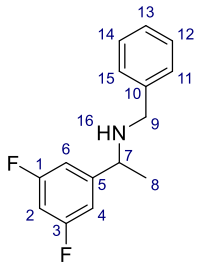

Synthesised from **7.3** (0.500 g, 2.04 mmol) using $NaBH_4$ (84.8 mg, 2.24 mmol) according to *general procedure C* to afford the product as a colourless liquid in 83% yield, (0.416 g, 1.68 mmol). **^{1}H NMR** (400 MHz, $CDCl_3$) δ (ppm): δ 7.41 – 7.15 (m, 5H, H_{15}-H_{11}), 6.99 – 6.79 (m, 2H, H_6, H_4), 6.68 (tt, *J* = 8.9, 2.4 Hz, 1H, H_2), 3.80 (q, *J* = 6.6 Hz, 1H, H_7), 3.67 (d, *J* = 13.2 Hz, 1H, H_9), 3.58 (d, *J* = 13.2 Hz, 1H, H_9), 1.54 (br s, 1H, H_{16}), 1.33 (d, *J* = 6.6 Hz, 3H, H_8). **^{13}C NMR** (101 MHz, $CDCl_3$) δ (ppm): 163.4 (dd, $^1J_{C\text{-}F}$ = 248.0, $^3J_{C\text{-}F}$ = 12.6 Hz), 150.4 (t, $^3J_{C\text{-}F}$ = 7.9 Hz), 140.3, 128.6, 128.2, 127.2, 109.7 – 109.2 (m), 102.3, (t, $^2J_{C\text{-}F}$ = 25.5 Hz), 57.2, 51.8, 24.6. **^{19}F NMR** (376 MHz, $CDCl_3$) δ (ppm): -110.0 – -110.1 (m). **FTIR** (neat) ν_{max} (cm^{-1}): 3391 (w), 3084 (w), 3062 (w), 3027 (w), 2925 (w), 2835 (w), 1623 (s), 1595 (s). **HRMS-ESI$^+$** (m/z): calc. for $[C_{15}H_{16}F_2N]^+$ expect 248.1245, found 248.1234.

N-Benzyl-2,2,2-trifluoro-1-phenylethan-1-amine, [**7.35**][215]

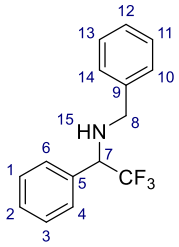

Synthesised from **7.8** (0.50 g, 1.90 mmol) using $NaBH_4$ (79.0 mg, 2.09 mmol) according to *general procedure C* and purified by FCC (20% EA & 10 % DCM in PE) to afford the product as a colourless liquid in 69% yield, (0.349 g, 1.32 mmol). **^{1}H NMR** (400 MHz, $CDCl_3$) δ (ppm): 7.60 –7.27 (m, 10H, Ar), 4.13 (q, *J* = 7.5 Hz, $1H_7$), 3.83 (d, *J* = 13.4 Hz, $1H_8$), 3.66 (d, *J* = 13.4 Hz, $1H_8$), 2.03 (s, br. 1H, H_{15}). **^{19}F NMR** (376 MHz, $CDCl_3$) δ (ppm): -73.9. **^{13}C NMR** (101 MHz, $CDCl_3$) δ (ppm): 139.1, 128.9, 128.8, 128.8, 128.7, 128.7, 128.3, 127.5, 125.6 (q, $^1J_{C\text{-}F}$ = 281.3 Hz), 63.5 (q, $^2J_{C\text{-}F}$ = 28.7 Hz), 51.1.Data in accordance with the literature[215]

4-(1-Benzylamino)ethyl)-3-methylphenol, [**7.26**]

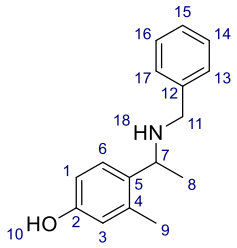

Synthesised from **7.6** (0.500 g, 2.09 mmol) using $NaBH_4$ (86.9 mg, 2.30 mmol) according to *general procedure C* to afford the product as a yellow amorphous solid 99% yield (0.500 g, 2.07 mmol). **^{1}H NMR** (400 MHz, MeOD-d_4) δ (ppm): 7.31 – 7.16 (m, 6H, $H_{6,13\text{-}17}$), 6.67 (dd, *J* = 8.4, 2.5 Hz, 1H, H_1), 6.57 (d, *J* = 2.5 Hz, 1H, H_3), 3.93 (q, *J* = 6.6 Hz, 1H, H_7), 3.61 (d, *J* = 13.0 Hz, 1H, H_{11}), 3.52 (d, *J* = 13.0 Hz, 1H, H_{11}), 2.05 (s, 3H, H_9), 1.27 (d, *J* = 6.6 Hz, 3H, H_8). **^{13}C NMR** (101 MHz, MeOD-d_4) δ (ppm): 156.9, 140.8, 137.9, 134.5, 129.6, 129.4, 128.1, 127.4, 117.9, 114.4, 52.3, 51.8, 22.9, 19.3. **FTIR** (neat) υ_{max} (cm^{-1}): 3313 (w), 3008 – 2484 br (w), 2931 (m), 1602 (s). **HRMS-ESI$^+$** (m/z): calc. for $[C_{16}H_{20}NO]^+$ expect 242.1539, found 242.1545.

N-(4-(1-Benzylamino)ethyl)phenyl)acetamide, [**7.27**]

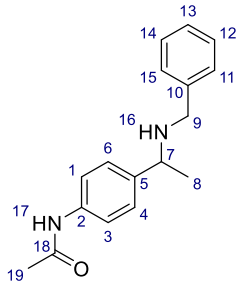

Synthesised from **7.7** (0.500 g, 1.88 mmol) using $NaBH_4$ (78.0 mg, 2.06 mmol) according to *general procedure C* to afford the product as a yellow amorphous solid in quantitative yield (0.502 g, 1.87 mmol). **^{1}H NMR** (400 MHz, $CDCl_3$) δ (ppm): 7.78 (s, 1H, H_{17}), 7.49 (d, *J* = 8.4 Hz, 2H, $H_{1,3}$), 7.40 – 7.13 (m, 7H, $H_{4,6,11\text{-}15}$), 3.78 (q, *J* = 6.5 Hz, 1H, H_7), 3.64 (d, *J* = 13.1 Hz, 1H, H_9), 3.57 (d, *J* = 13.2 Hz, 1H, H_9), 2.15 (s, 3H, H_{19}), 1.74 (s, 1H, H_{16}), 1.33 (d, *J* = 6.6 Hz, 3H, H_8). **^{13}C NMR** (101 MHz, $CDCl_3$) δ (ppm): 168.5, 141.5, 140.5, 136.7, 128.3, 128.0, 127.2, 126.8, 120.2, 56.9, 51.5, 24.4, 24.4. **FTIR** (neat) υ_{max} (cm^{-1}): 3292 (m), 3254 (m), 3198 (w), 3062 (w), 3087 (w), 3021 (w),

2962 (m), 2876 (w), 2836 (w), 2801 (w), 1661 (s), 1605 (s). **HRMS-ESI**$^{+}$ (m/z): calc. for $[C_{17}H_{20}N_2ONa]^+$ expect 291.1468, found 291.1472.

Methyl 4-(1-Benzylamino)ethyl)benzoate, [**7.28**]

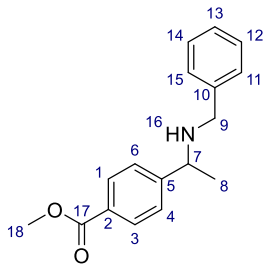

Synthesised from **7.8** (0.500 g, 1.87 mmol) using $NaBH_4$ (77.8 mg, 2.06 mmol) according to *general procedure C* to afford the product a pale yellow amorphous solid in 99% yield (0.497 g, 1.85 mmol). **^{1}H NMR** (400 MHz, $CDCl_3$) δ (ppm): 8.02 (d, J = 8.3 Hz, 2H, $H_{1,3}$), 7.44 (d, J = 8.2 Hz, 2H, $H_{4,6}$), 7.36 – 7.13 (m, 5H, $H_{11\text{-}15}$), 3.92 (s, 3H, H_{18}), 3.88 (q, J = 6.7 Hz, 1H, H_7), 3.64 (d, J = 13.2 Hz, 1H, H_9), 3.58 (d, J = 13.1 Hz, 1H, H_9), 1.37 (d, J = 6.6 Hz, 3H, H_8). **^{13}C NMR** (101 MHz, $CDCl_3$) δ (ppm): 167.0, 151.0, 140.2, 129.8, 128.9, 128.4, 128.1, 126.9, 126.7, 57.3, 52.0, 51.6, 24.3. **FTIR** (neat) ν_{max} (cm^{-1}): 3329 (m), 3028 (w), 2964 (w), 2886 (w), 2826 (w), 2805 (w), 1709 (s), 1609 (m), 1575 (m). **HRMS-ESI**$^{+}$ (m/z) calc. for $[C_{17}H_{20}NO_2]^+$ expect 270.1489, found 270.1494.

Amides:

N-Benzyl-*N*-1-phenylethylbenzamide [**3.7**][216]

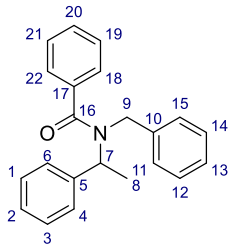

To a stirred solution of *N*-Benzyl-*N*-1-phenylethylamine **2.6** (44 mg, 0.21 mmol, 1 equiv) and Et_3N (29.3 µL, 0.21 mmol, 1 equiv) in CH_2Cl_2 at 0 °C benzoyl chloride (24.4 µL, 0.21 mmol, 1 equiv) was added dropwise. The reaction mixture was allowed to warm up to room temperature and was stirred for 1 hour after which the reaction was quenched with $NaHCO_3$ (aq., sat.), extracted with EtOAc, dried over Na_2SO_4 and concentrated *in vacuo*. The crude product was purified by flash column chromatography (15% EA in PE) to yield the product as a white solid (54.8 mg, 0.17mmol, 83%).**^{1}H NMR** (400 MHz, $CDCl_3$) δ (ppm): 7.68-6.89 (m, 15H, $H_{1\text{-}4,6,11\text{-}15,18\text{-}22}$), 5.24 (s, 1H, H_7), 5.03 (br. s, 1H, H_9), 3.97 (br. s 1H, H_7), 1.49 (d, J = 7.0 Hz, 3H, H_8). **^{13}C NMR** (101 MHz, $CDCl_3$) δ (ppm): 172.7, 140.4, 138.9, 129.4, 128.6, 128.3, 127.5, 127.1, 126.8, 126.4, 57.2, 45.3, 18.2. ^{1}H NMR is in accordance with the literature.[216]

General procedure D: Acylation of racemic reference amines

Et_3N (1.1 equiv) and Ac_2O (1.1 equiv) was added to a stirred solution of amine in MeCN (0.35 M). The reaction mixture was stirred at room temperature for 4 hours, then quenched with $NaHCO_3$ (aq., sat.), extracted with CH_2Cl_2, dried over Na_2SO_4 and concentrated *in vacuo* to yield the crude amide.

As for the benzyl amide **3.7** a mixture of rotamers was obtained for all the acyl amides. The rotamers were confirmed for a selected sample, through NMR analysis at 380 K. Chiral SFC analysis of the obtained amides revealed only two signals corresponding to the two enantiomers, further confirming the additional NMR signals being caused by rotamers. The NMR data given for the acylated amines below are for the major rotamer at 298 K.

General Procedure E: Acylation of crude screening mixture for reaction mixture e.e.

Acylation of amines in chapter 3 was carried out as follows: A small aliquot of the NMR sample was dried. Then Et_3N (4 µL) and Ac_2O (4 µL) was added to a stirred solution of amine in MeCN (0.5 mL). The reaction mixture was stirred at room temperature for 1 hour, then filtered through silica using MeCN as the eluent, and further filtered with a mixture of water and MeCN prior to be submitted for HPLC analysis.

General Procedure F: Acylation of crude screening mixture for crude reaction e.e.

Et_3N (100 µL) and Ac_2O (70µL) was added to a stirred solution of amine in MeCN (0.5 mL). The reaction mixture was stirred at room temperature for 4 hours, then quenched with $NaHCO_3$, taken into CH_2Cl_2, dried over Na_2SO_4 and concentrated. The amide was purified by prep TLC and extracted from the silica into 10% *i*-PrOH in *n*-hexane, filtered and analysed on the SFC.

N-Benzyl-*N*-(1-phenylethyl)acetamide, [**3.26**]

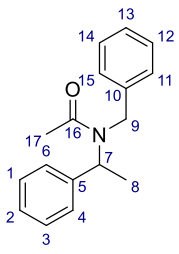

Synthesised from **3.6** (0.100 g, 0.473 mmol) using Ac_2O (50.0 µL, 0.521 mmol) and Et_3N (73.0 µL, 0.521 mmol) according to *general procedure D* and purified by FCC (10% EA in CH_2Cl_2) to afford the product as a white amorphous solid in 87% yield (104 mg, 0.411 mmol). **^{1}H NMR** (400 MHz, $CDCl_3$) δ (ppm): 7.39 – 7.19 (m, 8H, Ar), 7.09 (d, *J* = 7.4 Hz, 2H, Ar), 6.19 (q, *J* = 7.1 Hz, 1H, H_7), 4.41 (d, *J* = 17.9 Hz, 1H, H_9), 4.20 (d, *J* = 18.0 Hz, 1H, H_9), 2.06 (s, 3H, H_{17}), 1.44 (d, *J* = 7.2 Hz, 3H, H_8). **^{13}C NMR** (101 MHz, $CDCl_3$)

δ (ppm): 171.8, 141.0, 138.3, 128.6, 128.5, 127.6, 127.4, 127.0, 125.8, 51.4, 47.9, 22.5, 17.0. **FTIR**: (neat) ν_{max} (cm^{-1}): 2981 (w), 1630 (s), 1605 (m), 1512 (w). **HRMS-ESI$^+$**: calc. for $[C_{17}H_{20}NO]^+$ expect 254.1539, found 254.1541. **SFC Analysis:** CHIRAL-ART SA (CO_2/MeOH = 95/5, 2.5 mL min^{-1}, 40 °C) r_t= 5.32 (major), r_t= 6.49 (minor). SFC Analysis of sample prepared in accordance with *general procedure F:* 73% e.e. **HPLC Analysis**: Amylose-1 (MeCN:H_2O = 40:60, 1.5 mL min^{-1}, 25 °C) t_R = 37.29 (major), 57.23 (minor) minutes. Sample prepared according to *general procedure E*: 73 % e.e.

N-(4-Methoxyphenyl)-*N*-(1-phenylethyl)acetamide, [**3.78**]

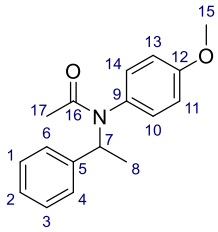

Racemic reduction was carried out following to *general procedure C* using **3.75** (0.20 g, 0.887 mmol) and $NaBH_4$ (36.9 mg, 0.977 mmol) to afford the crude product as a brown oil (153 mg). **^{1}H NMR** (400 MHz, $CDCl_3$) δ (ppm): 7.55 – 7.10 (m, 5H, Ar), 6.76 – 6.57 (m, 2H, Ar), 6.54 – 6.30 (m, 2H, Ar), 4.41 (q, *J* = 6.7 Hz, 1H, H_7), 3.69 (s, 3H, H_{15}), 1.54 (br. s, 1H, NH), 1.50 (d, *J* = 6.7 Hz, 3H, H_8). An aliquot of the crude product (55 mg) was submitted for acylation according to *general procedure D* using Ac_2O (35 µL, 0.417 mmol) and Et_3N (51 µL, 0.417 mmol). The crude acylation product was purified by FCC (20% EA in PE) to afford the product as a yellow liquid in 45% yield over two steps (51.1 mg, 0.228 mmol). **^{1}H NMR** (400 MHz, $CDCl_3$) δ (ppm): 7.42 – 7.13 (m, 7H, Ar), 6.73 – 6.63 (m, 1H, Ar), 6.53 – 6.36 (m, 1H, Ar), 6.29 (q, *J* = 7.2 Hz, 1H, H_7), 3.78 (s, 3H, H_{15}), 1.76 (s, 3H, H_{17}), 1.40 (d, *J* = 7.2 Hz, 3H, H_8). **^{13}C NMR** (101 MHz, $CDCl_3$) δ (ppm): 170.6, 159.1, 141., 131.6, 131.3, 128.1, 128.1, 127.4, 114.0, 55.3, 51.7, 23.4, 17.1. **HPLC Analysis**: Amylose-1 (MeCN:H_2O = 45:55, 1.5 mL min^{-1}, 25 °C) t_R = 11.27, 16.67 minutes. Sample prepared according to *general procedure E* was found to be racemic.

N-Benzyl-*N*-(1-phenylethyl)acetamide, [**3.80**][217]

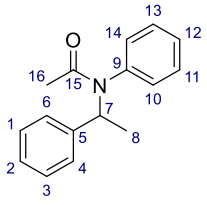

Racemic reduction was carried out following to *general procedure C* using **3.76** (0.15 g, 0.768 mmol) and $NaBH_4$ (32.0 mg, 0.845 mmol) to afford the crude product as a brown oil (153 mg). **^{1}H NMR** (400 MHz, $CDCl_3$) δ 7.52 – 7.17 (m, 5H), 7.09 (dd, *J* = 8.3, 7.5 Hz, 2H), 6.64 (t, *J* = 7.3 Hz, 1H), 6.52 (d, *J* = 7.8 Hz, 2H), 4.49 (q, *J* = 6.7 Hz, 1H, H_7), 1.52 (d, *J* = 6.7 Hz, 3H, H_8). An aliquot of the crude product (93 mg) was submitted for acylation according to *general procedure D* using Ac_2O (57 µL, 0.643 mmol) and Et_3N (79 µL, 0.643 mmol). The product was used crude for HPLC reference. **^{1}H NMR** (400 MHz, $CDCl_3$) δ 7.51 – 7.00 (m, 10H, Ar), 6.32 (q, *J* = 7.2 Hz, 1H, H_7), 1.77 (s, 3H, H_{16}), 1.42 (d, *J* = 7.2 Hz, 3H, H_8). **^{13}C NMR** (101 MHz, $CDCl_3$) δ (ppm): 169.9, 140.5, 138.3, 129.8, 127.8, 127.7, 127.5, 127.0, 106.1, 51.5, 22.8, 16.7.

Spectroscopic data is in accordance with the literature.[217] **HPLC Analysis**: Amylose-1 (MeCN:H_2O = 60:40, 1.5 mL min^{-1}, 25 °C) t_R = 8.10, 13.13 minutes. Sample prepared according to *general procedure E* was found to be racemic.

N-Phenylethyl-*N*-(1-phenylethyl)acetamide, [**3.85**]

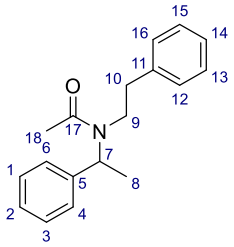

Synthesised from **3.84** (70.0 mg, 0.311 mmol) using Ac_2O (28.8 µL, 0.342 mol) and Et_3N (47.7 µL, 0.341 mmol) according to *general procedure D* and purified by FCC (10% EA in CH_2Cl_2) to afford the product as a yellow oil in 85% yield (70.8 mg, 0.265 mmol). **^{1}H NMR**[a] (400 MHz, $CDCl_3$) δ(ppm): 7.45 – 7.09 (m, 6H), 7.05 (d, *J* = 7.1 Hz, 2H), 6.93 (d, *J* = 7.0 Hz, 2H), 6.11 (q, *J* = 7.1 Hz, 1H, H_7), 5.11 (q, *J* = 6.9 Hz, 1H, H_7), 3.38 (ddd, *J* = 13.3, 11.6, 4.8 Hz, 1H, H, $H_{9/10}$), 3.29 – 3.09 (m, 3H, $H_{9,10}$), 2.79 (td, *J* = 12.0, 5.5 Hz, 1H, $H_{9/10}$), 2.68 – 2.56 (m, 1H, $H_{9/10}$), 2.68 – 2.56 (m, 1H, $H_{9/10}$), 2.52 (dd, *J* = 11.9, 7.2 Hz, 1H, $H_{9/10}$), 2.28 (s, 3H, H_{18}), 2.22 (s, 3H, H_{18}), 1.60 (d, *J* = 7.0 Hz, 3H, H_8), 1.56 (d, *J* = 7.1 Hz, 3H, H_8). **^{13}C NMR**[a] (101 MHz, $CDCl_3$) δ (ppm): 170.4, 170.3, 140.8, 140.4, 139.7, 138.2, 128.7, 128.6, 128.6, 128.4, 128.3, 128.2, 127.8, 127.6, 127.5, 126.8, 126.5, 126.0, 56.2, 50.9, 46.4, 45.1, 37.0, 35.0, 22.3, 21.9, 18.1, 17.0. **FTIR:** (neat) ν_{max} (cm^{-1}): 3063 (w), 3027 (w), 2977 (w), 2936 (w), 1635 (s), 1603 (m), 1583 (w). **HRMS-ESI$^+$** calc. for $C_{18}H_{22}NO^+$ expect 268.1696, found 268.1695. [a] NMR data for this compound contains both sets of rotamer peaks, since the rotamer peaks are ~1:1, which is why with the data in hand these cannot be distinguished and the carbon signals of both rotamers are included.

N-Butyl-*N*-(1-phenylethyl)acetamide [**3.88**]

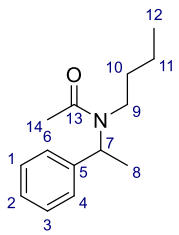

Synthesised from **3.87** (75.0 mg, 0.423 mmol) using Ac_2O (39.2 µL, 0.465 mmol) and Et_3N (64.9 µL, 0.465 mmol) according to *general procedure D* and purified by FCC (10% EA in CH_2Cl_2) to afford the product as a yellow oil in 61% yield (56.4 mg, 0.257 mmol). **^{1}H NMR** (400 MHz, $CDCl_3$) δ (ppm): 7.38 – 7.27 (m, 4H, $H_{1,3\text{-}4,6}$), 7.24 (d, *J* = 7.0 Hz, 1H, H_2), 6.01 (q, *J* = 7.1 Hz, 1H, H_7), 3.07 – 2.95 (m, 1H, H_9), 2.96 – 2.84 (m, 1H, H_9), 2.14 (s, 3H, H_{14}), 1.50 (d, *J* = 7.2 Hz, 3H, H_8), 1.22 – 1.03 (m, 2H, 4H, $H_{10,11}$), 0.79 (dd, *J* = 7.1, 5.8 Hz, 3H, H_{12}). **^{13}C NMR** (101 MHz, $CDCl_3$) δ (ppm): 170.6, 141.2, 128.3, 127.5, 127.2, 50.8, 44.4, 32.8, 21.9, 20.3, 16.8, 13.5. **FTIR** (neat) ν_{max} (cm^{-1}): 2959 (m), 2932 (m), 2873 (w), 1633 (s). **HRMS-ESI$^+$** calc. for $[C_{14}H_{22}NO]^+$ expect 220.1696, found 220.1698.

N-Benzyl-*N*-(1-(4-ethoxyphenyl)ethyl)acetamide, [**7.29**]

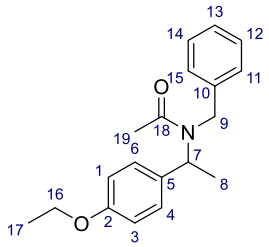

Synthesised from **7.21** (0.200 g, 0.783 mmol) using Ac_2O (73.5 µL, 0.862 mmol) and Et_3N (0.120 mL, 0.861 mmol) according to *general procedure D* and purified by FCC (10% EA in CH_2Cl_2) to afford the product as a beige liquid in 93% yield (217 mg, 0.730 mmol). **^{1}H NMR** (400 MHz, $CDCl_3$) δ (ppm): 7.30 – 6.96 (m, 7H), 6.83 (t, *J* = 8.2 Hz, 2H), 6.13 (q, *J* = 7.0 Hz, 1H, H_7), 4.35 (d, *J* = 17.9 Hz, 1H, H_9), 4.17 (d, *J* = 17.9 Hz, 1H, H_9), 3.98 (q, *J*= 6.9 Hz, 2H, H_{16}), 2.01 (s, H_{17}), 1.45 – 1.33 (m, 6H, $H_{8,19}$). **^{13}C NMR** (101 MHz, $CDCl_3$) δ (ppm): 171.4, 158.0, 138.1, 132.6, 128.5, 128.3, 126.7, 125.6, 114.1, 63.1, 50.6, 47.4, 22.3, 16.9, 14.6. **FTIR** (neat) ν_{max} (cm^{-1}): 3031 (w), 2979 (w), 2932 (w), 2876 (w), 1639 (s), 1610 (m), 1583 (w), 1510 (s). **HRMS-ESI$^+$**: calc. for $[C_{19}H_{24}NO_2]^+$ expect 298.1802, found 298.1801. **SFC Analysis**: Chiral-Art SA (CO_2/MeOH = 90/10, 2.5 mL min^{-1}, 40 °C) t_R = 3.74 (major), 4.40 (minor) minutes. Sample prepared according to general procedure X was found to be racemic. SFC Analysis of sample prepared in accordance with *general procedure F:* 67% e.e.

N-Benzyl-*N*-(1-(4-iodophenyl)ethyl)acetamide, [**7.30**]

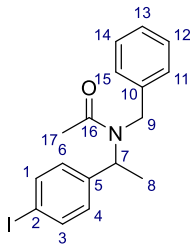

Synthesised **7.22** (0.200 g, 0.593 mmol) using Ac_2O (54.9 µL, 0.652 mmol) and Et_3N (91.0 µL, 0.652 mmol) according to *general procedure D* and purified by FCC (10% EA in CH_2Cl_2) to afford the product as a white amorphous solid in 90% yield (202 mg, 0.533 mmol). **^{1}H NMR** (400 MHz, $CDCl_3$) δ (ppm): 7.60 (d, *J* = 7.8 Hz, 2H), 7.37 – 6.99 (m, 6H), 6.94 (d, *J* = 7.2 Hz, 1H), 6.06 (q, *J* = 6.8 Hz, 1H, H_7), 4.39 (d, *J* = 17.9 Hz, 1H, H_9), 4.18 (d, *J* = 17.9 Hz, 1H, H_9), 2.04 (s, 3H, H_{17}), 1.38 (d, *J* = 7.1 Hz, 3H, H_8). **^{13}C NMR** (101 MHz, $CDCl_3$) δ (ppm): 171.5, 140.6, 137.7, 137.2, 129.3, 128.5, 126.9, 125.6, 92.8, 50.8, 47.8, 22.3, 16.6. **FTIR**: (neat) ν_{max} (cm^{-1}): 3059 (w), 3027 (w), 2970 (w), 2932 (w), 2876 (w), 1622 (s), 1585 (m). **HRMS-ESI$^+$**: calc. for $[C_{17}H_{19}INO]^+$: 380.0506 found 380.0507. **SFC Analysis**: Chiral-Art SB (CO_2/MeOH = 95/5, 2.5 mL min^{-1}, 40 °C) t_R =10.79, 11.49 minutes.

This sample was used for confirming the rotamer peaks for the acylated amines. **Figure SI-Exp-1** shows the H NMR spectrum at 298.15 K (top) and 380 K (bottom). Notice how the rotamers peaks have moved and merged at 380 K. The pseudo 2D spectrum in **Figure SI-Exp-2** shows the traces for how these signals merge.

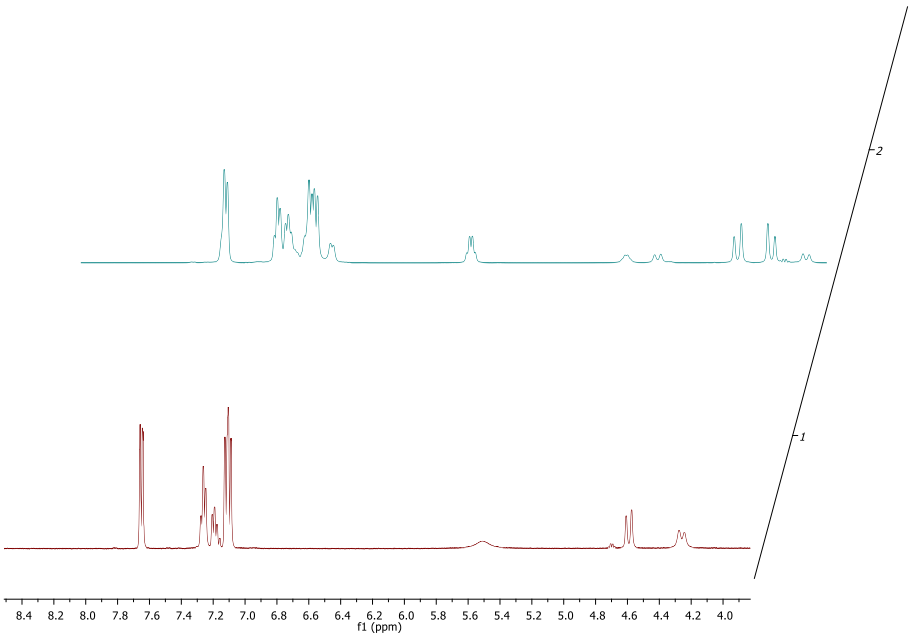

Figure SI-Exp-1: Top ^{1}H NMR at 298.15 K and bottom at 380 K in DMSO bottom.

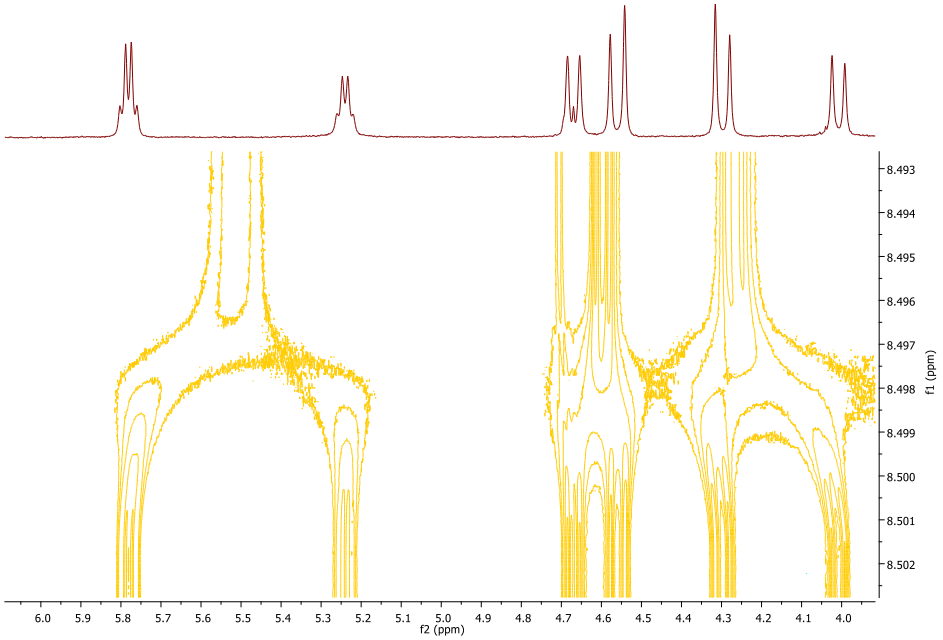

Figure SI-Exp-2: Pseudo-1D ^{1}H NMR showing how the signal merge together.

N-benzyl-*N*-(1-(3,5-difluorophenyl)ethyl)acetamide, [**7.31**]

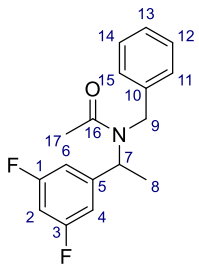

Synthesised **7.23** (0.206 mg, 0.833 mmol) using Ac_2O (77.1 µL, 0.916 mmol) and Et_3N (0.128 mL, 0.916 mmol) according to *general procedure D* and purified by FCC (10% EA in CH_2Cl_2) to afford the product as a colourless liquid in 91% yield (218 mg, 0.754 mmol). **^{1}H NMR** (400 MHz, $CDCl_3$) δ(ppm): 7.26 (t, *J* = 7.3 Hz, 2H), 7.21 – 7.15 (m, 1H), 7.07 (d, *J* = 7.5 Hz, 2H), 6.79 (d, *J* = 6.8 Hz, 2H, $H_{4,6}$), 6.61 (t, *J* = 8.7 Hz, 1H, H_2), 6.02 (q, *J* = 7.0 Hz, 1H, H_7), 4.44 (d, *J* = 17.9 Hz, 1H, H_9), 4.20 (d, *J* = 17.9 Hz, 1 H, H_9), 2.04 (s, 3H, H_{17}), 1.36 (d, *J* = 7.2 Hz, 3H, H_8). **^{13}C NMR** (101 MHz, $CDCl_3$) δ (ppm): 171.7, 162.9 (dd, $^1J_{C\text{-}F}$ = 248.5, $^3J_{C\text{-}F}$ = 12.8 Hz), 145.5 (t, $^3J_{C\text{-}F}$ = 8.2 Hz), 137.7, 128.6, 127.2, 125.7, 110.6 – 109.8 (m), 102.6 (t, $^2J_{C\text{-}F}$ = 25.4 Hz), 50.9, 48.0, 22.2, 16.8. **^{19}F NMR** (376 MHz, $CDCl_3$) δ(ppm): -109.5. **FTIR**: (neat) ν_{max} (cm^{-1}): 3063 (w), 3031 (w), 2985 (w), 2944 (w), 1643 (s), 1623 (s), 1594 (s). **HRMS-ESI$^+$**: calc. for $[C_{17}H_{18}F_2NO]^+$ expect 230.1351, found 230.1352. **SFC Analysis**: Chiral-Art SA (CO_2/MeOH = 95/5, 2.5 mL min^{-1}, 40 °C) t_R = 2.92 (major), 3.49 (minor) minutes. SFC analysis of sample prepared according to *general procedure F:* 50% e.e.

N-Benzyl-*N*-(2,3-dihydro-1H-inden-1-yl)acetamide, [**7.33**]

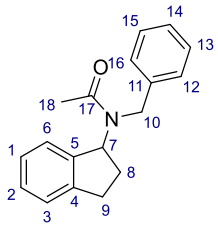

Racemic reduction was carried out following to *general procedure C* using **7.5** (0.23 g, 1.04 mmol) and $NaBH_4$ (43.3 mg, 1.14 mmol) to afford the crude product as a brown oil. **^{1}H NMR** (400 MHz, $CDCl_3$) δ (ppm): 7.61 – 6.91 (m, 9H), 4.33 (t, *J* = 6.7 Hz, 1H, H_7), 3.97 (d, *J* = 13.1 Hz, 1H_{10}), 3.92 (d, *J* = 13.1 Hz, 1H, H_{10}), 3.05 (ddd, *J* = 15.7, 8.6, 4.8 Hz, 1H_9), 2.84 (dt, *J* = 15.7, 7.8 Hz, 1H_9), 2.46 (dtd, *J* = 12.6, 7.7, 4.7 Hz, 1H, H_8), 1.99 – 1.79 (m, 1H, H_8), 1.61 (s, br. 1H, NH). The crude product was acylated using **7.25** (115 mg, 0.515 mmol), Ac_2O (47.7 µL, 0.566 mmol) and Et_3N (79.0 µL, 0.566 mmol) according to *general procedure D* and purified by FCC (CH_2Cl_2) to afford the product as an orange solid in 16% yield over two steps (22.0 mg, 83 µmol). **^{1}H NMR** (400 MHz, $CDCl_3$) δ (ppm): 7.68 – 6.93 (m, 9H, Ar), 6.44 (s,[a] 1H, H_7), 4.53 (d, *J* = 17.8 Hz, 1H, H_{10}), 4.20 (d, *J* = 18.0 Hz, 1H, H_{10}), 2.83 (s,[b] 2H, H_9), 2.37 (s,[c] 2H, H_8), 2.13 (s, 3H, H_{18}). **^{13}C NMR** (101 MHz, $CDCl_3$) δ (ppm): 172.5, 143.8, 141.9, 138.5, 128.8, 127.9, 127.2, 126.7, 125.8, 125.0, 124.1, 59.5, 48.3, 30.4, 30.3, 22.6. **FTIR:** (neat) ν_{max} (cm^{-1}): 3563 (w), 3451 (w), 3183 (w), 2938 (w), 1645 (m), 1607 (m). **HRMS-ESI$^+$:** calc. for $[C_{18}H_{19}NONa]^+$ expect 288.1359, found 288.1365 In low concentration samples the coupling for these signals are visible and appears as a quartet for [a], a triplet for [b] and a multiplet for [c].

N-Benzyl-*N*-(1-(4-hydroxy-2-methylphenyl)ethyl)acetamide, [**7.34**]

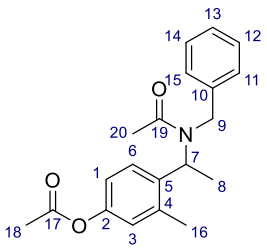

Synthesised from **7.26** (0.200 g, 0.829 mmol, 1 equiv) using Ac_2O (0.153 mL, 1.82 mmol, 2.2 equiv) and Et_3N (0.254 mL, 1.82 mmol, 2.2 equiv) according to *general procedure D* with 2.2 equiv of Ac_2O to allow for acetylation of both the secondary amine and the phenol. The crude product was purified by FCC (10% EA in CH_2Cl_2) to afford the product as a colourless oil in 74% yield (200 mg, 0.615 mmol). **^{1}H NMR** (400 MHz, $CDCl_3$) δ (ppm): 7.57 – 6.69 (m, 8H), 6.17 (q, *J* = 6.5 Hz, 1H, H_7), 4.38 (d, *J* = 17.6 Hz, 1H, H_9), 4.16 (d, *J* = 17.6 Hz, 1H, H_9), 2.31 (s, 6H, $H_{18,20}$), 2.11 (s, 3H, H_{16}), 1.48 (d, *J* = 6.9 Hz, 3H, H_8). **^{13}C NMR** (101 MHz, $CDCl_3$) δ (ppm): 171.0, 169.2, 149.9, 139.5, 138.0, 135.8, 128.4, 128.0, 127.0, 125.9, 123.5, 118.6, 48.9, 47.5, 22.4, 21.0, 19.2, 17.6. **FTIR:** (neat) ν_{max} (cm^{-1}): 3063 (vw), 3031 (w), 2975 (w), 2940 (w), 1757 (s), 1637 (s), 1586 (m). **HRMS-ESI$^+$** calc. for $[C_{20}H_{24}NO_3]^+$ expect 326.1756 found 326.1747. **SFC Analysis**: Chiral-Art SJ (CO_2/MeOH = 95/5, 2.5 mL min^{-1}, 40 °C) t_R = 4.19, 5.13 minutes. Sample prepared according to *general procedure F* was found to be racemic.

N-(1-4-Acetamidophenyl)-*N*-benzylacetamide, [**7.35**]

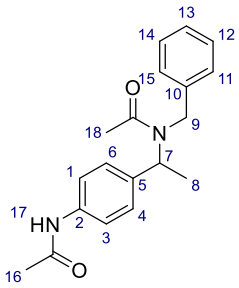

Synthesised from **7.27** (0.200 g, 0.745 mmol) using Ac_2O (69.0 µL, 0.820 mol) and Et_3N (0.114 mL, 0.820 mmol) according to *general procedure D* and purified by FCC (10% MeOH in CH_2Cl_2) to afford the product as a white amorphous solid in 98% yield (226 mg, 0.728 mmol). **^{1}H NMR** (400 MHz, $CDCl_3$) δ (ppm): 8.70 (s, 1H, H_{17}), 7.48 (d, *J* = 8.3 Hz, 2H, $H_{1,3}$), 7.34 – 7.06 (m, 7H, $H_{4,6,11\text{-}15}$), 6.10 (q, *J* = 7.0 Hz, 1H, H_7), 4.38 (d, *J* = 17.9 Hz, 1H, H_9), 4.18 (d, *J* = 18.0 Hz, 1H, H_9), 2.13 (s, 3H, H_{16}), 2.04 (s, 3H, H_{18}), 1.39 (d, *J* = 7.1 Hz, 3H, H_8). **^{13}C NMR** (101 MHz, $CDCl_3$) δ (ppm): 172.1, 169.1, 138.1, 137.8, 136.4, 128.7, 127.9, 127.1, 125.8, 120.1, 51.3, 48.0, 24.4, 22.6, 17.2. **FTIR:** (neat) ν_{max} (cm^{-1}): 3305 (w), 3273 (w), 3190 (w), 3115 (w), 3059 (w), 3027 (w), 2984 (w), 2936 (w), 1688 (m), 1666 (m), 1619 (s), 1601 (s), 1535 (s), 1514 (s). **HRMS-ESI$^+$** calc. for $[C_{19}H_{23}N_2O_2]^+$ expect 311.1754, found 311.1760. **SFC Analysis**: Chiral-Art SJ (CO_2/MeOH = 95/5, 2.5 mL min^{-1}, 40 °C) t_R =5.76, 6.31 minutes.

Methyl 4-(1-(*N*-benzylacetamido)ethyl)benzoate, [**7.36**]

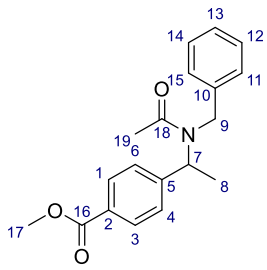

Synthesised from **7.28** (0.204 g, 0.757 mmol) using Ac_2O (70.1 µL, 0.833 mmol) and Et_3N (0.116 mL, 0.833 mmol) according to *general procedure D* and purified by FCC (10% EA in CH_2Cl_2) to afford the product as a colourless oil in 89% yield (209 mg, 0.672 mmol). **^{1}H NMR** (400 MHz, $CDCl_3$) δ (ppm): 7.97 (d, *J* = 8.1 Hz, 2H), 7.36 (d, *J* = 8.0 Hz, 2H), 7.31 – 7.25 (m, 1H), 7.22 (d, *J* = 6.7 Hz, 2H), 7.08 (d, *J* = 7.4 Hz, 2H), 6.16 (q, *J* = 7.1 Hz, 1H, H_7), 4.43 (d, *J* = 17.9 Hz, 1H, H_9), 4.18 (d, *J* = 17.9 Hz, 1H, H_9), 3.89 (s, 3H, H_{17}), 2.07 (s, 3H, H_{19}), 1.45 (d, *J* = 7.1 Hz, 3H, H_8). **^{13}C NMR** (101 MHz, $CDCl_3$) δ (ppm): 171.8, 166.7, 146.3, 137.8, 129.7, 129.2, 128.6, 127.4, 127.1, 125.7, 52.0, 51.3, 48.1, 22.4, 16.9. **FTIR**: (neat) ν_{max} (cm^{-1}): 3031 (w), 2984 (w), 2951 (w), 1717 (s), 1642 (s), 1609 (m), 1575 (w). **HRMS-ESI**$^+$calc. for $[C_{19}H_{22}NO_3]^+$ expect 312.1594, found 312.1596. **SFC Analysis**: Chiral-Art SJ (CO_2/MeOH = 95/5, 2.5 mL min^{-1}, 40 °C) t_R = 5.74 (major), 6.29 (minor) minutes. Sample prepared according to *general procedure F*: 39% e.e.

Indium(III) complexes

Indium(III) triflimidate [34]

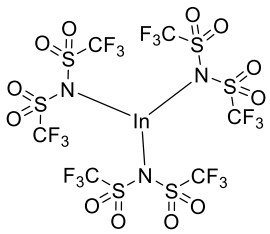

Indium(III) oxide (30.0 mg, 0.108 mmol, 1 equiv) and triflimidic acid (121.5 mg, 0.432 mmol, 4 equiv) was reflux in water (0.1 M) for 24 hours, then allowed to cool to ambient temperature. The resulting white beige suspension was filtered through celite, concentrated and dried *in vacuo* for 36 hours at 130 °C to afford the product as a white amorphous solid in 45% yield (46.0 mg, 48.1 µmol). **^{13}C NMR** (101 MHz, CD_3CN) δ (ppm): 118.3. **^{19}F NMR** (376 MHz, CD_3CN) δ (ppm): -80.2 (d, *J* = 1.3 Hz). **HRMS**[a] calc. for $C_6F_{18}InN_3O_{12}S_6$ expect 954.6558, found 954.6620. [a] run in negative mode on VION. Neutral mass observed. Observed m/z 953.6547.

[{In((*R*)-BINOLate)$_3$}{Na(THF)$_2$}$_3$]

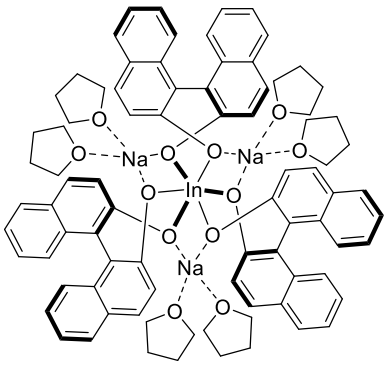

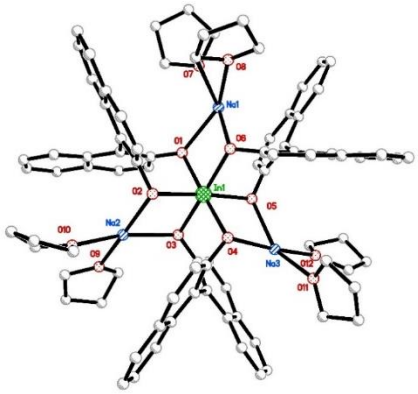

NaH (7.7 mg, 0.32 mmol, 33% in mineral oil, 6.6 eq.) was washed with hexane (3 · 1 mL) to remove the oil and dried. THF (0.5 mL) was added and the resulting suspension was cooled to 0 °C. To this stirred suspension (*R*)-BINOL (30.7 mg, 0.107 mmol, 2.2 eq.) was added. Everything was dissolved and the clear yellow solution was stirred allowed to warm to room temperature and stirred for 30 min. $InBr_3$ (17.3 mg, 0.049 mmol, 1 eq.) was added, and the formation of a white precipitate was observed, while the liquid turned colourless. This reaction mixture was stirred at room temperature for additional 19 hours, after which stirring was discontinued to allow the precipitate to settle. The supernatant was transferred to a dry flask. The THF was removed and the resulting light yellow-beige solid crystallised from THF and CH_2Cl_2 to yield colourless squared crystals. Storage in CH_2Cl_2 lead to the growing of longer needle shaped crystals. **^{1}H NMR**[a] (400 MHz, $CDCl_3$) δ (ppm): 7.98 (d, *J* = 7.9 Hz, 2H, Ar), 7.90 (d, *J* = 8.5 Hz, 2H, Ar), 7.45-7.29 (m, 7H, Ar), 7.16 (d, *J* = 7.6 Hz, 2H, Ar), 5.06 (s, br, 1H, OH), 3.75 (t, *J* = 6.2 Hz, 12H, THF), 1.86 (t, *J* = 6.4 Hz, 12H, THF). [a] of the dried crystals. The ^{1}H NMR spectrum of the dried crystals is very similar to the spectrum of BINOL. **FTIR** (neat) ν_{max} (cm^{-1}): 3284 br, 3045, 2971, 2873, 2337, 2151, 1615, 1589, 1558, 1501, 1461, 1423, 1352, 1338, 1273, 1244, 1211, 1177, 1143, 1126, 1051. The ^{1}H NMR spectrum of the complex in the crystallisation solution contains more aromatic signals than the spectrum for the dried crystals: **^{1}H NMR** (400 MHz, $CDCl_3$) δ (ppm): 7.96 – 7.75 (m, 14H), 7.73 – 7.67 (m, 1H), 7.64 – 7.54 (m, 1H), 7.49 – 7.32 (m, 6H), 7.18 – 6.72 (m, 17H). In addition, solvent signals are present. Unfortunately, there was not enough material for ^{13}C-NMR. However, for this complex the crystal structure contains all information about the actual structure of the complex. **MP**: Decompose at 150 °C. **X-Ray:** Access data in repository. https://doi.org/10.17863/CAM.34949

[{In((*R*)-BINOLate)$_3$}{Li(THF)$_2$}{Li(THF)}$_2$]

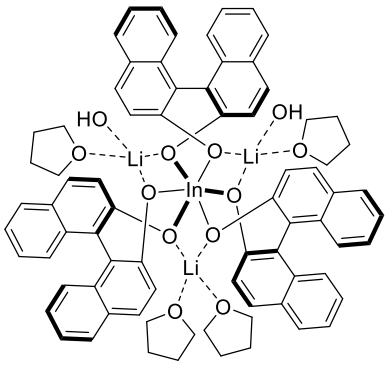

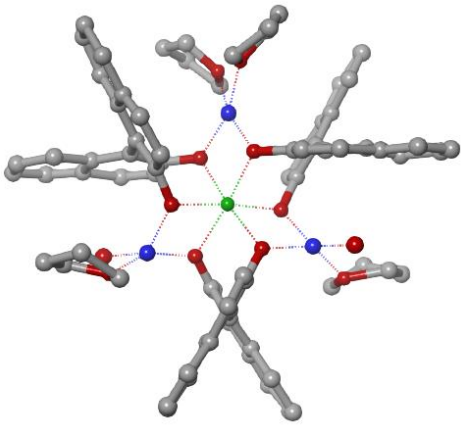

To a stirred solution of (*R*)-BINOL (45 mg, 0.157mmol, 3.1 equiv) in THF (0.5 mL) at 0 °C *n*-BuLi (197 µL, 1.6 M in hexane, 6.2 equiv) was added dropwise. The resulting yellow solution was allowed to warm to room temperature. $InBr_3$ (18 mg, 0.05 mmol, 1 equiv) was added and the suspension refluxed for two hours. The orange reaction mixture was allowed to cool to room temperature and concentrated to afford an orange solid. The solid was suspended in toluene and after 24 hours the suspension was filtered to remove the white salt of LiBr. The yellow liquid was concentrated and suspended in THF. The suspension was heated to 60 °C, followed by cooling to room temperature overnight, causing colourless square crystals to fall out. Dried crystals: **^{1}H NMR** (400 MHz, $CDCl_3$) δ (ppm): 8.00 (d, *J* = 8.9 Hz, 2H), 7.91 (d, *J* = 7.8 Hz, 2H), 7.44 – 7.30 (m, 7H + toluene), 7.22 – 7.11 (m, 2H + toluene), 5.04 (s, 1H), 4.46 (s, 1H), 3.77-3.73 (m, 4H, THF), 1.88-1.84 (m, 4H, THF). The ^{1}H-NMR spectrum of the dried crystals is very similar to the spectrum of BINOL. Dried crystals: **FTIR**: (neat) ν_{max} (cm^{-1}): 3383 br, 3042, 1616, 1588, 1557, 1498, 1466, 1454, 1424, 1344, 1272, 1246, 1209, 1143, 1072. The IR spectrum contains a broad strong signal at 3383, which is not reported in the literature.[160] However, IR in the literature may be of the solvated structure. Further comparison with the literature[160] does not reveal significant information, as the peaks between 1650 and 1000 in general exhibit similarity to the IR spectrum of BINOL. Solvated crystals in the THF solution: **^{1}H NMR** (400 MHz, $CDCl_3$) δ (ppm): 8.44 – 7.26 (m, 14H), 7.21 – 6.38 (m, 20H), 6.31 (d, *J* = 8.9 Hz, 1H), 5.78 (dd, *J* = 20.2, 8.5 Hz, 1H), 4.09 – 3.35 (m, 60H), 2.03 – 1.63 (m, 60H). A detailed comparison of the ^{1}H-NMR data with the literature[160] is not possible, as BINOLate protons in the literature[160] are reported from 6.62 ppm to 7.84 in a multiplet of 113 protons, which also include protons from toluene. **^{13}C NMR** (101 MHz, $CDCl_3$) δ (ppm): 148.7, 134.7, 133.8, 133.8, 133.8, 132.8, 130.6, 129.5, 128.8, 128.1, 128.1, 128.1, 127.8, 126.8, 125.8, 125.7, 125.7, 125.6, 125.3, 125.2, 124.4, 124.4, 124.4, 124.3, 123.8, 122.7, 122.0, 121.8, 120.9, 118.3, 67.9 (THF), 25.5 (THF). The majority of the signals in this carbon spectrum is borderline with regards to differing from baseline, even though 7000 scans were recorded. It is plausible that signals are missing *e.g.* from quartenary carbon atoms. Therefore, this carbon spectrum should not be used for any other conclusion than it is significantly different from BINOL. Both ^{1}H-^{1}H-COSY and ^{1}H-^{13}C-HSQC spectra were recorded. However, even though both

2D spectra contain certain distinct patterns, the complexity has not allowed for assignment of the signals in the ^{1}H NMR and ^{13}C NMR based on these recorded 2D spectra. In the literature a ^{13}C NMR spectrum with less signals is reported. This was recorded in C_6D_6, which could be a future possibility. However, the reported spectrum was from crystals which had been recrystallised from THF and toluene, and contained toluene in the crystal structure. **MP**: Decompose at 150 °C. **X-Ray**: Access data in repository: https://doi.org/10.17863/CAM.34949

Supplementary Tables:

Table SI-3.3.1: Examining factors affecting the conversion.

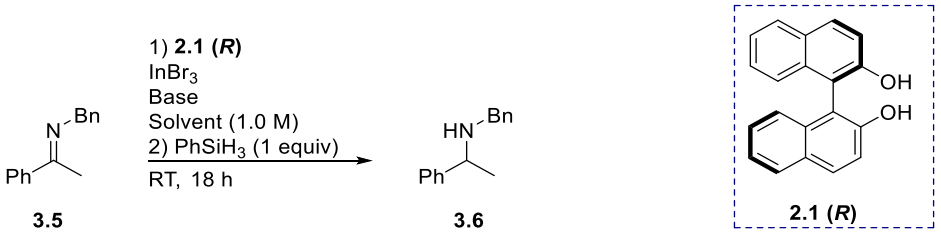

Entry	Solvent	Temperature [°C]	In(III) : 2.1 (*R*) [mol%]	DIPEA [mol%]	Conversion[a] [%]
1	CH_2Cl_2	40	10:10	20	81[b]
2	CH_2Cl_2	40	5:10	20	43
3	$CHCl_3$	40	10:10	20	71
4	CH_2Cl_2	40	10:10	20	40
5	CH_2Cl_2	40	10:10	20	58[c]
6	CH_2Cl_2	30	10:10	20	64
7	$CHCl_3$	40	5:10	40	20
8	CH_2Cl_2	RT	10:10	20[d]	24
9	CH_2Cl_2	RT	5:10	40[d]	0
10	CH_2Cl_2	RT	5:5	20	9[e]
11	CH_2Cl_2	RT	10:10	20	24[f]
12[g]	CH_2Cl_2	RT	15:15	30	46
13[g]	CH_2Cl_2	30	10:0	-	56
14[g]	CH_2Cl_2	30	5:0	10	10
15[g]	CH_2Cl_2	30	10:10	20	20[h]
16[g]	CH_2Cl_2	30	10:30	60	0
17[g]	CH_2Cl_2	30	10:10	50	10
18[g]	CH_2Cl_2	RT	10:10	10	38
19[g]	CH_2Cl_2	RT	0:0	-	0

[a] Conversion of imine to amine determined by crude NMR with 1,3,5-trimethoxybenzene as internal standard [b] 66% isolated yield. [c] 0.5 equiv silane. [d] Cy_2NMe used as base. [e] silane added before the imine. [f] $InBr_3$ and **2.1 (*R*)** were pre-dried *in vacuo* for 12 hours prior to used. [g] 0.7 M. [h] 1.5 equiv silane.

The reaction proceeds independent of the presence of ligand (entry 13, 14). However, the reaction needs In(III) to proceed (entry 19). Addition of increase amount of base decreases the conversion significantly (entry 16,17). Cy_2NMe resulted in a more pronounced decrease in conversion than DIPEA (entry 8,9).

Table SI-3.3.1.1: Solvent screen with and without base using ligand **2.1 (*R*)**.

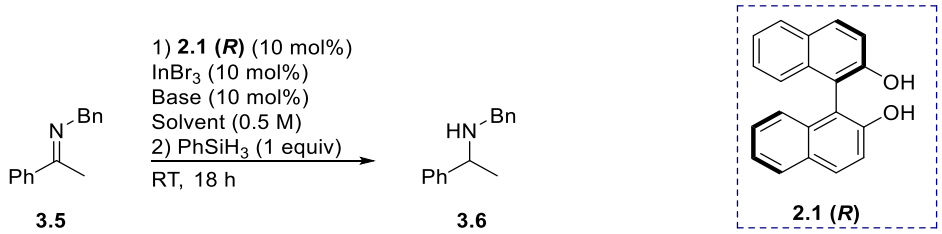

3.5 **3.6** **2.1 (*R*)**

Entry	Solvent	Base	Conversion[a] [%]	e.e.[b] [%]
1	MeOH	-	>99	0
2	MeOH	DIPEA	>99	0
3	EtOH	-	>99	0
4	EtOH	DIPEA	>99	0
5	MeCN	-	>99	0
6	MeCN	DIPEA	18	0
7	THF	-	66	0
8	THF	DIPEA	50	0
9	Et_2O	-	56	0
10	Et_2O	DIPEA	20	0
11	$C_2H_4Cl_2$	-	63	0
12	$C_2H_4Cl_2$	DIPEA	67	0
13	DMSO	-	67	0
14	DMSO	DIPEA	50	0
15	DMF	-	63	0
16	DMF	DIPEA	33	0
17	*n*-hexene	-	67	0
18	*n*-hexene	DIPEA	25	0
19	toluene	-	63	0
20	toluene	DIPEA	33	0

All reactions carried out with 253 µmol imine. [a] Conversion of imine to amine determined by crude NMR with 1,3,5-trimethoxybenzene as internal standard. [b] e.e. of amine determined by chiral stationary phase RP-HPLC

Unfortunately, all amine products were found to be racemic with **2.1 (*R*)** independent of the solvent and the presence of base.

Table SI-3.4.1: Testing amide formation

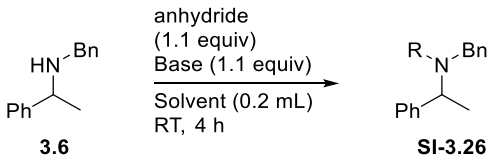

3.6 **SI-3.26**

Entry	Anhydride[a]	Base	Solvent	Crude HPLC analysis[b]
1	Ac_2O	Et_3N	THF	Full conversion, Excellent separation [c]
2	Ac_2O	Et_3N	MeCN	Full conversion, Excellent separation [c]
3	Ac_2O	Et_3N	CH_2Cl_2	Full conversion, Excellent separation [c]
4	Boc_2O	Et_3N	THF	Only **3.6**
5	Boc_2O	Et_3N	MeCN	Only **3.6**
6	Boc_2O	Et_3N	CH_2Cl_2	Low conversion
7	Boc_2O	$NaHCO_3$	THF:H_2O 1:1	Only **3.6**
8	Boc_2O	Et_3N, DMAP	THF	Low conversion

All reactions were carried out using 47 μmol amine. [a] Dimethyl carbonate was also for amine modification, but several compounds were found by chiral stationary phase RP-HPLC analysis. [b] Amylose-1, MeCN:H_2O 60:40. [c] separation between the two enantiomeric peaks. An impurity fronted the first enantiomer peak and on the crude amide prepared from In(III)-catalysed reactions further impurities were found. Excellent separation between both enantiomeric peaks and impurities were found at MeCN: H_2O 40:60. All flowrate 1 mL min^{-1}.

Acylation proceeded in full conversion (entries 1-3) and the enantiomers were easy to separate. Attempts to install a Boc group proceed in low-no conversion (entries 4-5).

Table SI-3.3.4.1: Lowering the catalyst loading.

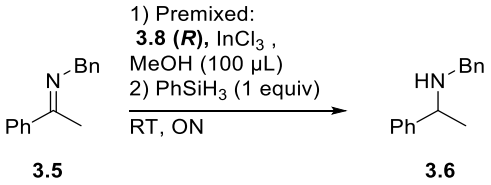

3.5 3.6

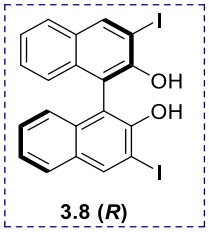

3.8 (*R*)

Entry	$InCl_3$ [mol%]	3.8 (*R*) [mol%]	Conversion[a] [%]	e.e.[b] [%]
1	2	8	94	34
2	1.5	6	94	35
3	1	4	90	33
4	0.5	2	88	32

[a] Conversion of imine to amine determined by crude NMR with 1,3,5-trimethoxybenzene as internal standard. [b] e.e. of amine determined by chiral stationary phase RP-HPLC

More than 90% conversion was achieved with both 1.5 and 2 mol% catalyst loading (entries 1,2), whereas the conversion decreased with further decrease in the catalyst loading (entries 3,4).

Table SI-3.3.4.2: Screening reducing agents.

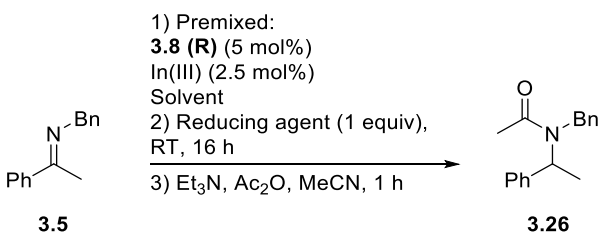

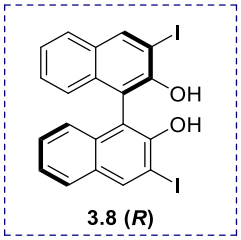

Entry	Solvent	[µL]	In(III) source	Premix temp, time	Reducing agent	Conversion[a] [%]	e.e.[b] [%]
1[c]	MeOH	200	$InCl_3$	RT, 1 h	Hantszch ester	0	-
2[c]	MeOH	200	$InCl_3$	RT, 1 h	TMDS	5	0
3[c]	MeOH	200	$InCl_3$	RT, 1 h	Hantszch ester[d]	0	-
4[c]	MeOH	200	$InCl_3$	RT, 1 h	TMDS[d]	4	0
5[e]	MeOH	100	$InCl_3$	RT, 1 h	TMDS	3	22
6[e]	MeOH	100	$InCl_3$	RT, 1 h	TMDSO	16	20
7[e]	MeOH	100	$InCl_3$	RT, 1 h	$PhSiHMe_2$	3	18
8[e]	MeOH	200	$InBr_3$	RT, 1 h	Et_3SiH	0	-
9[e]	MeOH	200	$InBr_3$	RT, 1 h	Et_3SiH	0	-
10[e]	CH_2Cl_2	200	$InBr_3$	RT, 1 h	Et_3SiH	0	-
11[e]	CH_2Cl_2[f]	200	$InBr_3$	RT, 1 h	Et_3SiH	0	-
12[e, g]	*i*-PrOH[f]	1000	$In(OTf)_3$	60 °C, 4 h	$LiBHEt_3$	0	-
13[e, g]	*i*-PrOH[f]	1000	$In(OTf)_3$	60 °C, 4 h	TMDS[h]	0	-
14[e, g]	*i*-PrOH[f]	1000	$In(OTf)_3$	60 °C, 4 h	TMDSO[h]	0	-
15[e, g]	*i*-PrOH[f]	1000	$In(OTf)_3$	60 °C, 4 h	Cl_3SiH	0	-
16[e]	MeCN	250	$InBr_3$	RT, 1 h	Et_3SiH	0	-
17[e]	MeCN[f]	250	$InBr_3$	RT, 1 h	Et_3SiH	0	-

[a] Conversion of imine to amine determined by crude NMR with 1,3,5-trimethoxybenzene as internal standard. [b] e.e. of the acylated amine determined by chiral stationary phase RP-HPLC. [c] 143 µmol imine. [d] 20 mol% Et_3N added. [e] 72 µmol imine. [f] 50 µL MeOH added. [g] 1 mol% **3.8 (*R*),** 0.5 mol% In(III). [h] 10 equiv.

TMSD and TMDSO were able to facilitate the reduction in MeOH (entries 5,6) but not in the optimised system (entries 13,14) even when excess reducing agent was added (10 equiv). In MeOH $PhSiHMe_2$ facilitated the reaction (entry 7), however, the e.e. was similar to the e.e. when $PhSiH_3$ was used. $PhSiHMe_2$ has not yet been examined in the optimised system. Et_3SiH was unable to facilitate the reducing, independent of the solvent employed (entries 8-11, 16-17). Hantszch ester was unable to

facilitate the reaction independent of the precense of base (entries 1,3). Cl_3SiH (entry 15) and $LiBHEt_3$ (entry 12) were unable to facilitate the reaction.

Table SI-3.4.3: Screening $In(OTf)_3$ in mixed solvent systems with MeOH and toluene; intial results from selected Denmark Ligands.

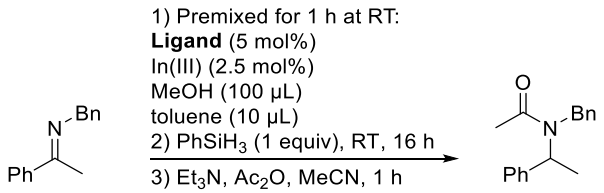

3.5 **3.26**

Entry	Ligand[a]	In(III) source	Conversion[b] [%]	e.e. [c] [%]
1	**3.55(*R*)**	$In(OTf)_3$	48	3
2	**3.50 (*R*)**	$In(OTf)_3$	45	2
3	**3.38 (*R*)**	$In(OTf)_3$	56	2
4	**3.25 (*R*)**	$In(OTf)_3$	29	0

All reactions carried out with 72 µmol imine. [a] Structure **Figure 3.7.1**. [b] Conversion of imine to amine determined by crude NMR with 1,3,5-trimethoxybenzene as internal standard. [c] e.e. of the acylated amine determined by chiral stationary phase RP-HPLC.

Unfortunately, all four ligands resulted in less than 5% e.e.

Table SI-3.4.5: Examining the effect of adding silver or tetrabutylammonium chloride.

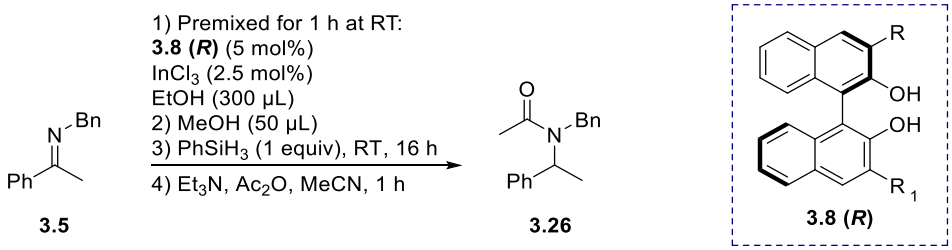

Entry	Additive	[mol%]	e.e. [a] [%]
1	$AgNO_3$	7.5	0
2[b]	$AgCO_3$	7.5	0
3	$AgCO_3$	7.5	4
4	tetrabutylammonium chloride	10	9
5	$AgBF_4$	7.5	15

All reactions with 72 µmol imine. All reactions went to full conversion (determined by crude NMR with 1,3,5-trimethoxybenzene as internal standard). [a] e.e. of the acylated amine determined by chiral stationary phase RP-HPLC. [b] No In(III) added.

Silver was found to catalyse a racemic reaction (entry 2). Addition of silver decreased the e.e. (entries 1,3,5). Addition of tetrabutylammonium chloride was found to decrease the e.e. (entry 4).

Table SI-3.5.2: Screening of other base additives.

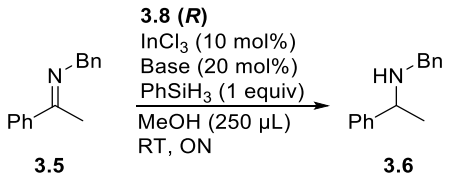

3.5 3.6

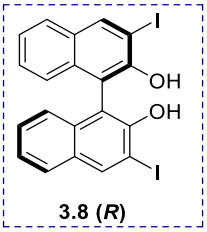

3.8 (*R*)

Entry	Base	Conversion[a] [%]	e.e. [b] [%]
1	$MeNH_2$	85	24
2	NH_3	96	23
3	pyridine	77	20
4	piperidine	22	29
5	DMAP	97	21
6	K_2CO_3	72	8
7	Piperidine[c]	0	-
8	DIPEA[c]	0	-
9[d]	DIPEA	50	32

[a] Conversion of imine to amine determined by crude NMR with 1,3,5-trimethoxybenzene as internal standard. [b] e.e. of the acylated amine determined by chiral stationary phase RP-HPLC. [c] 250 µL, no MeOH. [d] Reprinted from previous table for comparison.

When base was used as the reaction solvent, no imine reduction was facilitated (entries 7,8). Off the screened bases shown in this table, DIPEA afforded the highest e.e. (entry 9).

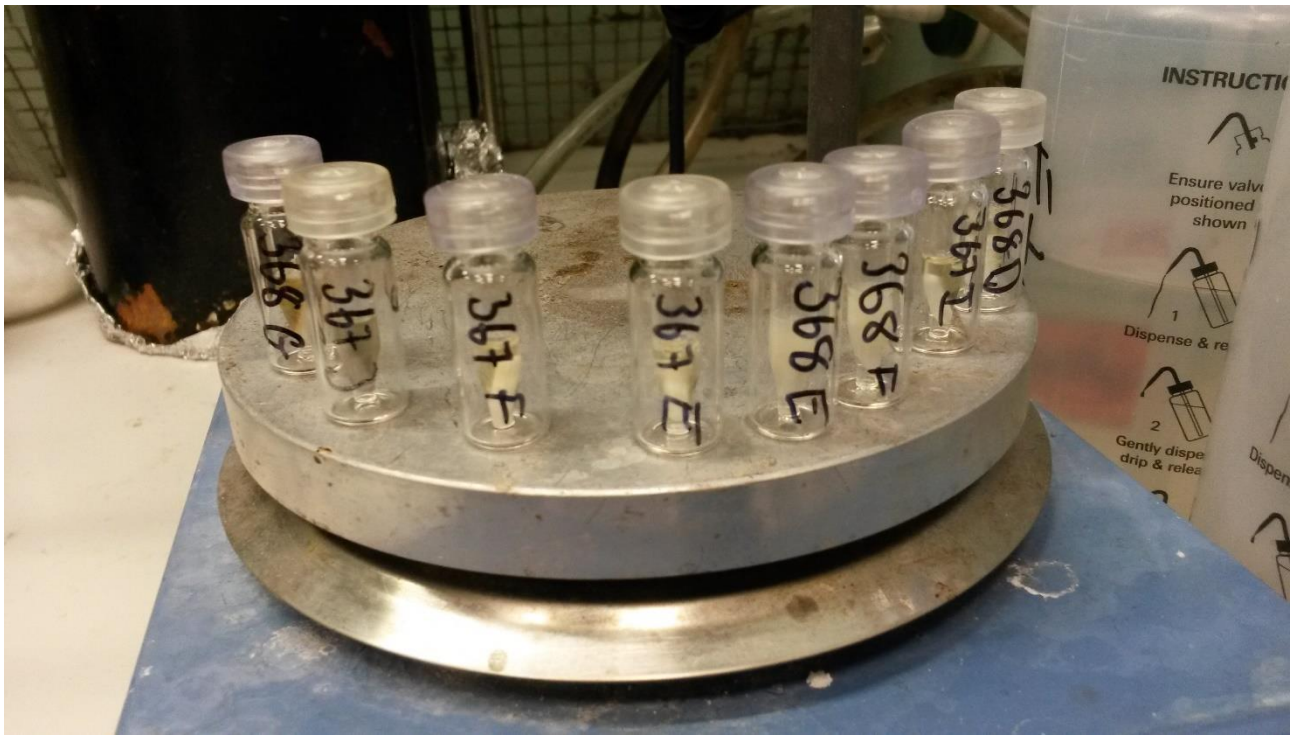

Figure SI-3.3.2.1: New reaction vessels – HPLC snapcap vials with 300 µL inserts.

Table SI-3.6.1: Screening In(III) compounds with alkoxy counterions.

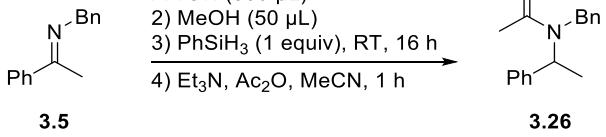

3.5 **3.26**

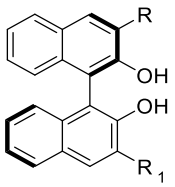

2.17 (*R*) R = (2,4,6-*i*-Pr)-Ph, R_1=I
3.8 (*R*), R,R_1=I
3.27 (*R*), R,R_1=(3,5-CF_3)-Ph
3.28 (*S*), (*S*)-VAPOL
3.29 (*R*), R,R_1=(3,5-Me)-Ph **H_8-BINOL**

Entry	Ligand	In(III) source	[mol%]	Additive	[mol%]	Conversion[a] [%]	e.e. [b] [%]
1	**2.17 (*R*)**	$In(OEt)_3$	0.5	HBF_4	0.5	98	4
2	**3.27 (*R*)**	$In(OEt)_3$	0.5	HBF_4	0.5	>99	0
3	**3.29 (*R*)**	$In(OEt)_3$	0.5	HBF_4	0.5	98	0
4	**3.28 (*S*)**	$In(OEt)_3$	0.5	HBF_4	0.5	91	22[c]
5[d]	**3.8 (*R*)**	$In(OTf)_3$	0.5		1.5	0	0
6[e]	-	$In(OEt)_3$	0.5	HBF_4	1.5	>99	0
7[e]	**3.8 (*R*)**	$In(OEt)_3$	0.5	HBF_4	1.5	>99	33
8	**3.8 (*R*)**	$In(OEt)_3$	0.5	HBF_4	1.5	>99	57
9	**3.8 (*R*)**[f]	$In(OEt)_3$	1	HBF_4	3	>99	42
10	**3.8 (*R*)**	$In(OEt)_3$	0.5	HBF_4	3	>99	44
11	**3.8 (*R*)**	$In(i\text{-PrO})_3$	0.5			>99	48
12[g]	**3.8 (*R*)**	$In(i\text{-PrO})_3$	0.5			0	-
13[e, g]	**3.8 (*R*)**	$In(i\text{-PrO})_3$	0.5			0	-
14[e, g]	-	$In(i\text{-PrO})_3$	0.5			0	-

All reactions performed with 72 µmol imine. [a] Conversion of imine to amine determined by crude NMR with 1,3,5-trimethoxybenzene as internal standard. [b] e.e. of the acylated amine determined by chiral stationary phase RP-HPLC. [c] (*S*)-enantiomer in excess [d] Hexafluoroisopropanol as solvent. [e] No MeOH added. [f] 2 equiv. [g] No silane added.

$In(i\text{-PrO})_3$ was not able to facilitate the reaction without addition of silane (entries 11-14). When hexafluoroisopronol was employed as solvent no conversion was observed (entry 5). Generally, no improvement in e.e. compared $In(OTf)_3$ as the source of In(III) was observed.

Table SI-3.6.1: Screening $In(NTf_2)_3$

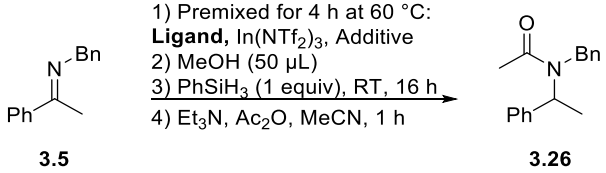

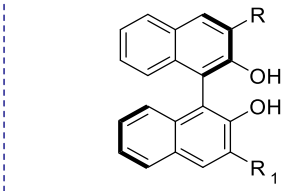

2.17 (*R*) R = (2,4,6-*i*-Pr)-Ph, R_1=I
3.8 (*R*), R,R_1=I
3.13 (*R*), R,R_1=Br
3.27 (*R*), R,R_1=(3,5-CF_3)-Ph
3.28 (*S*), (*S*)-VAPOL
3.29 (*R*), R,R_1=(3,5-Me)-Ph **H_8-BINOL**

Entry	Ligand	Additive	[mol%]	e.e. [a] [%]
1[b]	**3.8 (*R*)**	-	-	63
2[b]	**3.8 (*R*)**	NaOMe	2	46
3[b]	**2.17 (*R*)**	-	-	4
4[b]	**2.17 (*R*)**	NaOMe	2	10
5[b]	**3.29 (*R*)**	-	-	0
6[b]	**3.27 (*R*)**	-	-	5
7[b]	**3.28 (*S*)**	-	-	6 [c]
8[d]	**3.8 (*R*)**	-	-	46
9[d]	**3.13 (*R*)**	-	-	42
10[d]	**3.27 (*R*)**	-	-	2
11[d]	**3.27 (*R*)**	NaOMe	2	2
12[d]	**2.17 (*R*)**	-	-	3
13[d]	**2.17 (*R*)**	NaOMe	2	12
14[d]	**3.55 (*R*)** [e]	-	-	9
15[d]	**3.55 (*R*)** [e]	NaOMe	2	4
16[f]	**3.13 (*R*)**	-	-	16
17[g]	**3.13 (*R*)**	-	-	57
18 [g]	**3.27 (*R*)**	NaOMe	2	0
19[f]	**3.28 (*S*)**	NaOMe	2	2
20[f]	**3.27 (*R*)**	NaOMe	2	0
21[f]	**3.8 (*R*)**	-	-	24
22[g]	**3.8 (*R*)**	-	-	59
23[h]	**3.8 (*R*)**	-	-	62[i]

Table SI-3.6.1 continued: Screening $In(NTf_2)_3$

Entry	Ligand	Additive	[mol%]	e.e. [a] [%]
24 [h]	**3.13 (*R*)**	-	-	49
26 [j]	**3.13 (*R*)**	-	-	56
27 [k]	**3.8 (*R*)**	H_2O	0.1	59
28 [k]	**3.8 (*R*)**	H_2O	0.5	58
29 [k]	**3.8 (*R*)**	H_2O	1	58
30 [k]	**3.8 (*R*)**	H_2O	3	54
31 [k]	**3.8 (*R*)**	H_2O	5	52
32 [k]	**3.8 (*R*)**	H_2O	10	40

All reactions performed with 72 µmol imine. All reactions proceeded to full conversion. [a] e.e. of amide. [b] First batch $In(NTf_2)_3$ – contained In_2O_3 impurities. [c] (*S*)- enantiomer in excess. [d] Second batch $In(NTf_2)_3$ cleaned through celite plug and dried at 130 °C *in vacuo.* [e] Structure Figure 3.7.1 [f] First batch after subsequent celite plug and drying. [g] Third batch, partly decomposed as heated to 180 °C *in vacuo*. [h] Forth batch, dried *in vacuo* at RT, after celite plug. [i] average of two reactions. [j] Fifth batch, dried at 100 °C *in vacuo*. [k] Sixth batch, dried *in vacuo* for 36 h at 150 °C.

It was not possible to improve the e.e. by addition of water (entries 27-32). Addition of NaOMe had varying effect. How the In(III) triflimidate had been dried also had varying effect.